

PYROLYSIS AND THERMAL HYDROGASIFICATION OF HYDROCARBONS

---

by

Alberto Ignacio La Cava, Ingeniero Quimico, M.Sc., D.I.C.

DECEMBER, 1976

A thesis submitted for the degree of  
DOCTOR OF PHILOSOPHY  
OF THE UNIVERSITY OF LONDON

Department of Chemical Engineering  
and Chemical Technology  
Imperial College  
LONDON SW7

TO GUILLERMO DEMIAN,  
AND LIDIA

ABSTRACT

Some phenomena involved in the processes of industrial pyrolysis (thermal cracking) and hydrogasification of hydrocarbons have been studied, both theoretically and experimentally. Attention has been focused on the investigation of the mechanisms and kinetics of reaction.

Both reactions give a range of gaseous, liquid and solid products, and the experiments were performed at atmospheric pressure, using both a jet stirred reactor and a tubular flow reactor attached to a microbalance system. Ethane and butane were used as model hydrocarbons.

The production of gases has been found to involve mainly homogeneous reactions, largely independent of the surface. Using a jet stirred reactor, the gas phase product spectra from the pyrolysis of ethane in the presence and absence of hydrogen has been studied at high conversions. A mathematical model has been developed which gives good agreement with the results. The pyrolysis of butane in the presence and absence of hydrogen has been studied in a tubular flow microbalance reactor, and a model, based on free radical reactions, has been proposed to explain the effect of hydrogen. The use of free radical models for such more complex hydrocarbons has been approached using semiempirical modelling procedures.

Catalytic metal liners in the reactor wall have been found to affect the gas product composition initially, but the effect disappeared after short times on-line. The surface to volume ratio has been found to affect the gas product spectra.

The production of aromatic liquids has been studied by reacting butane in the tubular flow microbalance reactor, and the effect of the different operation variables has been studied. The presence of catalytic metal walls affected the production of aromatics when the reactor was first brought on line. Increases in the surface to volume ratio

produced a significant decrease in the production of aromatics. The mechanisms of aromatics production and the action of hydrogen have been discussed.

The formation of solid products has been studied using the pyrolysis of butane in a flow reactor combined with a C.I. microbalance. Carbon formation has been found to involve a catalytic and a non catalytic route. Hydrogen accelerated catalytic carbon formation and suppressed non-catalytic carbon. Catalytic carbon formation presented a complex three-zone activation energy in the Arrhenius plot, while non-catalytic carbon presented only one zone. Catalytic metal walls affected carbon deposition on non-catalytic surfaces. Increases in the surface to volume ratio in the reactor decreased the rate of carbon deposition per unit area. Models are presented, and catalytic and non catalytic carbon formation, surface to volume effects and condensation carbon deposition are discussed on this basis. Finally, the possible role of high molecular weight polycyclic aromatics as intermediates of non catalytic carbon formation, is discussed in the light of compounds found among the reaction products by mass - spectrometry.

ACKNOWLEDGEMENTS

I would like to thank my Supervisor, Dr. David L. Trimm for his help, friendship and guidance throughout this research project.

I like to thank my companions of the Catalysis Research Laboratory, particularly to Myra, Andy, Carlos, Chris and Wei for providing a cheerful atmosphere of work and free interchange of ideas.

I gratefully thank the institutions that have given financial support to myself and this project at different stages: The British Council, Air Products and Chemicals Inc. and the Consejo Nacional de Investigaciones Científicas y Técnicas de la República Argentina.

I wish also to thank the different institutions that have contributed, with a free exchange of ideas and suggestions, for the development of different parts of the present work, : Air Products and Chemicals Inc., and British Gas amongst many others.

Finally, my deepest acknowledgment to my wife Lidia, for all of her patience, love, companionship, understanding and financial support during hard times; and to Guillermo, my son, for the time of which he was deprived of me, due to this work .

LIST OF CONTENTS

TITLE	.....	1
ABSTRACT	.....	3
ACKNOWLEDGEMENTS	.....	5
LIST OF CONTENTS	.....	6
<u>CHAPTER I INTRODUCTION</u>	.....	12
1- GENERAL	.....	13
2- INDUSTRIAL THERMAL CRACKING	.....	14
a- Steam cracking	.....	14
b- Coke formation in steam cracking.	.....	16
3- INDUSTRIAL THERMAL HYDROGASIFICATION		
OF HYDROCARBON OILS.	.....	16
a- The future natural gas shortage.	.....	17
b- The development of the industrial process.	.....	19
c- Carbon formation in thermal hydrogasification.	.....	30
4- PYROLYSIS OF HYDROCARBONS	.....	33
a- Pyrolysis of light paraffins	.....	33
b- Pyrolysis of olefins.	.....	35
c- Pyrolysis in the presence of hydrogen.	.....	36
d- Pyrolysis and thermal hydrogenation of aromatics...		37
e- Surface effects during the thermal reactions		
of hydrocarbons.	.....	41
5- SYNTHESIS OF AROMATICS DURING THE THERMAL		
REACTIONS OF PARAFFINS AND OLEFINS.	.....	44
a- The mechanism of thermal synthesis of aromatics...		45
6- THE FORMATION OF CARBON DURING THE THERMAL		
REACTIONS OF HYDROCARBONS.	.....	48
a- The formation of carbon without the participation		
of catalytic metals.	.....	48

b- Metal - catalysed carbon formation, ..... 51

7- OBJECTIVES OF THE PRESENT RESEARCH. .... 54

CHAPTER II EXPERIMENTAL ..... 56

1- INTRODUCTION ..... 57

2- EXPERIMENTAL SYSTEM BASED ON A JET-STIRRED  
 REACTOR. .... 57

    a- Experimental procedure and variables studied. .... 62

3- EXPERIMENTAL SYSTEM BASED ON THE TUBULAR  
 MICROBALANCE REACTOR. .... 65

    a- The tubular microbalance reactor. .... 65

    b- Furnaces and temperature control. .... 70

    c- The gas analyzer ..... 75

    d- Liquid collection and analysis. .... 76

    e- Materials ..... 78

    f- Operation technique. .... 82

    g- Precautions taken with the manipulation  
     of polycyclic aromatics. .... 85

    h- Experimental operation conditions and variables  
     studied. .... 85

CHAPTER III RESULTS ..... 89

A- THE PRODUCTION OF THE MAJOR GASEOUS PRODUCTS ..... 92  
DURING THE THERMAL REACTION OF HYDROCARBONS.

1- Thermal reactions of ethane in a jet-stirred reactor,... 92

2- Thermal reactions of butane in a tubular flow  
 microbalance reactor. .... 105

    a- The effect of butane initial concentration  
     in mixtures with hydrogen. .... 105

    b- The effect of hydrogen concentration in the feed,..... 105

    c- The effect of reaction temperature. .... 107

d-	The effect of gas residence time.	107
e-	The effect of metal liners on the reactor wall.	112
f-	Minor compounds in the route towards aromatics.	112
g-	The effect of the surface to volume ratio in the reactor on the gas product composition.	117
B-	<u>THE PRODUCTION OF AROMATIC COMPOUNDS DURING THE THERMAL REACTION OF BUTANE</u>	120
a-	Effect of the residence time.	120
b-	Effect of hydrogen concentration	124
c-	Effect of butane inlet concentration in mixtures with hydrogen on the production of aromatics.	124
d-	Effect of temperature.	128
e-	Effect of metal liners on the reactor wall during the transient period.	135
f-	The effect of the surface to volume ratio in the reactor.	140
C-	<u>THE FORMATION OF CARBONACEOUS DEPOSITS DURING THE THERMAL REACTIONS OF BUTANE.</u>	143
1-	Experiments with pure butane.	143
a-	Carbon deposition on a silica foil.	143
b-	Carbon deposition on different metals.	145
c-	The effect of lining the reactor wall with different metals.	145
d-	Transient rates during the early stages of deposition.	147
e-	Effect of temperature on the rate of carbon deposition on copper sample foils.	153



2- Experiments with butane diluted with hydrogen and helium. ..... 160

    a- The effect of hydrogen and residence time ...  
        on the deposition over copper. .... 160

    b- The effect of hydrogen on the carbon  
        deposition over different metals. .... 160

    c- The effect of temperature on the deposition  
        over nickel and copper. .... 172

    d- Results of experiments with the reactor-  
        condenser scheme. .... 179

    e- Transient phenomena during carbon deposition. .... 188

    f- The effect of surface to volume ratio on  
        the rate of carbon deposition on a copper sample foil.. 192

D- REFERENCES TO THE FIGURES OF CHAPTER III. ..... 195

CHAPTER IV DISCUSSION ..... 214

1- GENERAL ..... 216

2- THE FORMATION OF THE MAIN GAS PRODUCTS. ..... 218

    a- Free- radical model at high conversions  
        in the presence of hydrogen; The thermal reaction of ethane. 219

    b- The effect of hydrogen on the rate of the  
        thermal decomposition of hydrocarbons. .... 232

    c- Semi-empirical modelling of thermal  
        hydrogenation reactions (hydrogasification). .... 237

    d- Effect of reactor surfaces on the production  
        of the major compounds. .... 241

3- THE PRODUCTION OF AROMATIC COMPOUNDS. ..... 242

    a- Introduction ..... 242

    b- The synthesis of aromatics from paraffins. .... 243

    c- Modelling of aromatics synthesis. .... 249

d-	Further reactions leading to the formation of polycyclic aromatics.	251
e-	The effect of hydrogen on aromatics formation	256
f-	The effect of surface to volume ratio in the reactor.	257
4-	<u>THE FORMATION OF CARBONACEOUS DEPOSITS</u> <u>ON SURFACES.</u>	258
	General	258
4-A	<u>The formation of carbon deposits without the intervention of catalytic metals.</u>	259
a-	General discussion of the experimental results.	259
b-	A model for non-catalytic carbon deposition.	262
c-	Simplified mathematical model. The effect of the operational variables.	264
d-	The effect of surface to volume ratio on carbon deposition.	273
e-	Mathematical modelling of the growth of coke particles by carbon deposition in a fluid bed during thermal hydrogenation.	277
f-	The deposition of carbonaceous material by physical condensation.	285
4-B	<u>The formation of carbon deposits on surfaces in the presence of catalytic metals.</u>	287
a-	Introduction	287
b-	Description of a qualitative model for carbon formation on catalytic metals.	288
	I- <u>Experiments with pure butane</u>	290
c-	Carbon deposition on different metals.	291
d-	The effect of lining the reactor wall with different metals.	291

e-	Transient effects during the early stages of deposition. ....	293
f-	Effect of temperature on the deposition of carbon over nickel. ....	293
II-	<u>Experiments with butane diluted with hydrogen and helium.</u> ....	294
g-	The effect of hydrogen on the carbon deposition over different metals. ....	294
h-	Transient phenomena in the presence of hydrogen....	296
5-	<u>THE INTER-RELATION AMONGST GAS MAJOR PRODUCTS, AROMATIC COMPOUNDS AND CARBON FORMATION.</u> ....	297
6-	<u>CONCLUSIONS</u> .....	301
	<u>APPENDIX I</u> .....	307
	<u>NOTATION</u> .....	314
	<u>REFERENCES</u> .....	319

## CHAPTER I

INTRODUCTION

1 - GENERAL	13
2 - INDUSTRIAL THERMAL CRACKING.	14
a - Steam cracking	14
b - Coke formation in steam cracking.	16
3 - INDUSTRIAL THERMAL HYDROGASIFICATION OF HYDROCARBON OILS.	16
a - The future natural gas shortage.	17
b - The development of the industrial process.	19
c - Carbon formation in thermal hydrogasification.	30
4 - PYROLYSIS OF HYDROCARBONS	33
a - Pyrolysis of light paraffins	33
b - Pyrolysis of olefins.	35
c - Pyrolysis in the presence of hydrogen.	36
d - Pyrolysis and thermal hydrogenation of aromatics.	37
e - Surface effects during the thermal reactions of hydrocarbons.	41
5 - SYNTHESIS OF AROMATICS DURING THE THERMAL REACTIONS OF PARAFFINS AND OLEFINS.	44
a - The mechanism of thermal synthesis of aromatics.	45
6 - THE FORMATION OF CARBON DURING THE THERMAL REACTIONS OF HYDROCARBONS.	48
a - The formation of carbon without the participation of catalytic metals.	48
b - Metal - catalysed carbon formation.	51
7 - OBJECTIVES OF THE PRESENT RESEARCH.	54

1-

GENERAL

The reactions of hydrocarbons at high temperatures have long been of industrial interest. Although the original thermal cracking route to gasoline has largely been replaced by catalytic processes, reactions such as pyrolysis, steam cracking and hydrogasification continue to be of paramount importance. This is largely as a result of the fact that steam cracking, the thermal treatment of ethane, propane, butane or naphtha, is the major route to ethylene and other light olefins, which are the corner stones of modern petrochemical industry.

In addition to this well-established reaction, attention is also being focused on pyrolysis of heavier oils in the presence of hydrogen (hydrogasification). The reaction, carried out at high pressures, leads to the production of methane and of aromatics, and offers future potential for the conversion of energy producing feedstocks from a less to a more desirable form.

Although these reactions are of considerable importance, there are difficulties in their operation. In particular, carbon formation poses many problems, since it deposits on the internal surfaces of the reactor and peripheral equipment to cause decreased thermal conductivity and to give tube blocking. The present research was initiated in order to study some aspects of this problem, in the context of hydrocarbon pyrolysis in the absence and presence of hydrogen.

This introductory chapter gives a short review and discussion of the state of knowledge in the fields concerned with the problem under consideration. An account of the industrial background and state of development of the technology is given in the first place, and a review and discussion of the literature in the aspects more related to the scientific background is presented later.

2-

INDUSTRIAL THERMAL CRACKING

Thermal cracking is defined as the thermal decomposition, under pressure, of large hydrocarbon molecules to produce smaller molecules. Lighter, more valuable hydrocarbons may thus be obtained from relatively low value heavy stocks.

It is believed that the thermal cracking of petroleum was discovered by accident in a small refinery in New Jersey, U.S.A. A bake still was used to separate oil into kerosene and lubricant residue. Due to lack of attention the temperature of the residue was allowed to rise enough to allow cracking to take place and the kerosene was found to be contaminated with thermally cracked gasoline. (Knight, et.al., 1973).

Thermal cracking of oil became commercial with the expanding demand for gasoline prior to World War I. Later it was noticed that the octane number of the cracked stock was higher than the corresponding straight run gasolines. With the advent of increasing compression ratios of automobile engines, this factor became as important as the yield increase. However, thermal cracking is now becoming obsolete, since the anti - knock requirements of modern automobile engines have outstripped the ability of the thermal cracking process to supply an economic source of high quality fuel.

a- Steam cracking

Although the original role of thermal cracking is now better covered by more modern processes (which provide higher quality gasoline), the principles of thermal cracking still have a part to play in the modern refinery. The most important use is in steam cracking, a thermal cracking process conducted at low pressure and high temperatures, in the vapour phase and with dilution of the hydrocarbon with steam. This process is primarily

used to produce light olefins ( ethylene, propylene, butenes and butadiene ) which are the raw materials of modern petrochemical industry.

According to Hardley , et.al. (1973), steam cracking of naphtha is by far the most important source of  $C_2$  to  $C_4$  petroleum chemical intermediates in West Europe and Japan. Products from hydrocracking and catalytic reforming, boiling in the naphtha range, are used to increase the straight - run material. The main product of the process is ethylene, although propylene, butanes and butadiene are important co-products. Another major co-product is the  $C_5 +$  liquid, containing mostly material which is an important source of benzene , toluene and isoprene.

In the endothermic steam-cracking process, the naphtha plus steam diluent is decomposed at temperatures between 700 and 900° C. The presence of steam lowers the partial pressure of the products, and thus reduces the rate of undesirable bimolecular reactions of the lower olefins into polycyclic aromatics and polymerised aromatics. These are responsible for the deposition of carbon in the reactor walls and coke in heat exchangers.

In the industrial plant operation, a mixture of steam and feedstock (usually naphtha) is cracked, generally in a coil-type furnace. (Zdomik , et.al. , 1970). Products from the furnace are usually quenched using transfer line heat exchangers, that allow the recovery of a large portion of the heat contained in the effluent. Dowtherm, or quench oil, are generally used as heat transfer media. (Zdomik , et.al. , 1970).

The normally liquid products (carbon number 5 or more) are first separated from the gases. The gases are then compressed and fractionally distilled at low temperatures, and the liquid is split into raw steam cracked gasoline and fuel oil plus tar. (Hardley et.al. , 1973).

b. Coke formation in steam cracking.

Steam cracking plants are expected to operate for a long time before cleaning is necessary. Plugging, high pressure drops and low heat transfer efficiency are produced by the deposition of carbonaceous materials on the reactor walls. Eventually, the operation of the plant has to be discontinued and the system cleaned. The expense of a shutdown is so great that the minor, slow reaction of carbon deposition is a very detrimental factor in the whole economy of the plant. (Nelson , 1958 ).

Direct observations from an industrial plant (Trimm , 1974 ) indicated that carbon did not deposit uniformly inside the furnace tubes. Very slow coke formation was noticed in the evaporation section of the apparatus. In the reaction zone, coke deposited steadily but became appreciable in the last sections of the tube. At the furnace outlet, in the quenching system (a transfer line heat exchanger ), coke was found to deposit on the exchanger walls and tubes.

3- INDUSTRIAL THERMAL HYDROGASIFICATION OF HYDROCARBON OILS.

In all the industrial countries of the world, there is an ever increasing demand for energy, and there are political pressures demanding that the preparation and conversion of this energy should be non-polluting. If it is possible to accept carbon dioxide and water as tolerable products of energy conversion, then natural gas is a fuel that provides a clean source of thermal energy. (Hebden et.al. , 1972 ).

The use of gas as a source of energy in towns and large cities for domestic consumption has also several advantages :

- a) Gas can be transported and distributed to the points of use through a pipeline network.
- b) No further treatments are required at the points of use ;



- c) Easy control and conversion to energy and
- d) The equipment for conversion is simple and cheap.

These advantages have led to a very widespread use of natural gas in modern society and hence to a fast consumption of a natural resource which is not available in unlimited amounts. The problem of the future depletion of the natural resources which originated the interest in transforming other fuels into a substitute natural gas, is discussed below.

a - The future natural gas shortage

There are several reasons for the imbalance between gas consumption and new gas discoveries. The search for gas had always taken second place to oil prospecting in most areas, due to low prices and to other restrictions imposed by governments. At the same time, technical advantages and lower prices have provided an incentive for the use of gas in many applications. For all these reasons, the United States and most of the European countries have predicted imminent shortages of natural gas, which will require either drastic cuts in consumption or the use of suitable replacements. (Lom, et.al., 1976). As an example, the perspectives of gas production and demands in the U.S.A. are given in figure I-1.

One possible way of filling the widening gap between demand and supply is the production of "synthetic" natural gas by chemical transformation of other fuels. Several processes have been developed recently that allow the transformation of different hydrocarbon oils distillates, crudes, heavy residues, and coal into a substitute for natural gas. The three main process routes involved in the gasification of fuels, each associated with a typical feedstock are :

- Steam reforming of light distillates

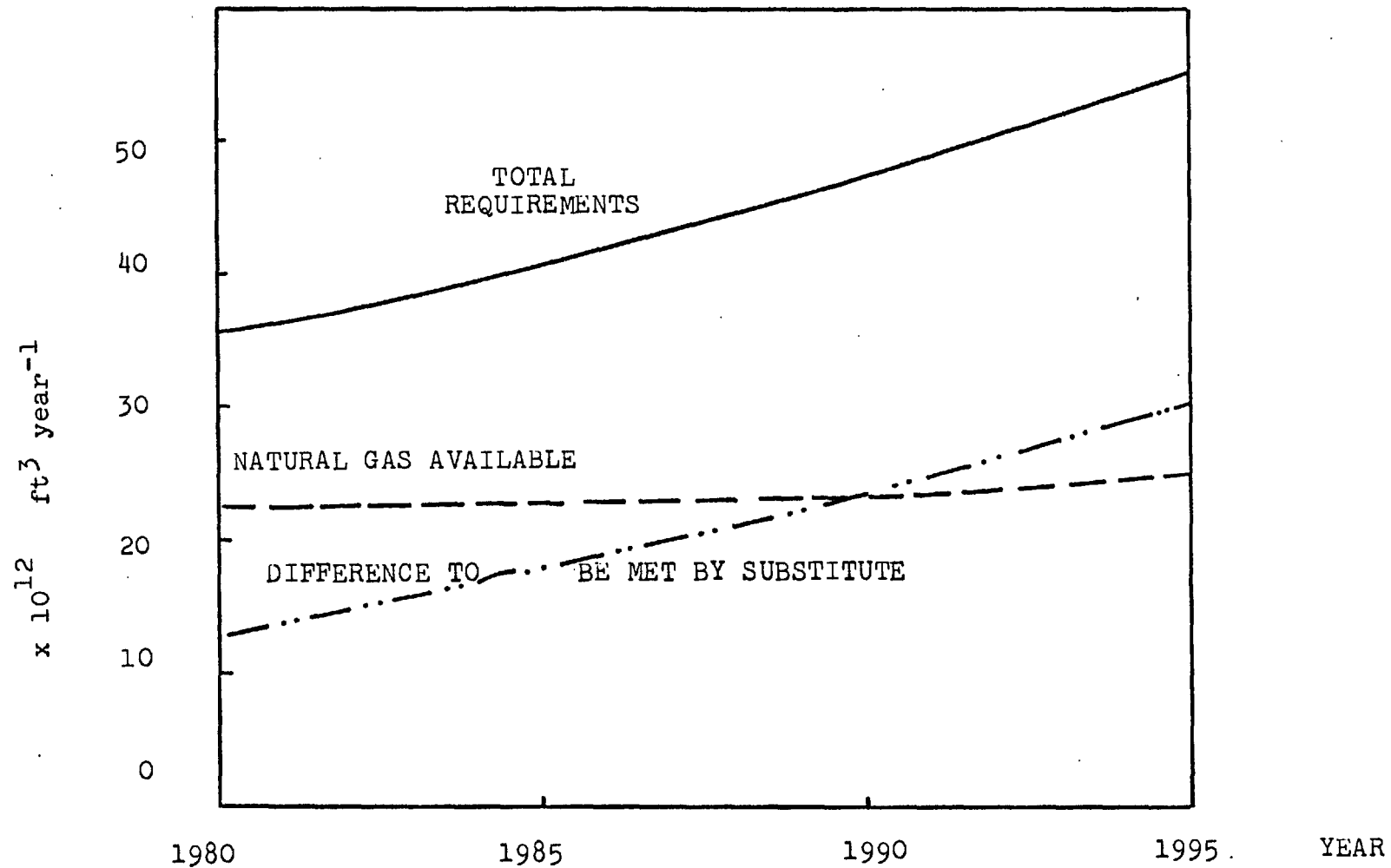


FIGURE I-1. ESTIMATES OF U.S.A. NEEDS FOR GAS ( Lom, W.L. et.al.,1976 )

- Thermal hydrogasification of middle distillates and residual fuels.
- Partial oxidation of residual fuels and coal.

During the present work , attention has been focused on thermal hydrogasification process. The main features and the steps in the development of the process are summarised below.

b- The development of the industrial process

The process of thermal hydrogasification of hydrocarbon oils was developed by the British Gas Corporation (previously The Gas Council) between the mid fifties and the mid sixties. The process was inspired by the same principles as were applied to the previously developed process of coal thermal hydrogasification. (Dent et.al. , 1957). The initial object seems to have been to provide a product that could be added to a Lurgi gas (coal gasification plant) to enrich the heating value. A further application seems to have been the production of a high heating value substitute natural gas (S.N.G.).

In essence, the thermal hydrogasification of oils is a process of high thermal efficiency, capable of transforming low value hydrocarbons into a gas composed mainly of methane. The process is a homogeneous thermal reaction, and the absence of a catalyst inside the reactor allows the processing of oils with considerable amounts of sulphur , metals and other catalyst poisons.

The first stages in the development of the process were carried out in a carbon gasification pilot plant. The technique used was to supply oil to a bed of coke particles at 700 - 900<sup>o</sup> C, fluidized with a hydrogen-rich gas at 20 -50 atm. The expected reactions were the breakdown of molecules into fragments and the addition of hydrogen to the resulting olefins :



The exothermicity of the second reaction is such as to compensate for the endothermicity of the pyrolysis, and reaction temperatures can be maintained by preheating the hydrogenating gas to 300° C - 600° C.

The functions of the fluid bed of coke particles were : (Dent et.al., 1957 ) .

- a) To maintain one uniform temperature throughout the reaction space.
- b) To receive any ash that comes with the oil and any carbon formed in the reaction.
- c) To act as a support and to provide heat for the vaporization of hydrocarbons that reach the bed in the liquid state.

Conclusions from the earlier experiments in the pilot plant were as follows :

- 1- The most desirable range of operation temperatures was between 700 - 900° C. Below 700° C the reaction was found to be very slow; at temperatures higher than 900° C tar vapours tended to crack and form soot.
- 2- The fluid bed gave good temperature control and retained the ashes of the oil, as expected.
- 3- In order to avoid carbon deposition, it was very important to get a good mix of hydrocarbon vapours and hydrogenating gas before they were admitted to the reactor.
- 4- No agglomeration occurred in the bed when hydrogenating light distillate or gas-oil, but the agglomeration and

caking of the fluid bed was found to be serious when hydrogenating crude or residual oils. It was found that the natural circulation of the fluid bed was not enough, and caking occurred mostly near the oil feed point .

The hydrogenation of a light distillate of boiling point 24-69° C gave 97 - 100 % gaseous products, up to 3 % benzene, 0.2 % naphthalene and 0.1 % higher aromatics . No carbon deposition was observed at 32 atm. and 715 - 740° C.

When hydrogenating a gas - oil of boiling range 210 - 368° C, 80.7 % gas was obtained, together with 12.6 % benzene, 4.3 % naphthalene, 2.4 % higher aromatics, without carbon deposition, at 32 atm. and 780° C.

To perform the hydrogenation of crude and residual oils, the initial reactor was modified. Figure I-2 shows an improved version of the modifications made to the fluid bed, intended to promote a higher recirculation rate in the coke particle medium. Model studies established that the coke recycle rate was high (of the order of 2000 lb/hr).

Experiments made with a crude oil, ( 31 % of it's weight distilled below 268° C) hydrogenating at 32 atm. and 765 - 820° C, gave 77 % gaseous products, 10 % benzene, 3 % naphthalene, 9 % higher aromatics and about 2.7 % of deposited carbon . No coking or agglomeration of the fluid bed occurred and the operation of the recycle reactor was successful.

The hydrogenation of a heavy fuel oil ( viscosity nominal Redwood N° 1 of 3000 sec.) in the same reactor gave 66 % gas, 9.5 % benzene , 6.4 % naphthalene, 13.3 % higher aromatics and 5 % of deposited carbon, when treated at 32 atm. and 755 - 785° C.

In parallel with the pilot plant scale developments , a series of laboratory experiments were performed , tending to establish the general behaviour of the system and provide more information for the pilot scale

operation. (Dent , et.al. , 1957)

Hydrogenation of light distillate in an empty tube at 700 - 800° C gave total conversion to gases , independent of the oil/hydrogen ratio at 10 seconds residence time. The gasification of gas-oil was more condition - sensitive, the conversion to gases increased with the temperature and decreased with the oil/hydrogen ratio. At 900° C some carbon deposition occurred.

The calorific value of the product gas increased with the oil/hydrogen ratio and reached a value of 1024 BTU / S ft<sup>3</sup> at 25 atm. and 700° C. The effect of using a longer residence time was checked; increases from 10 to 100 sec. produced a very slight increase in gas production. Raising the pressure from 25 to 50 atm. enhanced the yield of gaseous hydrocarbons produced.

Experiments were also made in a laboratory reactor filled with coke and operating in the fluidized conditions . In the new system, as with the empty reactor, the hydrogenation of light distillate to gas was complete, above 700° C. The hydrogenation of gas-oil, however, showed that the production of gaseous hydrocarbons decreased slightly (2 -4 % ) with respect to the empty tube, probably increasing the amount of aromatic products. At 700° C some xylenes were found in the condensate.

The effect of increasing the pressure of the fluid bed reactor when hydrogenating gas oil was found to be an increase of the yields of gaseous hydrocarbons and benzene and a decrease in the production of naphthalene and higher aromatics. The calorific value of the produced gas increased with the operation pressure.

A further stage of development of the industrial process was more concerned with the production of aromatic hydrocarbons, and particularly, benzene. (Moignard , et.al , 1959 ). The previous experiments with gasification of hydrocarbons had shown that certain amounts of aro-

atics were formed as by-products, and further research was devoted to establishing the conditions that would give higher yields of higher purity benzene. It had been established that, at 10 seconds residence time, the hydrogenation of a light distillate at  $700^{\circ}\text{C}$  and at a rate of 5 gallons of distillate /  $1000\text{ ft}^3\text{ H}_2$  gave complete conversion to gaseous products. When the distillate was fed in higher proportions ( 10 to 30 gallons /  $1000\text{ ft}^3\text{ H}_2$  ), aromatic hydrocarbons were synthesized at  $700 - 800^{\circ}\text{C}$  up to 20 - 25 % of the carbon contained in the feed.

Studies were then made with a laboratory silica-lined reactor that contained a fluidized bed of carbon particles ( 72 - 200 B.S.S. ). Pressures used were lower than in thermal hydrogasification, being of the order of 10 atm. ( Moignard, et.al., 1959 ). Typical experiments gave 82 % gas, 6.9 % benzene, 3.15 % toluene, 4.7 % of naphthalene and higher polynuclear aromatics. No carbon was deposited in the run. At a residence time of 10 seconds, the yield of aromatics increased with the distillate /  $\text{H}_2$  ratio up to a value of 28 gallons /  $1000\text{ ft}^3\text{ H}_2$ . Further increase in the distillate feed did not increase the yield of aromatics.

When the effect of reaction temperature was studied, the yield of aromatics was found to increase with temperature from 700 to  $800^{\circ}\text{C}$ . At the higher temperature range, higher amounts of other aromatics and carbon were formed.

Increasing the pressure in the reactor from 10 to 25 atm,

- a) increased the production of benzene and naphthalene and
- b) increased the deposition of carbon.

The authors considered that the effect of pressure was small ( Moignard, et.al., 1959 ).

Some of the experiments were more concerned with ideas about how aromatics are synthesized in hydrogasification. It had been postulated that benzene could be produced by dehydrogenation of cyclohexane present in the distillate, and an experiment was made with some pure hydrocarbons

to test this hypothesis.

In all the cases in the following table the conditions were: 750° C, 10 atm. and a rate of 8 gallons / 1000 ft<sup>3</sup> . H<sub>2</sub> .

TABLE I-1

PRODUCTS OBTAINED FROM HYDROGASIFICATION OF PURE HYDROCARBONS.

( From Moignard et.al. , 1959 )

COMPOUND % IN PRODUCTS	METHYL CYCLO HEXANE		METHYL CYCLO PENTANE	
	HEXANE	HEXANE	HEXANE	PENTANE
GAS	93.3	72.4	74.0	72.3
BENZENE	4.0	12.8	13.3	14.9
TOLUENE	0.5	2.8	2.4	3.4

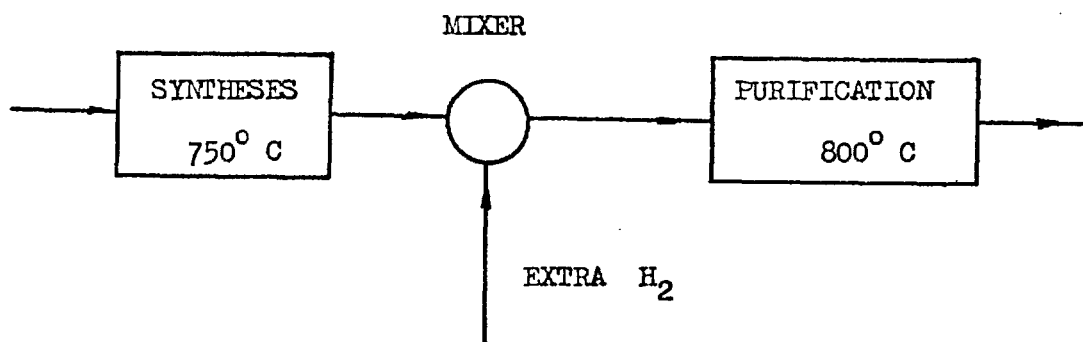
This table indicates that more aromatics were produced from cycloparaffins than from normal hydrocarbons, but that aromatics were produced in the absence of cyclic hydrocarbons. The fact that less toluene is produced from methyl - cyclohexane than from cyclohexane puts a serious objection to the idea that aromatics were produced by dehydrogenation of cycloparaffins. It should be noticed also that the amounts of benzene and toluene obtained from 5 membered cycloparaffins is the same as obtained from 6 membered cycloparaffins, contrary to what should be expected from a direct dehydrogenation route.

Some other experiments were made in the laboratory fluidized reactor, concerned with the demethylation of toluene. The experiments showed that a maximum of 98% of benzene could be obtained from the demethylation of toluene at 800° C, (10 atm. , at 10 seconds residence time ) with a feed of 3.5 gallons of toluene / 1000 ft<sup>3</sup> of H<sub>2</sub> . The yield



of benzene from toluene was found to increase with temperature, with higher  $H_2$  / Toluene and with residence time.

The principles of demethylation were also applied to the purification of the liquid condensate produced in the synthesis process, using a reactor assembly as shown in the diagram below :



The conditions in the purification stage were  $800^{\circ}C$  and 25 atm. The amount of carbon deposited was high ( 6.5 - 7.4 % ), but xylenes and polycyclics disappeared. The liquid condensate contained benzene, traces of toluene and some naphthalene, but the higher aromatics were destroyed to give benzene. In the overall process, 20 % of the carbon contained in the feed was transformed to benzene.

In all the previous experiments, the benzene produced could be purified by simple distillation to give a product that would fulfill all the specifications of purity, with the exception that the content of sulphur compounds was very high. This sulphur comes from the distillate feed to the reactor, and from the coke particles used in the fluid bed.

Experiments were made with a sulphur - free distillate ( $< 1$  ppm) and the reactor was filled with commercial silica - alumina particles. The first run gave a high carbon deposition ( 8 % ) and a higher proportion of aromatics. In the following runs, carbon deposition fell to 2 % , the amount of aromatics decreased, and a pure benzene (by simple distillation) was obtained.

At this stage of the development, the major features of the processes were concerned with the use of the fluid bed and the recirculating fluid bed reactors. A new way of effecting the hydrogenation of light distillates was then considered. (Murthy , et.al. , 1963). With light distillates, carbon deposition can be avoided because the distillate is completely evaporated and mixed with hydrogen before entering the reaction vessel. The new concept was, then, to produce the thermal hydrogasification of light distillate in an empty reactor with internal gas recycle , as shown in figure I-3.

When the mixture of distillate and hydrogenating gas is injected at high velocity into one end of the inner tube, the contents of the vessel circulates down the central tube and up the annulus. This ensures a good uniformity of temperatures inside the reactor. Model work showed that the jet can entrain 20 times its own volume, so that the gas can circulate about 20 times before leaving the reactor.

The products from the gas - recycle - hydrogenator (G.R.H.) were 30 % gases and 10 % condensates. Carbon did not deposit in the reactor except at low pressures (70 psig. ) or high distillate / hydrogen ratio ( 7.4 gallons of distillate / 1000 ft<sup>3</sup> H<sub>2</sub> ). The benzene produced contained high amounts of sulphur compounds . Otherwise, the benzene obtained by simple fractionation was of the highest quality.

The G.R.H. was used successfully with fractions of hydrocarbons of higher boiling point. (Thompson , et.al. , 1966). When a fraction of boiling point up to 335<sup>o</sup> C was hydrogenated, the preheater blocked in a short time and there were signs that vaporization before the hydrogenator was incomplete.

Runs were made in a pilot plant G.R.H. to check the effect of pressure on the calorific value of the gas produced from a low boiling point distillate. Gas of 1000 BTU / ft<sup>3</sup> was prepared at 450 , 650

and 900 psig. Traces of carbon deposition were found at 450 and 650 psig. but more were formed at 900 psig.

The successful operation of the G.R.H. seemed to depend on very few restrictions, that can be analyzed at this stage of the review. Most of these correspond to the fact that the G.R.H. cannot operate under conditions which carbon is formed, and this has been found to limit severely the use of the reactor. As an example, this restriction does not allow, up to the present, the use of the G.R.H. to hydrogasify crude or heavy oils. In the first place, it is very difficult to vaporize completely a heavy oil. In most cases, the vaporization temperature falls within the range of liquid pyrolysis, which—due to the high concentration of the liquid hydrocarbons could be very fast and could produce the blockage of inlet tubes and nozzles.

If droplets of unvaporized hydrocarbon reaches the reaction chamber, there is a high probability that the drop would undergo pyrolysis to carbon formation instead of vaporizing, mixing with hydrogen and reacting to produce methane.

Secondly, from the experiments done by the British Gas Council, it was found that crude and residual oils always give some carbon. Thus the technology that would allow thermal-hydrogasification of these oils would also have to suppress the formation of carbon and to produce a way of gasifying the liquid feed.

On the other side, the older technique of putting a fluid bed of solid particles inside the reactor, follows the idea that, provided that carbon will be formed inside the reactor, a collection surface provides a way of "trapping" the carbon in such a way as to avoid its deposition in inconvenient places.

As a result of these type of arguments, opinion is divided as to the relative merits of the FBH and the G.R.H., and many recent develop-

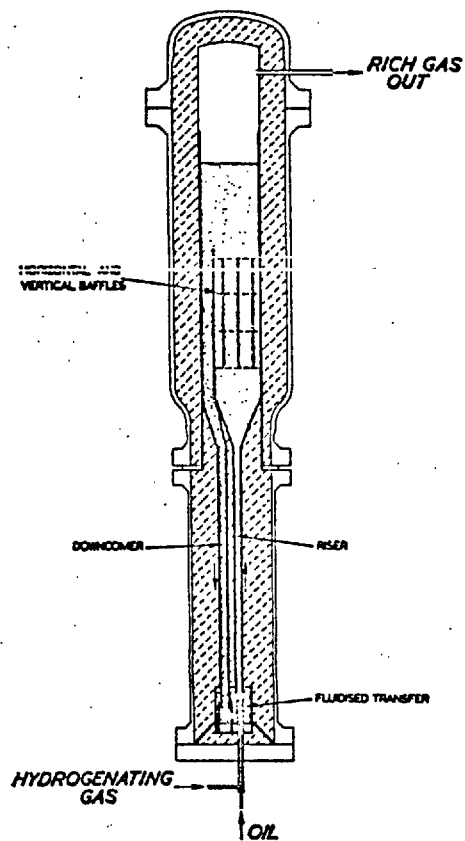


FIGURE I-2. THE FLUIDISED BED HYDROGENATOR FOR CRUDE PETROLEUM INCORPORATING A DOWNCOMER AND RISER OUTSIDE THE BED

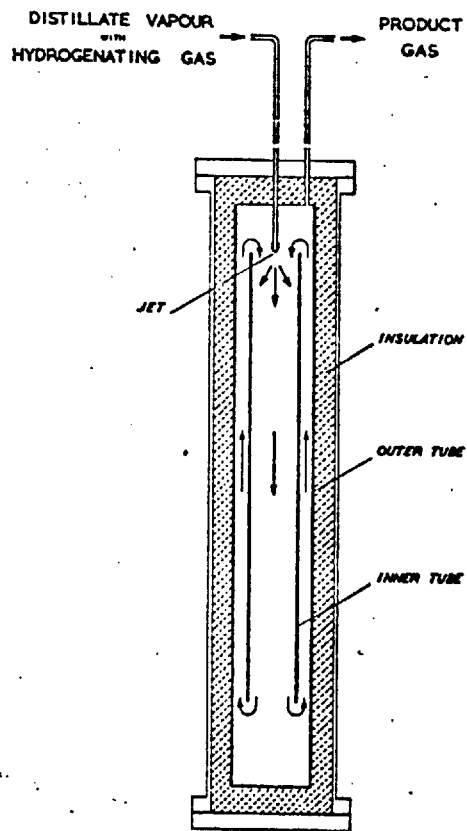


FIGURE I-3. THE GAS RECYCLE HYDROGENATOR

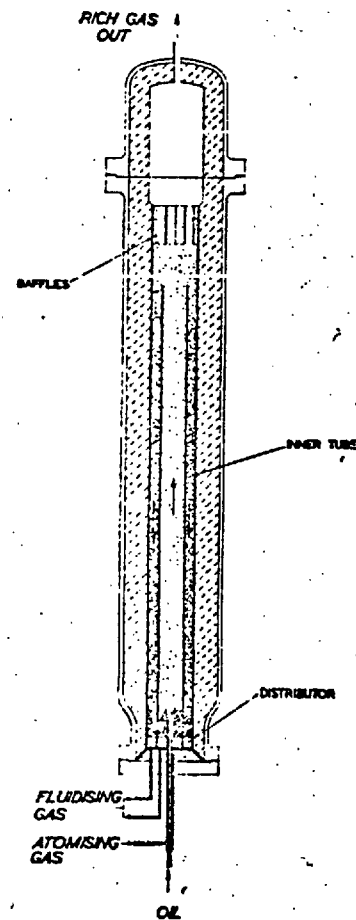


FIGURE I-4. THE SIMPLIFIED FLUIDISED BED HYDROGENATOR

( From Thompson et. al., 1966)

TABLE I-2

## THE DEVELOPMENT OF THE INDUSTRIAL THERMAL HYDROGASIFICATION.

TYPE OF REACTOR	FEATURES	DISADVANTAGES
Fluid bed of coke particles	Hydrogenate light distillates	Caking of the bed with heavier fractions
Recirculating fluid bed	Hydrogenates light, heavy distillates and crudes	Complicated design to recirculate bed.
Gas Recycle Hydrogenator	Hydrogenates light and medium distillates	Not having particles to collect carbon formed , severe carbon problems with higher fractions and crudes.
Simplified recirculating fluid bed	Hydrogenates light, heavy distillates and crudes.	Has a fluid bed inside.

ments show features of both systems . Thus, for example, a recent Gas Council process is, in essence, a G.R.H. inverted and modified to hold a fluid bed of carbon particles (fig. I-4 ). This unit is cheaper and it's performance in the hydrogenation of crude oils is excellent. (Thompson et.al. , 1966).

Thus it can be seen that the application of the hydrogasification reaction has involved a trend of development and that the optimum reactor configuration is still open to question.

Table I-2 summarizes the different stages in the development of the process of thermal hydrogasification in pilot plant and semiindustrial scale. The details on the formation of carbon in the G.R.H. are given below.

c - Carbon formation in thermal hydrogasification.

The presence of severe carbon formation problems became evident when British Gas was developing the industrial process associated with the gas - recycle - hydrogenator. (Thompson et.al. , 1966). There were two differences from the previously developed technology : the pressure was lower in the new process and a certain amount of  $\text{CO}_2$  was present in the hydrogenating gas.

Pilot plant experiments were carried out to study the effect of the new operating conditions. Carbon was formed in the hydrogenator when the pressure was reduced but this formation was suppressed by lowering the operation temperature from  $750^\circ\text{C}$  to  $700^\circ\text{C}$ . Carbon deposits reappeared as soon as  $\text{CO}_2$  was allowed into the reactor. The temperature could not be further reduced for reasons of reactor thermal stability, but these final traces of carbon formation were eliminated by adding 5 to 10 % of steam to the feed. Successfull experiments were then performed in the pilot plant.

Carbon formation troubles started again when the first

commercial plant was set into operation. Since the pilot plant experiments were carried out with sulphur containing distillates while the commercial unit used a purified feedstock, the lack of sulphur in the feed was blamed for the production of carbon. This was shown to be true when the carbon formation problems were solved by adding 10 p.p.m. of sulphur to the feed. (Thompson et.al., 1966)

Pilot plant studies were then performed with purified distillates in the presence of sulphur at different levels in the feed. When the amount of sulphur was less than 2 ppm, soot appeared in the outlet stream of the reactor and when the unit was opened, there was a thick layer of sooty carbon all over the internal surfaces of the reactor. Further experiments showed that 10 ppm of sulphur was a safe margin for operation of the plant. This did not suppress the formation of a hard layer of carbon in the internal walls, but did minimize soot formation. Hard carbon was found to depend on sulphur as shown below.

<u>AMOUNT</u>	<u>OF</u>	<u>SULPHUR</u>	<u>AMOUNT</u>	<u>OF</u>	<u>CARBON</u>
10	ppm		300	gr.	
100	ppm		50	gr.	
300	ppm		Nil.		

The internal walls in pilot plant and industrial reactor were 18 / 8 stainless steel. Knowing the catalytic properties of this material for carbon formation, the question arose whether, instead of adding sulphur, it was not better to use another material for the wall. Tests on carbon formation tendencies of metals were made, and copper was found to be inert to carbon formation. On this basis new hydrogenator internals were made from copper such that only this material was in contact with the gas at high temperature. It was difficult to start the reaction in the new system, but once started, considerable quantities (4000 g) of carbon

were produced. This carbon was : a) hard carbon adjacent to the metal surface and

b) sooty carbon adhering to the hard carbon layer.

Traces of nickel were found in the carbon and it was assumed that this material probably carried by the distillate from the internal surfaces of the vaporizer , was causing the high carbon formation . The material of the vaporizer was changed to copper and the reaction was performed again : the amount of carbon formed was as high as before.

This series of experiments ruled out copper as a wall material in the gas - recycle hydrogenator. Stainless steel with traces of sulphur in the feed seemed to offer a better solution.

These experiments , with pilot and industrial plants for the thermal hydrogasification of oils, show that carbon formation and deposition on the reactor surfaces can be a serious source of trouble in the operation of commercial plants. A better knowledge and understanding of the phenomena involved in carbon formation , which may allow forms of reducing the problem, is seen to be very desirable.



4- PYROLYSIS OF HYDROCARBONS.

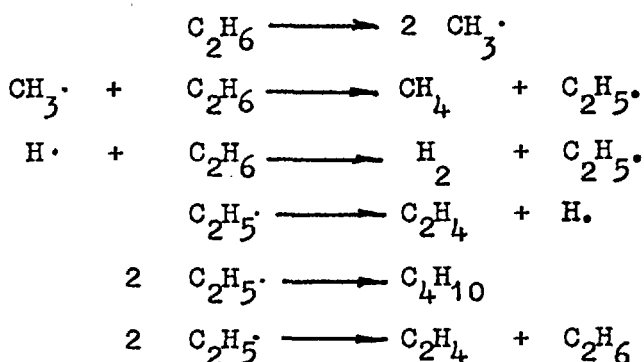
The chemical reactions involved in the pyrolysis of hydrocarbons play an important role in the processes studied in this research. It is now firmly established that these reactions proceed following Rice - Herzfeld radical chain mechanisms. (Leathard et.al. , 1970). A review of some mechanisms is given below.

a - Pyrolysis of light paraffins

The pyrolysis of methane is the simplest mechanism of free-radicals breakdown, but the true sequence of steps as yet to be established. A review of the system was given by Khan et.al. (1970). Shock tube studies give values of activation energy greater than those obtained in conventional reactors, indicating the possibility of heterogeneous effects on the reaction.

Mathematical modelling of the free - radical mechanism of methane pyrolysis and the estimation of the kinetic parameters using quasilinearisation techniques was made by Denis et.al. (1974) , and reasonable agreement was obtained between model predictions and experimental results.

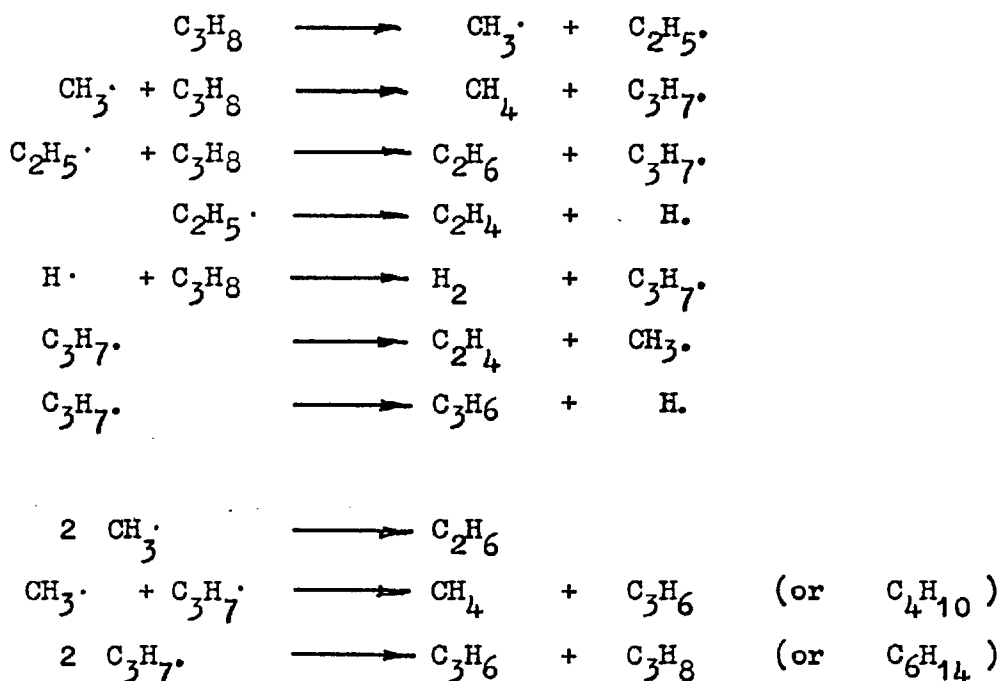
The mechanism of ethane pyrolysis was discussed by Quinn (1963) . The following sequence of reactions was proposed to represent the reaction at low conversions :



Mathematical modelling of the sequence of free-radical

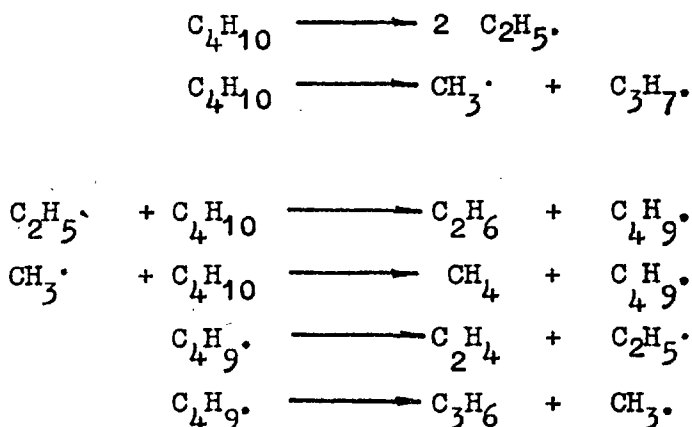
reactions was attempted by Snow et.al. (1959), Snow (1966) and Pacey et.al. (1972). A simplified molecular model was proposed by Robertson et.al. (1975) for purposes of optimisation of ethane pyrolysis plants.

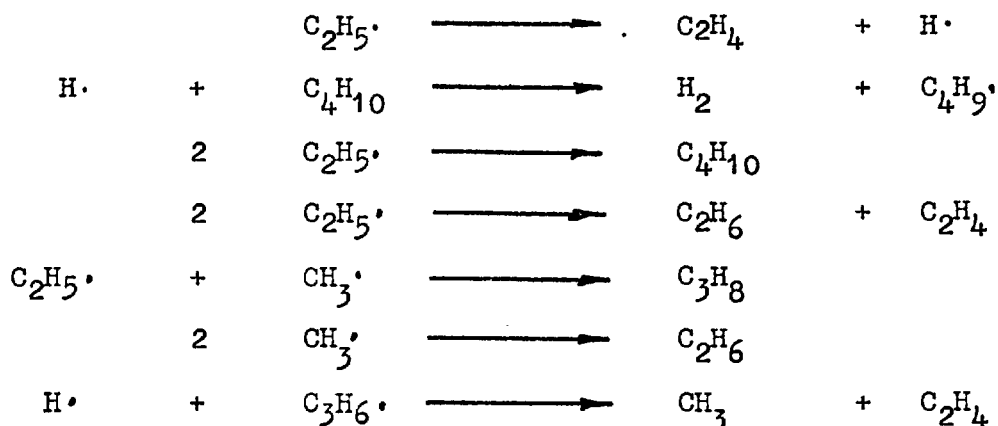
A mechanism for the pyrolysis of propane at low conversions was proposed by Herriot et.al. (1972), based in the following sequence of reactions :



A set of constants for a model, based upon the above reactions, was also proposed by Herriot et.al. (1972).

Pacey et.al. (1972) mathematically modelled the pyrolysis of butane at low conversions, with the sequence :





Modelling of the pyrolysis of higher paraffins and modelling of high conversions of either short or long chain paraffins, result in a large number of elementary free-radical reactions involving free-radical species reacting with primary and secondary products of the reaction. Models involving too many reactions do not have any theoretical interest and, as the computational effort is very large, are not practical. The solution is to use simplified approaches and semiempirical methods. Thus for example, Murata et.al. (1975), have solved the difficulty with semiempirical models representing the network of kinetic reactions and empirical parameters simulating the total behaviour of the reaction. Still more simplified ways of obtaining product compositions during industrial pyrolysis (steam cracking) have been given by Zdonik et.al. (1970)

#### b- Pyrolysis of olefins

The pyrolysis of ethylene was studied by Kunugi et.al. (1969) and the main products of the reaction were found to be hydrogen, methane, ethane, propylene, 1-butene and 1-3 butadiene. The minor products were found to be acetylene, cyclopentene, cyclopentadiene, cyclohexene and benzene. Trace amounts of cis and trans 2 butene, cyclohexadiene, toluene, xylene isomers, styrene and polycyclic aromatics (mainly naphthalene) were identified. Carbon deposits in the reactor wall were found to be less than 0.04 weight % of converted ethylene. A series of free-radical reaction

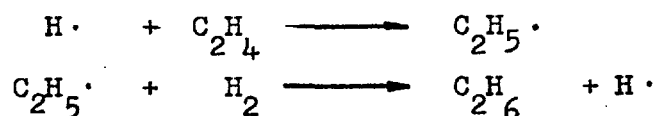
steps were studied to explain the experimental observations.

The thermal reaction of propylene were studied by Kunugi , et.al. (1970). In this case, the main products were found to be ethylene, methane, hydrogen, butenes and butadiene. Minor products were cyclopentadiene, methylcyclopentene, hexadienes, cyclopentene, benzene, toluene, ethane, acetylene and polycyclic aromatic hydrocarbons (mainly naphthalene). Traces of allene, methylacetylene, propane, cyclohexane, cyclohexadiene, 4-methylcyclohexene, xylenes and styrene were also identified. Deposition of carbon on the reactor wall was very small and was generally neglected. An overall kinetic law based on a three halves order can explain the behaviour of propylene decomposition with  $k = 10^{15.06} \exp\left(-\frac{63200}{RT}\right) \text{ cc}^{1/2} / (\text{mole}^{1/2} \text{ sec.})$ .

A free radicals mechanism to explain the previous results has also been developed (Kunugi , et.al. , 1970 a).

#### c- Pyrolysis in the presence of hydrogen

The presence of hydrogen during the thermal decomposition of paraffins is expected to hydrogenate olefins produced during the reaction. (Dent, et.al. , 1957). The thermal hydrogenation of olefins proceeds normally through a free-radical chain, as given by Benson (1968):



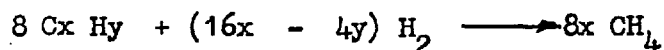
Apart from its effect on the unsaturated products of the primary decomposition, hydrogen has an accelerating effect on the decomposition of paraffins, with the exception of ethane. (Thompson et.al. , 1973). The effect of hydrogen on the rate of decomposition of paraffins can be represented by the equation:

$$\text{RATE} = \left\{ C_1 + C_2 \left[ \text{H}_2 \right] \right\} \left[ \text{HYDROCARBON} \right]$$

Experiments with a series of hydrocarbons gave the values of the Arrhenius parameters given in the following table: (Brooks , 1967).

Hydrocarbon	log A (no H <sub>2</sub> )	log A (90 % H <sub>2</sub> )	E (keal/mole)
Ethane	17.5	17.5	90
Isobutane	14.5	15.2	64
n-Butane	17.3	17.6	71.4 , 71.8
Neopentane	12.1	12.3	50.7
Cyclopentane	11.3	11.9	60.

All the above values are calculated on a simplified model for the decomposition :

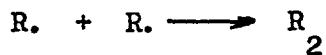


First order reaction with respect to the hydrocarbon was assumed.

To explain the accelerating effect of hydrogen , it is generally proposed that the less reactive alkyl radicals are replaced by the more reactive hydrogen atoms via the methathesis reaction : (Benson , 1965)



Another explanation may be that the above reaction would compete with the termination:

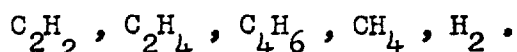


and hence would increase the chain length and increase the decomposition of the hydrocarbon.

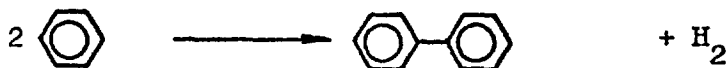
#### d- Pyrolysis and thermal hydrogenation of aromatics

Aromatic systems can undergo different thermal reactions, as follows: (Thompson et.al. 1973).

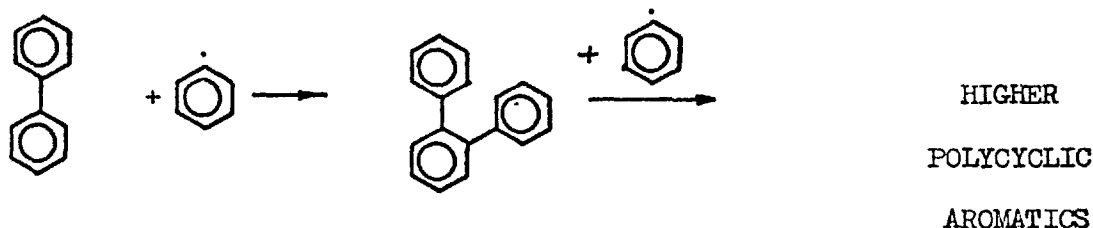
- 1- Reactions involving side chains, such as dealkylation, alkylation, condensation of rings through side chains and reactions of the side chains.
- 2- Polymerisation of the aromatic system, with the formation of polyphenyls and hydrogen.
- 3- Breakdown of the aromatic ring, to give several smaller fragments, such as



The pyrolysis of benzene starts at about  $700^{\circ}C$ , showing the high stability of the aromatic ring. Up to approximately  $780^{\circ}C$ , the principal reaction is: (Thompson et.al. 1973)

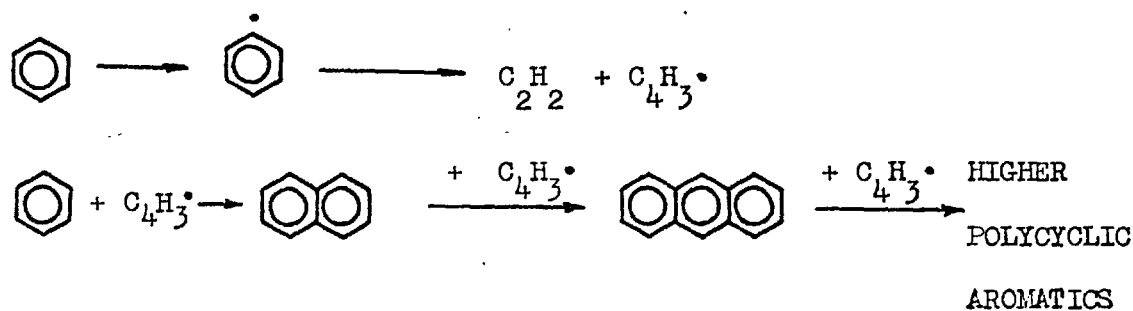


The production of higher molecular weight aromatics can proceed in the following way: (Badger, 1965)



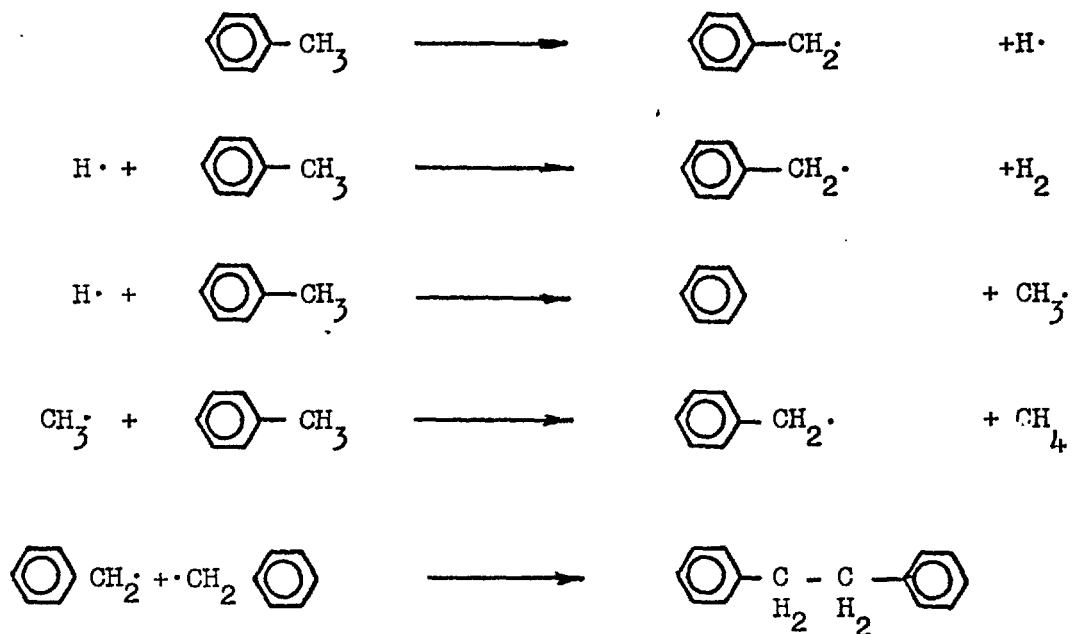
Virk et.al. (1974) consider the above route as a possible route to carbon during aromatic pyrolysis. Their theory, however, does not take into account that phenyl polymerisation is a slow process and that carbon can be formed in a few milliseconds in the gas phase. Other processes may build polycyclic structures towards carbon. The breakdown of the aromatic ring may produce building blocks that may construct polycyclic molecules as follows: (Thompson

et.al. , 1973).



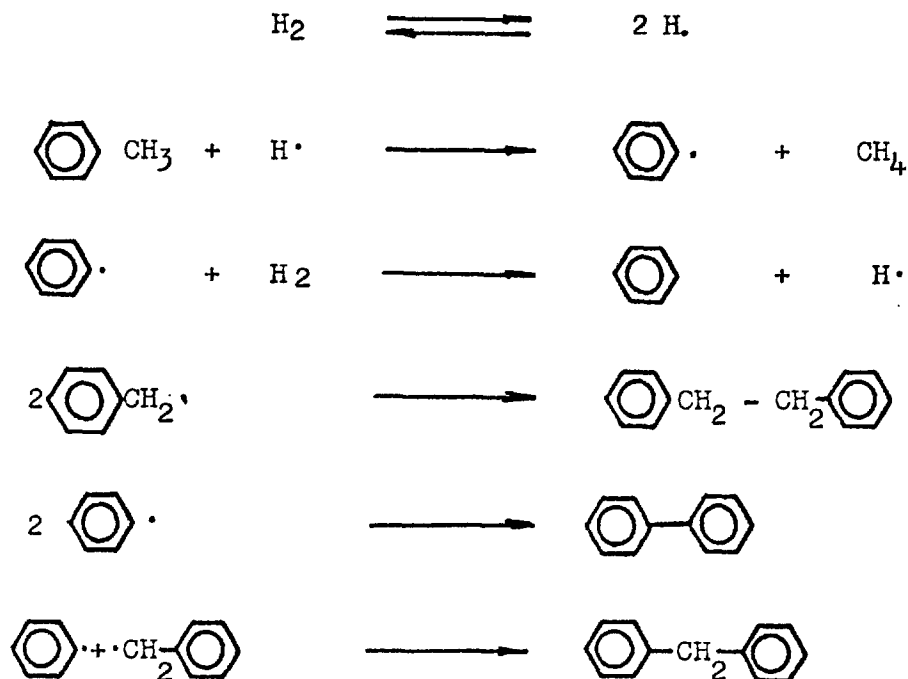
Ring fission takes place at temperatures above 780° C and will produce the evolution of methane and light hydrocarbons.

According to Brooks et.al. (1971) the pyrolysis of toluene proceeds according to the following mechanism:



In the presence of hydrogen the mechanism changes to:

(Weiss , et.al. , 1963)



According to Thompson et.al. (1973), while benzene decomposition is very insensitive to hydrogen pressure, toluene pyrolysis is significantly accelerated by hydrogen.

The thermal hydrocracking of n-butylbenzene was studied at low temperature by Slotboom et.al. (1974). The main reaction was the side chain cracking, resulting in styrene, toluene and propenylbenzene. Benzene was formed by dealkylation of butylbenzene. Products from cyclisation reactions, such as tetralin, naphthalene and other bicyclics were detected at low concentrations. The partial pressure of hydrogen had only a minor effect on the rate and selectivity.

The major products from the pyrolysis of naphthalene were found to be the binaphthyls. (Fitzer et.al. , 1971). Secondary products were perylene, benzofluoranthene, terylene and higher ternaphthyls. At above 700° C, some ring fission produced benzopyrene (Badger, 1965). The activation energy for the decomposition of naphthalene, calculated as a first order reaction is about 80 Keal/mole. (Lahaye et.al. , 1968).

The pyrolysis of anthracene produces six isomers of bianthril bi-



anthrene and dibenzoperylene. (Fitzer et.al. , 1971). Via a similar mechanism, the pyrolysis of phenanthrene gives dibenzo <b,n> perylene and dibenzo <b,k> perylene. Higher condensed products are also formed. The pyrolysis of phenanthrene in the presence of excess hydrogen is carried on with the participation of hydrogen atoms acting as chain carriers. In the first place, phenanthrene is hydrogenated thermally to give 1-2-3-4 tetrahydrophenanthrene and 9-10 dihydrophenanthrene. The aliphatic ring is then hydrocracked to give different products. (Penninger et.al, 1973).

The pyrolysis of fluorene, tetralin and indane proceed in the same form in the presence of excess hydrogen. Hydrogen atoms produce the scission of the non - aromatic rings and the fragments are hydrocracked. (Penninger et.al. 1973a , Penninger et.al. , 1973b).

To summarise then, the general trends in decomposition reactions involving aromatics can be given as follows: (Fitzer et.al. , 1971).

- 1- Unsubstituted aromatics react by chemical condensation to form polynuclear aromatics. The aromatics having the anthracene configuration are the most reactive.
- 2- Alkyl - substituted aromatics are more reactive than unsubstituted aromatics, the effect being more pronounced the greater the number and the length of the alkyl groups.
- 3- The alkyl groups are in the position where the formation of new aromatic systems take place.
- 4- The highest reactivity is exhibited by aromatics containing five - numbered ring systems.

e- Surface effects during thermal reactions of hydrocarbons.

Chemical reaction processes can occur either in a gas homogen-

eous phase and in the solid gas interphase . Both types of reactions are of widespread use in practice, as catalytic (mainly surfaces) or homogeneous processes.

During the thermal reaction of hydrocarbons, there is at least the hypothetical possibility of a heterogenous process taking place on the reactor walls, simultaneously with the homogeneous, free radical reactions that occur in the gas phase. This possibility brings under discussion other hypothetical phenomena : that processes in the wall may affect the homogeneous reactions and that reactions in the gas phase may affect surface processes.

One way in which homogeneous and heterogeneous processes can interact is through the main molecular species involved in the reaction. The reactor wall may exhibit catalytic activity, which means that molecular compounds are absorbed on the surface, react and desorb, promoting increased conversion in some of the reactions. An example of this type of interaction is given by Slotboom et.al. (1974), when they report several transient effects attributed to the reactor wall and find that certain reactions involving aromatics are affected by the ageing of the reactor wall.

Another type of interaction involve free radicals and reactor surfaces. Termination reactions of the free radicals at the wall can end a chain reaction and hence will affect the homogeneous process. Hydrogen atoms, for example, would recombine preferently at the wall, for energy-transfer reasons . A rapid calculation applied to a laboratory reactor (surface to volume ratio :  $1 \text{ cm}^{-1}$  ) with the kinetic theory of ideal gases, indicates that the efficiency of collision with the wall that will give to the wall termination reactions the same importance as the homogeneous radical recombination, is of the order of  $10^{-4}$  . This result indicates that the nature of the surface

in contact with the gas could have a profound effect on the gas phase processes. Several effects of this nature were reviewed by Leathard et.al. (1970). The effect of some impurities over certain surfaces, such as oxygen and oxides, were found to disturb markedly the homogeneous reaction. The nature and conditioning of the carbon layer deposited on the reactor walls was also found to be very important. (Blackemore, et.al., 1973).

Initiation of free radicals at the reactor wall is another form of interaction between surface and gas phase that may be present during hydrocarbon pyrolysis. No results have been reported that could indicate that this effect may be significant.

The existence of parallel reaction free-radical chains in the gas and on the surface is also possible, at least hypothetically. Makarov et.al. (1969 and 1974) assume the existence of surface free radical chains that compete with gas reactions. His model was applied to methane pyrolysis in the presence of carbon particles.

One experimental method, widely used in homogeneous kinetics research can be used to identify the presence of heterogeneous effects. The technique is to change the surface to volume ratio in the reacting system. If no change in the rates are observed, it is assumed that the reaction is purely homogeneous.

The criteria seems quite logical, but fails to take into account that the system could exhibit lack of parameteric sensitivity towards the surface to volume ratio under certain circumstances, even though the surface may be playing an important role in the reaction. In the results presented by Slotboom et. al. (1974), such a failure becomes evident. A change in  $S/V$  from 3.1 to 13.3  $\text{cm}^{-1}$  did not produce any change in conversion rates and product selectivity. This experimental fact could have taken as a proof of no participation of the surface in the reaction, but a temperature history effect was observed that could only be attributed to

surface conditioning and interaction with the homogeneous reactions.

As a conclusion from this example, the lack of observable effect of S/V on the reaction does not prove the absence of heterogeneous effects. Surface effects in homogeneous reactions are poorly understood and constitute a very important field of research, with theoretical and practical implications.

#### 5- SYNTHESIS OF AROMATICS DURING THE THERMAL REACTION OF PARAFFINS AND OLEFINS.

In the pyrolysis of paraffins and olefins, a certain amount of liquid condensate or solid is formed as a byproduct of the reaction. This condensate is generally made up of benzene, toluene, and small amounts of polycyclic aromatics. This observation was made in the first pyrolysis experiments published by Berthelot. (Badger, 1965)

When pyrolyzed at 750° C in the presence of hydrogen and at the stoichiometric amount required to produce methane, a series of pure hydrocarbons gave the following yield of aromatics : (Brooks , 1967).

HYDROCARBON	H <sub>2</sub> /HC	% BENZENE	% TOLUENE
n-hexane	6	3.2	0.3
n-butane	3	3.7	0.5
neopentane	3	5.3	1.1
isobutane	4	6.1	1.3
cyclopentane	5	12.1	3.1

Percentage olefins in the initial breakdown products of hydrocarbons  
at 560° C (Thompson et.al. , 1973).

HYDROCARBON	INITIAL % OLEFINS
n-Butane	25.0
neo-pentane	33.6
iso-butane	52.0
n -hexane	58.7
cyclo-pentane	98.0
cyclo-hexane	95.0

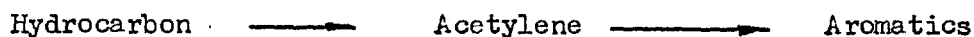
In the above experiments, the order of efficiency of production of aromatics seems to be correlated with the initial amount of olefins produced initially by the hydrocarbon in its early stages of breakdown. Apparently then, olefins and their derivatives play a role in the formation of aromatics. In the above reactions, most of the gas product was methane, with small amounts of ethane, ethylene and hydrogen. In the liquid, 2 % was diphenyls and polynuclear aromatics. The yield of aromatics was found to rise with temperature, approximately doubling in the range of 700° C to 760° C.

The total pressure seemed to have little effect on the production of aromatics. The proportion of hydrogen present in the reactant mixture, on the other side, seemed to play a decisive role in the production of aromatics. The amount of aromatics decrease with increasing the hydrogen / aromatic ratio.

a- The mechanism of thermal synthesis of aromatics

The experimental observation that acetylene pyrolysis gave benzene and other aromatics, made Berthelot suggest that the mechanism

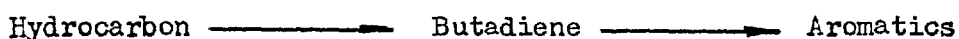
of synthesis was (Badger, 1965)



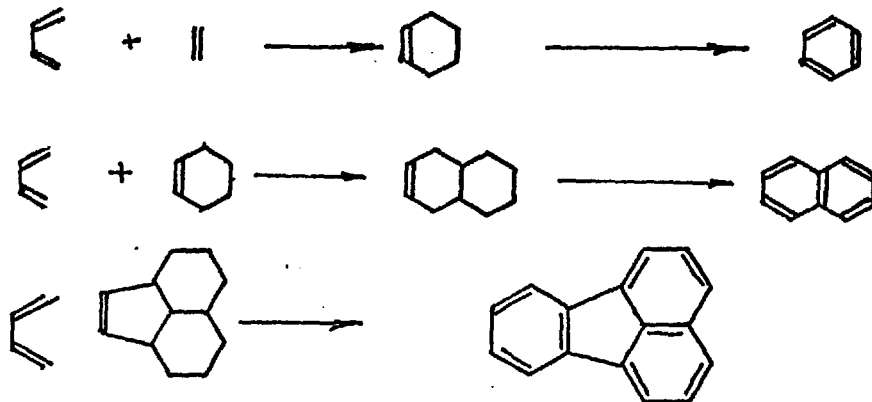
aromatics being produced via a process of polymerization of acetylene.

The idea has the inconvenience that acetylene is not an important product in pyrolysis of hydrocarbons.

The butadiene intermediate hypothesis:



originated from the observation that the pyrolysis of butadiene gave a tar with 25% benzene and 20% naphthalene. According to this hypothesis, aromatics are formed by a series of Diels - Alder reactions involving alkenes and butadiene or aromatics and butadiene: (Fitzer et al., 1971).



The pyrolysis of butadiene gave cyclohexene, cyclohexadiene and  $C_8$  aromatics at  $550^\circ C$ . (Badger, 1965). At  $700^\circ C$  complete conversion of the acyclic and alicyclic components to aromatics occurred, and benzene, toluene, and polynuclear aromatics were observed among the products.

Ethylene and propylene have been seen to react with butadiene to give the Diels - Alder adducts cyclohexene and 3 methylcyclohexene, and with increased contact time - benzene formation was observed in the

presence of ethylene and toluene formation in the presence of propylene. There is thus good evidence that a type of Diels - Adler reaction can occur at high temperatures, and it seems likely that this reaction plays a part in some pyrolysis.

Although butadiene is formed from many hydrocarbons under pyrolytic conditions, recent evidences suggest that it cannot be an important intermediate in the synthesis of polynuclear aromatics at high temperatures. For example, the the pyrolysis of a mixture of pyrene and butadiene gave a yield of benzopyrenes only very slightly greater than obtained from the pyrolysis of butadiene itself.

At higher temperatures, the relative energies for the diene addition and for radical addition suggests that synthesis proceeds by radical and not by molecular addition. Attention should be given, amongst others, to the hypothesis that the pyrolysis of hydrocarbons can give  $C_3$  fragments and that the synthesis of aromatic hydrocarbons proceeds from these units. It was suggested, for example, that the thermal abstraction of H from allene would give a stabilized carbene: (Badger , 1965 )



and the dimerisation of this fragment is expected to give benzene.

Although this last example has not gained popularity, it seems more probable that the synthesis of aromatics takes place via a free-radical mechanism than molecular addition. This applies more to the higher temperature regimes of pyrolysis, in which, although the mechanism is not known, the abundance and diversity of existing free radicals makes one assume that the fast build up of higher molecular weight aromatics takes place via free-radicals.

Some attention should also be paid to the possibility that walls could act as catalyst for aromatization reactions. It is known that reactor walls can play a role in increasing the amount of polynuc-

-lear aromatics (Brook, 1967), although the effect decreases with time due to wall conditioning, probably by coverage with carbon. However the real role of the steady state or aged surface in the production of aromatics is unknown.

6- THE FORMATION OF CARBON DURING THE THERMAL REACTIONS  
OF HYDROCARBONS.

The study of the mechanisms that produce the formation of carbonaceous deposits on the reactor walls, or the formation of gas phase carbon particles, could be divided to consider the cases where a transition metal is or is not involved as a catalyst. The thermodynamic principles involved in the formation of carbon from pyrolyzing hydrocarbons (either catalytic or non catalytic) were described by Fitzer et.al. , (1971) and will not be discussed here.

a- The formation of carbon without the participation of  
catalytic metals

When dealing with the mechanism of carbon formation that is not promoted by the presence of a metal, there could be a tendency to call it "non - catalytic carbon" or "homogeneous produced carbon", but a second consideration would prove that the idea associated with both names is wrong. At temperatures and conditions of industrial pyrolysis and hydrogenolysis of hydrocarbons, the weak catalytic activity of the carbon surface may play an important role. Thus for example Tesner (1973) has proposed a Langmuir type of kinetics that allows one to explain the inhibiting effect of hydrogen on carbon deposition from methane on soot particles. This fact is important if it is considered that in pyrolysis and hydrogasification, all the surfaces in contact with the gas will be covered with carbon after a short period of time, and that the nature of the deposit changes with temperature and composition in the gas phase.



From the review of Palmer et.al. (1965 ) it is possible to consider the following qualitative chemical models of carbon formation:

- 1- The  $C_2$  theory: This suggests that solid carbon results from the polymerization of  $C_2$ .
- 2- The atomic C theory : This suggests that monoatomic carbon may possibly be a significant species in nucleation.
- 3- The  $C_3$  theory : This supports the idea that solid carbon in flames arises by condensation of carbon vapor, the major component of which is believed to be  $C_3$  .
- 4- The acetylene theory (Prado , 1972) : Advanced by Berthelot in 1866. The essence of the theory is that carbon particles are formed from acetylene by simultaneous polymerization and dehydrogenation.
- 5- Hydrocarbon polymerization theories: These theories assume that fuel undergo a polymerization process that ends in carbon. Some assume that liquid polymers or polymers of high molecular weight are formed as intermediates. Some suspicion exists that polycyclic and polynuclear aromatics could be intermediates in the path towards carbon.
- 6- The surface decomposition theory: Tesner (1973) is the principal advocate of a theory in which carbon is formed through a surface chemical reaction of the original hydrocarbon on a carbon surface.
- 7- Condensation theory: This theory has been revived recently by Lahaye et.al. (1974) in a model for the formation of carbon blacks in a tubular reactor. According to their model, the initial hydrocarbon is transformed by a gas phase reaction into macromolecules. The partial pressure of the macromolecules increases with reaction time until the supersaturation is high

enough to induce condensation of the macromolecules into droplets. The formation of the liquid nuclei eliminates the supersaturation and the formation of additional liquid nuclei becomes impossible. The macromolecules which continue to be formed maintain the nuclei growth. The liquid droplets are further pyrolyzed into a solid material.

The results of the mathematical model seem to agree with the experimental results.

Direct evidence against the theory of droplets formation has been presented recently. Graham et.al. (1975) studied the formation of soot aerosols in a shock tube from benzene and other aromatics.

The system was provided with instrumentation able to measure the concentration of aromatics, the amount of drops or particles formed (by light scattering) and the absorption at  $3.39\mu\text{m}$  produced by the formation of solid carbon. They have found that the appearance of the aerosol is simultaneous with the onset of absorption in the  $3.39\mu\text{m}$  produced by solid carbon, so no drops of condensate appeared before the formation of solid carbon.

The success of the condensation theory is that it allows an explanation of most of the experimental facts in soot nucleation and the effect of the operation variables on the particles formed. The fact that it has been proved wrong indicates only that the basic phenomena is not homogeneous physical nucleation and condensation, but must be a very similar phenomena in its mathematical formulation. In this sense, a chemical nucleation mechanism, as proposed by Tesner (1973), is worth considering.

The intermediates that, through the yet unknown mechanism, finally form the carbon particles or deposit, are still the object of controversy. Experiments with carbon formation in flames tend to support the idea that acetylene is the intermediate that polymerises (forming

polyacetylenes) which grow until the particle is formed. (Palmer et.al., 1965). Research in pyrolysis and thermal hydrogenation of hydrocarbons tends to support the feeling that aromatics and polycyclic aromatics are involved in some way in the formation of carbon. (Fitzer , et.al. ,1971; Virks et.al. ,1974, Thompson et.al. , 1973 and Bokros , 1969) It is impossible to rule out the possibility that several different mechanisms could be operative in different conditions.

With respect to the deposition of carbon on surfaces, very little has been reported that could give a quantitative description of the phenomena and less to explain the mechanism. The treatment of Tesner (1973) of the deposition of carbon over particles assume a surface reaction of the parent hydrocarbon, which allows him to explain the inhibition produced by hydrogen, but neglects any effect of the homogeneous pyrolytic reactions. Other models, reviewed by Bokros (1969), correlate the conditions of deposition over particles in a fluid bed with the physical properties of the carbons, but do not try to explain the mechanism of deposition.

#### b- Metal-catalysed carbon formation

Metals such as iron, cobalt and nickel, exhibit a marked catalytic effect towards carbon formation and tend to affect the nature of the carbon formed. Early research on the subject was concerned with the formation of carbon from carbon monoxide on iron, related to the Fisher - Tropsch process. Recently, the use of metal catalysts in reforming and steam reforming processes and the interest in avoiding carbon deposition on the walls of reactors and heat exchanges has directed more attention to the study of carbon deposition from hydrocarbons on metals. (Figueiredo (1975).

Detailed reviews of the bibliography in catalytic carbon formation have been presented recently by Lobo (1971), Derbyshire (1974),

Figueiredo (1975), and Rostrup - Nielsen (1975) which make unnecessary<sup>52</sup> a detailed review and discussion here. Only the main conclusions and a few particular aspects will be considered here.

According to Figueiredo (1975) the literature on catalytic carbon formation reveals several common features in different systems, which are given below:

- 1- At low temperatures ( $350 - 550^{\circ} \text{C}$ ) rates of deposition remain constant for considerable periods of time.
- 2- The presence of metals in carbon deposits has been reported for deposition from hydrocarbons and  $\text{CO}$ .
- 3- The presence of carbides has been reported under similar conditions.
- 4- A maximum rate of carbon formation has been observed at temperatures in the region  $550 - 600^{\circ} \text{C}$ , and approximately zero order kinetics have been determined for temperatures below the maximum.
- 5- Hydrogen has been generally found to increase the rates of deposition.
- 6- The rate determining step has been associated with a solid-state diffusion mechanism, both at low temperatures ( $< 350^{\circ} \text{C}$ ) where carbides are the final solid products, and at higher temperatures, where carbon is formed ( $350 - 550^{\circ} \text{C}$ ).

Lobo (1971) studied the formation of carbon from light hydrocarbons, in the presence and absence of hydrogen over foils of Fe, Co, Ni, Pt, Cu, Ag and Au for the range of temperatures  $300 - 800^{\circ} \text{C}$ . The study covered both the kinetics of deposition and the structure and properties of the deposits formed. For nickel a complex temperature dependence was observed for the rates of deposition, with a maximum at  $500 - 550^{\circ} \text{C}$  and a minimum at  $600 - 650^{\circ} \text{C}$ , defining three regions in the Arrhenius plot. In the low temperature region the rates of deposition were found to be independent of the nature and partial pressure of the hydrocarbons and exhibited activation energies in the range of 29-34 Kcal/mole. At temperatures

above 600 - 650° C , the carbon forming mechanism has been attributed to the homogeneous pyrolysis of the hydrocarbons, while in the intermediate region negative activation energies were observed and the rate of the process was found to depend on the partial pressures of the hydrocarbon and hydrogen.

Lobo et.al. (1972) proposed the following mechanism of carbon formation on nickel foils:

The absorption of olefins on the surface is followed by dehydrogenation and hydrogenolysis reactions to produce carbon atoms, which migrate through the nickel to active growth centres.. Disruption of the nickel takes place and crystallites are carried with the growing carbon and catalyse further carbon production. The rate determining step at low temperatures is considered to be the diffusion of carbon atoms through the nickel.

Figueiredo (1975) studied carbon formation from propylene on nickel catalysts and nickel foils, under conditions of pyrolysis and steam reforming conditions. At low temperatures (below 500° C), the specific rate of carbon deposition was found to be the same over both foils and supported catalysts. Nickel crystallites were found to be carried with the growing carbon and the kinetic results have been explained in terms of the diffusion of carbon through nickel being rate - determining.

Carbon deposition over substrates of nickel, cobalt and iron foils at higher temperatures (500 -1000° C) was studied by Derbyshire (1974). A characteristic of the rate data obtained was the coincidence of laminar graphite formation with a particular type of carbon uptake - time behaviour, where the rate of growth falls to zero after a significant reaction time. In every case, the final weight uptake correspond to the solubility of carbon in nickel at the reaction temperature. The formation of laminar graphite on cobalt and nickel was explained through a dissolution - reprecipitation mechanism.

## 7- OBJECTIVES OF THE PRESENT RESEARCH

The object of this research was to try to elucidate the nature and mechanism of some processes that take place in industrial pyrolysis and thermal hydrogasification of hydrocarbons. The principal interest was focused on the processes that led to the formation of carbon on the internal surfaces of the reactors. The areas of knowledge reviewed in this introduction reveal the insufficient understanding of some key steps in the chain of events taking place during the thermal reaction of hydrocarbons. Some of them are listed below:

- a- Incomplete understanding of the effect of hydrogen on the homogeneous free-radical pyrolysis of hydrocarbons.
- b- Incomplete knowledge of the mechanism of synthesis of aromatics during the thermal reaction of other hydrocarbons.
- c- Lack of complete information on the kinetics and the effect of the operational variables on the amount and nature of aromatics formed.
- d- Insufficient knowledge about the mechanism of carbon deposition on non - catalytic surfaces, the chemical intermediates that produce the deposition, how the intermediates are formed and what is the effect of the operational variables on the deposition.
- e- Lack of information on the deposition of carbon on catalytic surfaces under high conversion pyrolysis conditions. Insufficient information on the effect of reactor wall nature on the homogeneous pyrolysis, aromatic synthesis and carbon deposition over different surfaces. Insufficient understanding of the effect of the surface to volume ratio in the reactor over the different processes taking place.

During the present work, attention was paid to those aspects where the understanding is insufficient and experiments

were performed to elucidate some of these problems.

The experimental system was designed to provide maximum versatility and instrumented to obtain the chemical composition of the reaction products over a wide range, covering compounds from methane to 3-4 benzopyrene by gas chromatography. The kinetic study of carbon deposition on surfaces suspended inside the tubular flow reactor was performed with the aid of a microbalance, which offered a continuous register of the changes in weight of the surface.

The experimental work was performed with the system operating at atmospheric pressure. This condition is different from the high pressure used generally in thermal hydrogasification or in industrial thermal cracking, and the conclusions from this work should be extrapolated to industrial conditions having this fact in mind. The basic nature of the phenomena involved, however, is expected to remain the same.

CHAPTER IIEXPERIMENTAL

1- INTRODUCTION	.....	57
2- EXPERIMENTAL SYSTEM BASED ON A JET STIRRED REACTOR	.....	57
a- Experimental procedure and variables studied.	.....	62
3- EXPERIMENTAL SYSTEM BASED ON THE TUBULAR MICROBALANCE REACTOR.	.....	65
a- The tubular microbalance reactor	.....	65
b- Furnaces and temperature control	.....	70
c- The gas analyzer	.....	75
d- Liquid collection and analysis	.....	76
e- Materials	.....	78
f- Operation technique	.....	82
g- Precautions taken with the manipulation of polycyclic aromatics.	.....	85
h- Experimental operation conditions and variables studied.		85



## 1- Introduction

During the present research, attention has been paid to the features of homogeneous processes taking place in the gas phase, as well as to heterogeneous processes taking place on the surfaces that are in contact with the gas. Two experimental systems were used during the study. The first in which the main interest was to follow the homogeneous gas reactions, and the second in which the experimentation was directed at surface processes and aromatic hydrocarbons formation: This latter was carried over a wide range of operation conditions. Both sets of equipment are described below.

## 2- Experimental system based on a jet-stirred reactor.

The equipment represented in figure II-1 was used to obtain kinetic information on the thermal reactions of ethane at high conversions. It is based on a silica jet-stirred reactor, a system to control the flow of gases and temperature, and an analyzer to determine the composition of the gas streams.

Ethane, hydrogen, nitrogen and oxygen were obtained from head pressure regulation valves at 10 psig. Ethane and hydrogen were used as reactants, oxygen to burn off the carbon layer deposited after a run and nitrogen was used to flush the system before and after the admission of oxygen. The gas circuit was arranged so that each stream could be sent to a bubble flowmeter (see fig. II-1).

Once the flow was measured, the corresponding rotameter was used to control the constancy of the stream. A mercury manometer was connected to measure the pressure drop in the reactor jet. This pressure was always

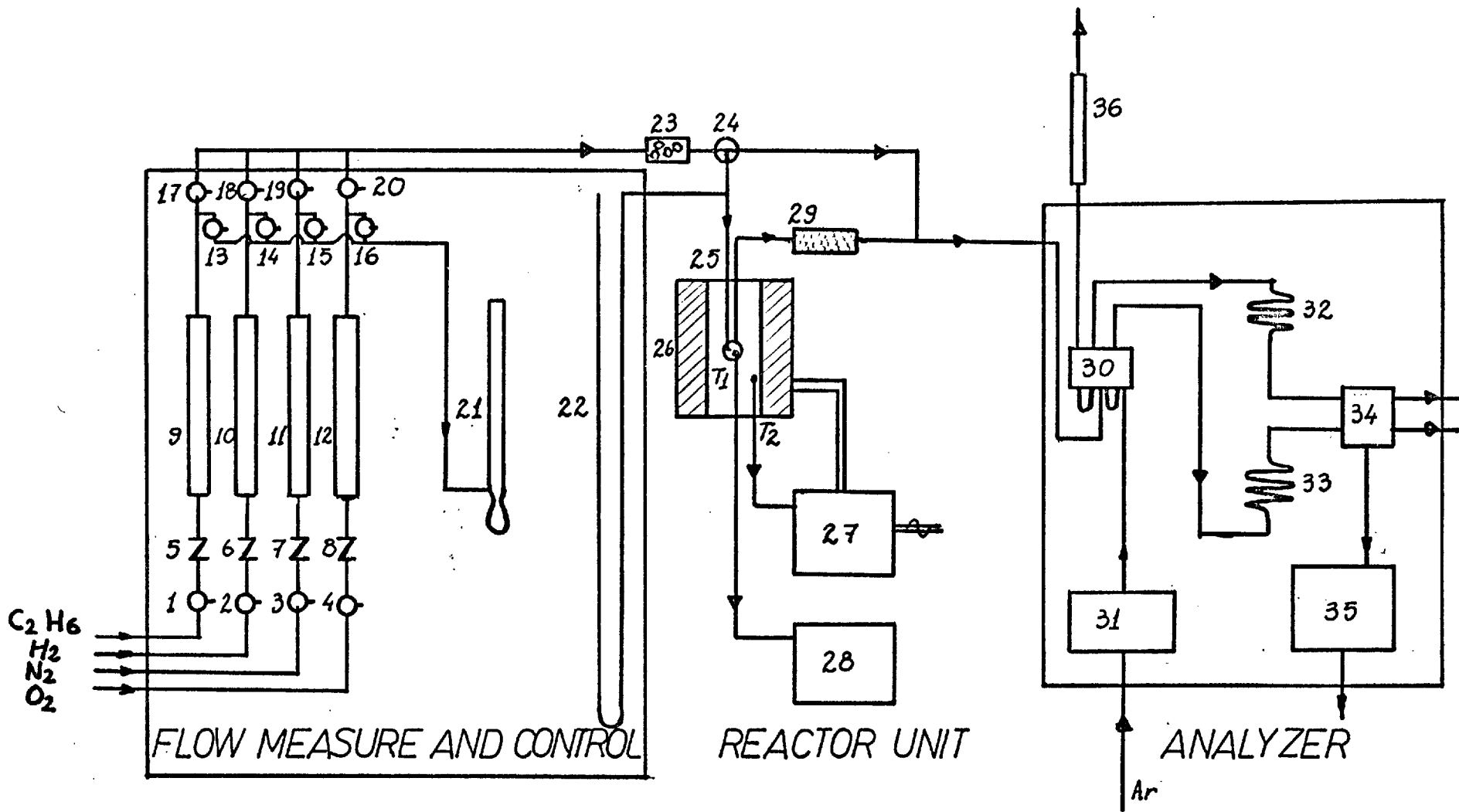


FIGURE II-1. EXPERIMENTAL EQUIPMENT FOR ETHANE PYROLYSIS  
IN A JET STIRRED REACTOR

References of Figure II-1

- 1,2,3,4      Flow interruption toggle valves.
- 5,6,7,8      Precision flow regulating valves.
- 9,10,11,12      Rotameter type flow-meters.
- 13,14,15,16      Toggle valves to send any flow to the  
17,18,19,20      gas bubble flowmeter.
- 21      Gas bubble flowmeter.
- 22      Differential manometer to measure reactor pressure.
- 23      Beads-type gas mixer.
- 24      Three ways valve to send input feed to analyzer.
- 25      Jet-stirred silica reactor.
- 26      Heating furnace.
- 27      Furnace P.I.D. Controller.
- 28      Reactor temperature measuring unit.
- T1      Reactor thermocouple.
- T2      Furnace thermocouple.
- 29      Tars filter.
- 30      Two way pneumatic sample valve.
- 31      Flow regulator
- 32      Silica gel column.
- 33      Activated alumina column.
- 34      Micro katharometer detector.
- 35      Amplifer, recorder and integration unit.

less than 12 mmHg.

The small jet-stirred tank reactor was designed according to Bush (1969) and a diagram is shown in figure II-2. The volume of the reactor was measured by weighing when filled with distilled water and the value was found to be 6.63 cm.<sup>3</sup>. The reactor was constructed in silica to support the high reaction temperatures of pyrolysis. A thin chromel-alumel thermocouple was placed in the reactor to measure the temperature of the gaseous mixture.

The reactor was placed in a furnace whose temperature was measured with a chromel-alumel thermocouple and controlled to  $\pm 1^{\circ}$  C with an electronic proportional-integral-derivative electric heating controller. The reaction temperature was measured to  $\pm 1^{\circ}$  C with a potentiometer. (See figure II-1).

Once the reacted stream left the reactor it was filtered through a glass-wool packing to remove the aromatic tars that were formed as secondary products of the reaction, and was sent to the analyzer unit.

The unit has two gas chromatographic columns (see fig. II-1). The external column operates at room temperature and was a stainless steel tube of 2 m. x  $\frac{1}{8}$ " filled with activated silica gel. The other is an internal column placed in the oven of a "PYE panchromatograph" operated at 125<sup>o</sup> C. It consisted of a stainless steel tube of 3 m. x  $\frac{1}{8}$ ", filled with activated alumina. The sample valve was a pneumatic 10 port type valve that was installed in the same oven as the internal column to operate also at 125<sup>o</sup> C and was suitable for sampling condensable streams. The valve was operated to deliver one sample to one column and, when the analysis was finished, a second sample was sent to the other column for analysis. The silica gel column was used to separate nitrogen, hydrogen and methane and the activated alumina column for the remaining components. The detector was a Servomex micro katharometer operated at 125<sup>o</sup> C,

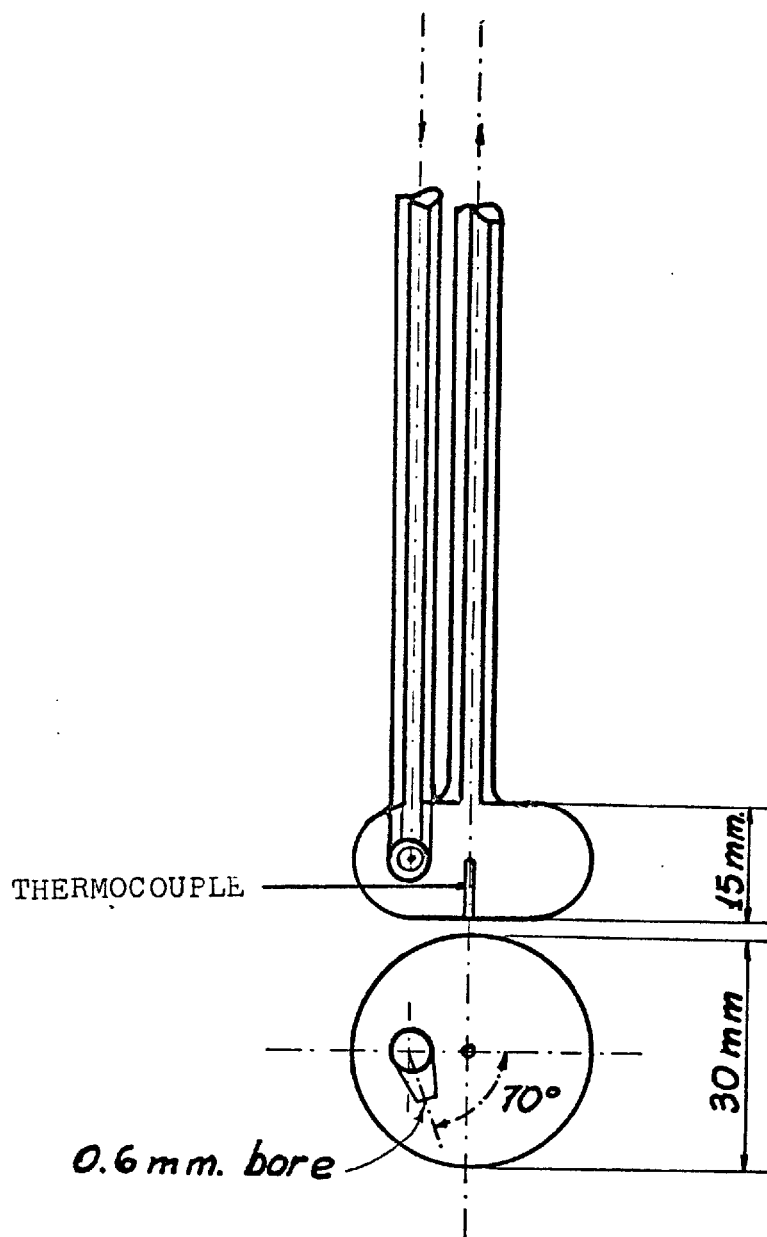


FIGURE II-2

## THE JET STIRRED TANK REACTOR

whose signal was amplified, recorded and integrated to obtain the composition of each sample. A flow of 25 ml. min<sup>-1</sup> of argon was provided by a PYE gas flow regulation equipment.

The analyzer was calibrated to operate with nitrogen, hydrogen, methane (silica gel column), ethane, ethylene, acetylene, propane, propylene and butane (alumina column). The calibration was done by injection of several volumes of pure gases onto the corresponding column and integrating the area of the resulting peaks. The information was correlated by least squares polynomial regression to fit the equation:

$$\text{Volume (ml)} = a_1x + a_2x^2 + a_3x^3 + a_4x^4 + a_5x^5 \quad (\text{IV.1})$$

where x is defined as attenuation times area of peak in integrator counts units. The parameters obtained in the calibration are listed in Table II.1. A computer program was written using these parameters to speed up the calculations and to give the composition of gaseous streams in molar fractions.

a- Experimental procedure and variables studied

The reactor was heated to operation temperature while flushing with nitrogen. Reactant flows were measured with the bubble flowmeter and then admitted to the reactor. The temperature was adjusted then to give the desired temperature inside the reactor. After 6-10 minutes (the time in which the system was assumed to reach steady state) a duplicate analysis of the products was done. A measure of the outlet flow was taken to check the carbon balance in the system. When the run was finished, the carbon layer in the reactor was burned off by passing oxygen through the reactor at 800° C.

TABLE II.1

Calibration parameters for different gases

<u>Compound</u>	<u>a<sub>1</sub></u>	<u>a<sub>2</sub></u>	<u>a<sub>3</sub></u>	<u>a<sub>4</sub></u>	<u>a<sub>5</sub></u>
Nitrogen	$4.798 \times 10^{-5}$	0.0	0.0	0.0	0.0
Hydrogen	$-5.913 \times 10^{-5}$	$5.077 \times 10^{-6}$	$1.257 \times 10^{-11}$	$2.165 \times 10^{-16}$	$-6.723 \times 10^{-22}$
Methane	$1.758 \times 10^{-5}$	0.0	0.0	0.0	0.0
Ethane	$1.999 \times 10^{-5}$	0.0	0.0	0.0	0.0
Ethylene	$2.203 \times 10^{-5}$	0.0	0.0	0.0	0.0
Acetylene	$1.835 \times 10^{-5}$	0.0	0.0	0.0	0.0
Propane	$2.262 \times 10^{-5}$	0.0	0.0	0.0	0.0
Propylene	$2.312 \times 10^{-5}$	0.0	0.0	0.0	0.0
Butane	$2.227 \times 10^{-5}$	0.0	0.0	0.0	0.0

TABLE II.2

Spectrum of variables studied with the jet-stirred reactor

<u>Temperature</u>	<u><math>\tau_1</math> (sec)</u>	<u><math>\tau_2</math> (sec)</u>	<u><math>\tau_3</math> (sec)</u>	<u><math>\tau_4</math> (sec)</u>	<u>Feed Ethane</u>	<u>Feed Hydrogen</u>
700° C	1.90	3.04	5.07	12.19	1.0	0.0
750° C	0.85	2.78	7.58	11.02	1.0	0.0
800° C	0.80	2.68	7.92	11.83	1.0	0.0
830° C	0.80	2.62	7.10	10.43	1.0	0.0
700° C	0.91	2.54	6.30	8.72	0.548	0.451
750° C	0.86	2.42	6.01	8.32	0.548	0.451
800° C	0.82	2.31	5.73	7.93	0.548	0.451
850° C	0.79	2.21	5.47	7.57	0.548	0.451
900° C	0.75	2.11	5.23	7.24	0.548	0.451
950° C	0.72	2.03	5.03	6.96	0.548	0.451



The experimental conditions were selected to cover the range of industrial interest in temperatures and inlet residence times, but working at atmospheric pressure. Conditions where no hydrogen was included in the feed tended to give more carbon deposition and to form more tars than the conditions where hydrogen was one of the reactants.

Table II-2 presents the set of variables covered during the study with the jet-stirred reactor.

### 3- Experimental system based on the tubular microbalance reactor

The equipment represented in figure II-3 was designed to study the rates of carbon deposition over sample surfaces, and at the same time to obtain the composition of major gas products and aromatics produced during the thermal reactions of n-butane. The system was based on a silica cylindrical tubular reactor coupled to a microbalance. Gases were metered and the flows controlled by a gas controlling board, and then delivered to the base of the tubular reactor. A sample surface, in the shape of a rectangular foil, hung from one arm of a microbalance, which sensed the changes in weight of the sample produced by deposition of carbonaceous material from the reacting gas. The stream of products emerging from the reactor went either to a low temperature trap (where the aromatic tars were condensed) or through a tar filter into two gas sample valves that allowed the on-line chromatographic analysis of the gas stream.

During the runs, a stream of nitrogen was passed through the microbalance head to avoid the possibility of contamination of the head with aromatic tars. The efficiency of the flushing stream is improved by a flow director, as represented in figure II-4.

#### a- The tubular microbalance reactor.

When considering a chemical reaction where processes are

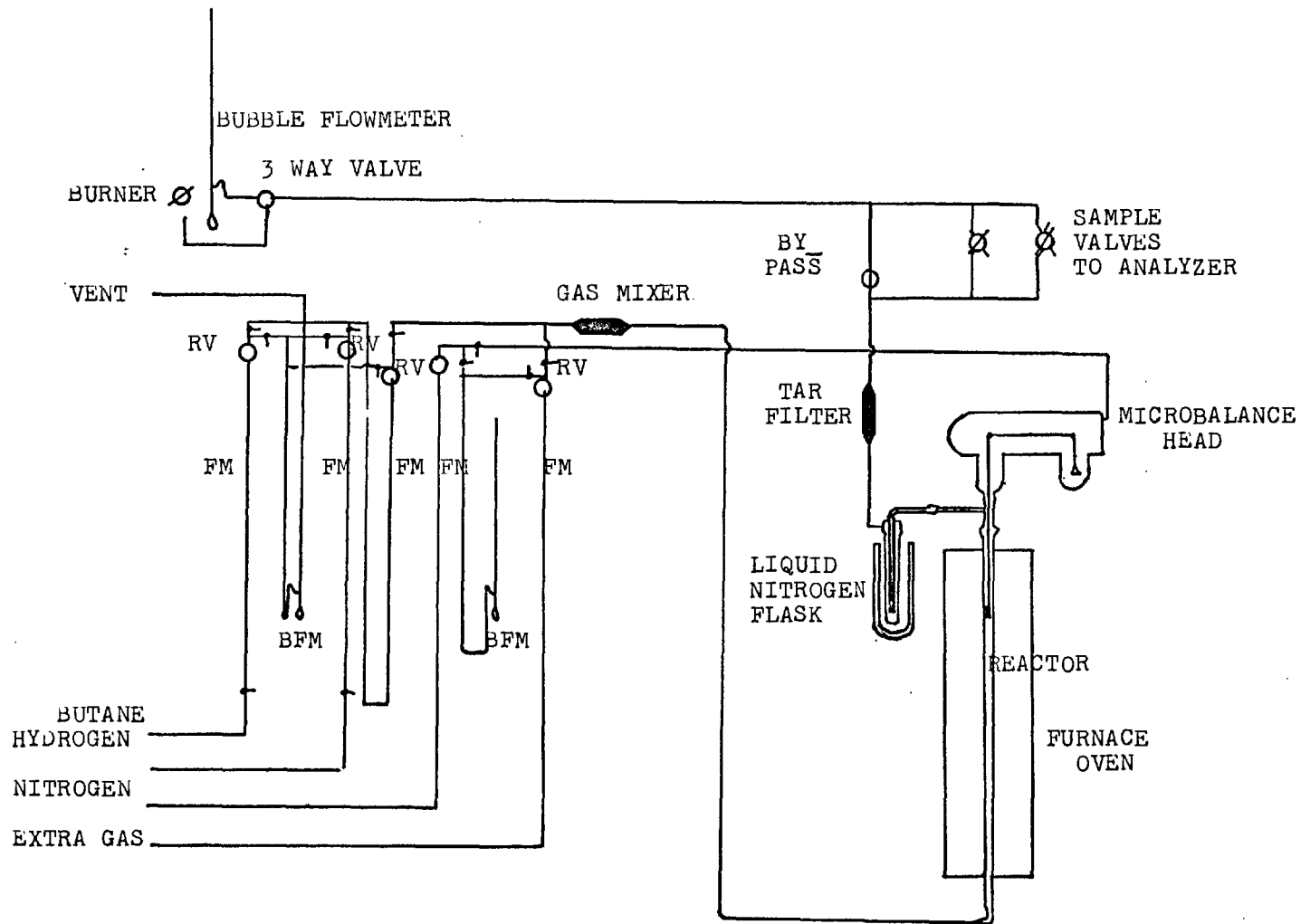


FIGURE II-3. EXPERIMENTAL SYSTEM FOR BUTANE PYROLYSIS IN A TUBULAR FLOW MICROBALANCE REACTOR.

RV: regulation valve. FM: Flow meter. BFM: Bubble flow meter

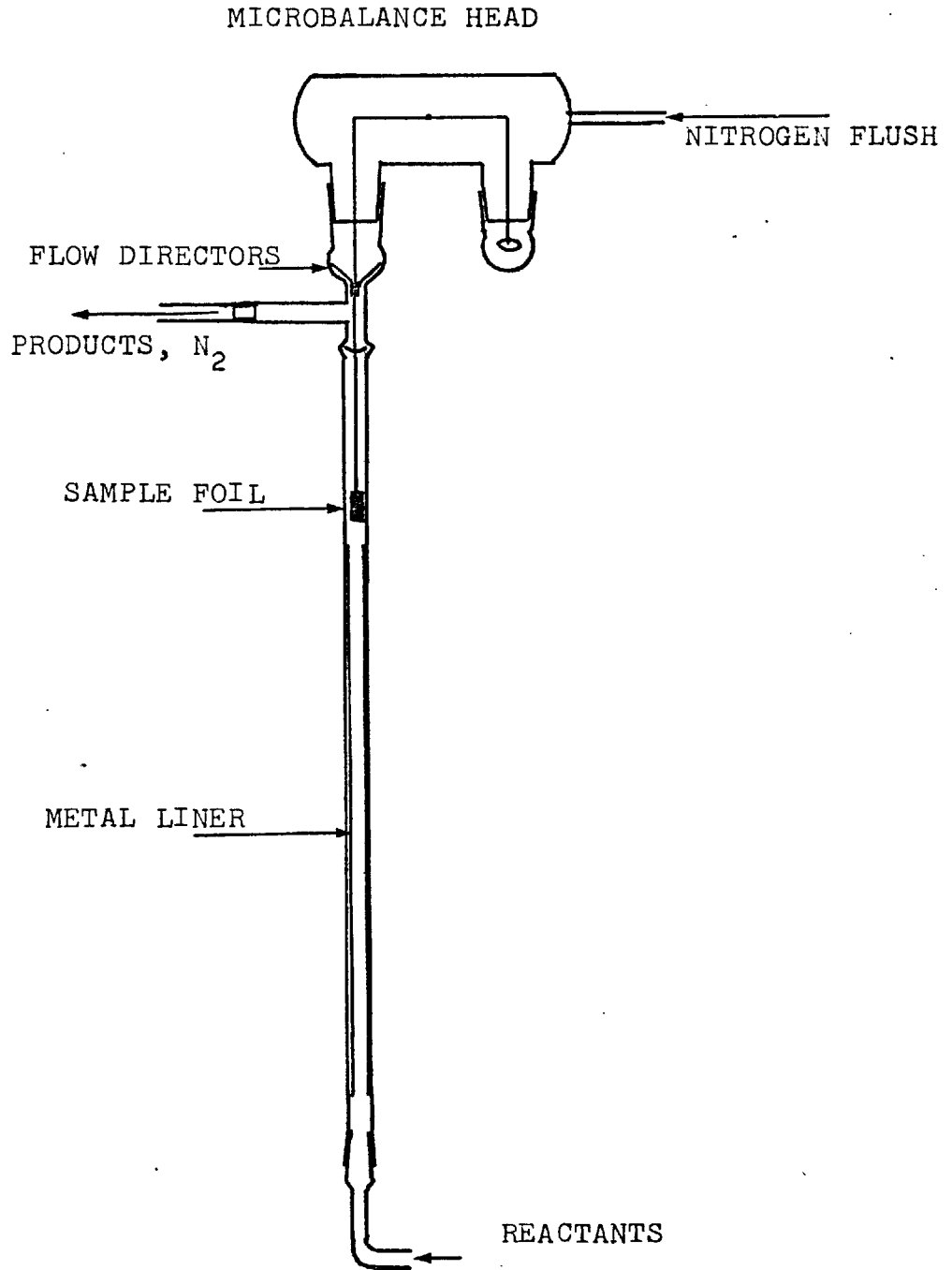


FIGURE II-4. THE TUBULAR FLOW MICROBALANCE REACTOR.

occurring both in the gas and on the surfaces in contact with the gas, several aspects have to be taken into account in the design of the experimental system. In the first place, the features of the homogeneous reaction should be perfectly defined. In flow systems, the temperature distribution and the flow pattern should be known, and it is desirable that the reactor should operate as near as possible to the behaviour of an ideal system (either a differential, a perfectly stirred or a tubular plug flow reactor ).

The selection of a tubular flow reactor offered several advantages. A sample foil could be positioned inside the reactor to simulate a surface in contact with the reacting gas. The changes in weight on the sample could be sensed continuously with the aid of a microbalance: Being constructed in silica, the internal surfaces could be lined with metal foils to simulate a metal reactor, and the reactor could be packed with thin wire mesh to produce changes in the surface to volume ratio. In a complete series of experiments, each half of the reactor could be kept at different temperatures to simulate a "reactor" followed by a "condenser" and the sample foil used to measure changes in weight inside either zone.

The wide versatility of the tubular-microbalance reactor brought, however, some disadvantages. The presence of a hanging sample foil and the need to put liners and packings inside the reactor did not allow the measurement of temperature inside the reactor, and the temperature was measured at the external tube wall. The tube had to be straight and the internal diameter large enough to allow the presence of the sample foil and liners. This geometry leads to the need to use furnaces that presented deviations from isothermal.

In this research, versatility was considered essential and the tubular-microbalance reactor was adopted in spite of these dis-

advantages. In conditions where some limitations in possibilities could be accepted. The jet-stirred microbalance reactor, as used by Turner (1976), reduce these disadvantages considerably.

The reactor was made from a silica tube of 1.09 cm internal diameter and 45 cm long. The upper part ended in a silica ball ground joint that allowed the alignment of the sample foil inside the reactor. The lower end was provided with a cone ground joint that connected the reactor with the reactants feed line.

A C.I. Electronics MK 2B vacuum microbalance head was used in a pyrex glass vacuum bottle with conical glass connections. The balance head was connected to the control unit and to a Honeywell recorder ( 1 mV full scale) via a matching unit (provided by C.I. Electronics ); damping and range extending facilities were provided in the matching unit.

The reactor was connected to the reactor head through a pyrex glass T adaptor, as shown in figure II-4. The adaptor had a cone joint to connect to the balance head and a ground ball joint to fit with the silica reactor joint. A third arm, provided with a cone joint, was used to let the exit gases out of the system. A flow director was installed, to protect the microbalance head from contamination with tarry liquid products, this also improved the efficiency of nitrogen flushing.

Sample foils were cut into rectangular pieces of 0.7 x 2 cm or 0.5 x 2 cm. A little hole was made near one edge and the foil was hung from the microbalance arm with the aid of two pieces of hooked silica fibre.

Metal liners were prepared by cutting a foil to a size of 5 x 15 cm. This was scrolled to a diameter of 1 cm and fitted into the reactor with a support of silica wool. During runs of the series III , two pieces were inserted into the reactor, giving a liner of total length

30 cm.

The surface to volume ratio in the reactor was modified by introducing a copper wire screen, scrolled to form a cylinder of the same diameter as the reactor. The geometrical dimensions of the wire mesh were : wire diameter : 0.02 cm, 15 mesh  $\text{cm}^{-1}$ , surface area (calculated) : 1.88  $\text{cm}^2$  per square centimeter cross section of screen, maximum surface area when 30 cm of screen scroll were inside the reactor : 565  $\text{cm}^2$ . The surface to volume ratio inside the reactor was varied from 4  $\text{cm}^{-1}$  (empty tube) to 18.8  $\text{cm}^{-1}$  by the introduction of different lengths of the screen roll.

b- Furnaces and temperature control

Two sets of furnace arrangements were used to heat the reactor in the different series of experiments. Series I and II (see later) were performed with a two section furnace. Each section could be set at different temperatures and controlled independently by separate controllers to within  $\pm 1^\circ \text{C}$ . Most of the experiments in series I and II were performed with the arrangement shown in figure II-5. The lower section was set at  $400^\circ \text{C}$  and used to preheat the reactants. The upper section was used as the reaction furnace. The metal sample foil was positioned 30 mm. from the top of the upper section.

In the "reactor-condenser" series of experiments, the lower section was used as the reaction furnace, and set to a constant  $900^\circ \text{C}$ . The upper section simulated a condenser and the temperature was varied to study the deposition of high boiling point aromatics on a sample foil. (See fig. II-6).

During the third series of experiments another furnace was also used. It was designed and built with the purpose of improving the temperature distribution along the axis of the reactor. The sample

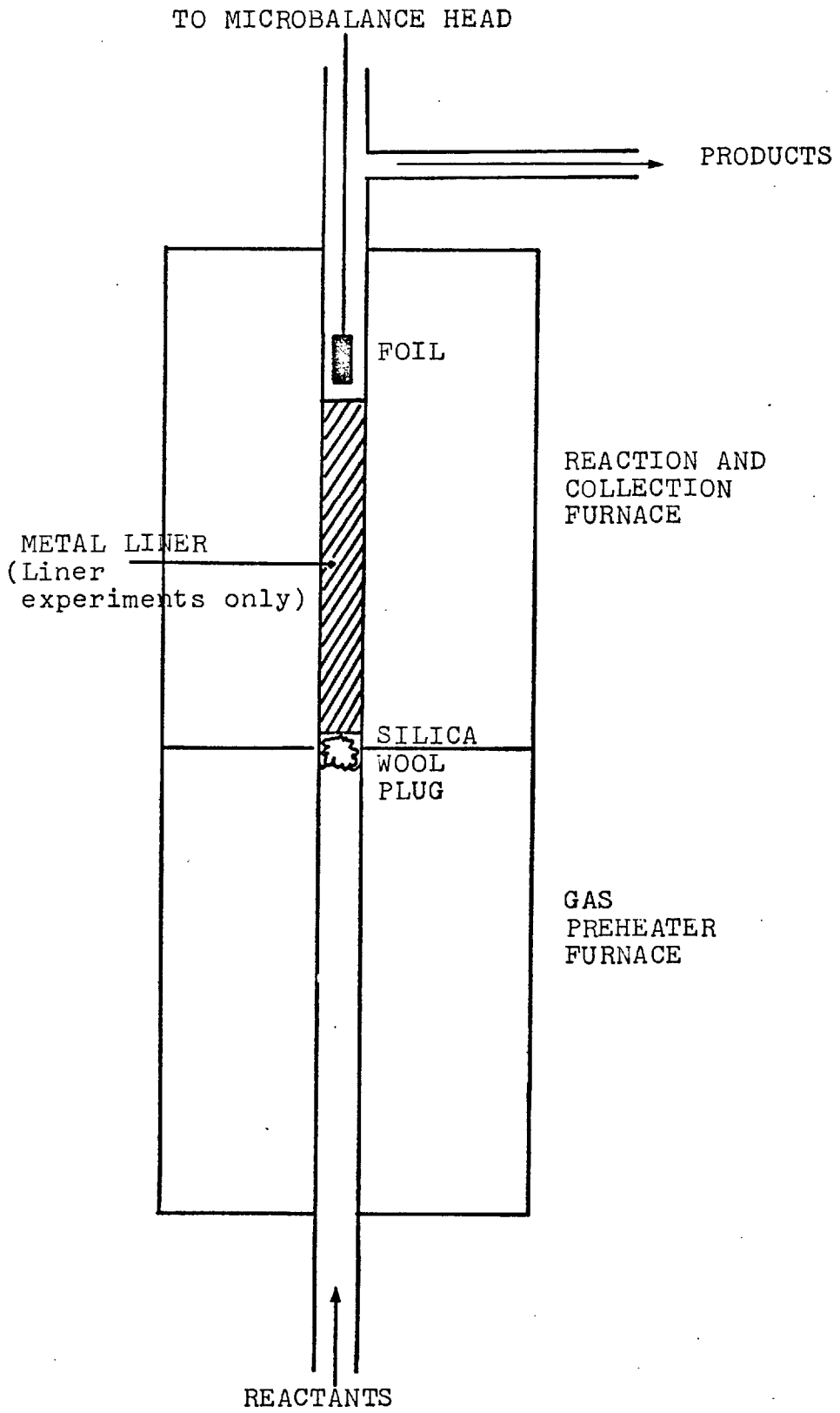


FIGURE II-5. SCHEME OF PREHEATER- REACTOR.

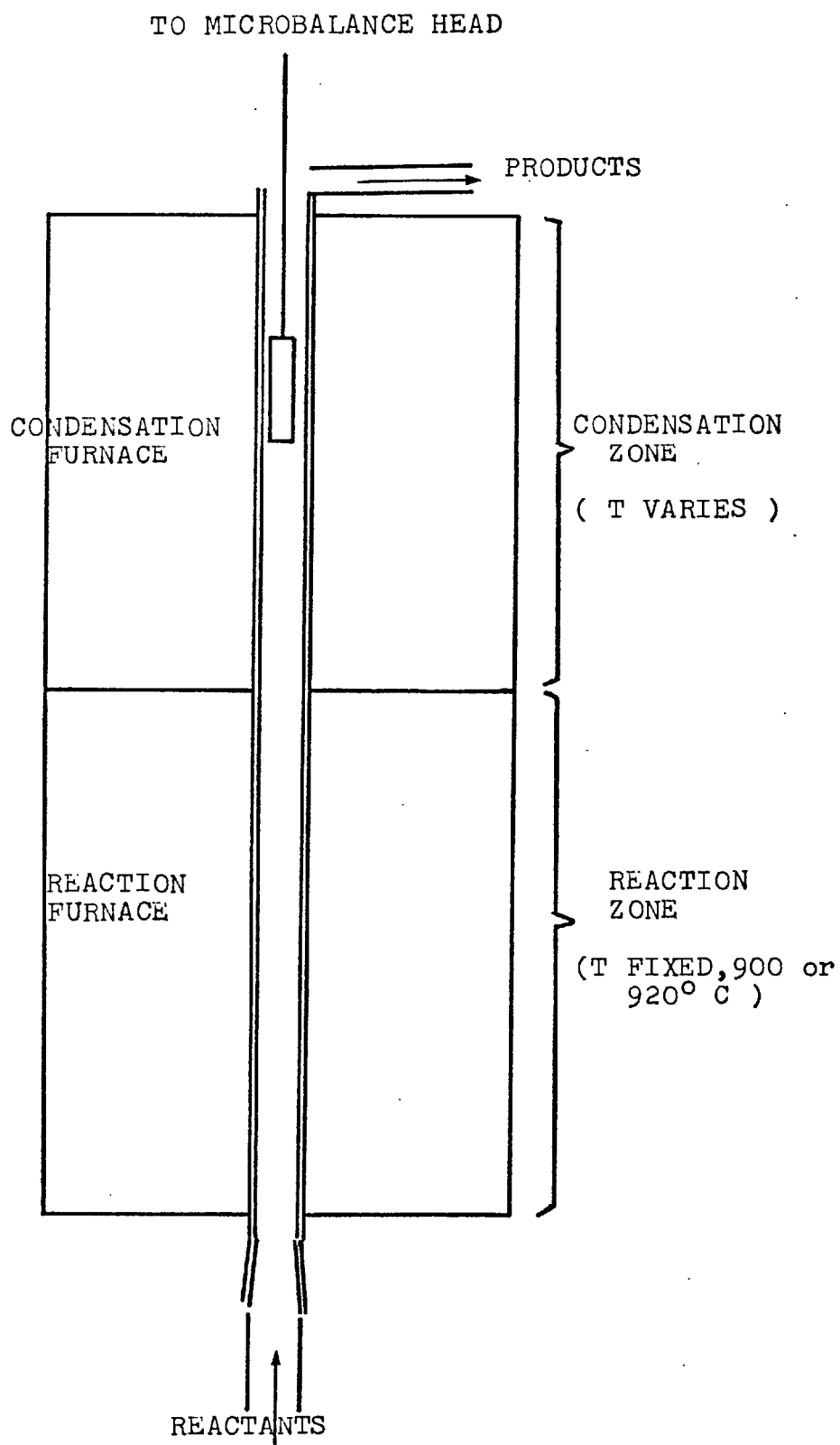


FIGURE II-6. SCHEME OF REACTOR- CONDENSER.



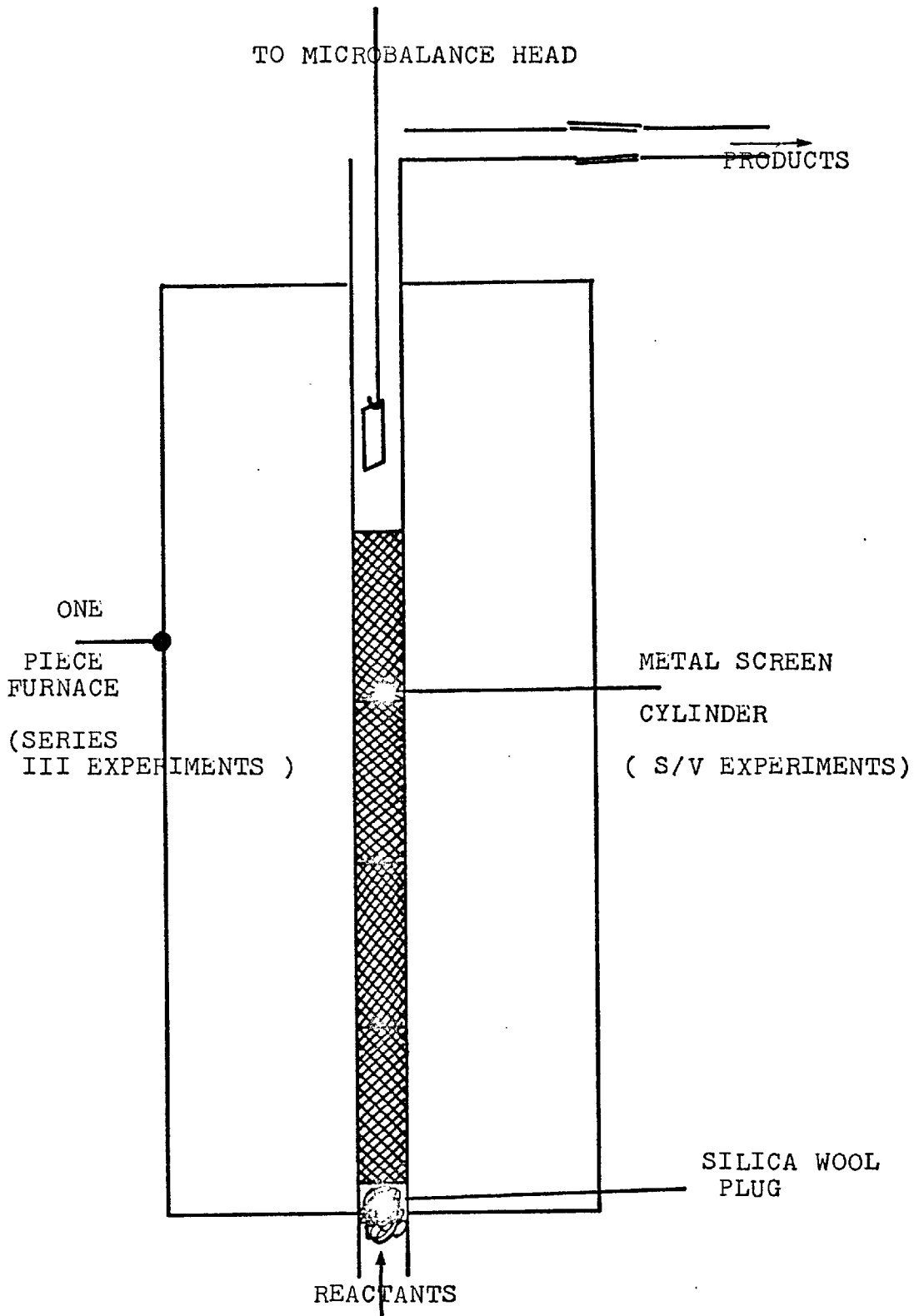


FIGURE II-7. ONE PIECE FURNACE ARRANGEMENT.

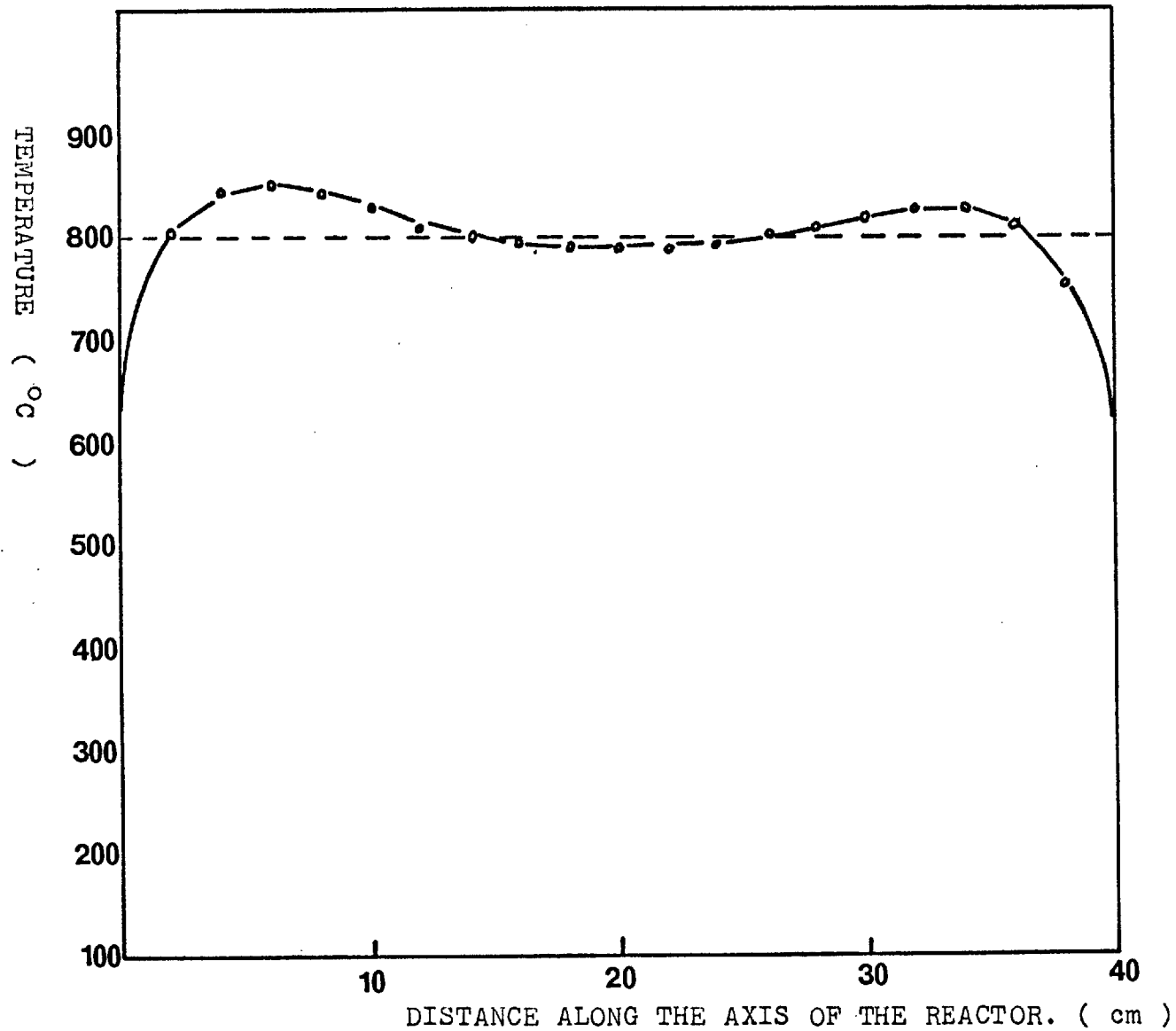


FIGURE II-8. TEMPERATURE DISTRIBUTION IN THE REACTOR AXIS WITH THE FURNACE OF FIGURE II-7.

foil was positioned 50 m m. from the furnace top. The arrangement of the system and the temperature distribution inside the reactor are shown in figures II-7 and 8.

Both temperature controllers were designed and built in the departmental Electronics Workshop. The controllers were of the type P.I.D. and were used in conjunction with chromel alumel thermocouples.

c- The gas analyzer

The gas coming out of the reactor went through a tar filter (glass wool) and was sampled through two PYE gas sampling valves. One of the samples was sent to a 1.5 m. stainless steel column packed with activated silica gel, in which hydrogen and nitrogen were separated; detection was carried out using a Servomex microkatharometer. The silica gel column operated at 25° C.

The other sample was sent for analysis to a G.C.D. Pye Gas Chromatograph equipped with a dual flame ionization detector. Methane, ethane, ethylene, propane, propylene, butane, butadiene, cyclohexane, cyclohexadiene and benzene were separated in a 2.5 mts x  $\frac{1}{8}$ " stainless steel column packed with activated alumina. A temperature program was used to achieve the separation: 4 min at 75° C, followed by a linear increase of 16° C min<sup>-1</sup> up to 300° C, where the last peaks were left to elute.

Identification of compounds was performed by injection of the pure gases and comparing them with the unknown on a retention time basis. A small amount of an unidentified compound eluted after 1-3 butadiene. It was marked as "unknown 1". According to the retention time, the compound could be a cyclopentene or pentadiene.

The quantitative evaluation of the concentration of

hydrogen and nitrogen was performed on the basis of a calibration of the areas of the peaks with known volumes of the pure gases. With the hydrocarbons it was found that the calculated correction factors (Kaiser, 1963) corresponded quite closely with the experimental calibration and were adopted to calculate the composition.

The calculation of the composition, in moles per cent, was made with the aid of a computer program. A sample printout is given in figure II-9.

#### d- Liquid collection and analysis

Liquid and solid aromatic hydrocarbons are produced during the thermal reaction in small quantities. To obtain information on their composition and nature, a liquid trapping device was designed and installed. (See figure II-10). Several traps were built and a heating wire was fitted around the outlet tubes from the reactor (able to keep the temperature to 400° C) to avoid condensation of aromatics before reaching the collection trap. Ice was used, in a test experiment, as a cooling agent, but the efficiency of collection was increased by 37% by the use of liquid nitrogen. Liquid nitrogen seemed to be more efficient in the precipitation of the tar aerosol and was finally adopted for the experimental work.

When the collection was completed, the trap was allowed to reach room temperature slowly. After weighing, the content was dissolved in 10 ml of chloroform and kept in sealed vials in the dark until analysis could be completed.

The mixture of aromatics, with compounds ranging from benzene to 3-4 benzopyrene and higher polycyclic aromatics, was analyzed in a G.C.D. Pye Gas Chromatograph with dual flame ionisation detectors. The columns were glass coils of 2.5 m length and 2 mm internal diameter, packed

---

G A S C O M P O S I T I O N											
R U N 130											
HYDROGEN	NITROGEN	METHANE	ETHANE	ETHYLENE	PROPANE	PROPYLENE	BUTANE	BUTADIENE	UNKNOWN 1	UNKNOWN 2	BENZENE
		(HYDROCARBONS)									
		52.08	5.63	38.67	0	1.36	.04	.06	.48	0	1.68
		(TOTAL)									
14.57	25.93	28.90	3.12	21.46	0	.76	.02	.04	.27	0	.93
		(FREE OF NITROGEN)									
25.08		39.02	4.22	28.98	0	1.02	.03	.05	.36	0	1.26

---

FIGURE II.9. SAMPLE PRINTOUT OF THE COMPUTER PROGRAM THAT CALCULATES THE COMPOSITION OF THE MAJOR GAS PRODUCTS.

with 3 % OV-1 on Gas Chrom Q , 80-100 mesh (Phase Separations Ltd. ). Injector parts and detectors were held at 375° C. The separation was achieved with a temperature program as follows: 5 min at 35° C, followed by an increase of 16° C min<sup>-1</sup> and holding at 350° C until all the components were eluted. A typical trace is shown in figure II-11.

Benzene, toluene, ethylbenzene, ethyltoluene, naphthalene, diphenyl, acenaphthene, fluorene, stilbene, anthracene-phenanthrene, fluoranthene, pyrene, chrysene, and 3-4 benzopyrene were identified by comparing the retention times of the peaks with those corresponding to the pure compounds. Methyl-propyl benzene (or diethyl benzene), methyl-naphthalene, acenaphthylene and methyl-anthracene were identified by the use of a retention time-boiling point correlation. Some compounds were not identified and were marked as unknown from 1-5.

Correction factors were estimated following the theoretical procedure outlined by Kaiser (1963). The calculation of concentration was performed with the aid of a computer program. A sample printout of a typical analysis is shown in figure II-12.

#### e- Materials

Most of the gases used were C.P. grade (with the exception of n-butane that was Instrumental grade) and no further purification was attempted. Butane, ethane and hydrogen were analyzed by gas chromatography and the level of oxygen was found to be below the level of detection of the micro-katharometer. Methane, ethane, acetylene, propane, butane and helium were provided by Matheson Co. and nitrogen, hydrogen, ethylene, propylene, oxygen and argon (carrier for chromatography) by British Oxygen Co..

Metal foils, in sheets of 150 x 150 mm and 0.125 mm thickness were provided by Goldfellow Metals Ltd. Purities were as

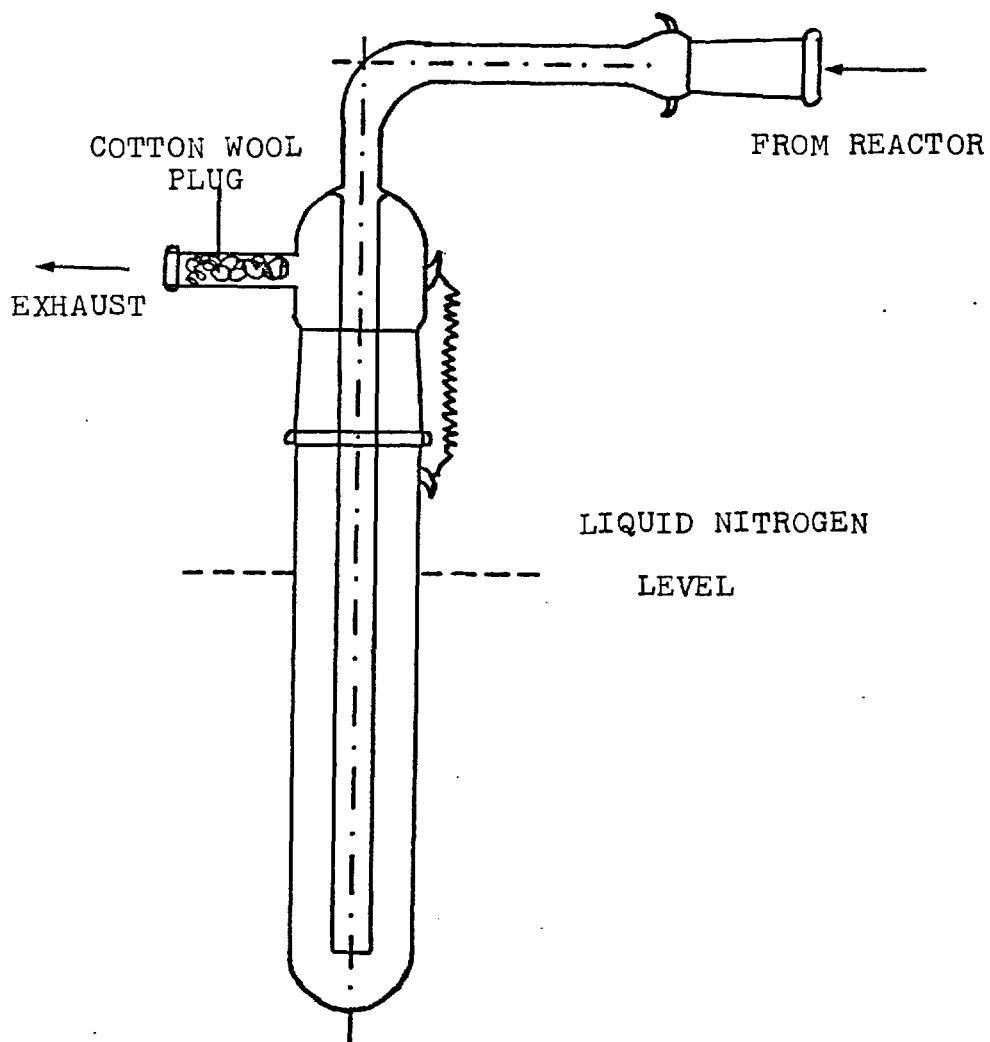


FIGURE II-10. LIQUID COLLECTION TRAP.

FIGURE II-11. TYPICAL GAS CHROMATOGRAPHIC TRACE OF THE ANALYSIS OF HEAVY TARS, CONDITIONS AS IN THE TEXT.

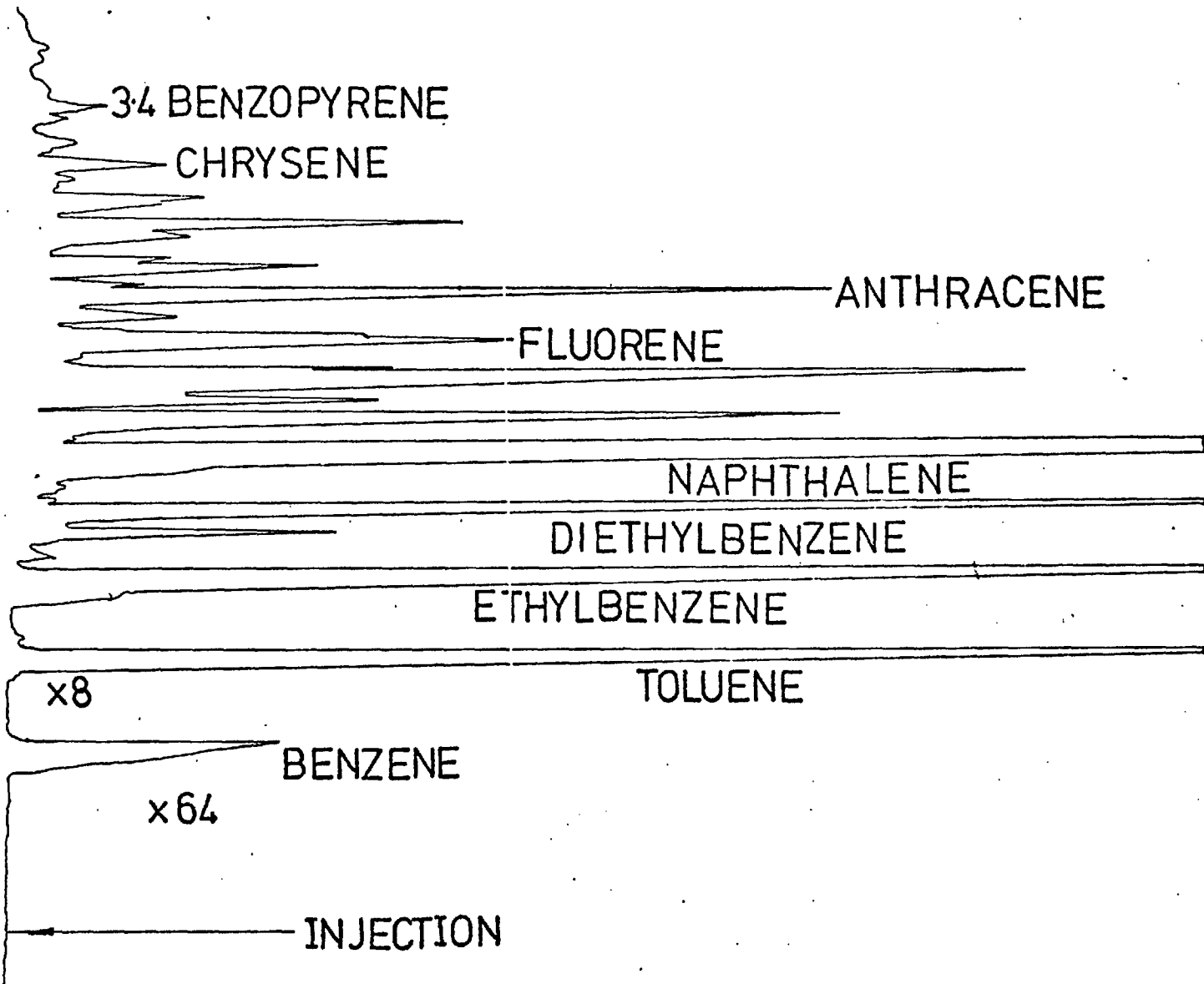




FIGURE II-12. SAMPLE PRINTOUT OF THE PROGRAM THAT CALCULATES AROMATICS COMPOSITION

RUN 113  
-----

TOTAL MASS CONCENTRATION OF AROMATICS = .205480MGR./ML.  
LIQUID COMPOSITION  
-----

	MASS PERCENT (LIQUID)	MASS CONCENTRATION (GAS)	MOLES PERCENT (LIQUID)	MOLAR CONCENTRATION (GAS)
BENZENE	54.92	.112854	68.81	.00144400
TOLUENE	2.21	.004537	2.35	.00004924
ETHYLBENZENE	3.54	.007283	3.27	.00006860
ETHYLTOLUENE	.07	.000138	.05	.00000115
METH.PROP.BENZ.	1.41	.002898	1.03	.00002159
NAPHTHALENE	18.50	.038023	14.13	.00029664
METHNAPHTHALENE	.88	.001803	.60	.00001268
DIPHENYL	.97	.001989	.62	.00001292
ACENAPHTHYLENE	3.99	.008191	2.56	.00005302
ACENAPHTENE	0	0	0	0
FLUORENE	1.13	.002312	.66	.00001391
STILBENE	.26	.000532	.14	.00000295
ANTHRACENE AND PHENAN.	3.20	.006576	1.76	.00003691
METH.ANTHRACENE	.77	.001585	.39	.00000827
FLUORANTHENE	1.37	.002805	.66	.00001399
PYRENE	2.06	.004241	1.00	.00002099
UNKNOWN 1	.48	.000975	.23	.00000484
CHRYSENE	1.18	.002424	.51	.00001062
UNKNOWN 2	.43	.000885	.18	.00000387
UNKNOWN 3	.57	.001179	.25	.00000517
3-4 BENZOPYRENE	1.06	.002184	.41	.00000865
UNKNOWN 4	.38	.000782	.15	.00000310
UNKNOWN 5	.62	.001271	.24	.00000504

follows: copper : 99.9 %, iron : 99.5 % and nickel : 99.8 %.

f- Operation technique

The following operation sequence was established in all runs where carbon deposition, aromatics composition and gas product spectrum were to be determined. When only partial information was required, the corresponding steps were deleted.

- 1- Once a week, the calibration of the microbalance and microkatharometer was verified.
- 2- At the start of a new run, a new sample foil was hung from the microbalance. The reactor was closed and the oven positioned. A liquid collection tube was packed loosely with cotton wool and fitted into place, to filter the tars produced during the initial and ageing periods.
- 3- Passing hydrogen through the reactor, the system was heated up to the desired working temperature and reduced for one hour.
- 4- The flow of the reactant gases and microbalance flush nitrogen, were adjusted to the desired valves.
- 5- The gas mixture was admitted to the reactor and a record of the weight of the sample foil VS time was started. A period of about half an hour was spent under these conditions, to allow for the conditioning of the inside of the reactor and sample surface.
- 6- The gas flow was stopped and, in a rapid operation, the cotton wool filled trap was replaced by a previously weighed empty trap. The dewar was positioned and filled with liquid nitrogen.

7- Gas was again admitted to the reactor and liquid products were condensed for 15 to 30 minutes, while a record of the weight changes in the sample foil was obtained.

8- The gas flow was stopped and the condensed liquid was allowed to reach 0° C slowly, while condensed gases evaporated from the trap. Then the trap was removed, both ends plugged loosely with cotton wool and left to reach equilibrium with room conditions before weighing

9- Another cotton wool trap (not cooled) was placed at the reactor outlet, Gas was admitted again to the reactor and the weight register re-started. After a stabilisation period, the gas analysis was performed. Hydrogen and nitrogen were analyzed first, and then the gaseous hydrocarbons.

10- At this point, the run was finished. Another run could be started, repeating all the procedure from the point 4. If the runs of the complete set covering a variable was finished, air was admitted to the reactor, to burn the carbon and the carcinogenic tars.

11- The tar traps were weighed after the collection with an analytical balance. Tars were dissolved in 10 ml of chloroform and transferred to vials. These were sealed with plastic stoppers and plastic tape and kept in the darkness for further analysis.

12- Tar composition was determined by gas chromatography, as described previously. The rates of carbon deposition were found by measuring the slopes of the recorded weight-time plots. Several measurements were taken.

Gas analysis was performed to  $\pm 2\%$  reproducibility and tar collection to  $\pm 3.3\%$ . Reproducibility in the aromatics analysis (concentration

FIGURE II-13

Example of carbon balance

(Run II-134)

		mg. carbon min <sup>-1</sup>
<u>Input</u> :	96.87 ml butane min <sup>-1</sup>	190.25
<u>Output</u> :	223.57 ml gas min <sup>-1</sup>	
	44.8 % CH <sub>4</sub>	49.17
	2.52 % C <sub>2</sub> H <sub>6</sub>	5.53
	27.93 % C <sub>2</sub> H <sub>4</sub>	61.31
	.76 % C <sub>3</sub> H <sub>6</sub>	2.50
	.45 % C <sub>4</sub> H <sub>6</sub>	1.96
	<u>Total gas</u>	<u>120.47</u>
	60.75 mg liquid min <sup>-1</sup>	
(assumed 93.75 % carbon in liquid )		56.96
carbon deposited (assumed same rate in reactor as on the foil )		5.58
	<u>Total carbon</u>	<u>183.01</u>
	Difference	- 7.24
	Error in balance :	3.8 %

calculated in the outlet gas) was  $\pm 9.6\%$  for benzene, and the reproducibility of analysis of a liquid aromatic sample was  $\pm 1.83\%$  for benzene. Reproducibility for carbon formation rates was found to be poor, as previously found by Figueiredo (1975) and Lobo (1973). The value for the series of runs (III-119 to 122) gives a reproducibility of  $\pm 7.8\%$ .

An example of the overall mass balance of the carbon in the system is given in figure II-13. An error of  $3.8\%$  in the balance is not surprising, considering that the result is a combination of measurements (concentrations, flows and weights) that are themselves subject to error.

g- Precautions taken in the manipulation of polycyclic aromatics

The presence of at least one very carcinogenic aromatic compound (3-4 benzopyrene) in the tars produced during the experiments gave the constraint of taking all possible precautions to avoid contact of the material with the skin and the laboratory atmosphere.

Disposable plastic gloves were used to manipulate the materials. The operations where there was a risk of contaminating the atmosphere were carried on in a fume cupboard. The outlet stream from the reactor was discharged into the flame of a Bunsen burner and the carbon tars from inside the reactor were burned in situ before opening the reactor to the atmosphere.

h- Experimental operation conditions and variables studied.

All the experiments were performed at atmospheric pressure. The temperature in the furnace was measured and controlled at the level where the foil was positioned. The gas residence time in the reactor was defined as the reaction volume divided the gas flow rate at the inlet and at the reaction temperature. The time thus defined was called the "inlet

residence time."

The variables studied were reaction temperature, inlet residence time, reactant concentration, hydrogen concentration and diluent concentration. Other effects studied were the influence of different metal liners, the influence of different metal and silica sample foils, influence of changing the surface to volume ratio in the reactor and the influence of the time on-line.

Experiments were performed in three different series, marked as series I, II and III. Series I were performed with undiluted butane. No analysis of gas products or liquid aromatics was performed. Runs I-1 to 5 were performed at 800° C, covering residence times 2 to 5 sec and using a silica foil as a sample surface. Runs I-6 and 7 repeated the same study with a nickel sample foil, I-8 with iron and I-3 with copper. Run I-10 was devoted to study of the effect of temperature, between 800 and 900° C, at constant residence time, using a copper sample foil.

Runs I-11 to 15 were devoted to the study of the effect of reactor liners, at 800° C, with copper sample foils and using the residence time as a variable. Runs I-11 and 14 were performed with iron liners, runs I-12 and 15 with nickel liners and run I-13 with a copper lining foil.

The second series of experiments were performed with butane and mixtures with hydrogen and helium. A gas analysis was made for each run of this series.

Runs II-1 to 15 covered the effect of the concentration of butane in hydrogen, at constant residence time ( 1.6 sec ), 800° C and using nickel as sample material. Runs II-16 to 23 were devoted to study the effect of hydrogen at constant butane concentration, using helium as diluent. Nickel foils were used, at 800° C and 1.6 sec residence time.

Runs II-24 to 31 were dedicated to the effect of the concentration of butane in hydrogen, using iron sample foils at  $800^{\circ}$  C and 1.3 sec residence time. The same experiments were repeated in runs II-32 to 37, using copper sample foils.

The combined effect of temperature and the presence of hydrogen was studied with nickel sample foils at a residence time of 1.3 sec (calculated at  $800^{\circ}$  C). Runs II-38 to 46 used 20 % of butane in hydrogen as a feed and runs II-47 to 52 used 20 % of butane in helium. The same experiments were performed using copper sample foils. Runs II-53 to 58 involved 20 % butane in helium, and II-59 to 63 used 20 % of butane in hydrogen.

A study of the combined effect of temperature and residence time was performed using copper sample foils and pure butane feed. Runs II-64 to 75 were devoted to this study.

Several runs were performed with the "reactor-condenser" scheme, previously described in this chapter. Copper sample foils were used and a constant temperature of  $900^{\circ}$  C was fixed in the "reactor" section. Runs II-76 to 86 were made with pure butane feeds, while in runs II-87 to 100, a mixture of 33 % of butane in hydrogen was reacted. In runs II-101 to 105, nickel sample foils were used.

During the third series of experiments, gas and liquid tars analysis was performed for every run. In runs III-101 to 104, the effect of residence time at  $800^{\circ}$  C was studied, using copper sample foils and a feed of 50 % of butane in hydrogen. The effect of the concentration of hydrogen was studied at  $800^{\circ}$  C, at 25 % of butane in the feed and using helium as a diluent (runs III-105 to 108). The effect of temperature was established during runs III-109 to 118, in the presence of 50 % of either hydrogen or helium, using copper sample foils.

The effect of reactor liners as a function of the time on-line was also studied, in runs III-119 to 122 using copper liners and copper sample

foils, and in runs III-123 to 126 with iron liner and copper sample foil. 50 % of butane in hydrogen was used as a reactor feed, at 800° C.

In runs III-127 to 130, the effect of changing the surface to volume ratio in the reactor was established, at 800° C, with 50 % of butane in hydrogen in the feed and using copper sample foils. Runs III-131 to 134 were performed to establish the influence of the butane concentration in hydrogen on the production of aromatic tars, at 800° C and using a copper sample foil.



## CHAPTER III- RESULTS

A- <u>THE PRODUCTION OF THE MAJOR GASEOUS PRODUCTS DURING</u> <u>THE THERMAL REACTION OF HYDROCARBONS.</u> .....	92
1- Thermal reactions of ethane in a jet-stirred reactor. ....	92
2- Thermal reactions of butane in a tubular flow microbalance reactor. ....	105
a- The effect of butane initial concentration in mixtures with hydrogen. ....	105
b- The effect of hydrogen concentration in the feed. ....	105
c- The effect of reaction temperature. ....	107
d- The effect of gas residence time. ....	107
e- The effect of metal liners on the reactor wall. ....	112
f- Minor compounds in the route towards aromatics. ....	112
g- The effect of the surface to volume ratio in the reactor on the gas product composition. ....	117
B- <u>THE PRODUCTION OF AROMATIC COMPOUNDS DURING THE THERMAL</u> <u>REACTION OF BUTANE.</u> .....	120
a- Effect of the residence time. ....	120
b- Effect of hydrogen concentration. ....	124

c-	Effect of butane inlet concentration in mixtures with hydrogen on the production of aromatics. ....	124
d-	Effect of temperature. ....	128
e-	Effect of metal liners on the reactor wall during the transient period. ....	135
f-	The effect of the surface to volume ratio in the reactor. ....	140
C-	<u>THE FORMATION OF CARBONACEOUS DEPOSITS DURING THE THERMAL REACTIONS OF BUTANE.</u> ....	143
1-	Experiments with pure butane. ....	143
a-	Carbon deposition on a silica foil. ....	143
b-	Carbon deposition on different metals. ....	145
c-	The effect of lining the reactor wall with different metals. ....	145
d-	Transient rates during the early stages of deposition. ....	147
e-	Effect of temperature on the rate of carbon deposition on copper sample foils. ....	153

2- <u>Experiments with butane diluted with hydrogen and helium.</u>	160
a- The effect of hydrogen and residence time on the deposition over copper. ....	160
b- The effect of hydrogen on the carbon deposition over different metals. ....	160
c- The effect of temperature on the deposition over nickel and copper. ....	172
d- Results of experiments with the reactor-condenser scheme. ....	179
e- Transient phenomena during carbon deposition. ....	188
f- The effect of surface to volume ratio on the rate of carbon deposition on a copper sample foil. ....	192
D- REFERENCES TO THE FIGURES OF CHAPTER III .....	195

A- THE PRODUCTION OF THE MAJOR GASEOUS PRODUCTS DURING THE  
THERMAL REACTION OF HYDROCARBONS

1 THERMAL REACTION OF ETHANE IN A JET-STIRRED REACTOR.

Results on the thermal reactions of ethane in the presence and absence of hydrogen were obtained with the object of studying the reaction under relatively high ethane conversion levels. The results obtained were used to build mathematical models of the reaction under these conditions.

Product composition as a function of the residence time, obtained from pure ethane feeds at different temperature levels, are presented in figures III-1 to III-4. The corresponding results when ethane-hydrogen mixtures were fed to the reactor are shown in figures III-5 to III-10.

In the lower temperature range (700-750 ° C), the main reaction trend appears to be the simple decomposition of ethane into hydrogen and ethylene, with little methane being formed. At higher temperature, the formation of methane became more important. Methane production increased with residence time in all cases.

Ethylene production increased with residence time at the lower temperatures. At higher temperatures, the yield went through a maximum in residence time, the maximum being followed by a decay in concentration at longer residence times.

To establish a comparison between results in the presence and absence of hydrogen, yields of products and conversion of ethane were plotted as a function of temperature in figures III-11 and III-12. The yield of methane was not sensibly affected by the presence of hydrogen in the feed, but the maximum yield of ethylene

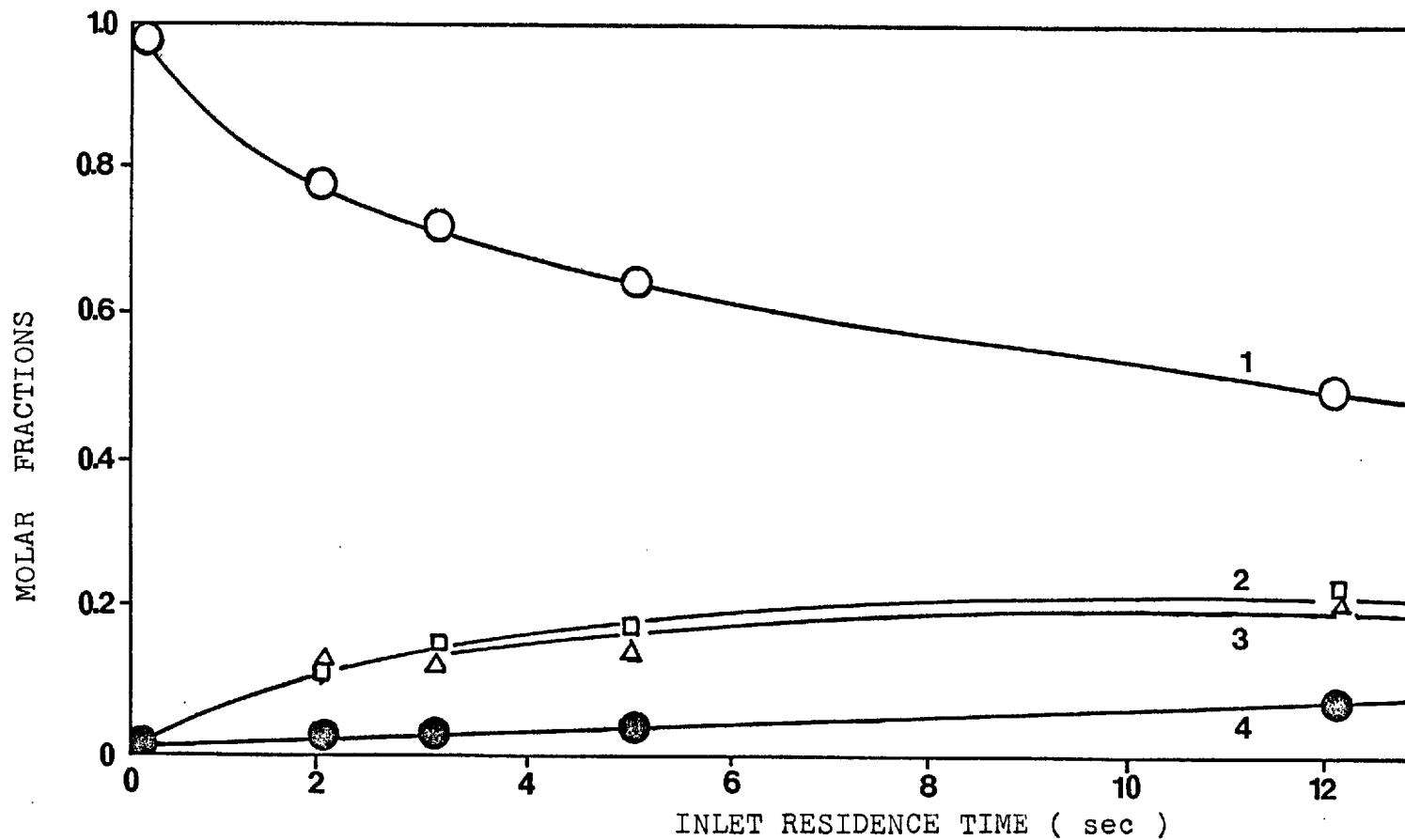


FIGURE III-1. PRODUCTS COMPOSITION FROM THE THERMAL REACTION OF ETHANE IN A JET-STIRRED REACTOR.

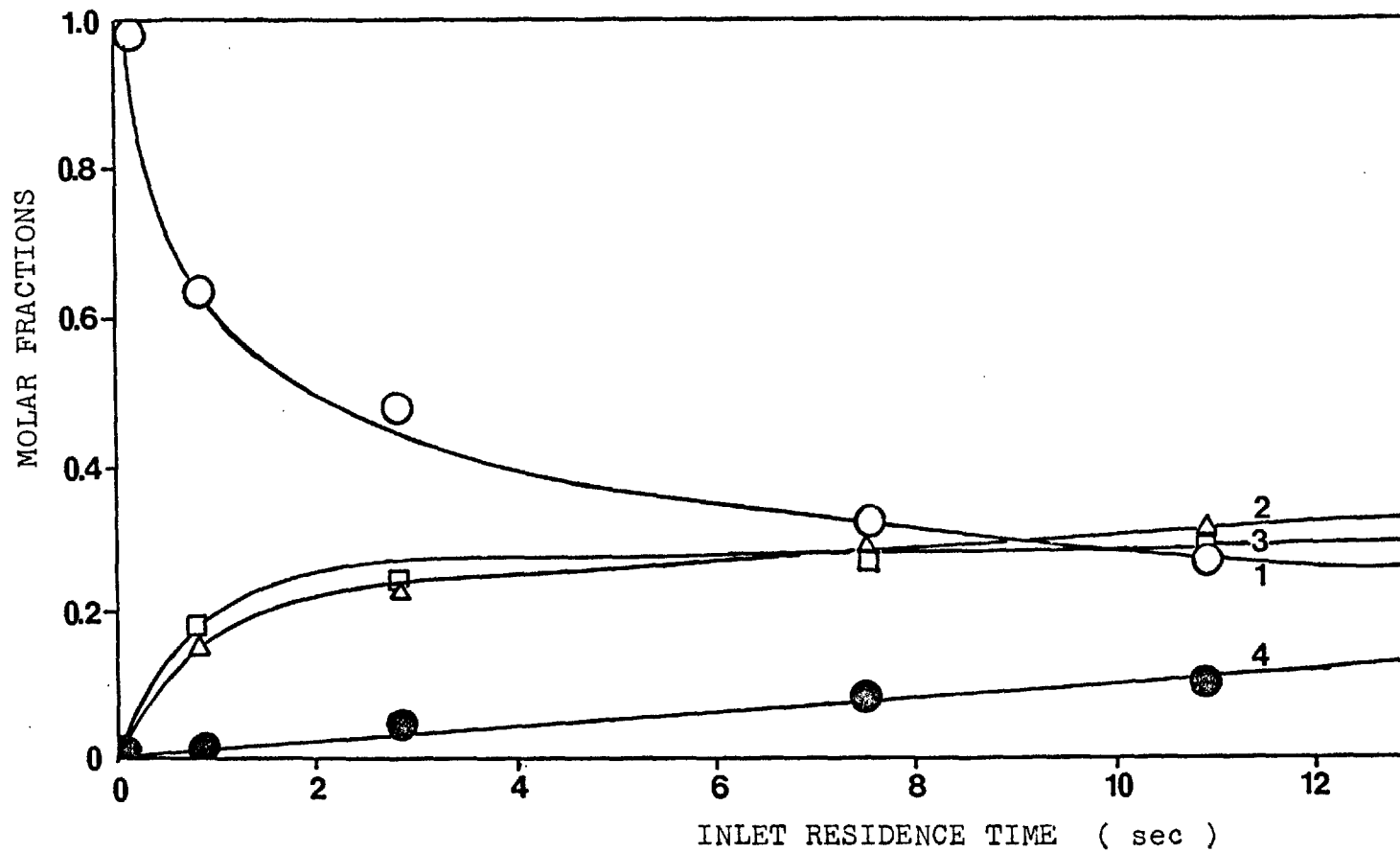


FIGURE III-2. PRODUCTS COMPOSITION FROM THE THERMAL REACTION OF ETHANE IN A JET-STIRRED REACTOR.

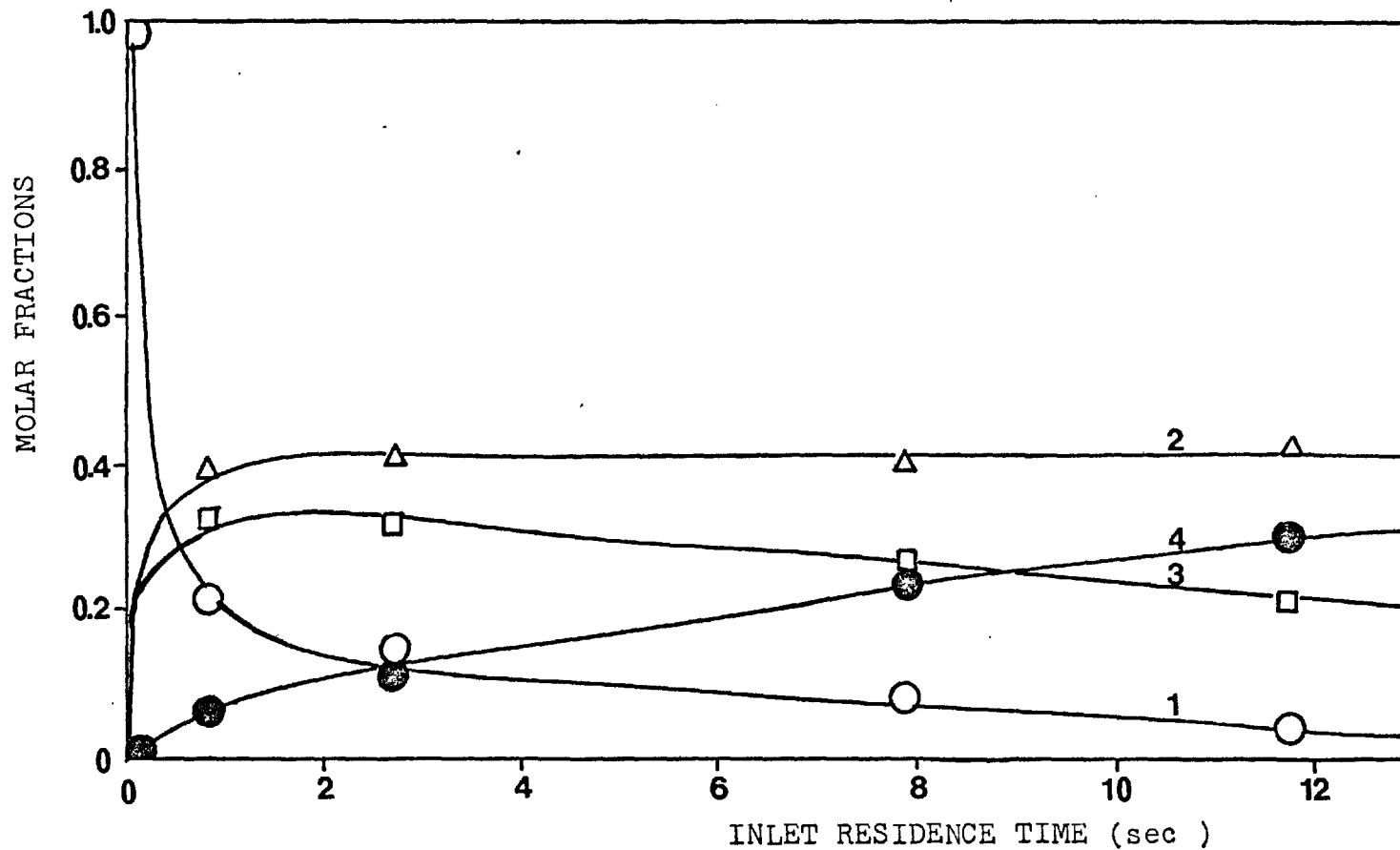


FIGURE III-3. PRODUCTS COMPOSITION FROM THE THERMAL REACTION OF ETHANE IN A JET-STIRRED REACTOR.

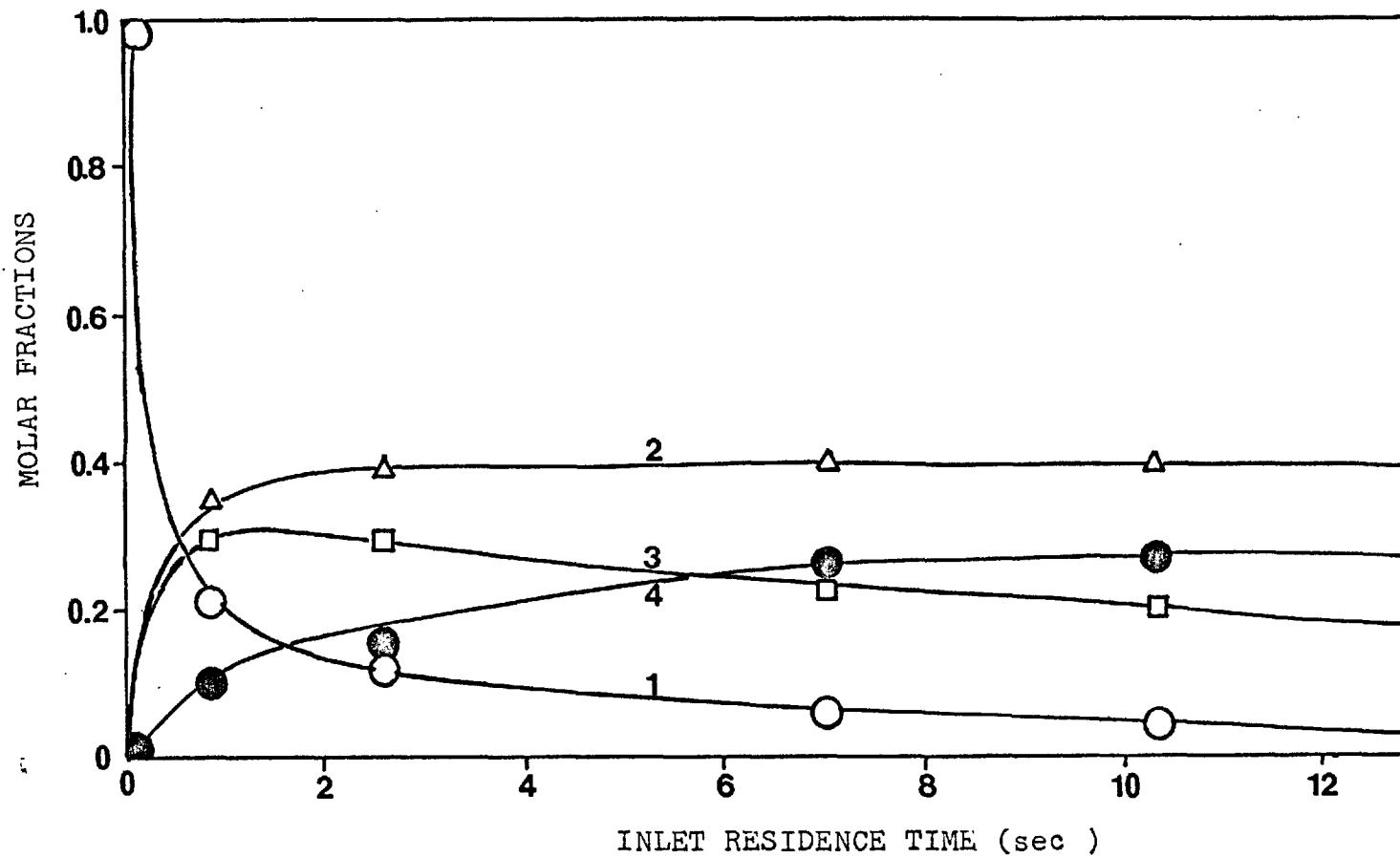


FIGURE III-4. PRODUCTS COMPOSITION FROM THE THERMAL REACTION OF ETHANE IN A JET STIRRED REACTOR.



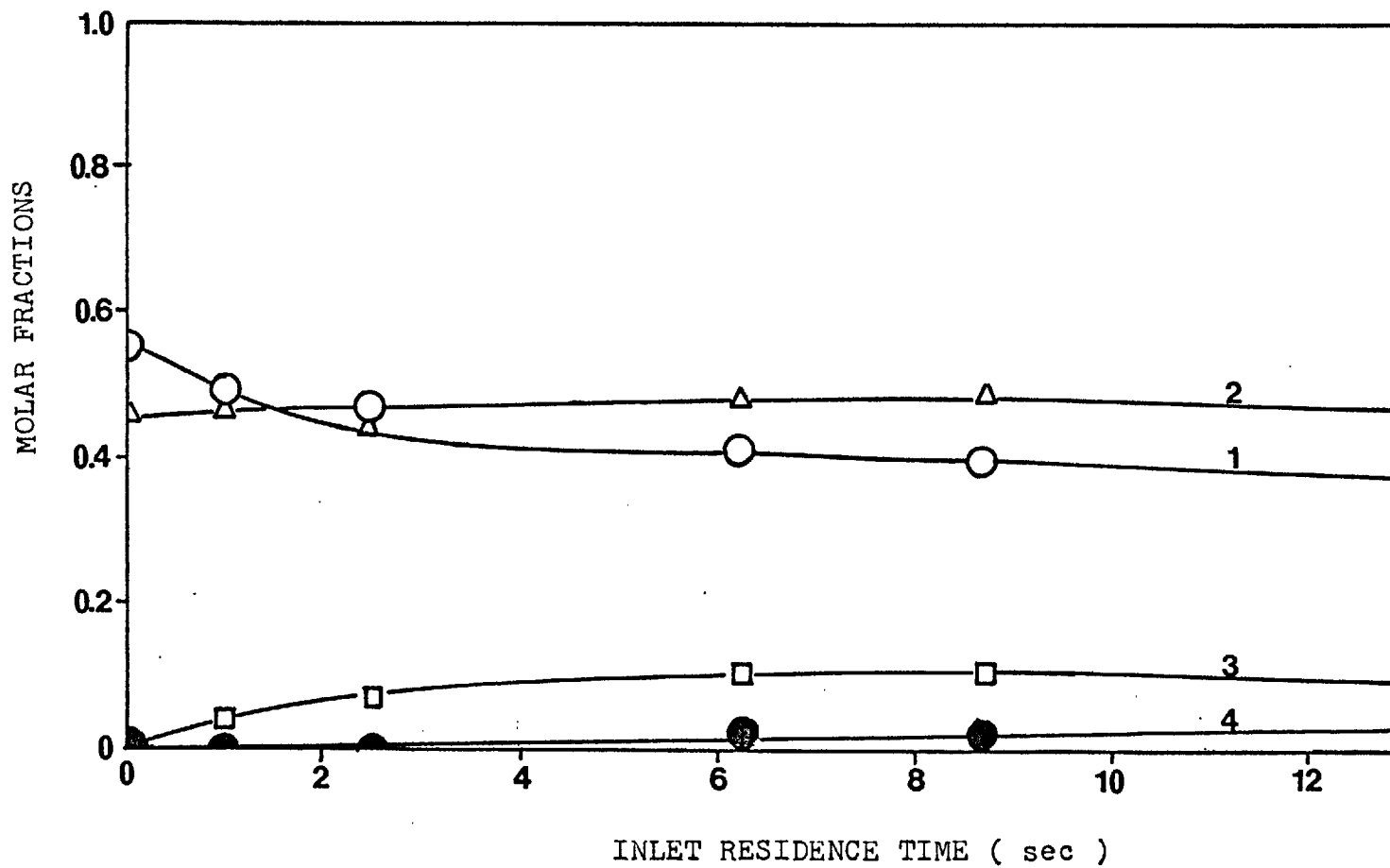


FIGURE III-5. PRODUCTS COMPOSITION FROM THE THERMAL REACTION OF ETHANE IN A JET-STIRRED REACTOR.

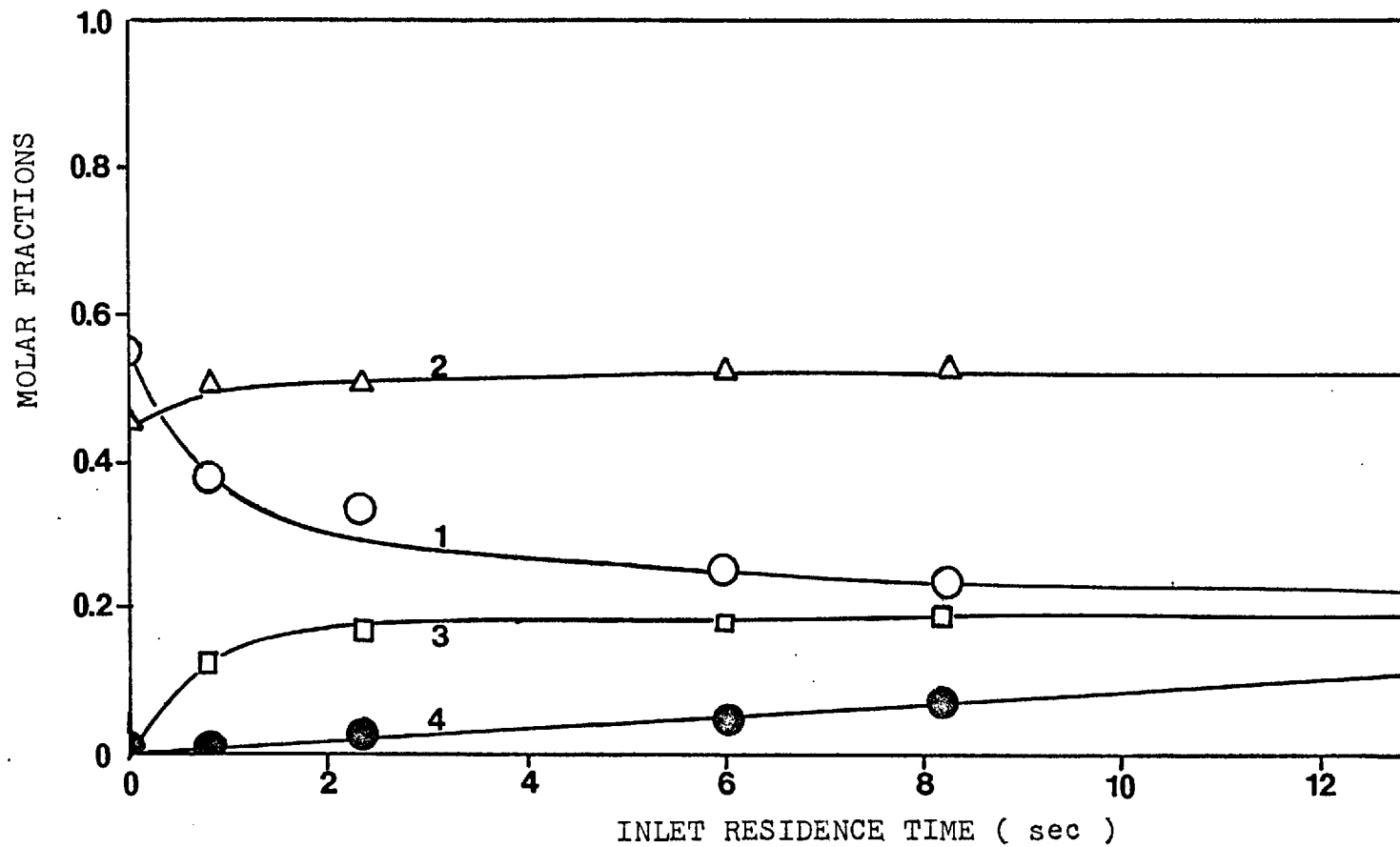


FIGURE III-6. PRODUCTS COMPOSITION FROM THE THERMAL REACTION OF ETHANE IN A JET-STIRRED REACTOR.

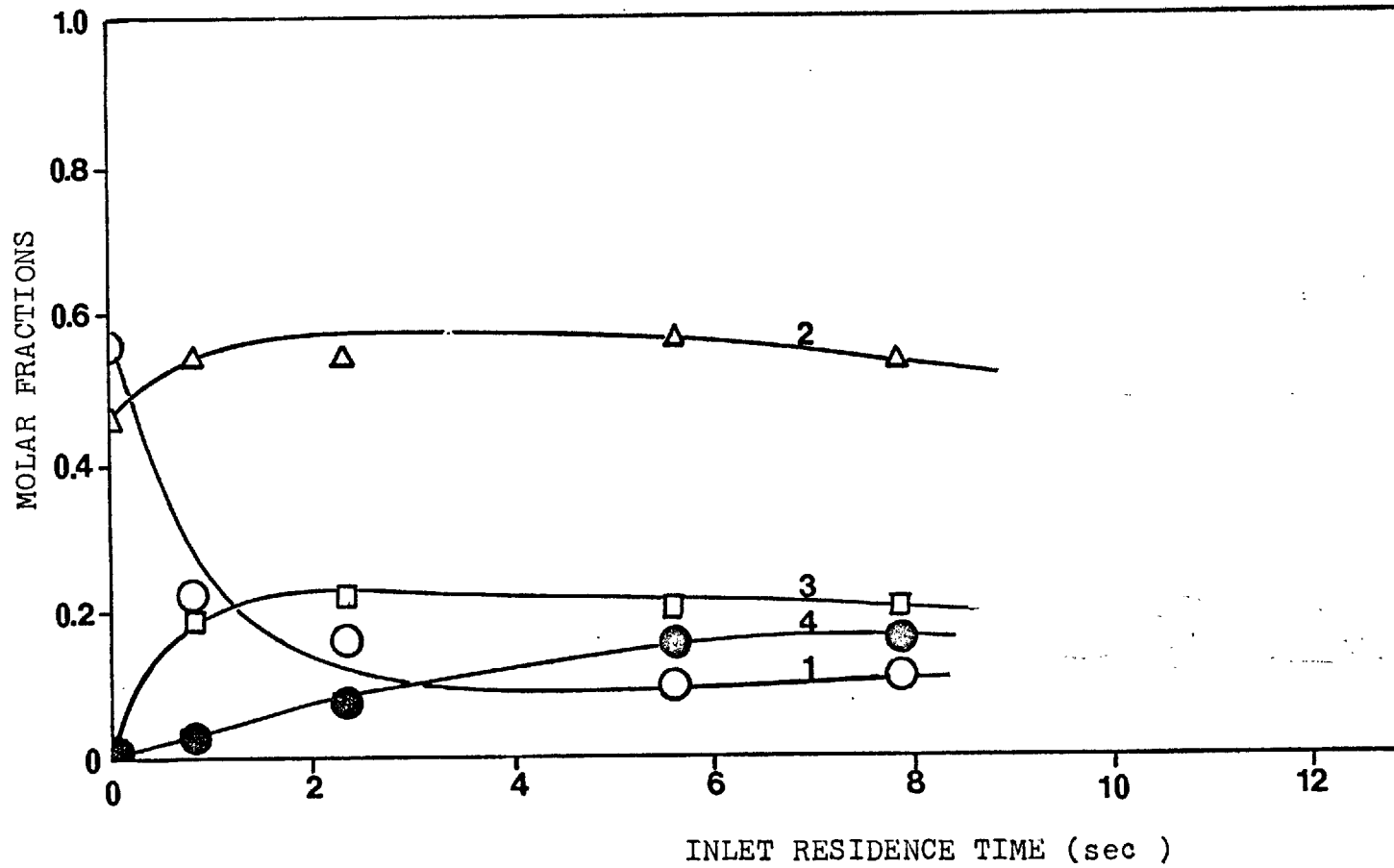


FIGURE III-7. PRODUCTS COMPOSITION FROM THE THERMAL REACTION OF ETHANE IN A JET-STIRRED REACTOR.

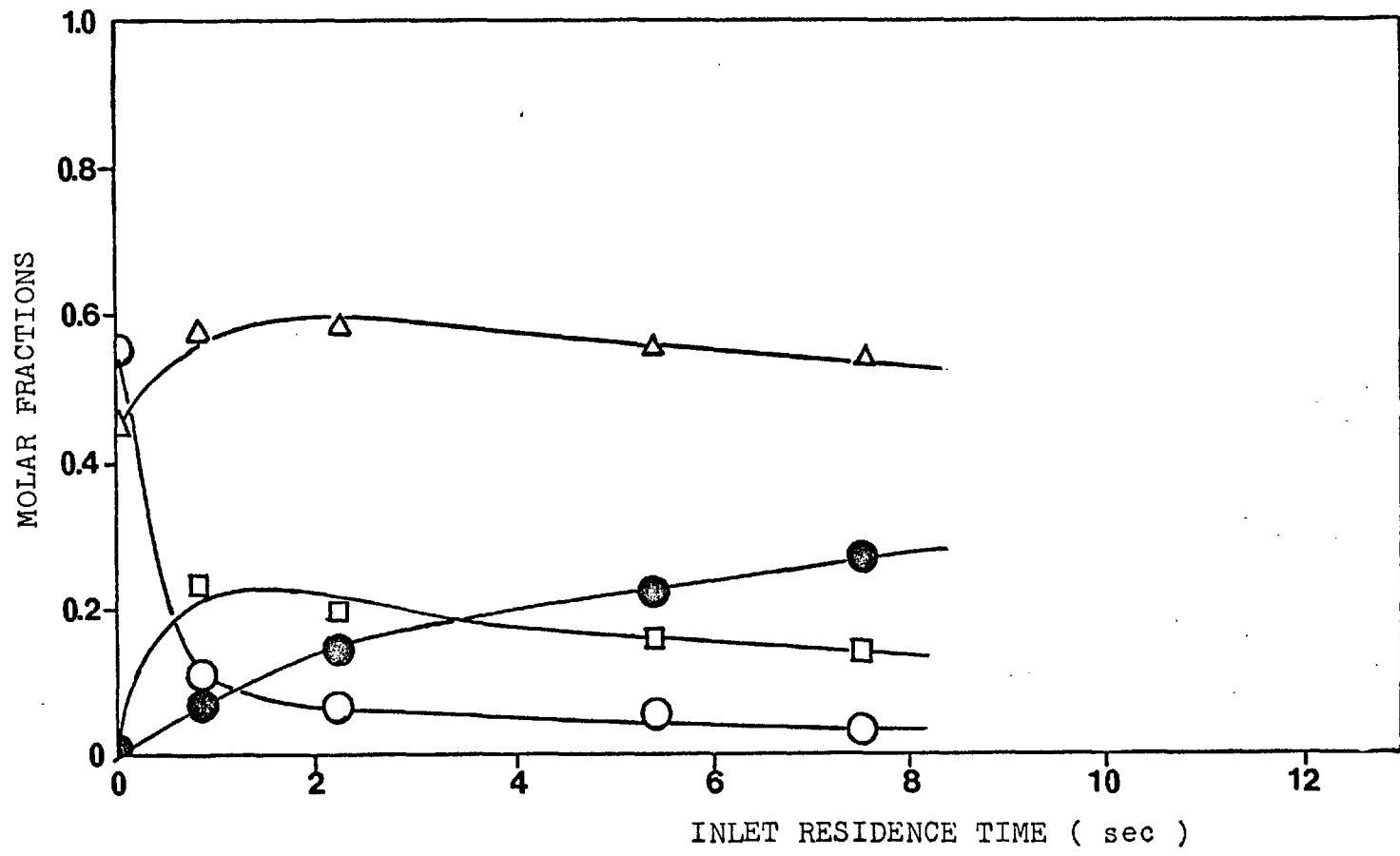


FIGURE III-8. PRODUCTS COMPOSITION FROM THE THERMAL REACTION OF ETHANE IN A JET-STIRRED REACTOR.

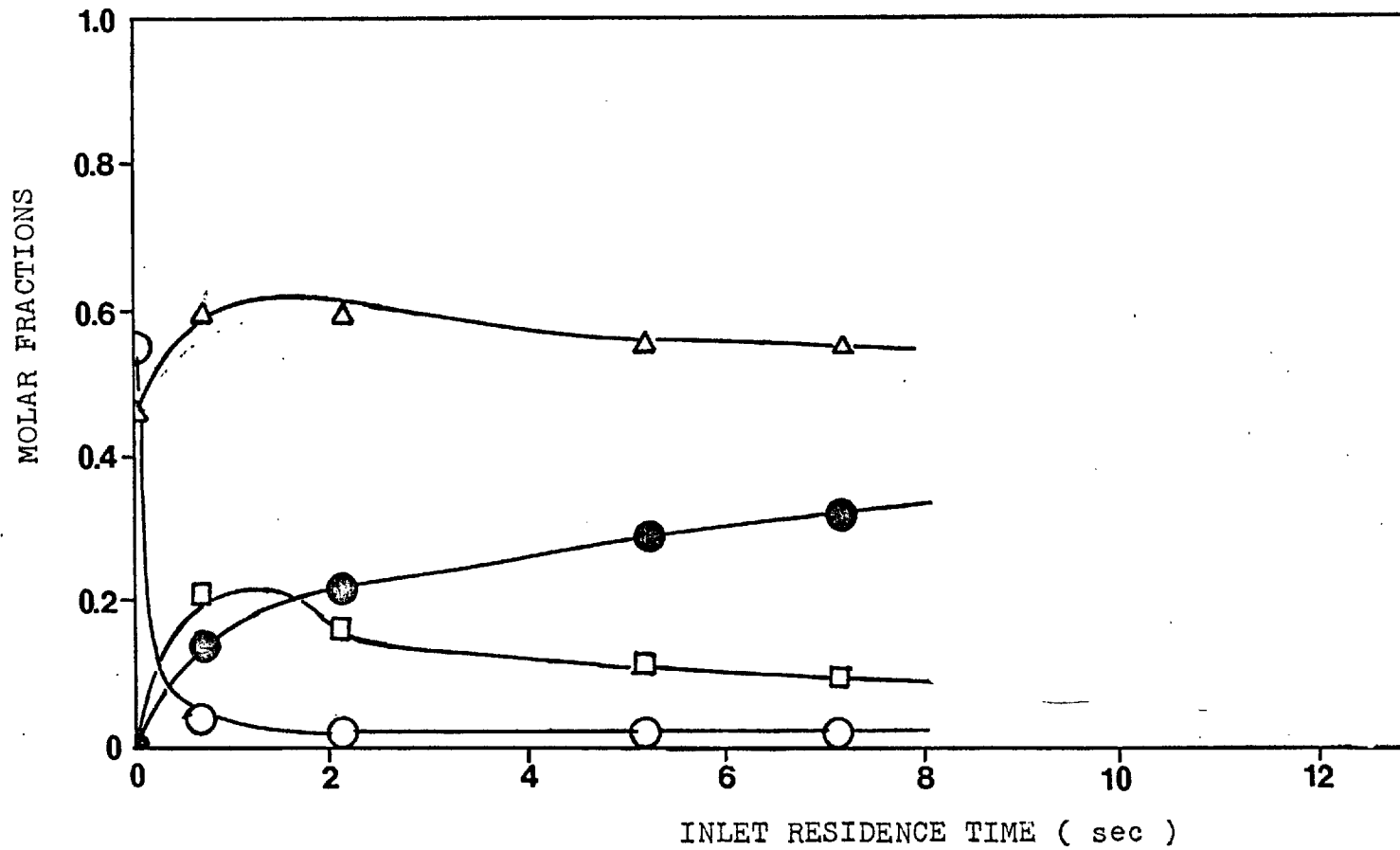


FIGURE III-9. PRODUCTS COMPOSITION FROM THE THERMAL REACTION OF ETHANE IN A JET-STIRRED REACTOR.

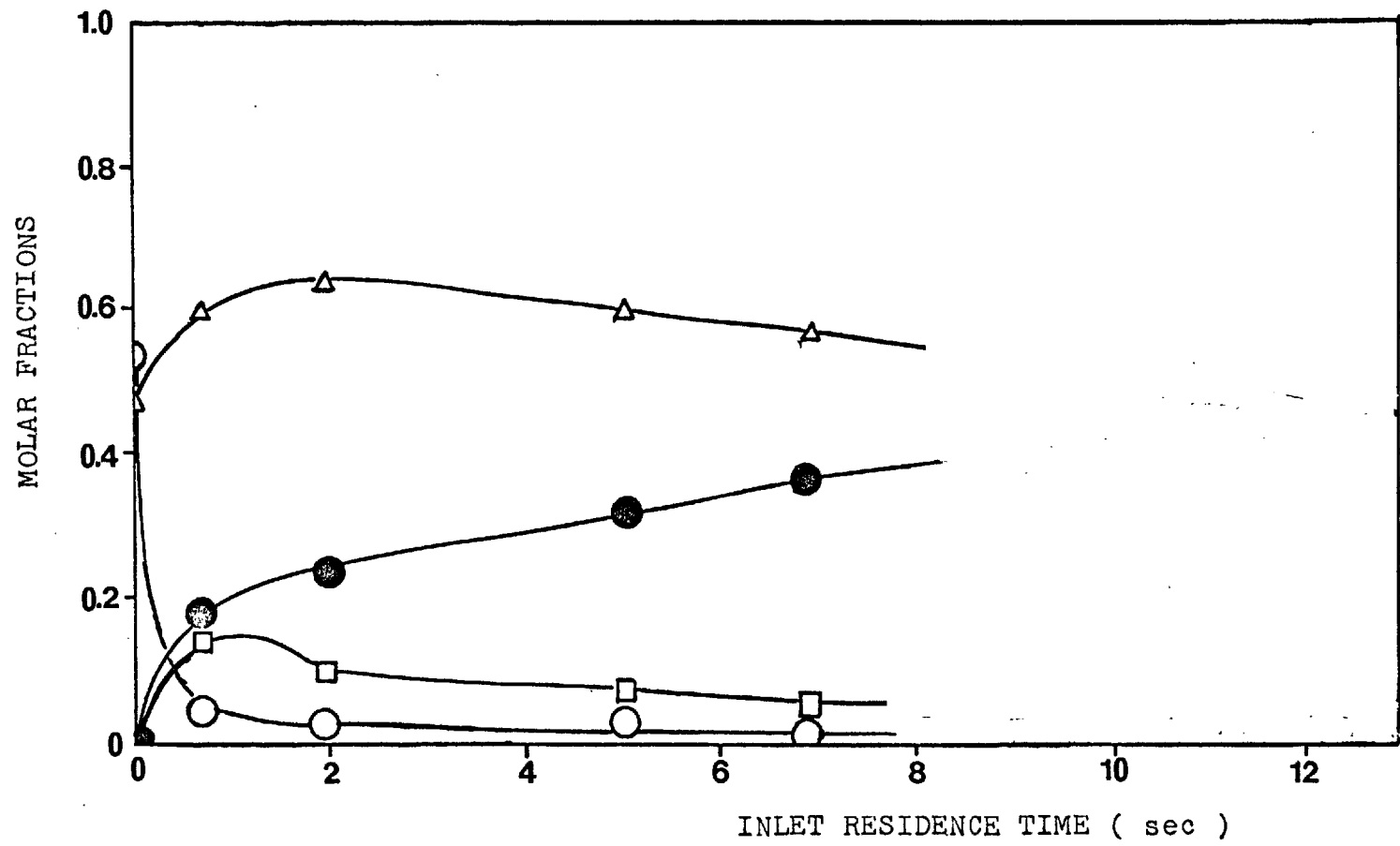


FIGURE III-10. PRODUCTS COMPOSITION FROM THE THERMAL REACTION OF ETHANE IN A JET-STIRRED REACTOR.

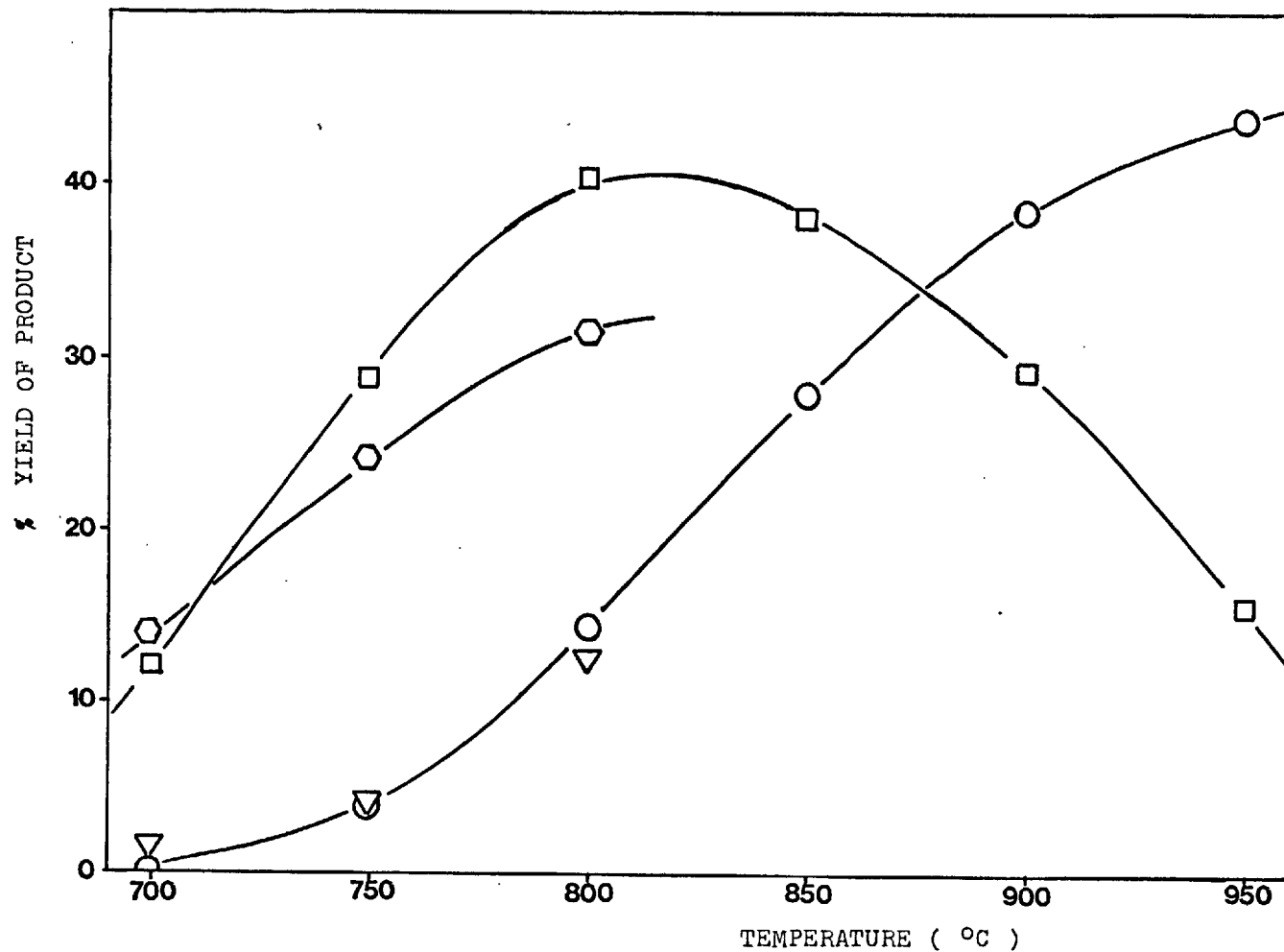
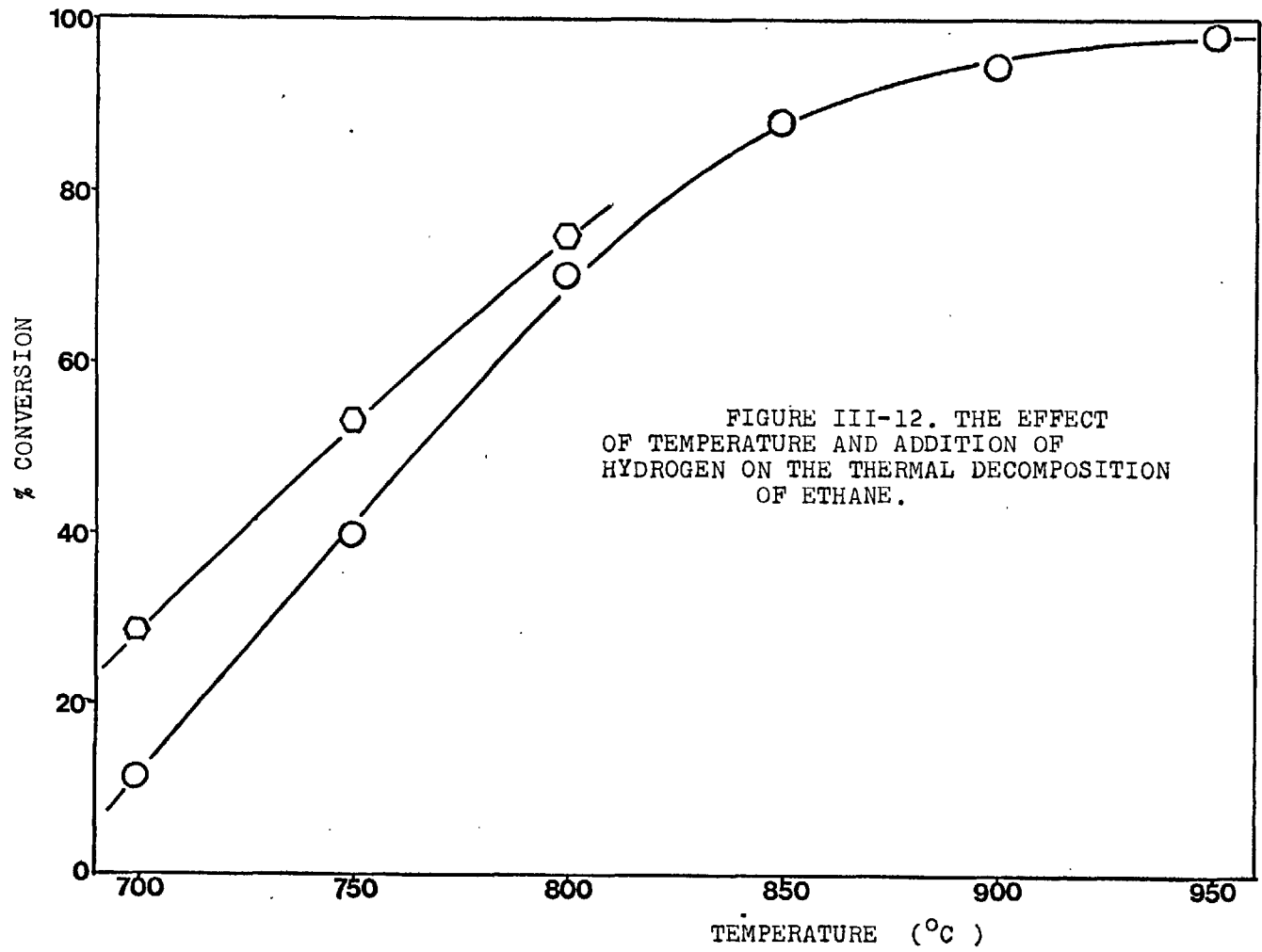


FIGURE III.11. THE EFFECT OF TEMPERATURE AND THE ADDITION OF HYDROGEN ON THE YIELD OF ETHYLENE AND METHANE DURING THE THERMAL REACTION OF ETHANE.





was increased by dilution with hydrogen. Ethane conversion was found to decrease with the addition of hydrogen.

## 2- THERMAL REACTION OF BUTANE IN A TUBULAR FLOW MICROBALANCE REACTOR

Results on product composition from the thermal reactions of butane at high conversions were obtained from a complementary study.

The information was primarily obtained with the aim of relating the gas products spectrum with carbon formation and to understand the mechanism of carbon deposition from pyrolyzing hydrocarbons. (See section C of this chapter).

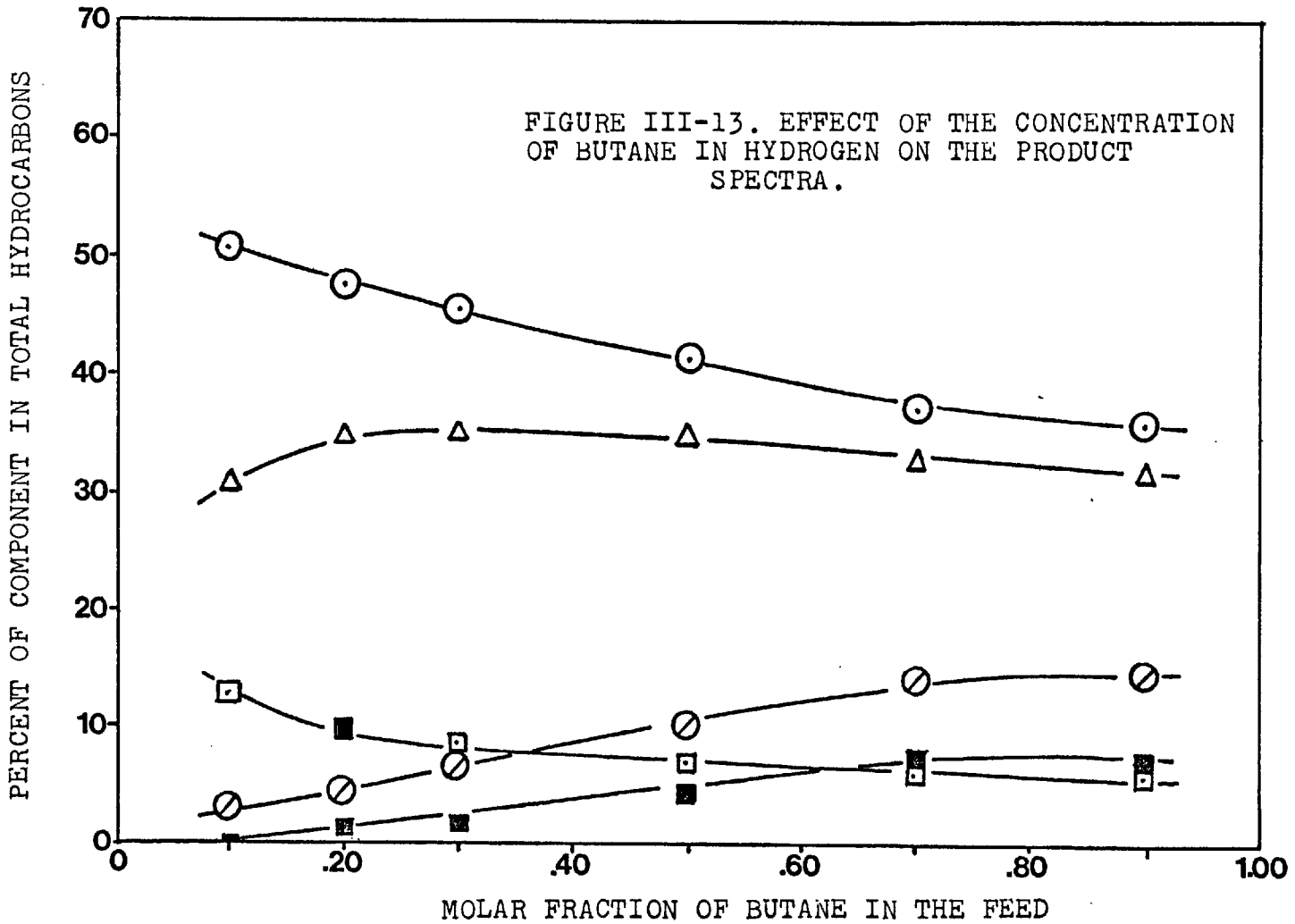
### a- The effect of butane initial concentration in mixtures with hydrogen.

When mixtures of butane and hydrogen were reacted, changes of product spectra occurred. The relative composition of hydrocarbons as a function of butane initial concentration is presented in figure III-13.

Conversion of butane was found to increase at low initial butane concentrations. Yields of methane and ethane were found to fall with an increase of butane concentration, propylene to increase and ethylene went through a maximum at about 20-30% of butane in the feed.

### b- The effect of hydrogen concentration in the feed

To establish the influence of hydrogen in the feed, a diluent was used (helium), the feed concentration of butane and the total inlet flow rate being kept constant.



The results from the experiments are shown in the figure III-14. Butane conversion is increased by the presence of hydrogen. Methane and ethane yields are improved by the presence of hydrogen, while olefins(ethyleneand propylene) are significantly suppressed.

c- The effect of reaction temperature

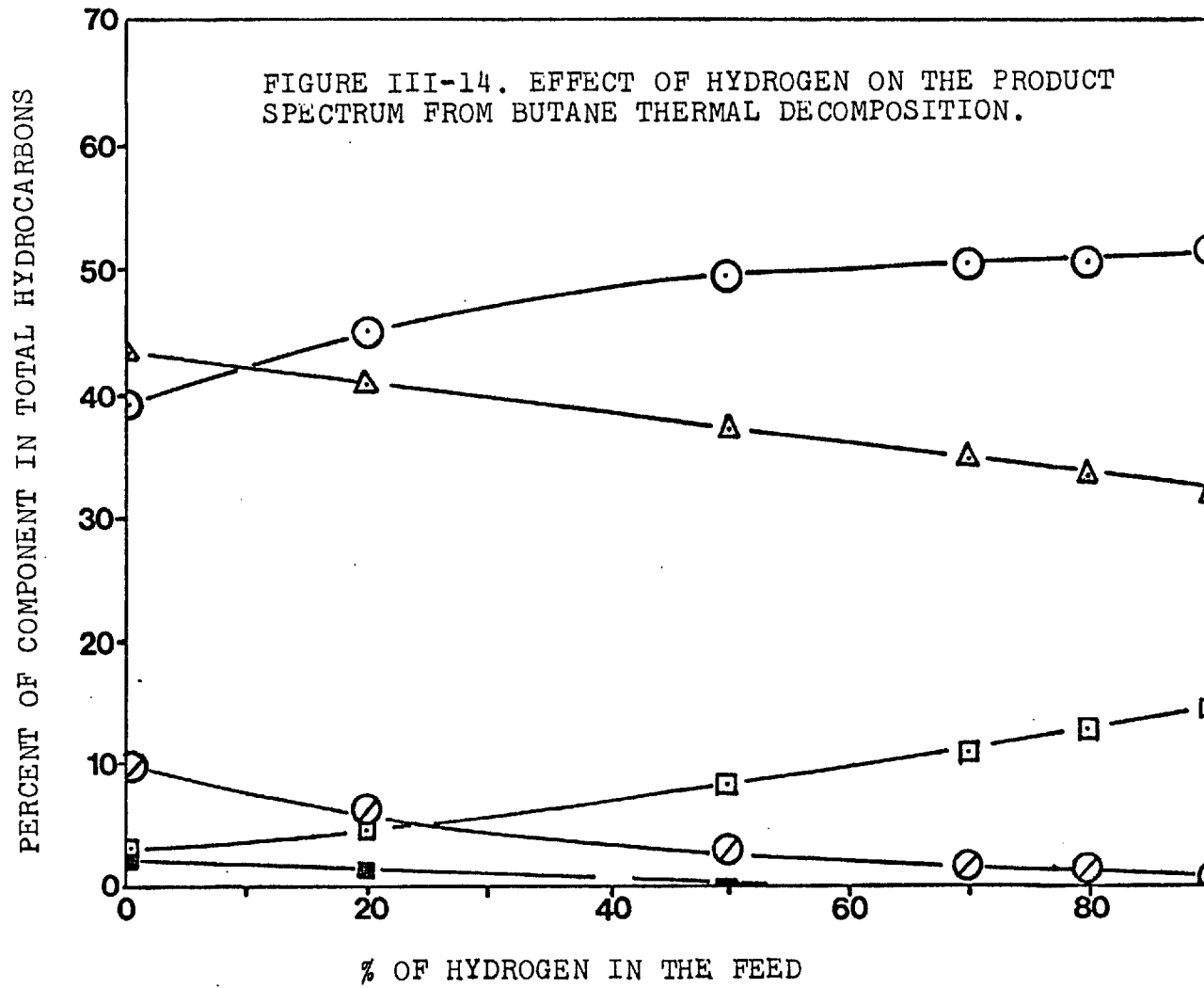
The products composition at different levels of temperature with the addition of hydrogen or helium was studied, and results obtained are shown in figures III-15 and III-16.

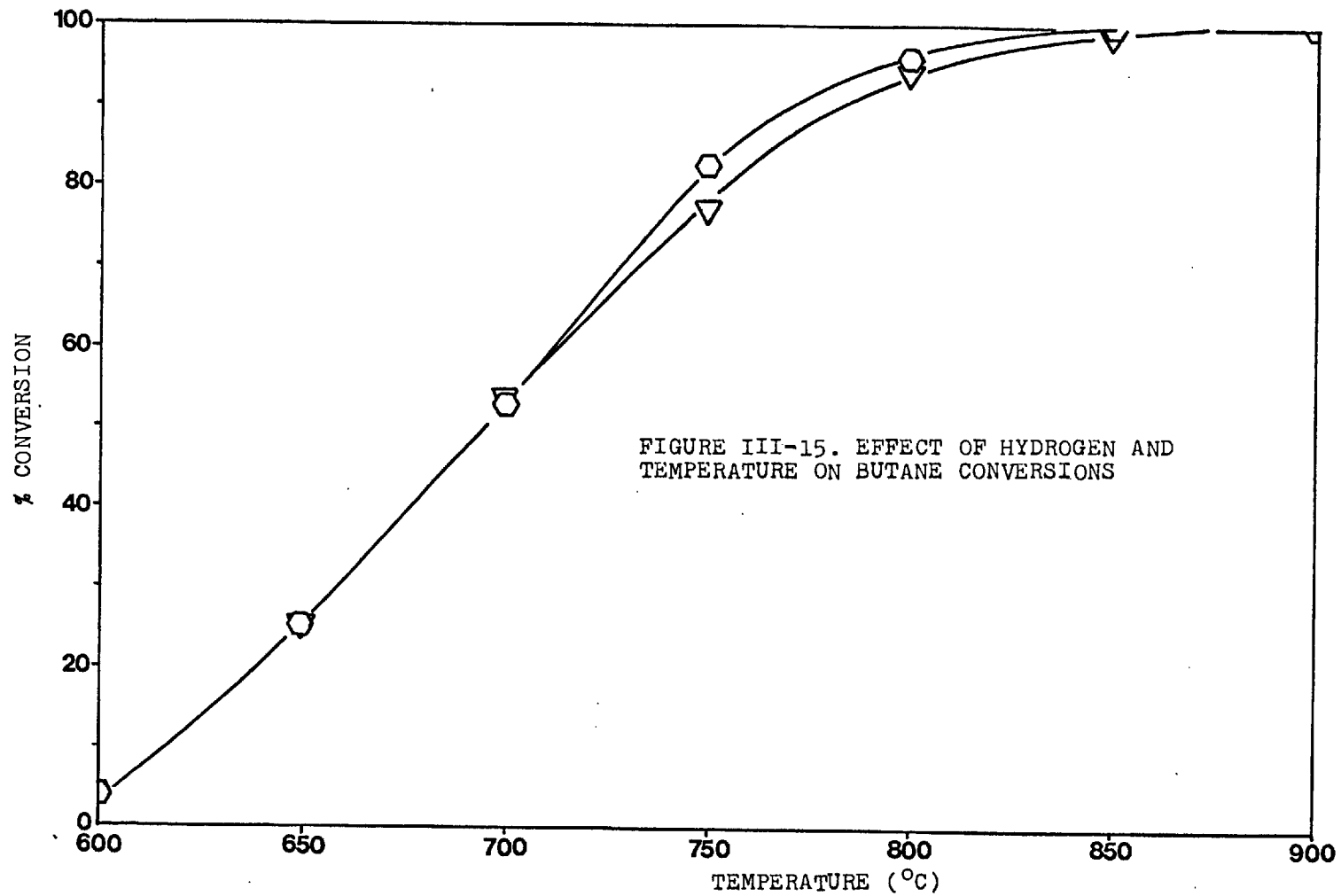
The presence of hydrogen was found to increase butane conversion only above 700 °C, the gas having an insignificant effect at lower temperatures. Hydrogen had the effect of increasing methane yields at the higher temperatures. Both ethylene and propylene yields reached a maximum with temperature. The absence of hydrogen in both cases enhanced the maximum possible yield and the temperature at which the maximum occurs is higher for propylene when hydrogen is added with the feed.

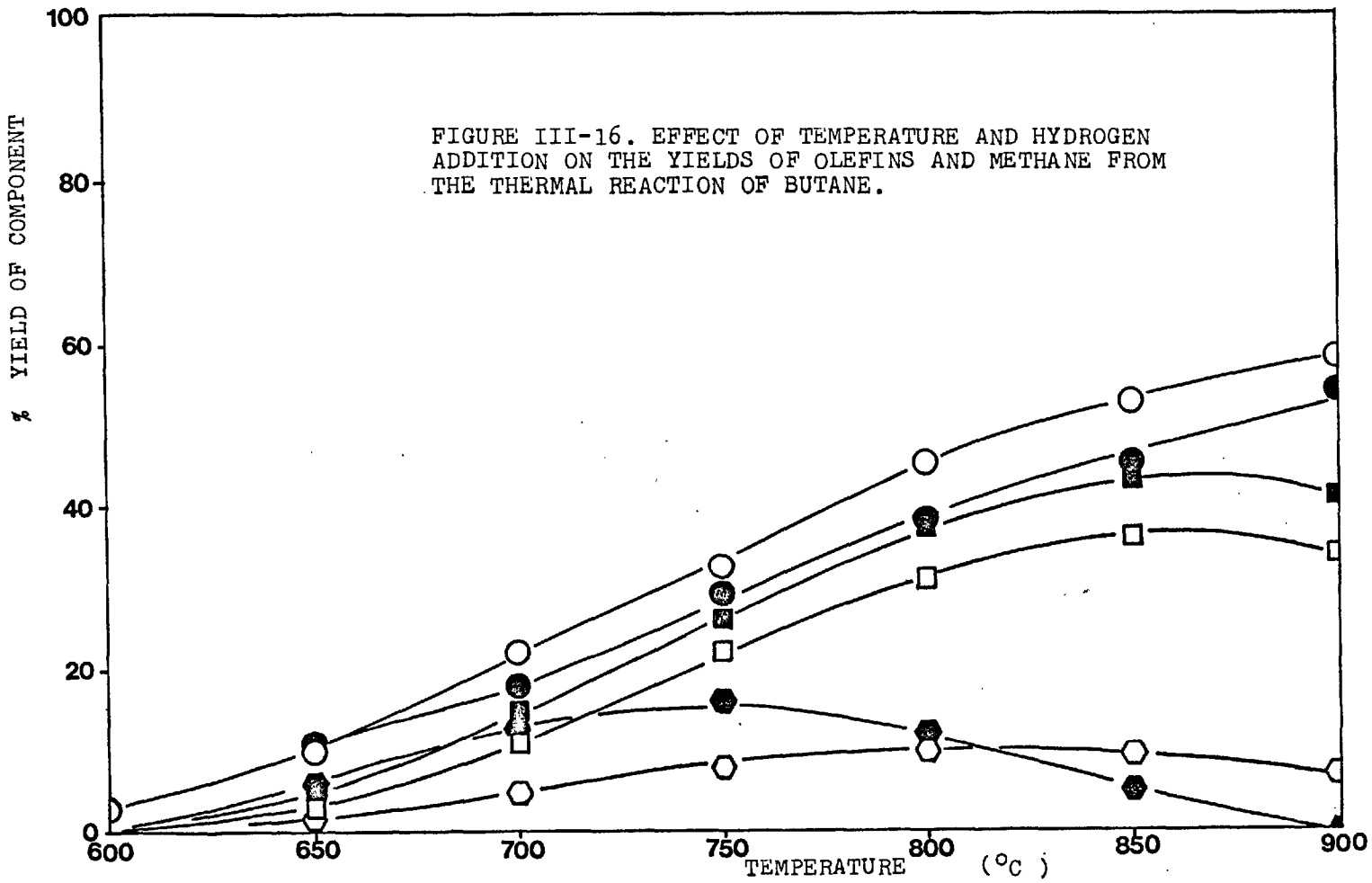
The use of small metal foils inside the reactor to measure the rates of carbon deposition (probably having a catalytic role, see later) raises the question of whether there is any effect of the nature of the sample foil on the gas products spectrum. Figure III-17 gives the product distribution at different temperatures from experiments where Ni and copper foils were used: no significant difference was found between the two cases.

d- The effect of gas residence time

The residence time has been defined in this work as the







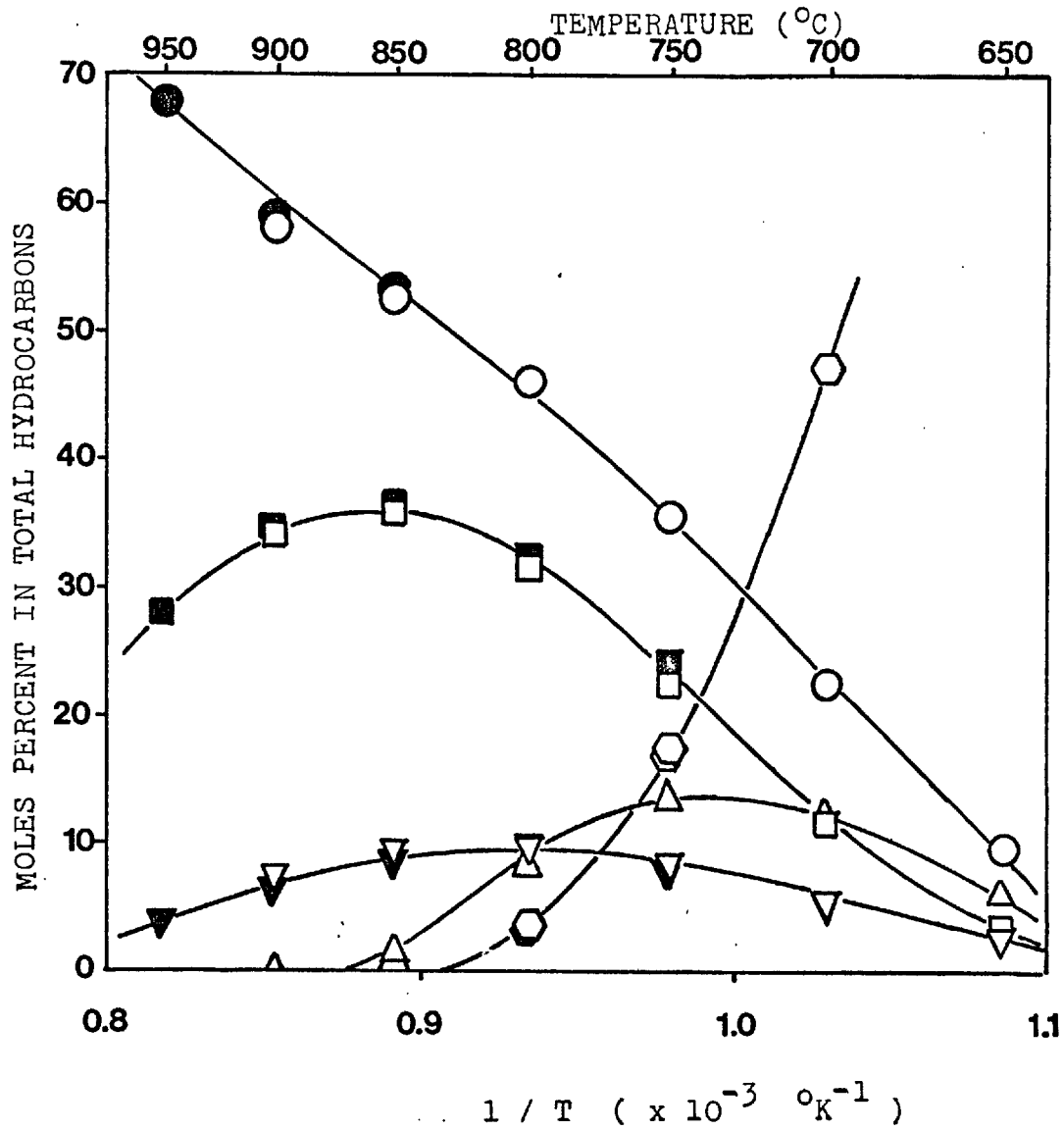


FIGURE III-17. THE EFFECT OF TEMPERATURE AND SAMPLE FOIL MATERIAL.

volumetric flow of reactants at the temperature of the reactor (but before suffering expansion by chemical reaction) divided by the volume of the reactor.

The effect of residence time on products composition at different temperatures when pure butane is reacted, is shown in figures III-18 to III-20. Methane and hydrogen yields were found to increase with residence time. Propylene and ethylene went through a maximum, followed by a decay at longer residence times. Ethane was found to reach a constant concentration, after the early formation stages.

Figure III-21 shows the effect of residence time when butane-hydrogen mixtures were pyrolyzed at 800 ° C. The behaviour is similar to pure butane pyrolysis.

e- The effect of metal liners on the reactor wall

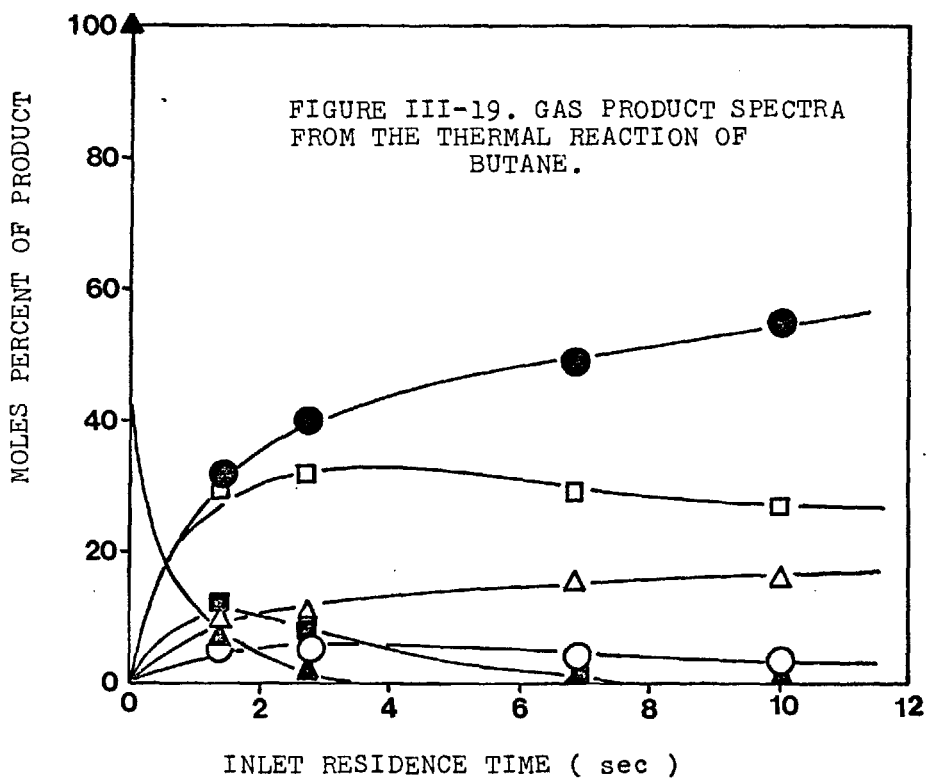
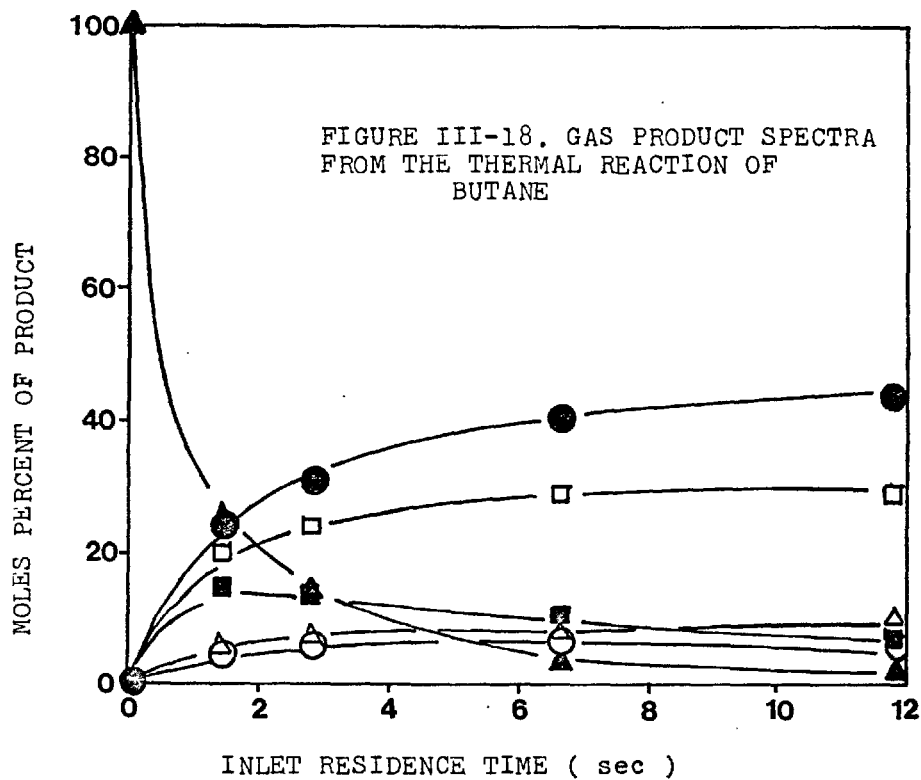
Experiments were performed in which metal foils were placed inside the reactor against the wall. Samples of the outlet stream were analyzed as a function of time on-line.

The results are presented in figure III-22. There is an appreciable difference between the gas compositions from different metal liners during the early stages of reaction. A decreased yield of methane and ethylene, and an increased production of hydrogen is observed when results from iron-lined reactor are compared with copper-lined reactor products spectrum. When time increased, the differences died off, indicating that both reactors give the same composition of gas products in the steady state.

f- Minor compounds in the route towards aromatics

Composition trends of minor gaseous hydrocarbons that appeared





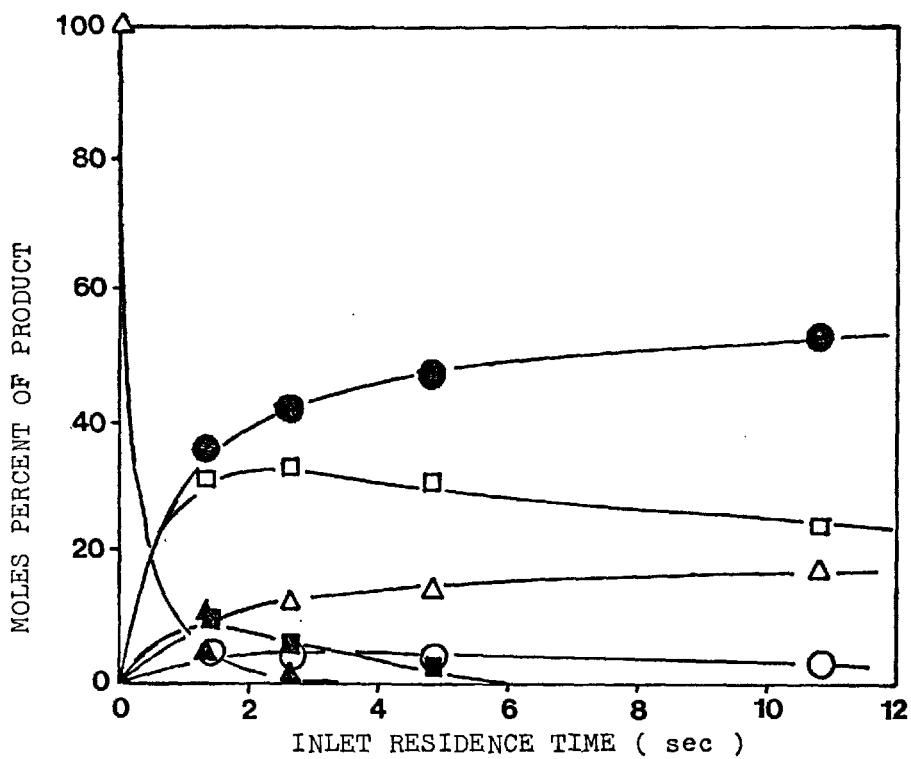


FIGURE III-20. GAS PRODUCT SPECTRA FROM THE THERMAL REACTION OF BUTANE.

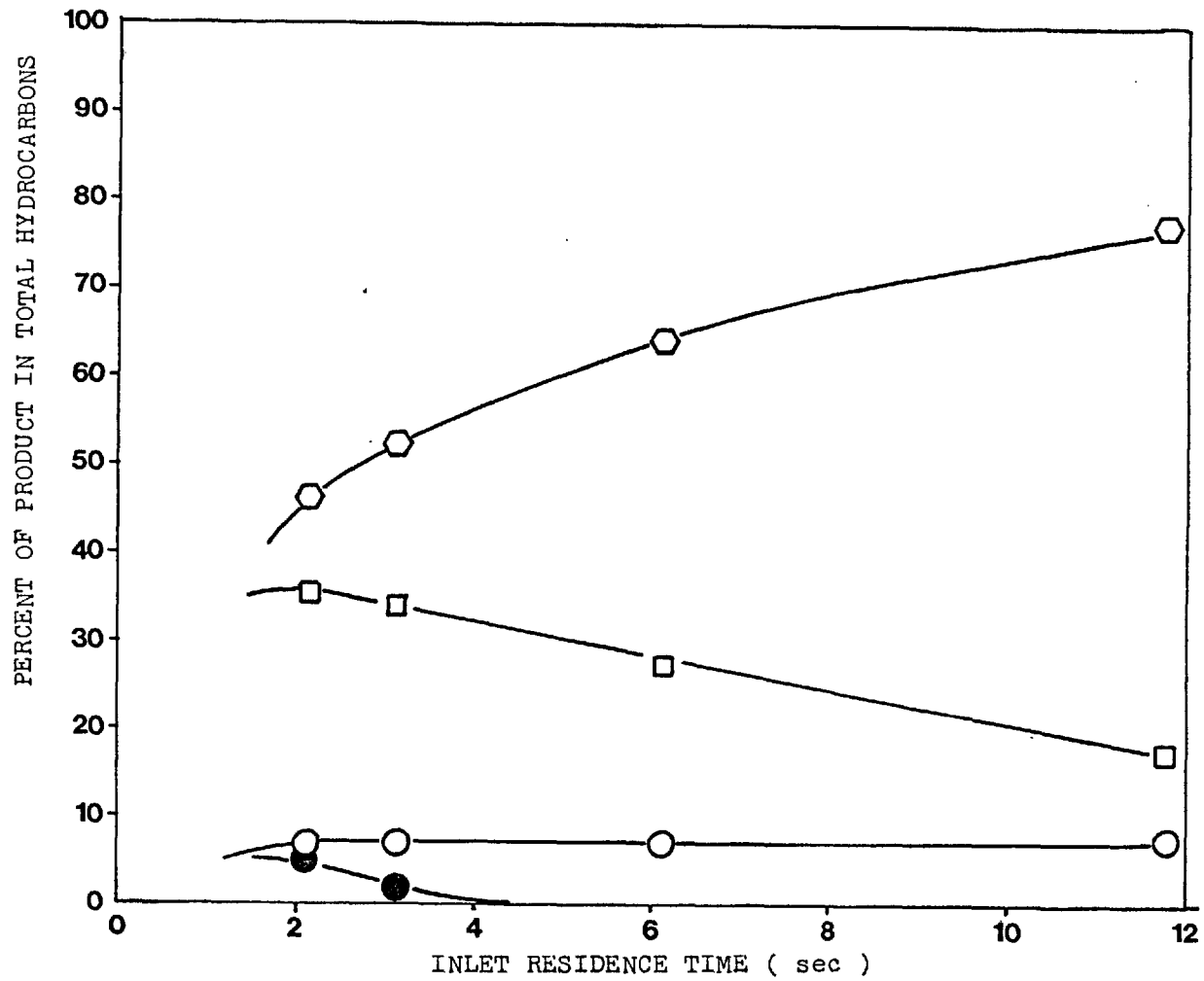
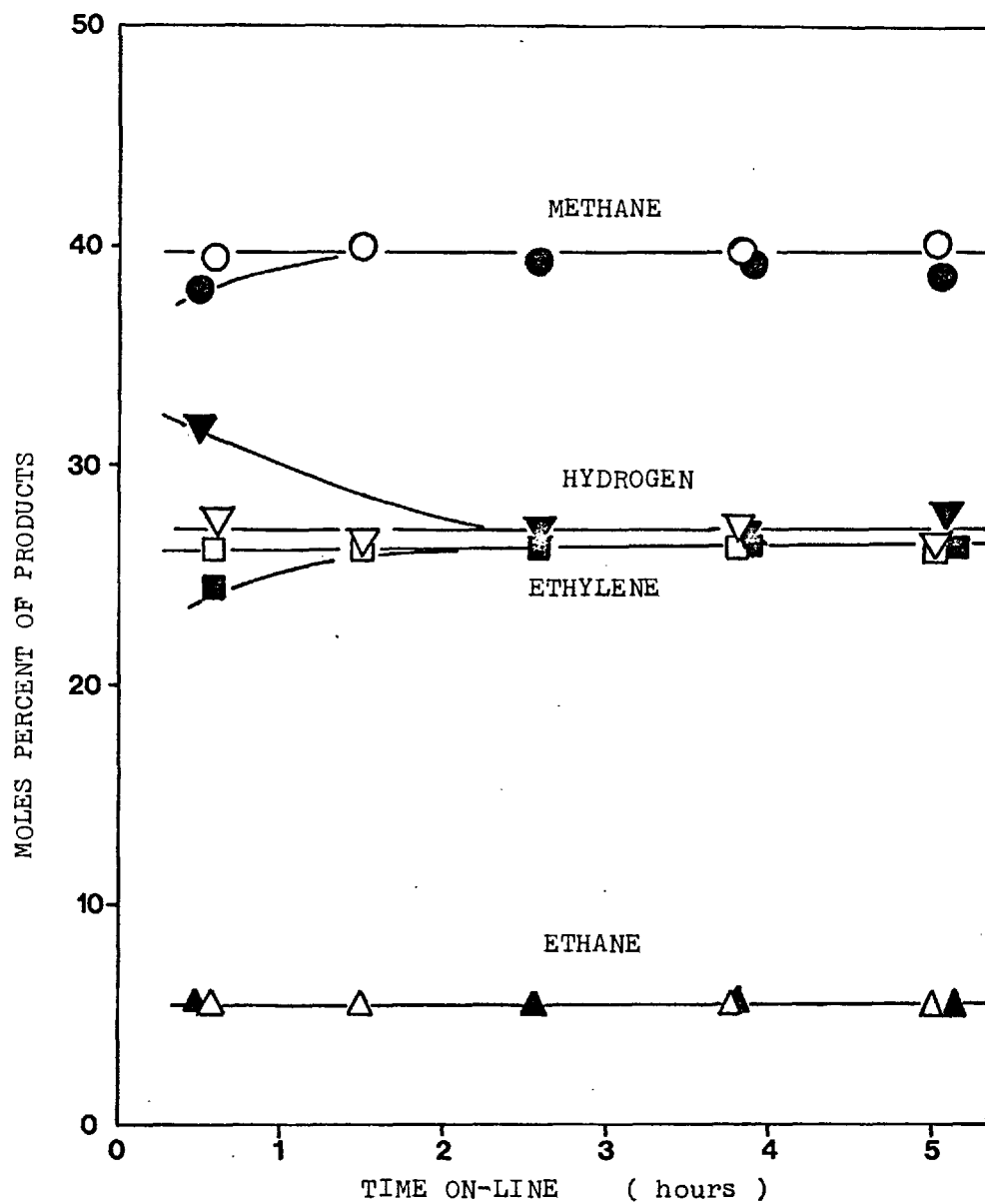


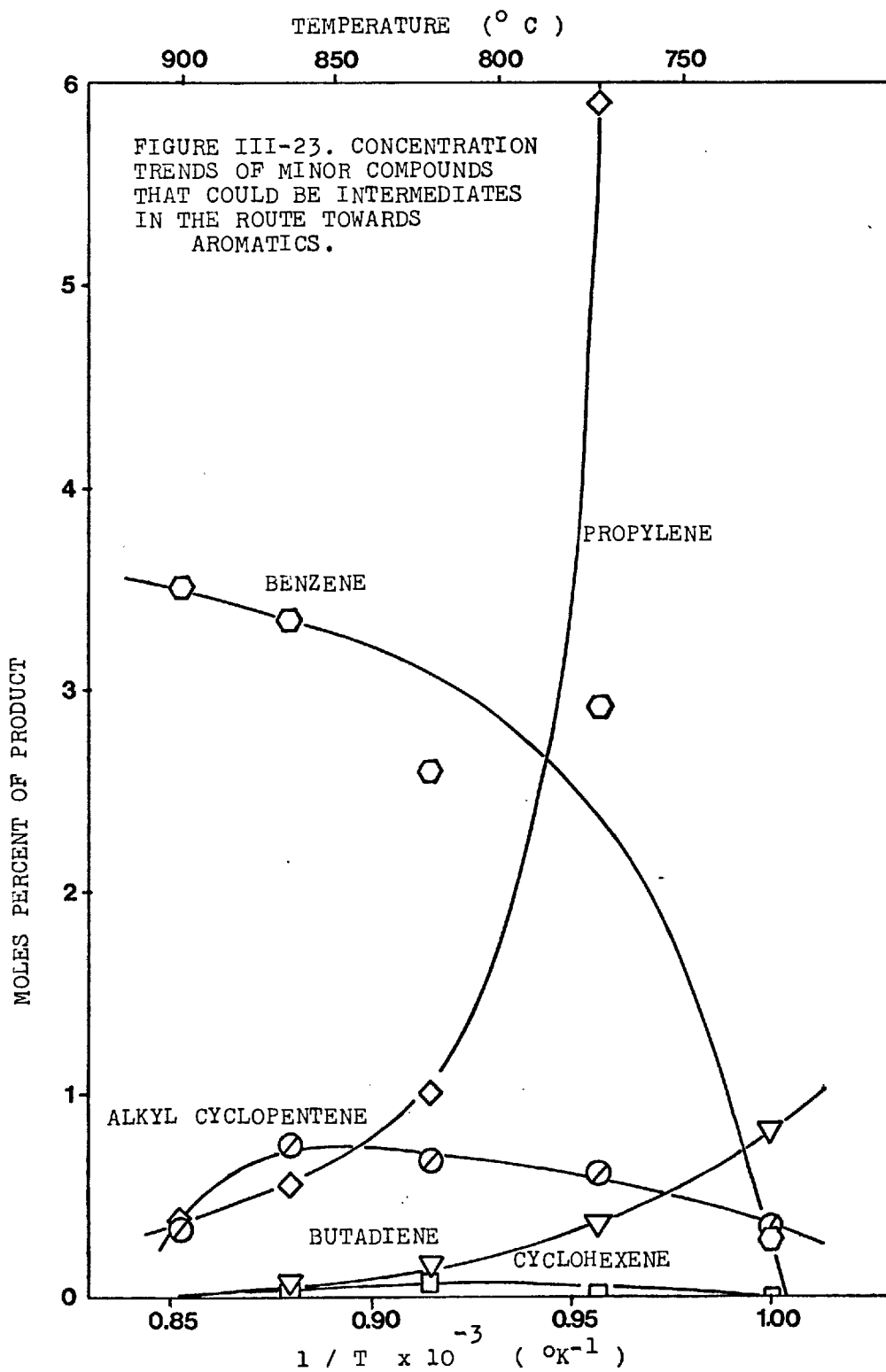
FIGURE III-21. EFFECT OF RESIDENCE TIME AND HYDROGEN ON THE PRODUCTS COMPOSITION.

FIGURE III.22. THE EFFECT OF METAL LINERS.  
GAS COMPOSITION CHANGES DURING TRANSIENT

in the reactor outlet gas stream may give indications as to the mechanism of formation of aromatics. Figure III-23 shows the composition spectrum of minor compounds as a function of temperature, revealing the presence of several potentially aromatics forming intermediates. The appearance of benzene is also shown.

g- The effect of the surface to volume ratio in the reactor on the gas product composition.

Figure III-24 show the effect of modifying the surface to volume ratio on the main products distribution. Changes of composition are of the order of 6 to 7%. The production of ethylene, propylene and ethane increased with surface to volume ratio, while a decrease is noticed in methane and benzene production.



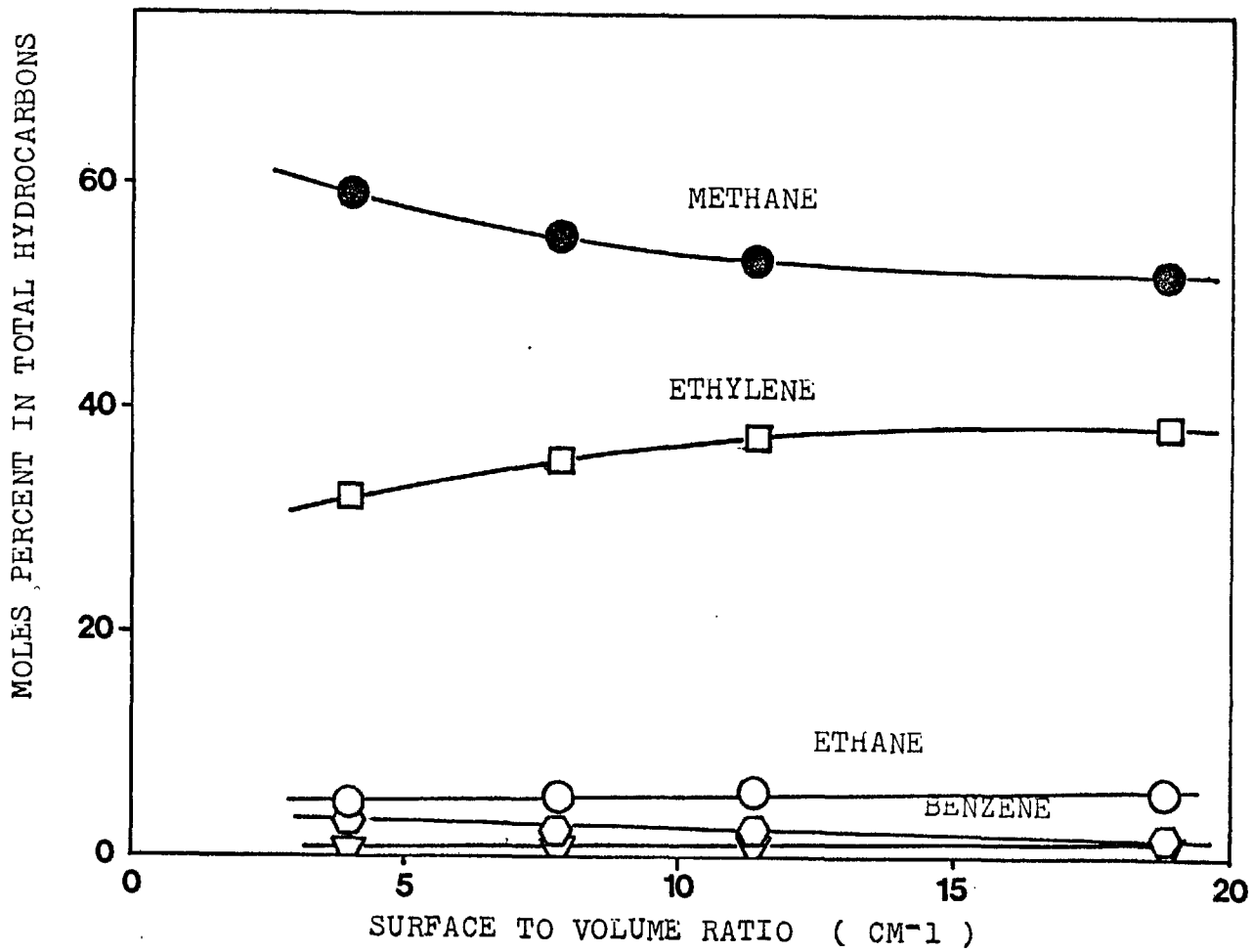


FIGURE III-24. THE EFFECT OF SURFACE TO VOLUME RATIO IN THE REACTOR ON THE GAS PRODUCT COMPOSITION.

B THE PRODUCTION OF AROMATIC COMPOUNDS DURING THE THERMAL REACTIONS  
OF BUTANE.

Information on the amounts of liquid aromatics condensed in the reactor outlet, as well as its composition, were obtained in the tubular flow microbalance reactor. These aromatic compounds (ranging from benzene to 2-3 benzopyrene) could act as precursors for carbon formation during pyrolysis under the conditions studied. In industrial conditions, these can also deposit solid carbonaceous material on the walls of cooling equipment, by physical condensation of heavy aromatics.

a- Effect of the residence time.

The total mass concentration of aromatics in the outlet gas stream for the pyrolysis of a butane:hydrogen mixture is shown as a function of the residence time in figure III-25. The general shape of the curve is a sharp rise from a positive, non-zero value of the residence time, increasing to a maximum and then decreasing slowly at longer residence times. The duplicated values at  $\tau=2$  and 12 seconds show that the reproducibility of the values is poor. This is probably due to imperfect collection of the tars in the liquid trap.

The composition of the liquids collected at different residence times is given in figure III-26. Changes in the relative composition of the condensates are observed. The proportion of benzene is approximately constant; polynuclear aromatics increase, while substituted benzene compounds decrease with residence time.

A clearer picture of the reaction trend can be gained from the actual concentration of each compound at the outlet of the reactor. These concentrations can be calculated from the amount and composition of the condensates and the results are presented in



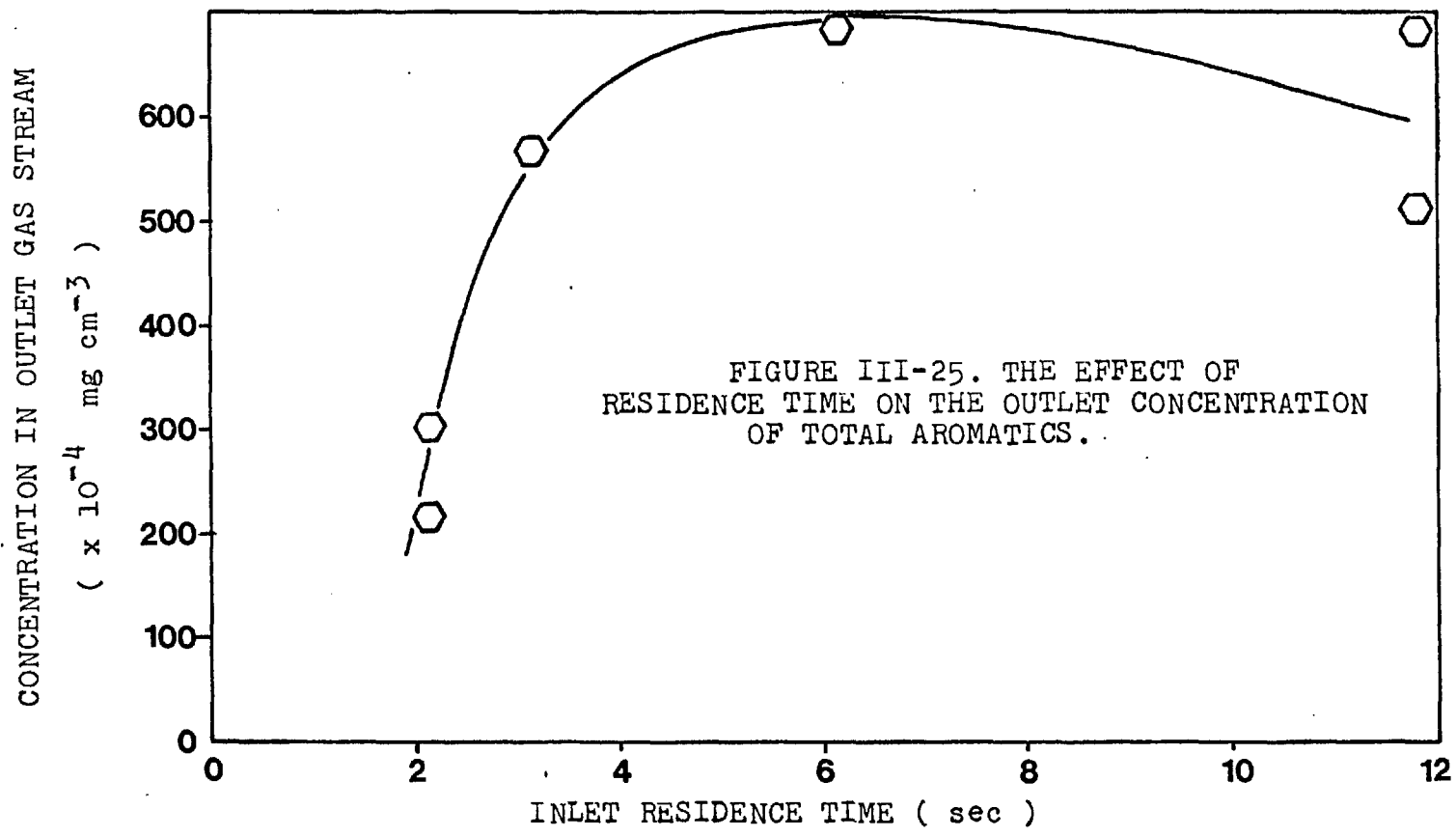


FIGURE III-25. THE EFFECT OF RESIDENCE TIME ON THE OUTLET CONCENTRATION OF TOTAL AROMATICS.

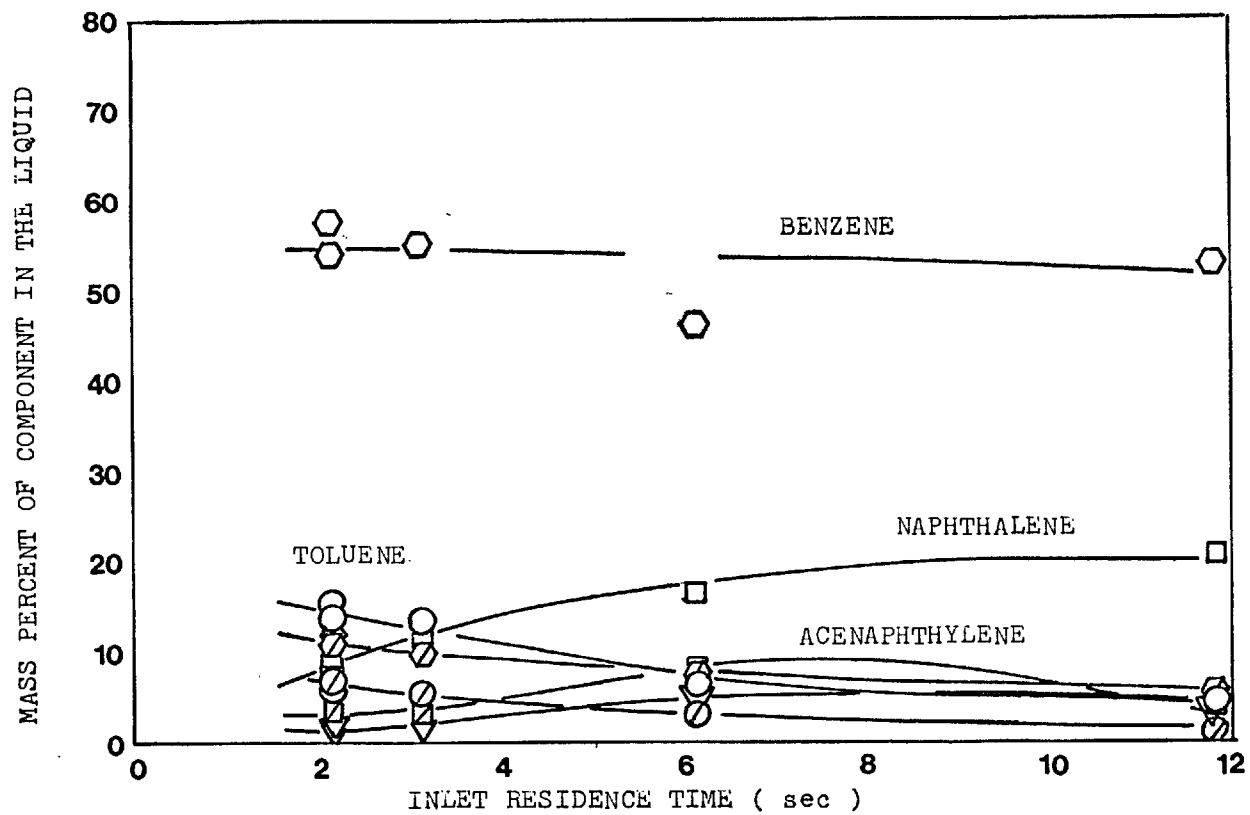


FIGURE III-26. EFFECT OF RESIDENCE TIME ON THE COMPOSITION OF THE AROMATIC LIQUID COLLECTED AT THE REACTOR OUTLET.

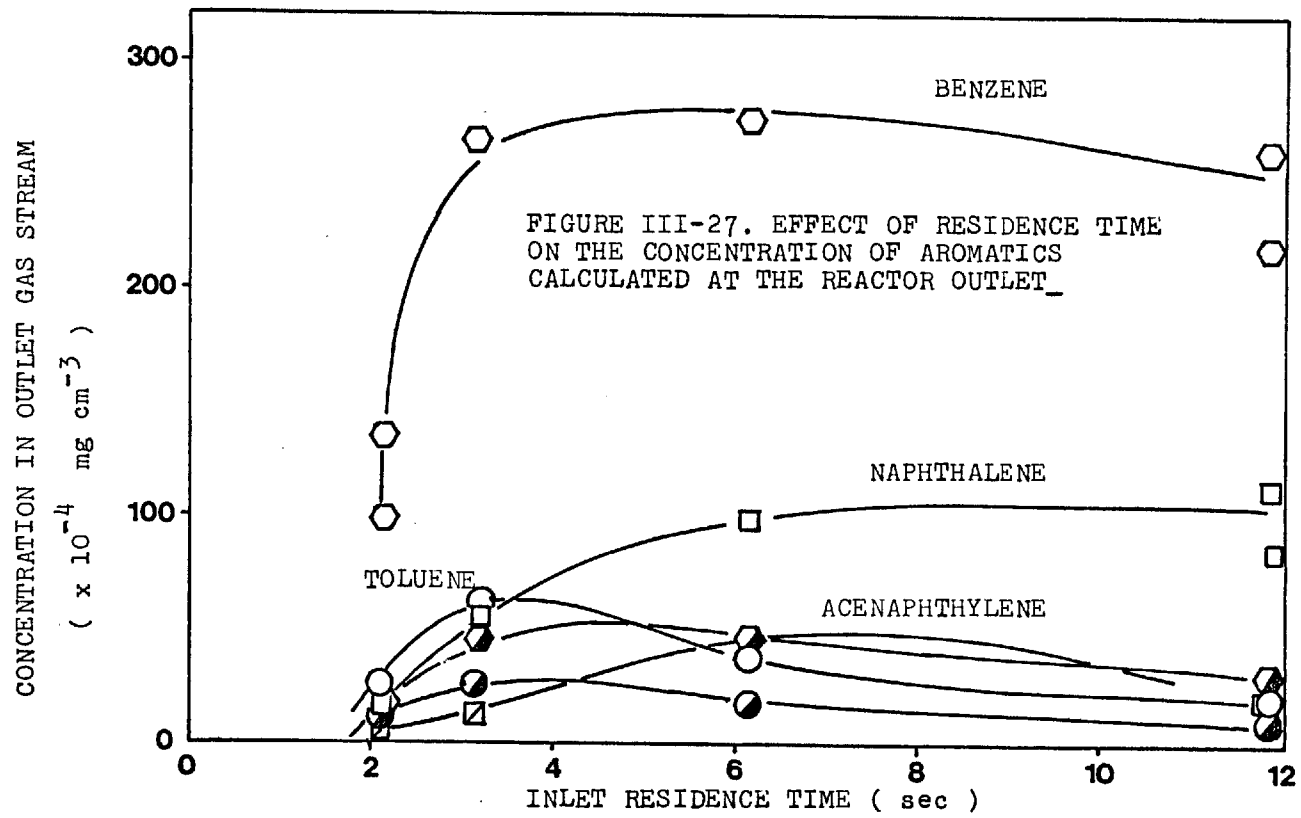


figure III-27.

All aromatics start to be formed at a certain threshold of residence time and their concentration grows with time. Substituted benzene compounds (toluene, ethylbenzene and methyl-propyl benzene) go through a maximum with residence time and their concentrations decay at longer times. Benzene also reaches a maximum, but its decay is slower with time.

Naphthalene concentration grows with time and does not reach a maximum in the concentration range studied. The same happens with anthracene-phenanthrene and chrysene (not shown). Acenaphthylene concentration goes through a maximum followed by decay.

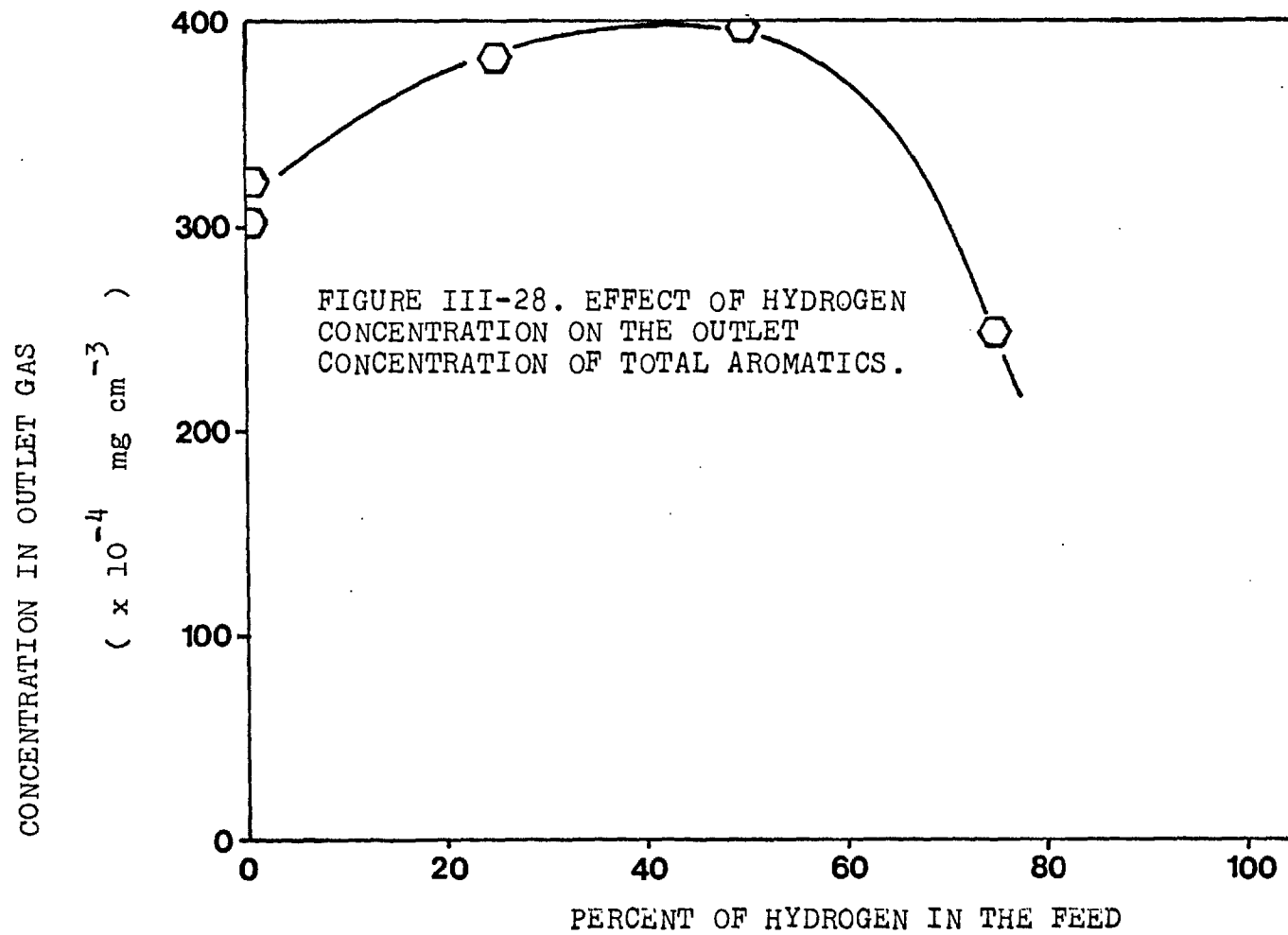
b- Effect of hydrogen concentration.

The effect of hydrogen at 25 % molar concentration of butane was studied using helium as a diluent.

Figure III-28 shows that the total liquid concentration in the reactor outlet has a maximum at intermediate concentrations of hydrogen. The composition of the liquids collected show that higher proportions of benzene are favoured by increasing the concentration of hydrogen. (Fig. III-30).

Concentrations of benzene have a maximum at 50 % of hydrogen in the feed, decreasing at higher concentrations of hydrogen. Higher polynuclear aromatics decrease with hydrogen (fluorene, acenaphthylene and anthracene) while naphthalene, toluene and ethylbenzene present a maximum at intermediate concentrations of hydrogen, but this is less marked than in the case of benzene.

c- Effect of butane inlet concentration in mixtures with hydrogen on the production of aromatics.



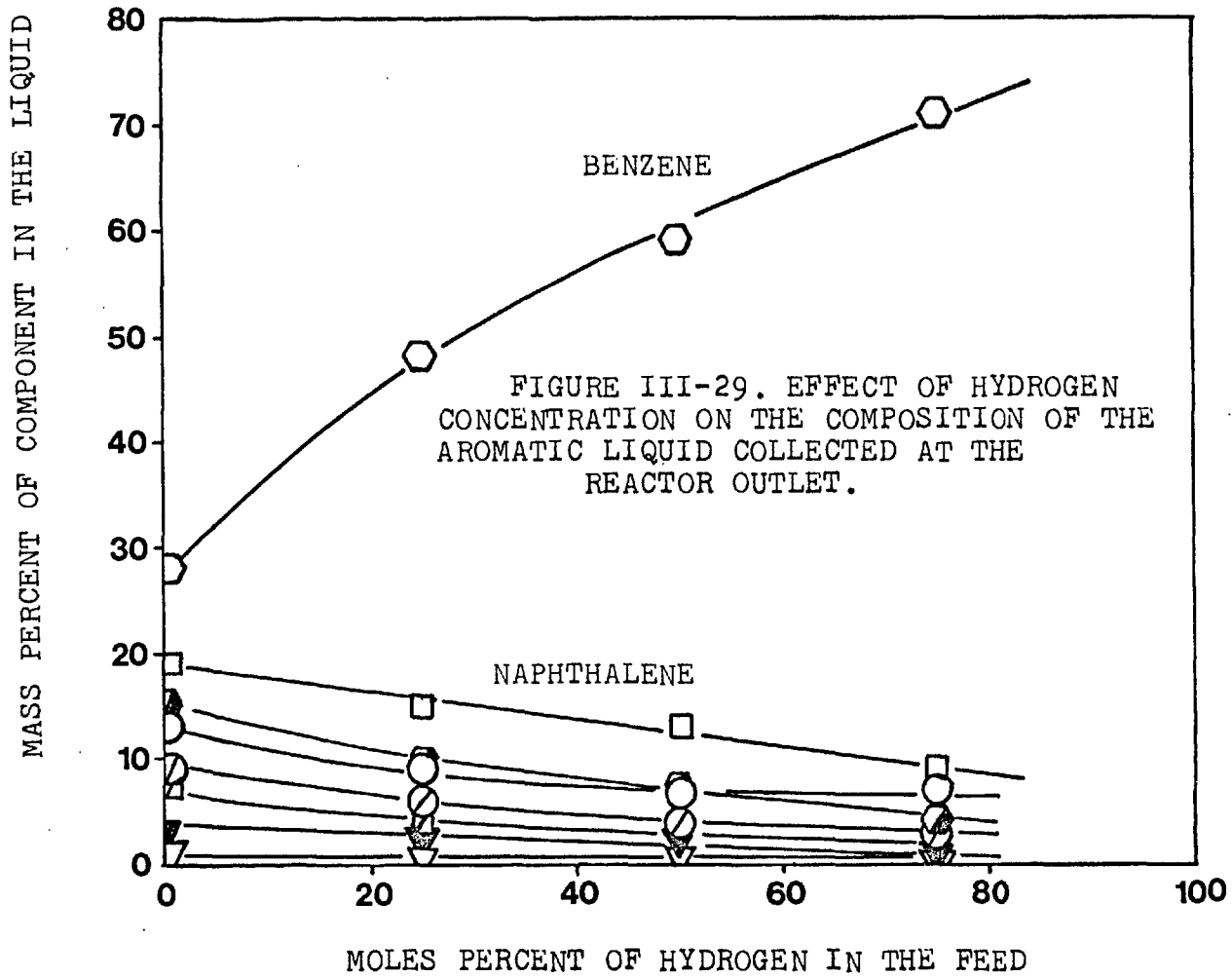
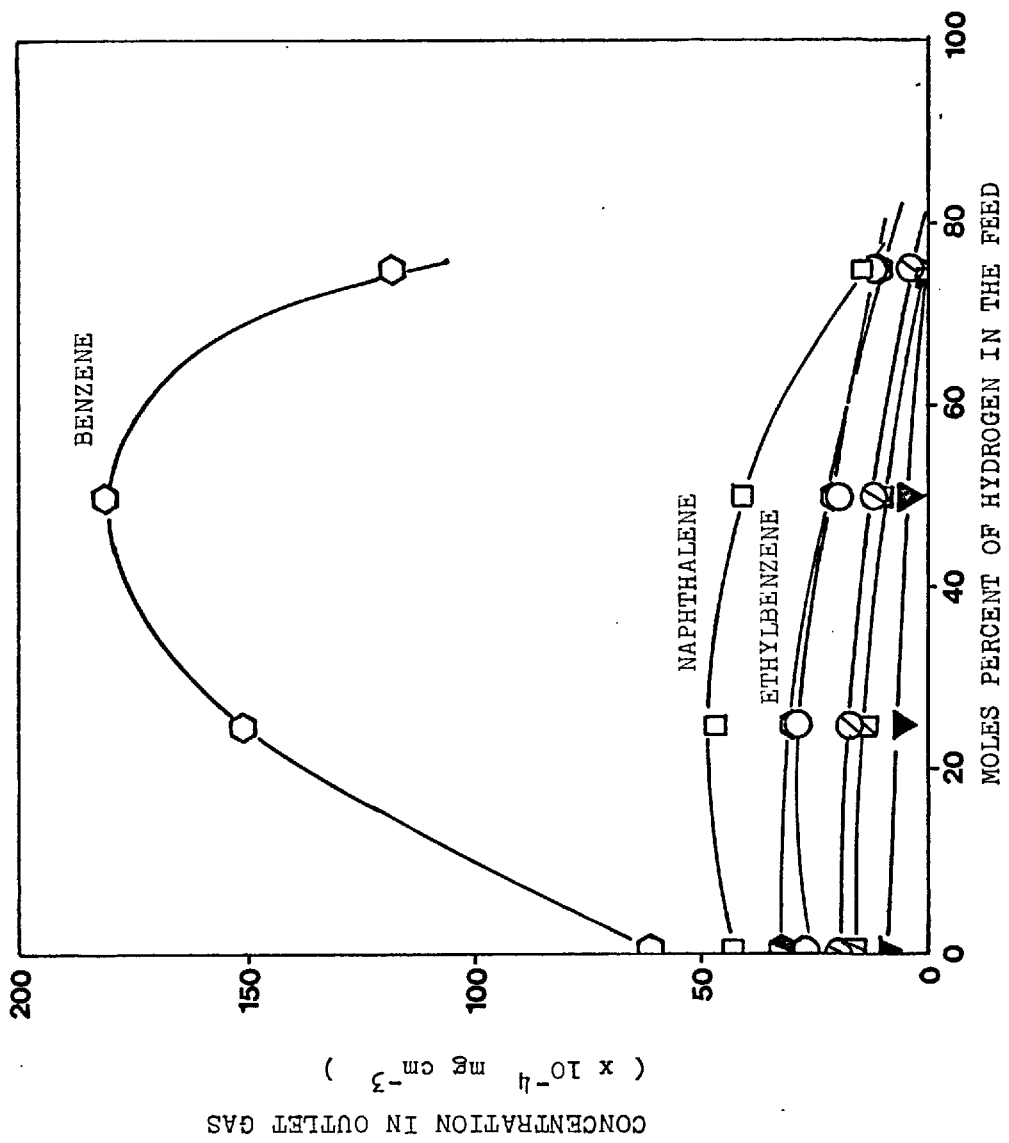


FIGURE III-30. EFFECT OF HYDROGEN CONCENTRATION ON THE COMPOSITION OF AROMATICS CALCULATED AT THE REACTOR OUTLET.



Figures III-31 and 32 show the effect of the initial concentration of butane on the production of aromatic compounds during the reaction. The effect in all cases is more complex than a linear relationship, being more than first order with respect to the initial concentration of reactant at low percentages of butane, and less than first order in the higher concentrations. The production of heavier polycyclic aromatics is favoured by high butane proportions in the initial mixture.

d- Effect of temperature

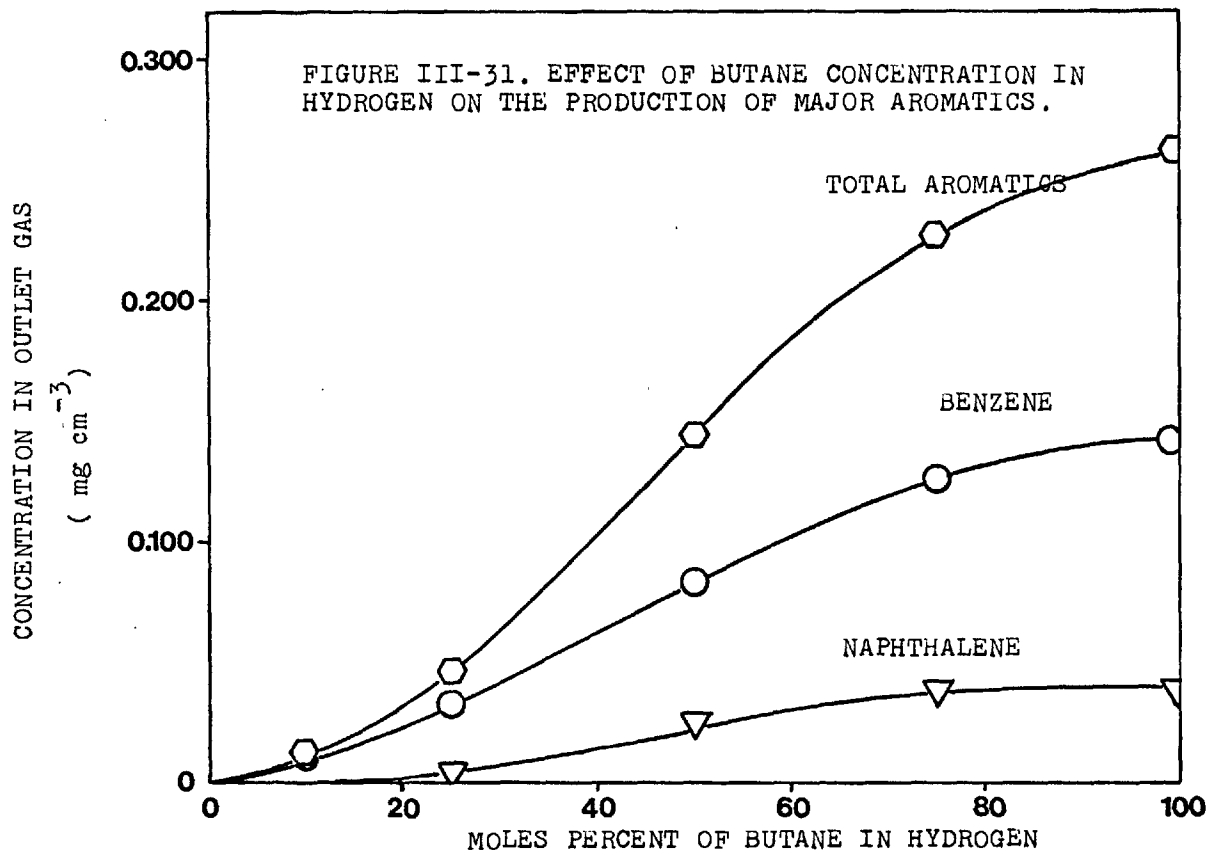
The effect of temperature on the production of aromatics during the thermal reactions of butane was studied with mixtures of 50 % hydrocarbon in hydrogen or helium.

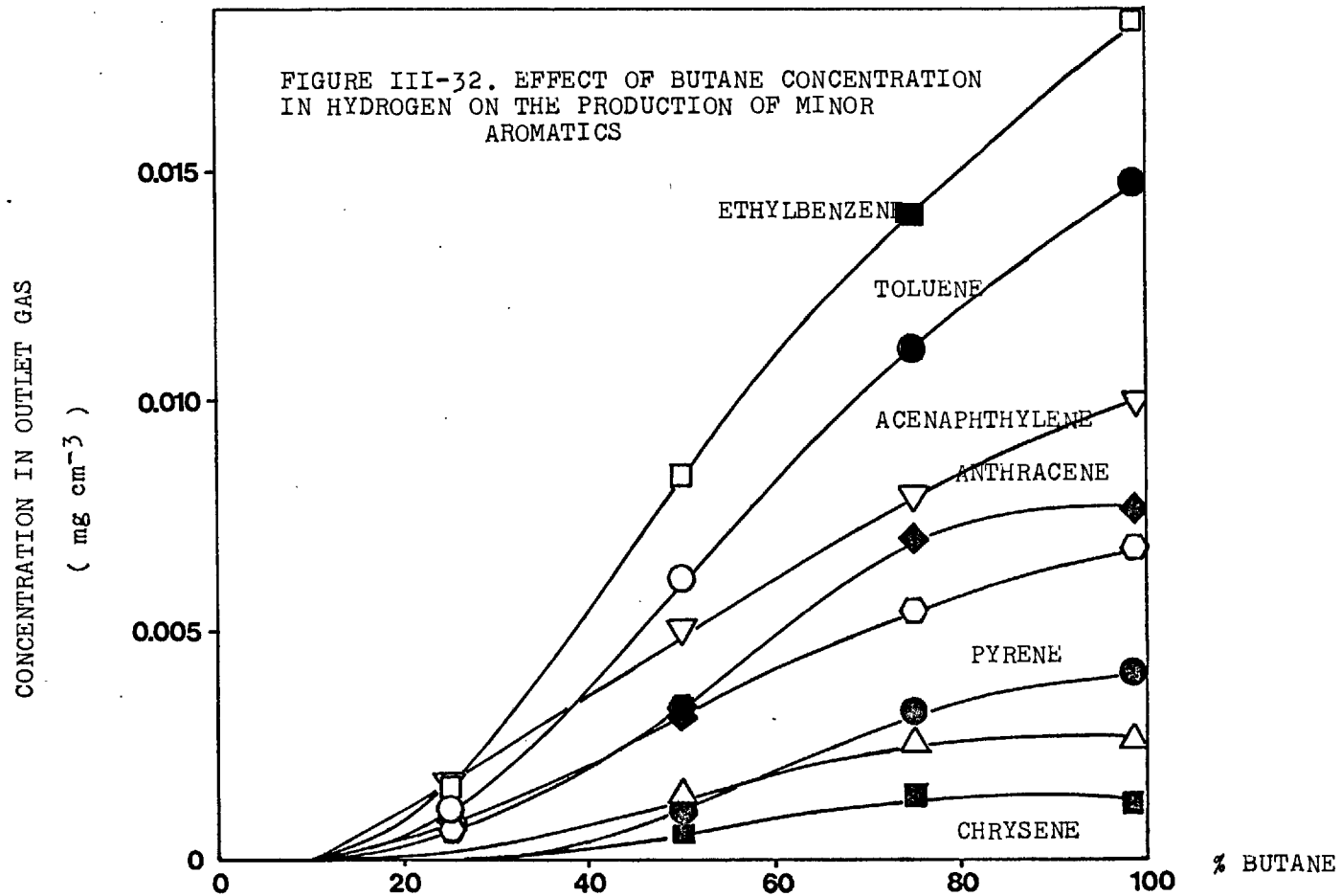
The rate of total production of aromatics as a function of temperature is presented in figure III-33. Within the range of temperatures under study, the rate of aromatics formation was found to increase with temperature. The presence of hydrogen in this case decreased the rate of formation at temperatures below 800 °C, while no appreciable effect is shown at higher temperatures.

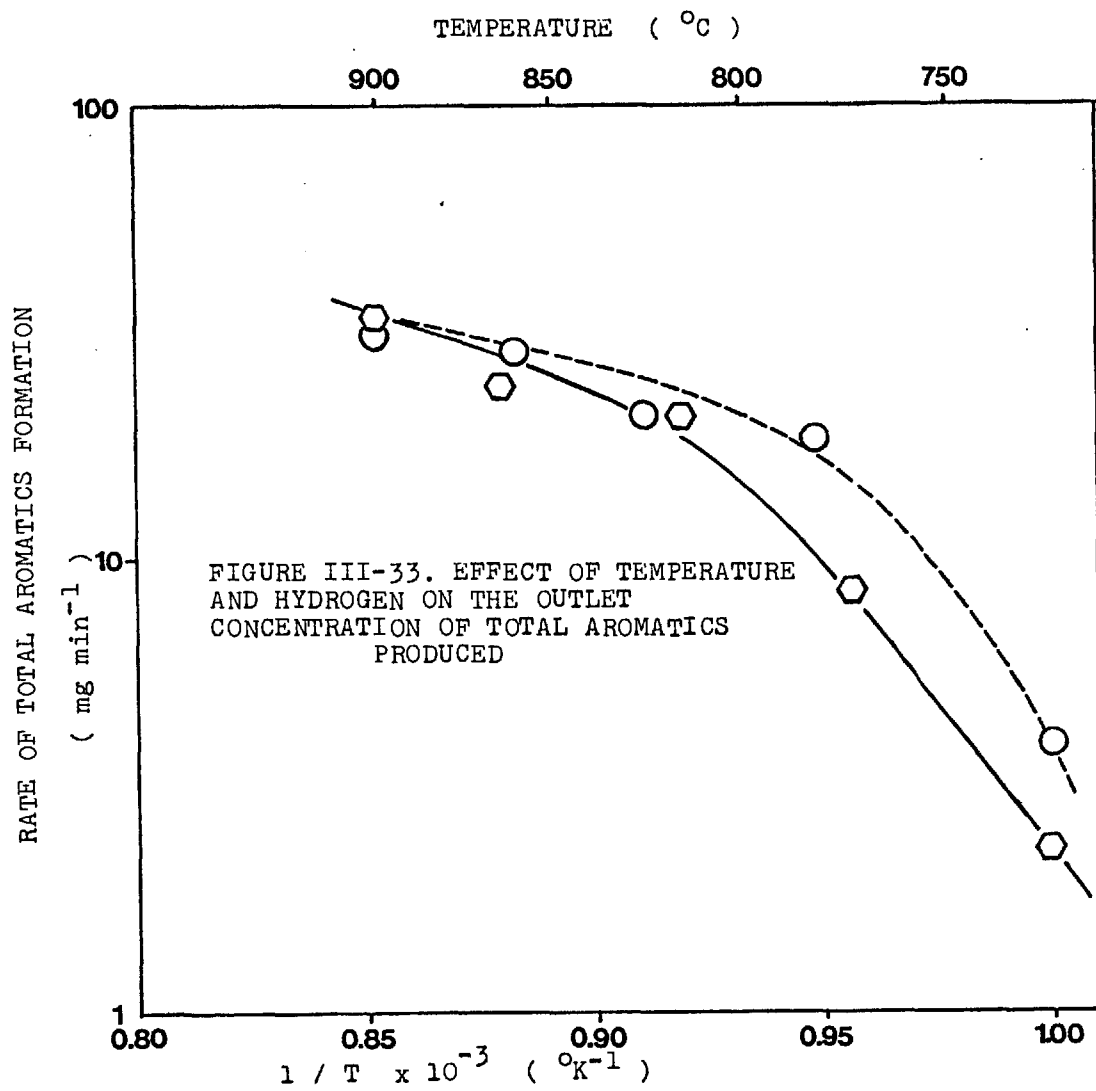
The composition of the condensates collected during the experiments is shown in figures III-34 and III- 35 In both series of runs, the proportions of benzene and toluene were found to decrease with increases of temperature, while naphthalene showed the opposite behaviour, increasing with temperature. Hydrogen was found to increase the proportion of benzene in the liquid, the toluene decreasing at the same time.

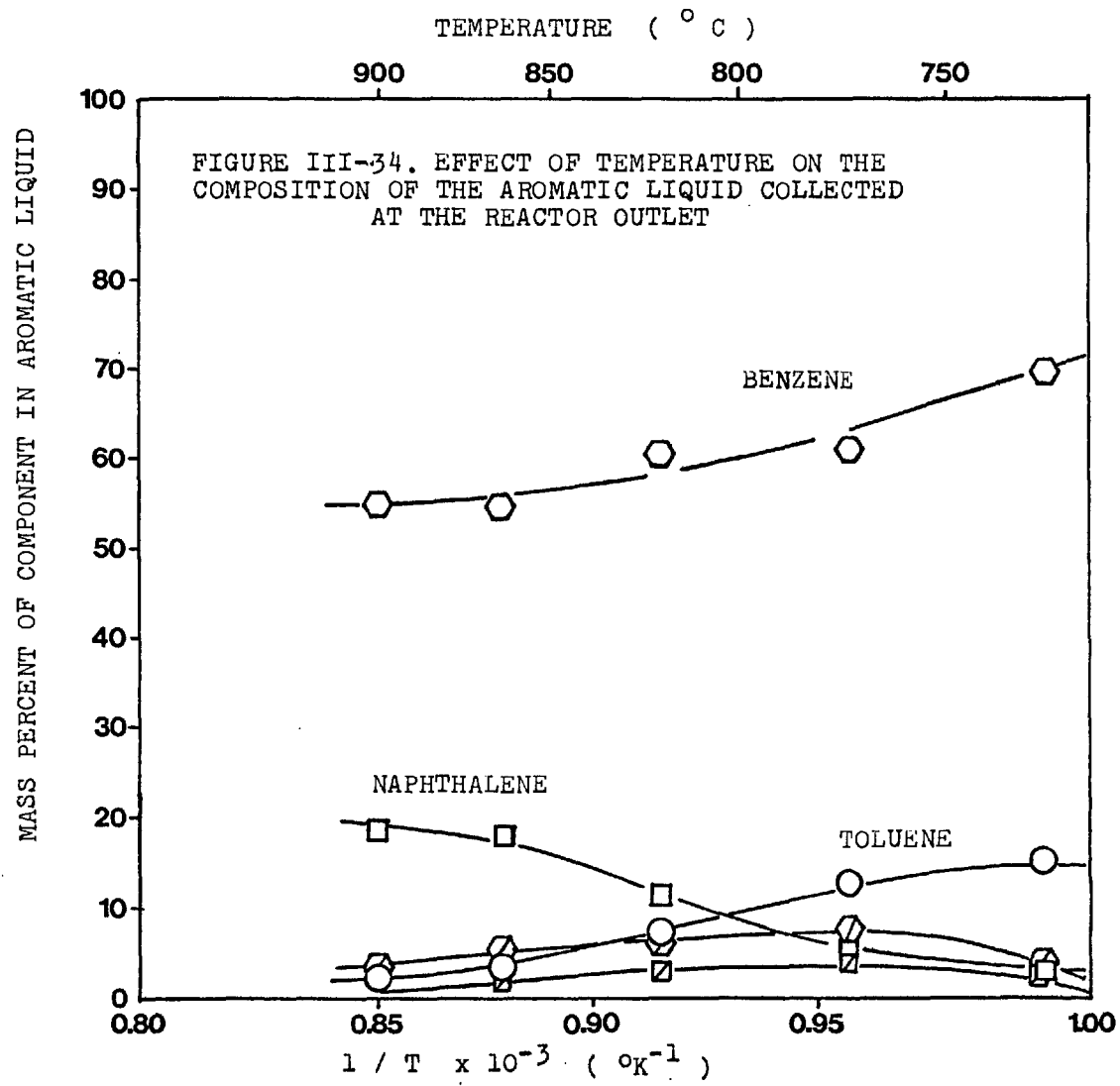
The effect of temperature and hydrogen on the concentration of benzene and naphthalene in the outlet stream is shown in figure III-36. The effect of hydrogen is to increase the concentration of naphthalene.

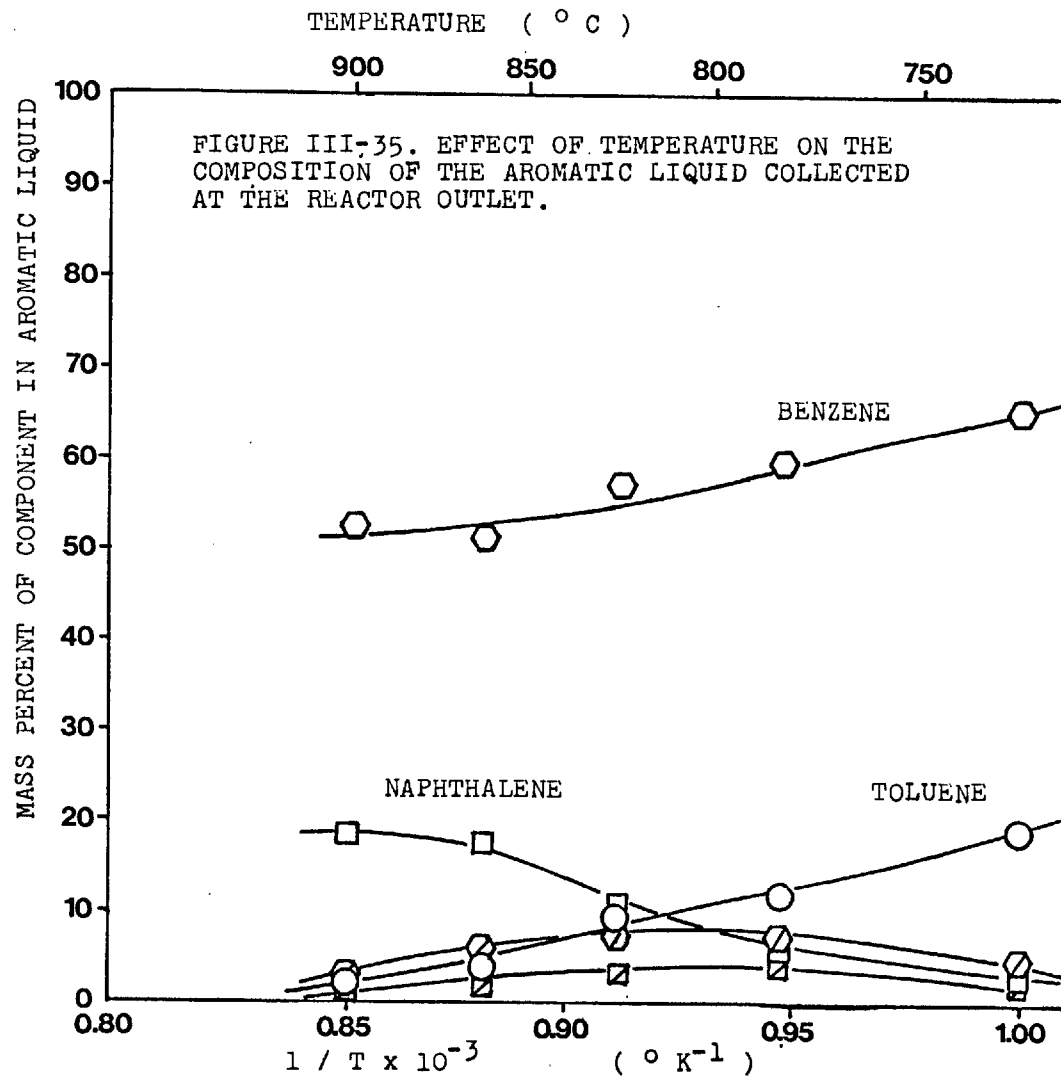


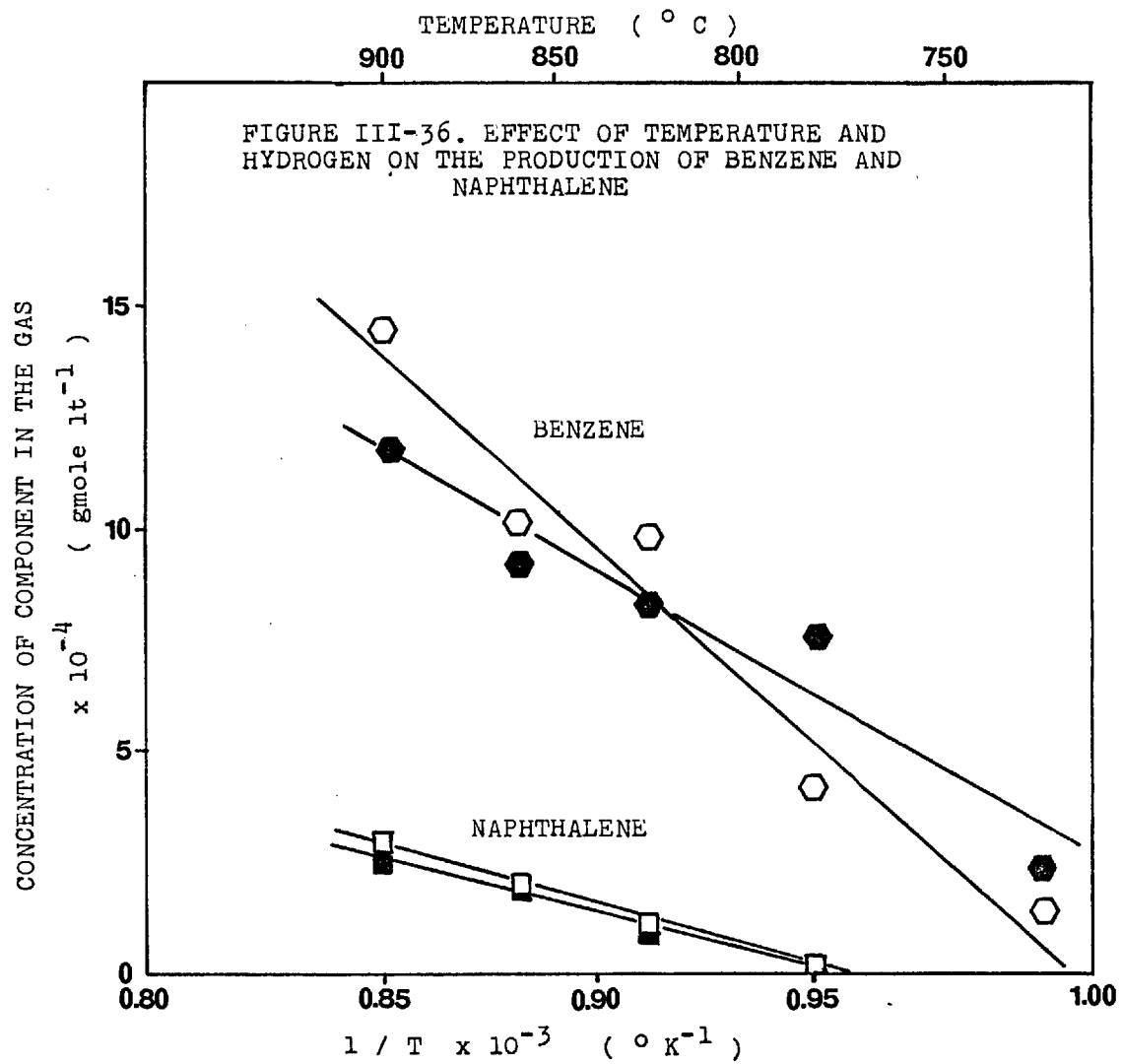












With benzene the effect is to decrease the concentrations at low temperature and to increase them at higher temperatures, with respect to the results obtained with helium as a diluent. The temperature at which the concentrations from both series of results are equal is about 820 °C.

e- Effect of metal liners in the reactor wall during the transient period

The study of the effect of the nature of the reactor wall on the production of aromatics was performed at constant conditions and collecting samples of condensate as a function of time on-line.

Figure III-37 shows the difference of behaviour between copper and iron liners in the production of aromatics. Results with copper show a fast increase of concentration, followed by slight changes, decreasing first and increasing later. Iron results show a definite delay in reaching the same values as copper, but yields are slightly higher later in the reaction. After one hour run, the results are approximately similar in both cases.

Changes in the composition of the liquid are shown in figure III-38. The results from copper lined walls are approximately constant throughout the experiment. Results from iron lined wall change as follows: at the early stages of reaction, benzene production is lower and naphthalene and toluene higher than the corresponding results from the copper lined reactor. Later the benzene proportion is higher and naphthalene lower than the constant copper results. Finally, the liquid composition become equal to the copper case for longer times.

Figures III-39 and III-40 present the results of outlet concentrations for several aromatics. In all cases, the values for iron lined reactors are lower in the early stages of reaction and tend to be

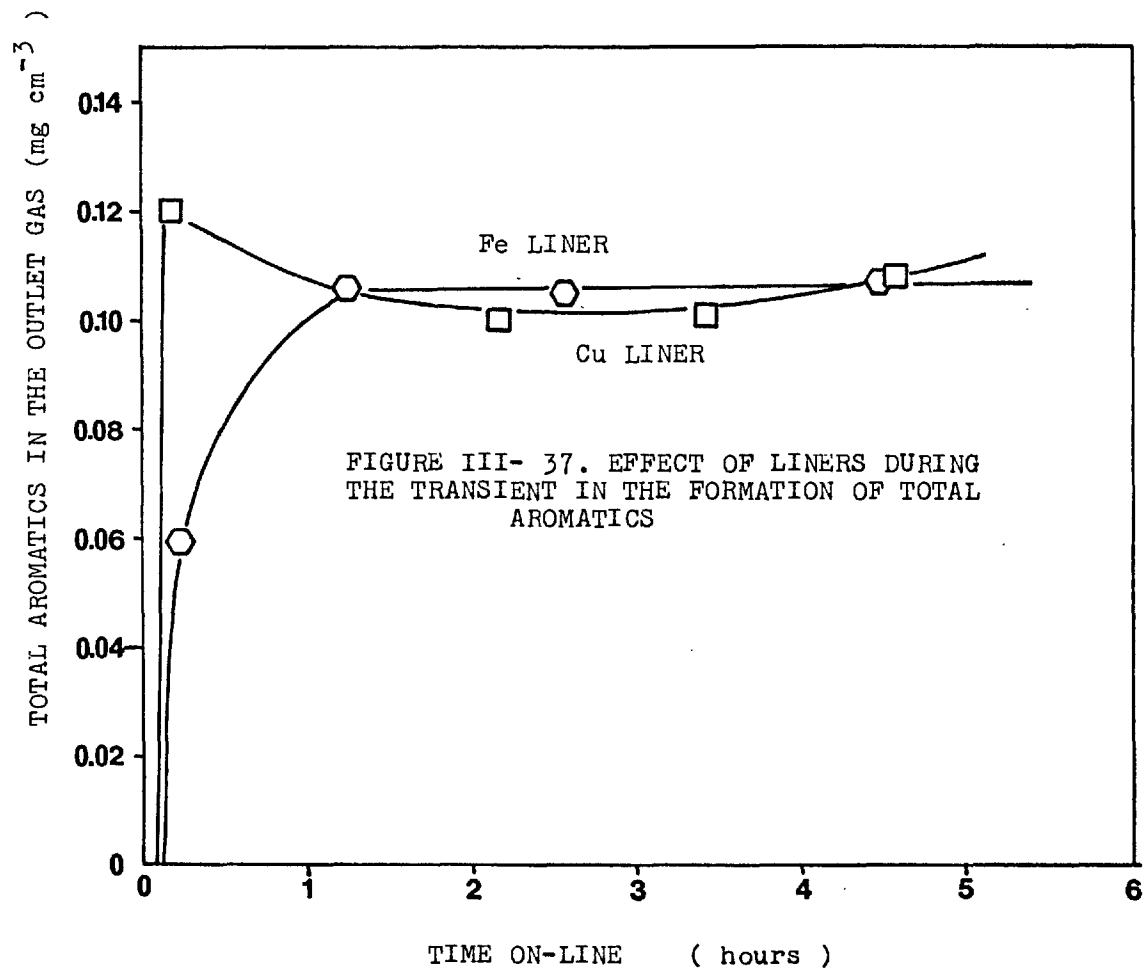
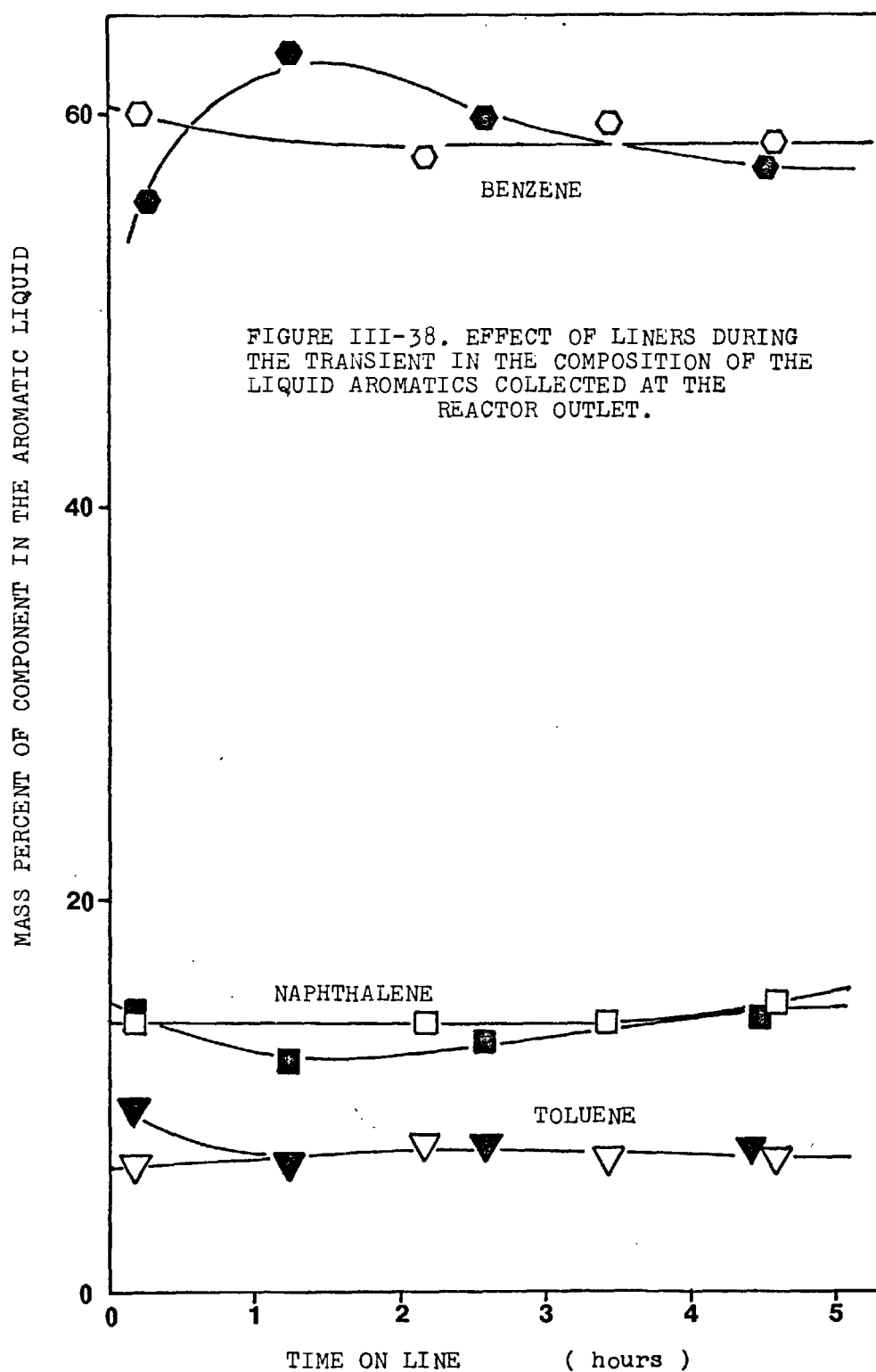
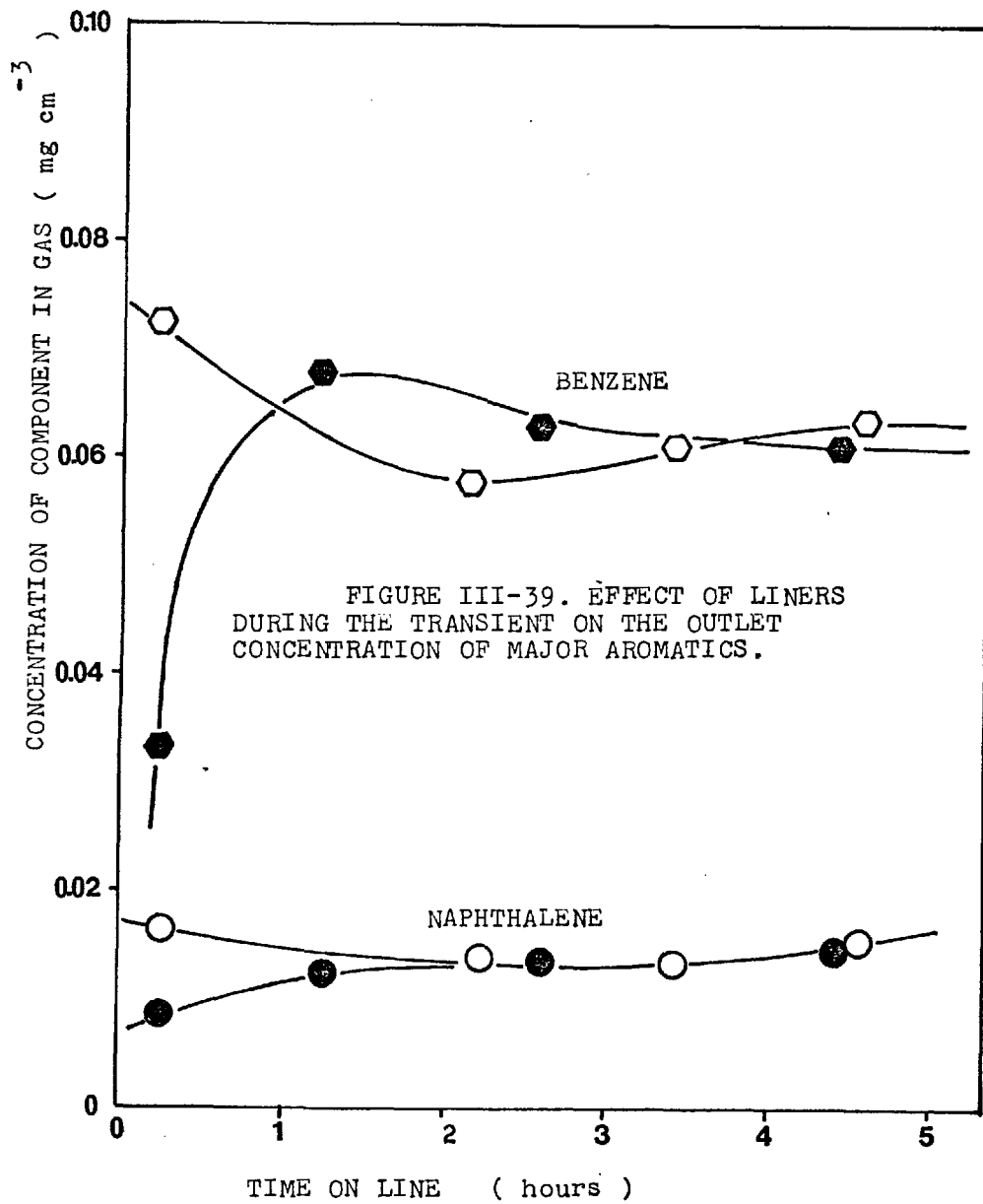
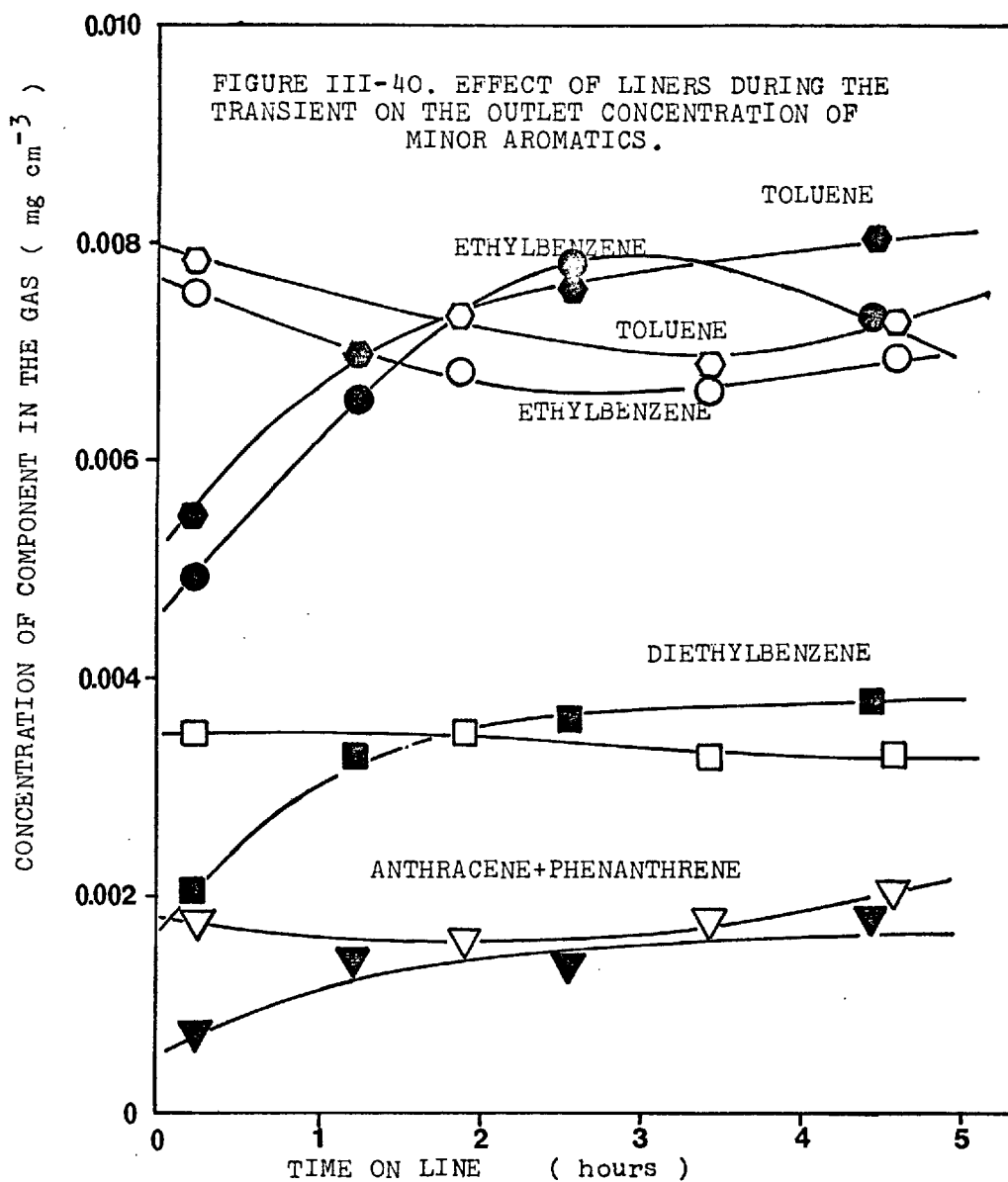


FIGURE III- 37. EFFECT OF LINERS DURING THE TRANSIENT IN THE FORMATION OF TOTAL AROMATICS







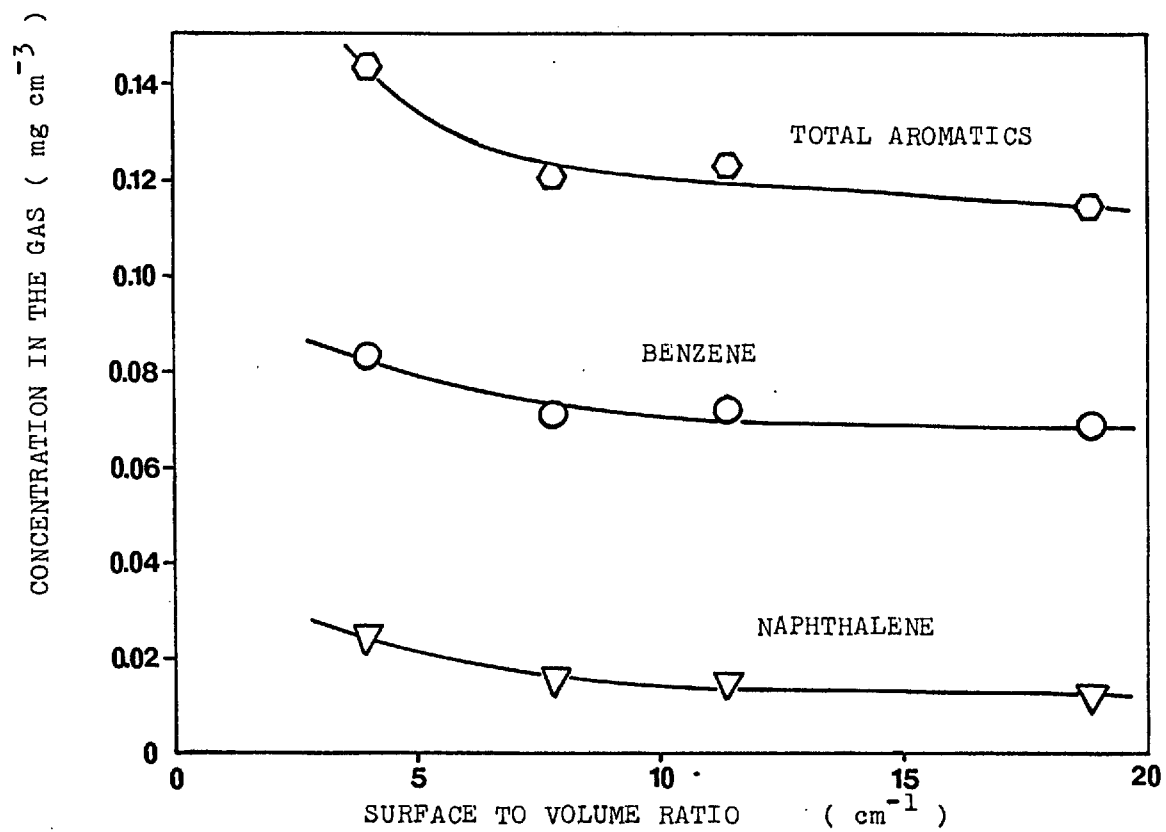


approximately equal at longer times.

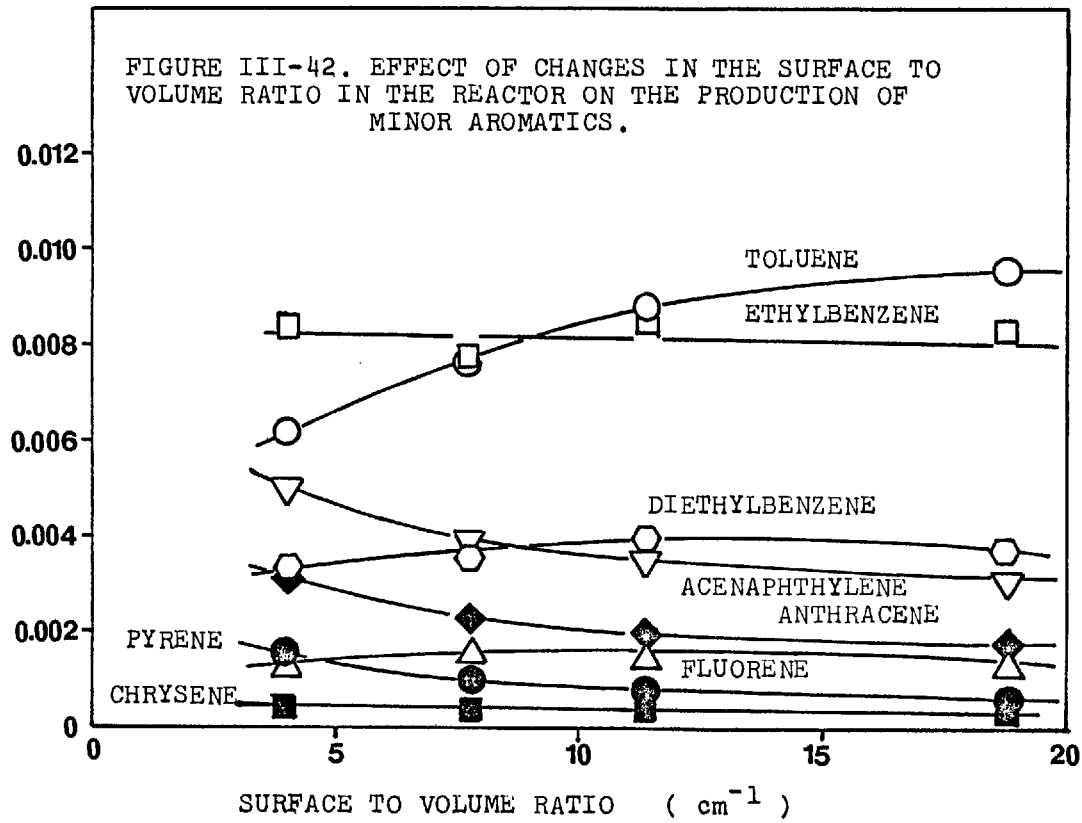
f- The effect of the surface to volume ratio in the reactor on the production of aromatics.

Changes in surface to volume ratio had an effect on the production of total and major aromatics, as shown in figure III-41. A decrease of the order of 20% was noticed in the production of total aromatics as a result of the changes in the ratio of surface to volume studied. The effect on the production of minor aromatics is shown in figure III-42. The production of acenaphthylene, anthracene, pyrene and chrysene decreased with increases of surface to volume ratio.

FIGURE III-41. EFFECT OF CHANGES IN THE SURFACE TO VOLUME RATIO IN THE REACTOR ON THE PRODUCTION OF TOTAL AND MAJOR AROMATICS.



CONCENTRATION OF PRODUCT IN THE GAS  
(  $\text{mg cm}^{-3}$  )



C- THE FORMATION OF CARBONACEOUS DEPOSITS DURING THE THERMAL REACTIONS OF BUTANE

1- EXPERIMENTS WITH PURE BUTANE

The first series of carbon formation runs was performed in the tubular microbalance reactor. Pure butane was reacted in the absence of any diluents. Analysis of the gas products or liquid condensates was not performed during this part of the work.

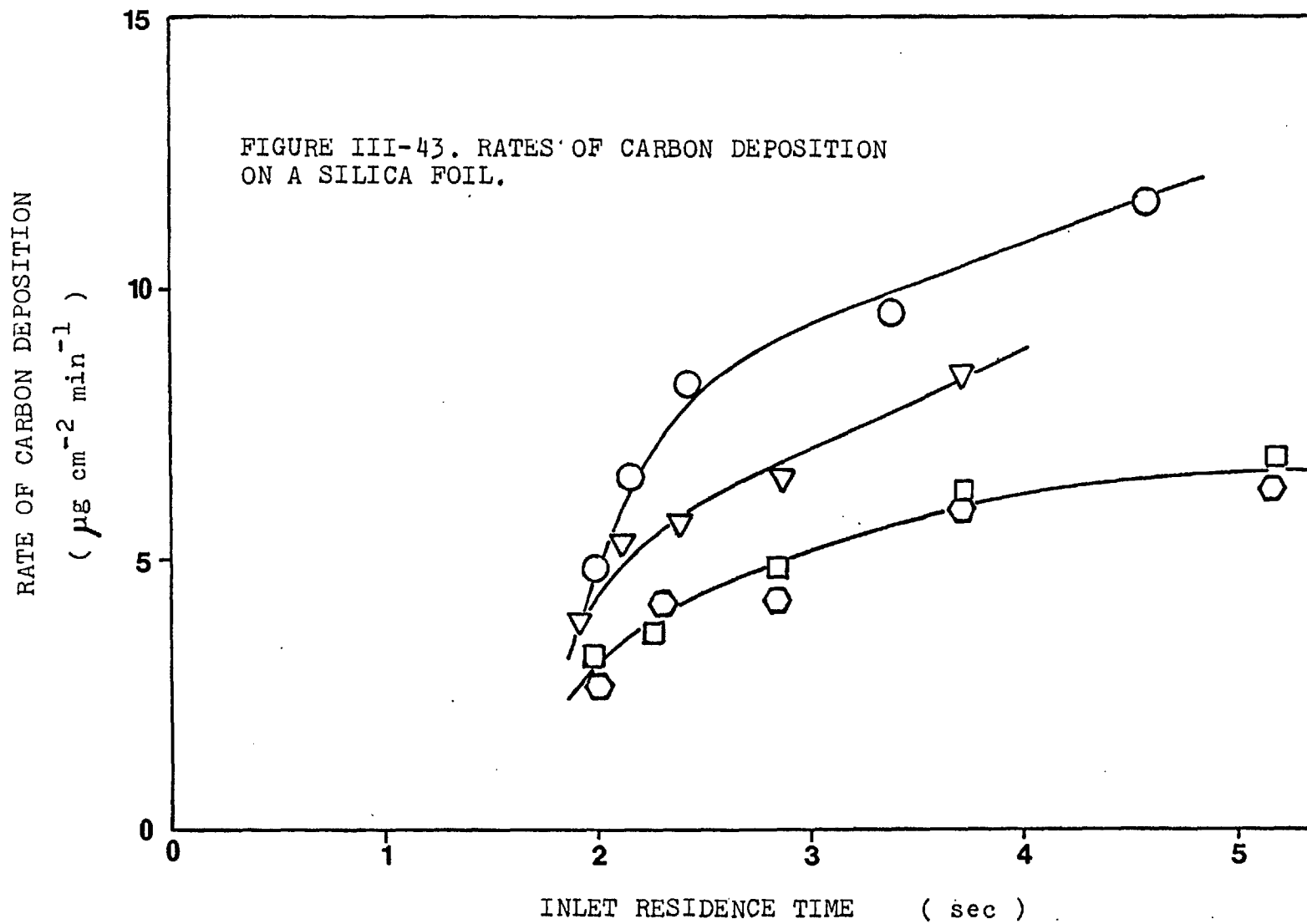
a- Carbon deposition on a silica foil

A series of runs were performed where the carbon deposited on a silica foil ( geometric area of  $3.96 \text{ cm.}^2$  ) was measured and recorded with the microbalance system. The intention of the runs was to check the reproducibility of the experimental system, using silica, (considered to be an inert material for carbon deposition).

Between runs, the carbonaceous layer that was deposited in the reactor and on the sample foil was removed by passing air through the reactor at  $800 \text{ }^\circ\text{C}$ . Hydrogen was passed during one hour, following the burning.

It became evident (see fig. III-43) that the rates of deposition were decreasing between consecutive runs, indicating that the surface of the silica was sensitive to the treatments (carbon deposition, oxidation and reduction at  $800 \text{ }^\circ\text{C}$ ).

This ageing effect was considered to be detrimental to the reproducibility of the experimental results. No further experiments were performed with silica sample foils.





b- Carbon deposition on different metals

In the following experiments, different metal foils were hung from the microbalance and subjected to deposition from pyrolyzing butane at 800 ° C. The procedure was repeated with nickel, copper and iron foils. A period of one hour at the reaction temperature under hydrogen was allowed to reduce the foils before starting the reaction. Hydrogen was also passed between experiments during the period required to re-adjust the gas flows.

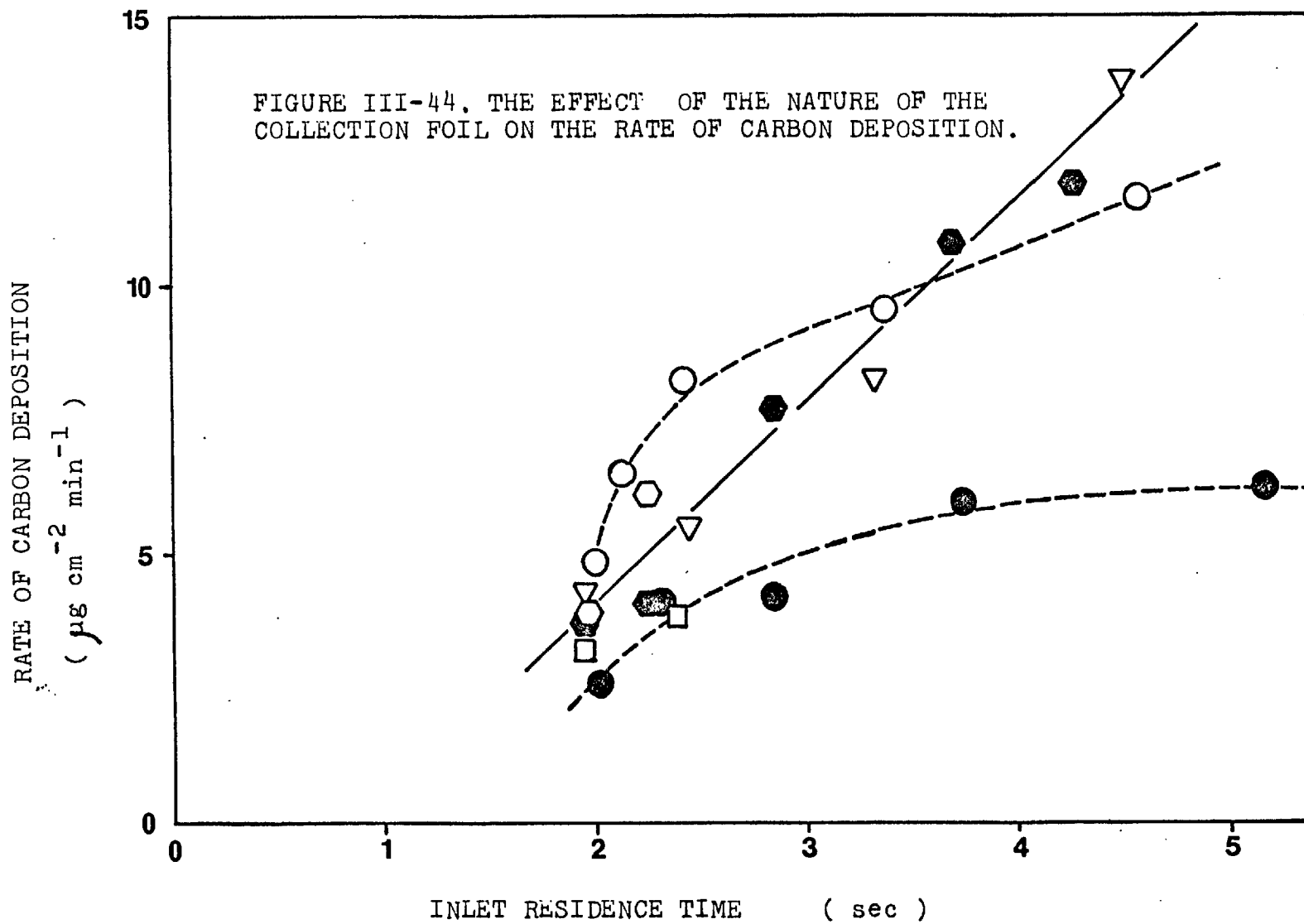
The steady state rates of carbon deposition are shown in figure III-44. The transient phenomena that happens at the early stages of deposition, which are discussed in detail later in this chapter gave differences in the behaviour of the metals with respect to early carbon deposition, but no significant differences could be seen in the steady state. The rates, for all metals, fall approximately on a straight line.

The results of deposition on a new and an aged silica foil are shown in the same figure. Significant differences can be appreciated in the shape of the curves obtained with silica and metals.

c- The effect of lining the reactor wall with different metals.

A series of runs were performed to study the effect of the nature of the reactor wall on the deposition of carbon on a sample foil.

The procedure of lining and the sizes of the metal foils fitted in the reactor wall was described earlier. In all cases, copper foils were hung from the microbalance as sample collection surfaces, copper was selected because it is known to be catalytically inert for carbon formation and gave reproducible results in carbon deposition experiments.



When the reactor wall was lined with copper, results were found to change with time in a form indicated in figure III-45. When conditions of flow were changed, the initial rate was found to be higher than the steady state rate.

The steady state rates of deposition were found to be the same as in the case of the reactor without lining.

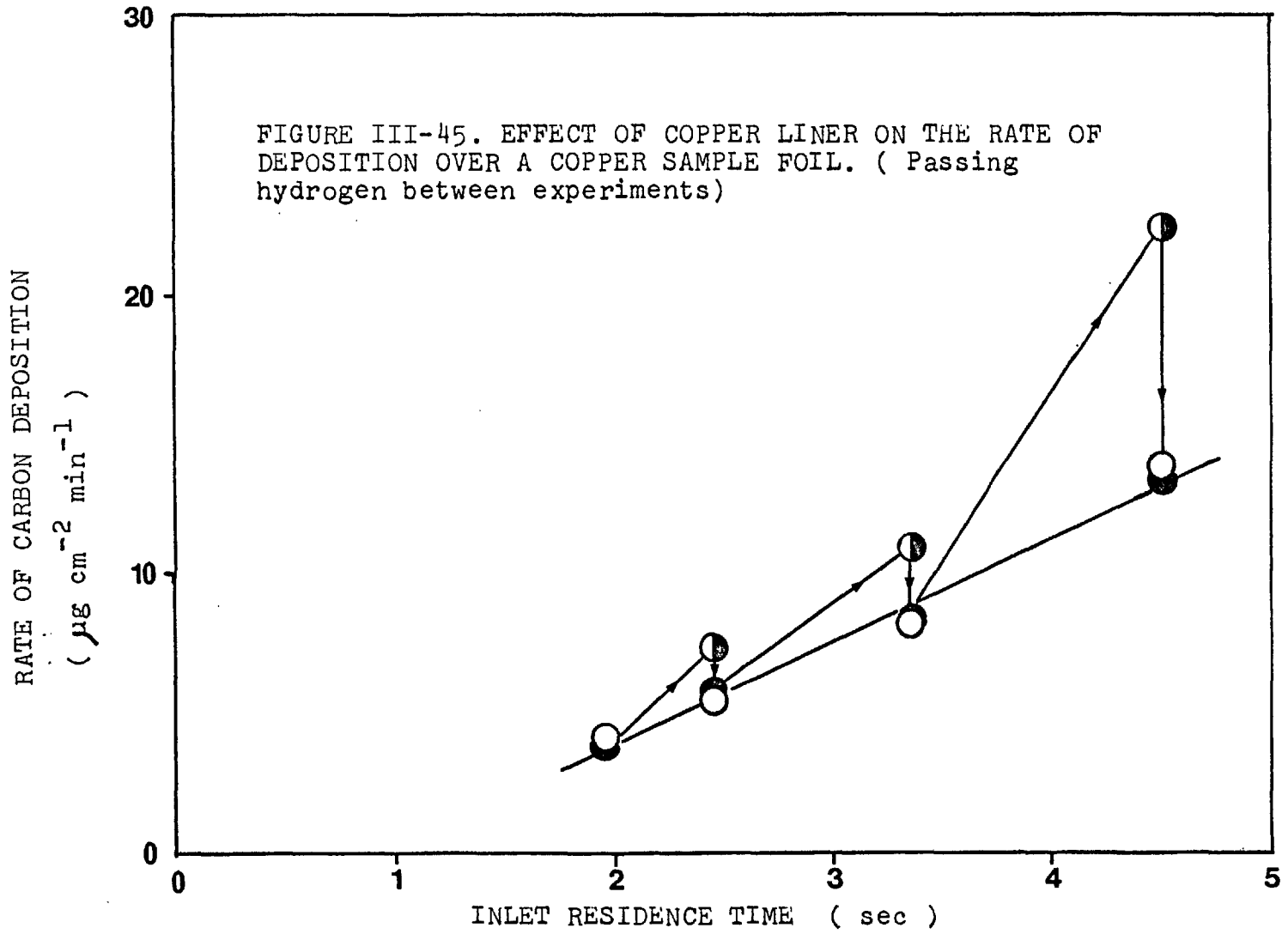
When iron was used as a liner, the behaviour of the rates was similar to copper-lined results. (See figure III-46). Differences were observed in that the steady state rates were higher than those corresponding to the no-liner experiments.

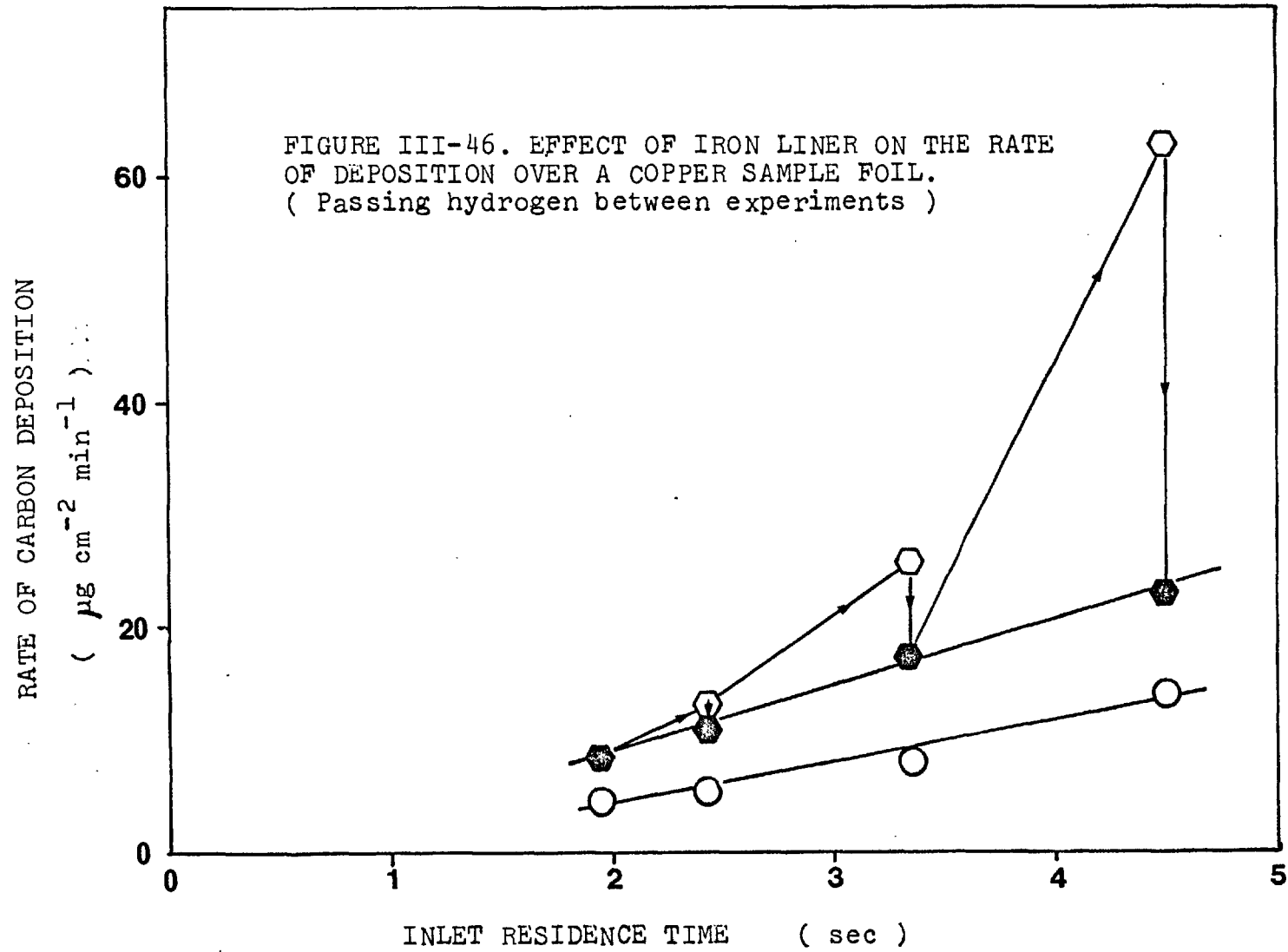
No higher initial rates were found when nickel was used as liner. The steady state rate was reached after a very short period of time. Figure III-47 shows the steady state rates of deposition for the different metal liners. Under the conditions studied, metal liners were found to enhance carbon deposition on a second metal surface. Iron was the more active, followed by nickel. Copper did not enhance deposition, compared with the non-lined silica reactor wall.

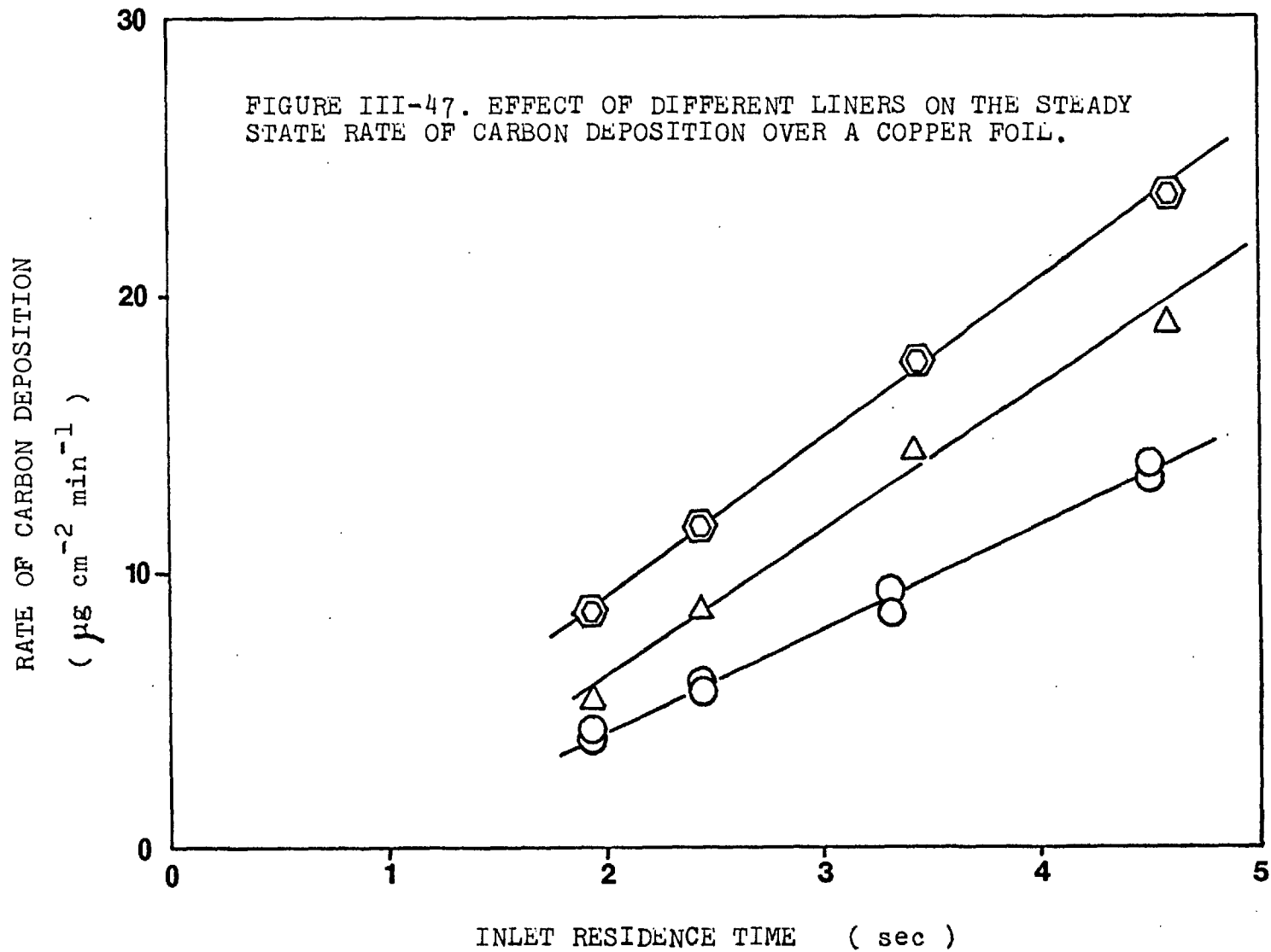
Some runs were performed changing the order of the sequence of operation (i.e. starting with new foils at the highest residence time and performing the operation decreasing residence time at each step). Figures III-48 and III-49 show the difference between experiments increasing and decreasing residence time with iron and nickel liners. In both cases, the difference in operation sequence gave different results, indicating the sensitivity of the final rate towards the previous history of the reactor and deposition surfaces.

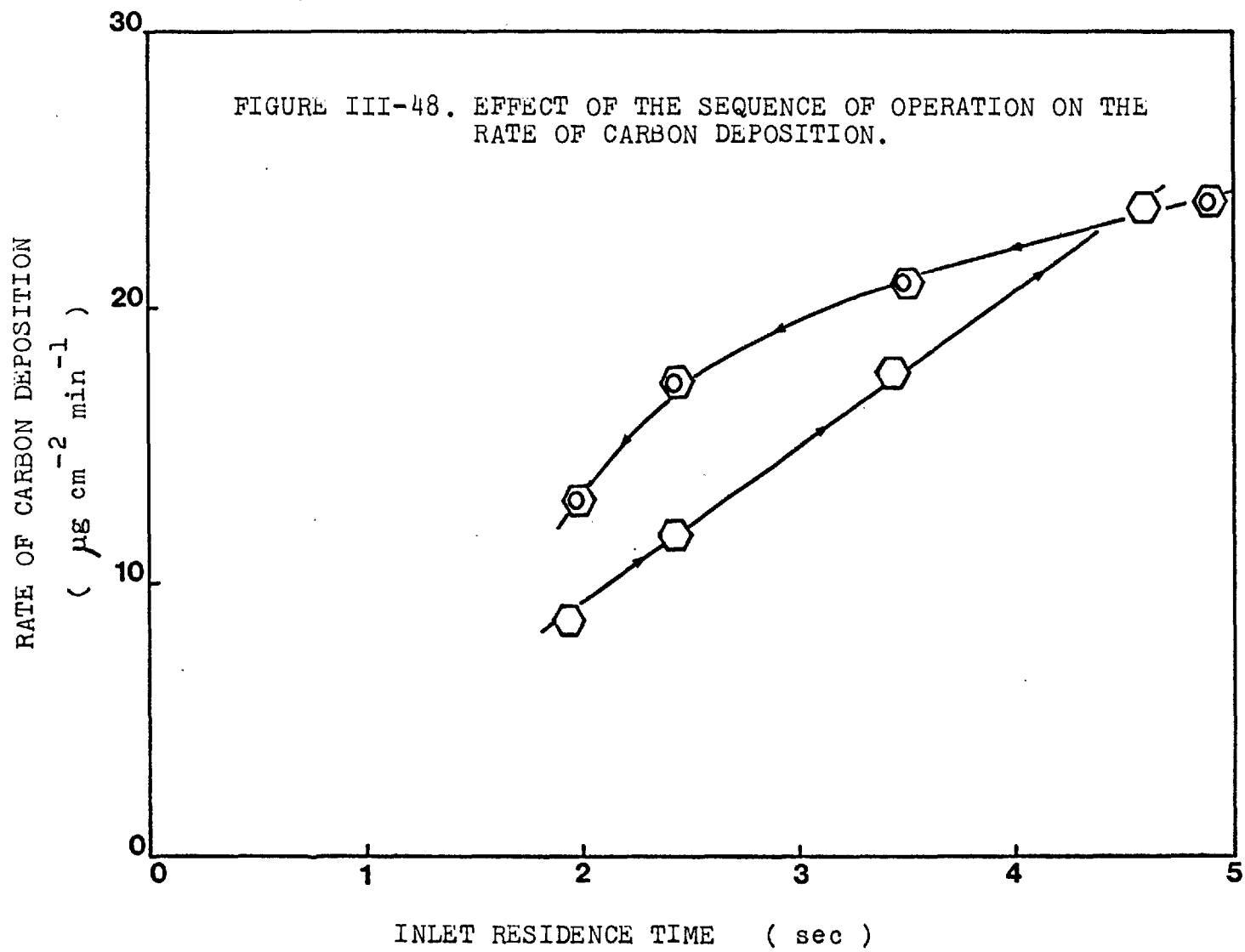
#### d- Transient rates during the early stages of deposition

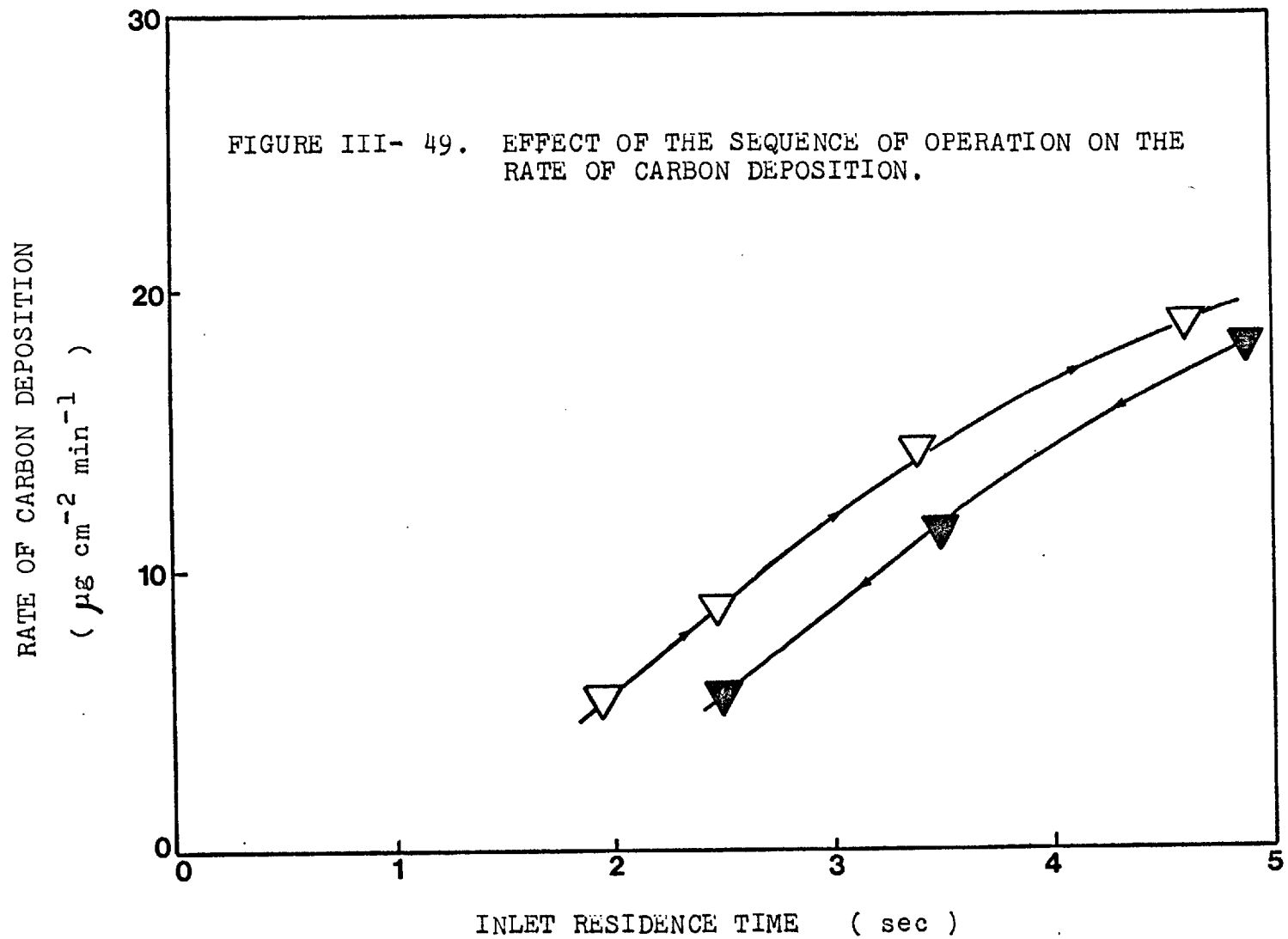
During the experiments, several effects were noticed that disappeared after a few minutes on-line. A detailed study was













performed on some of these phenomena, because they may add information on the processes happening on the surfaces under study.

When foils of different materials were hung from the microbalance, the steady state rates were found not to be significantly different. However, figure III-50 shows that there are important differences in the transient behaviour of each material. Iron shows a short period during which the rate of carbon uptake is ten times higher than the steady state. Other materials did not show large differences, but small changes in the behaviour are observed.

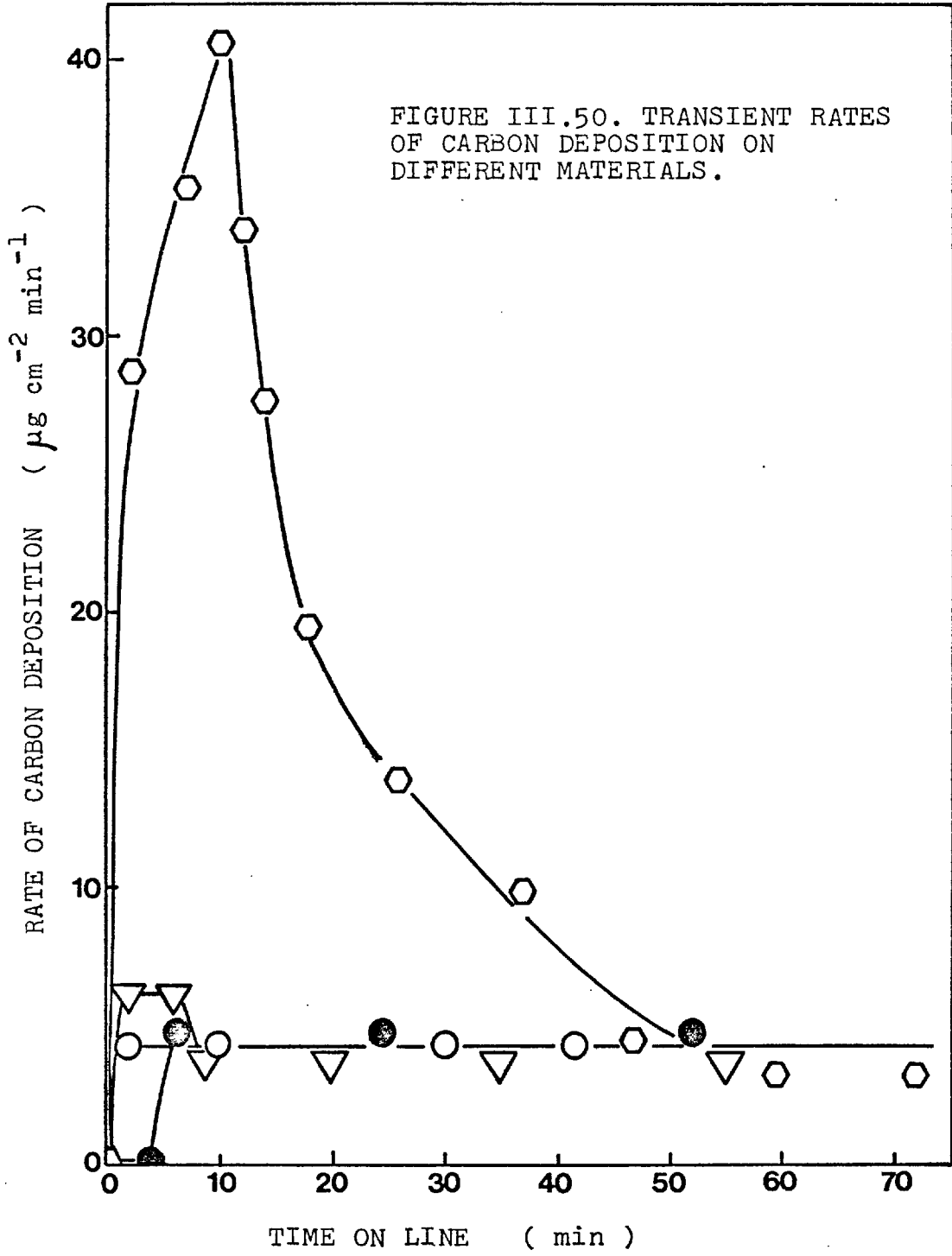
Figure III-51 show the transient produced in the rate of deposition when nickel was used as liner at large residence times. No important transient was observed with nickel liners at low residence time ( $\tau = 2$ ).

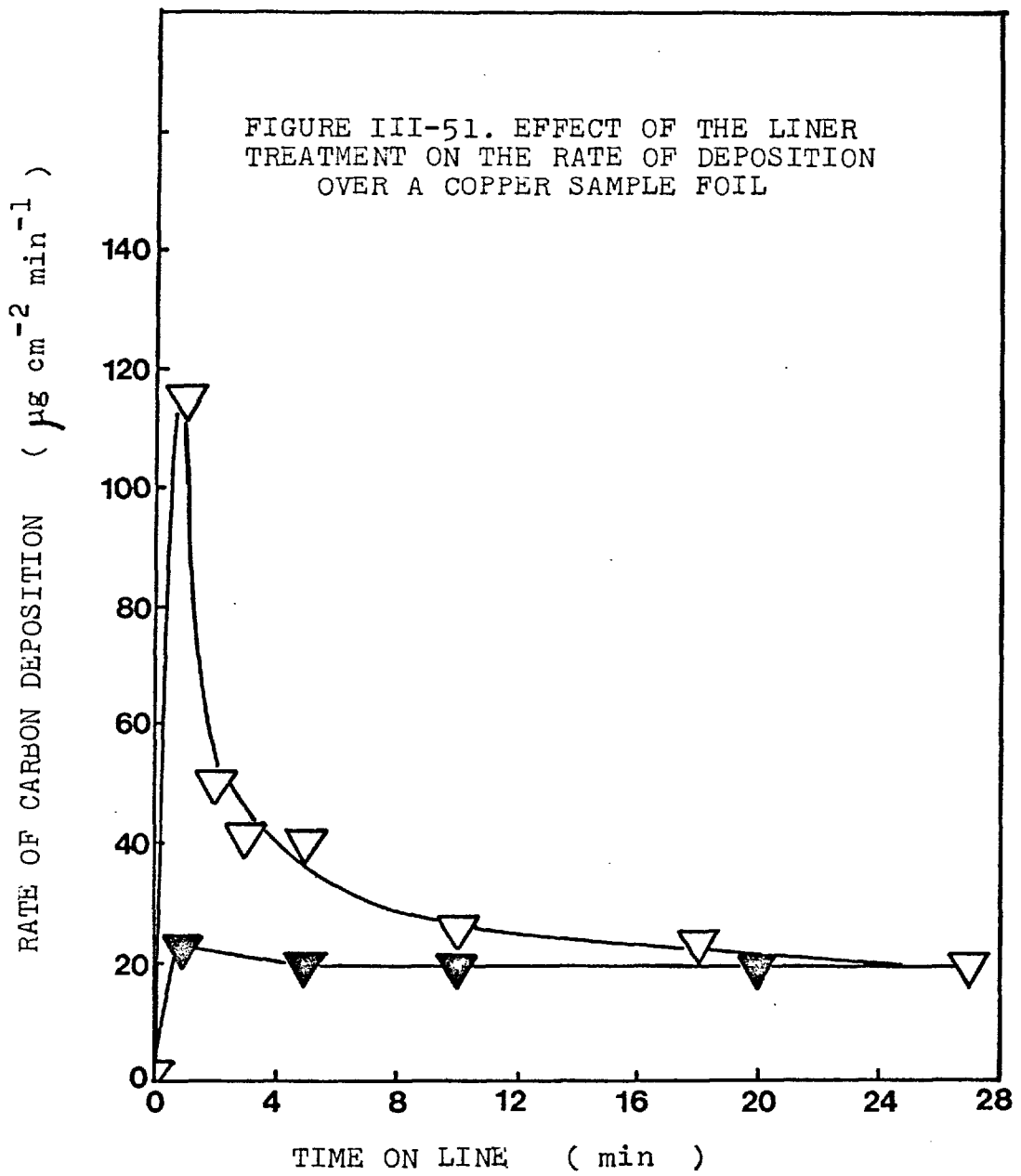
After a run in which the effect of iron lining was studied, the carbon deposited on both liner and collector foils was burned with air. The foils were reduced with hydrogen and the carbon deposition experiment re-started. The result is shown in figure III-52. A significantly high rate of deposition was found initially with the treated foils.

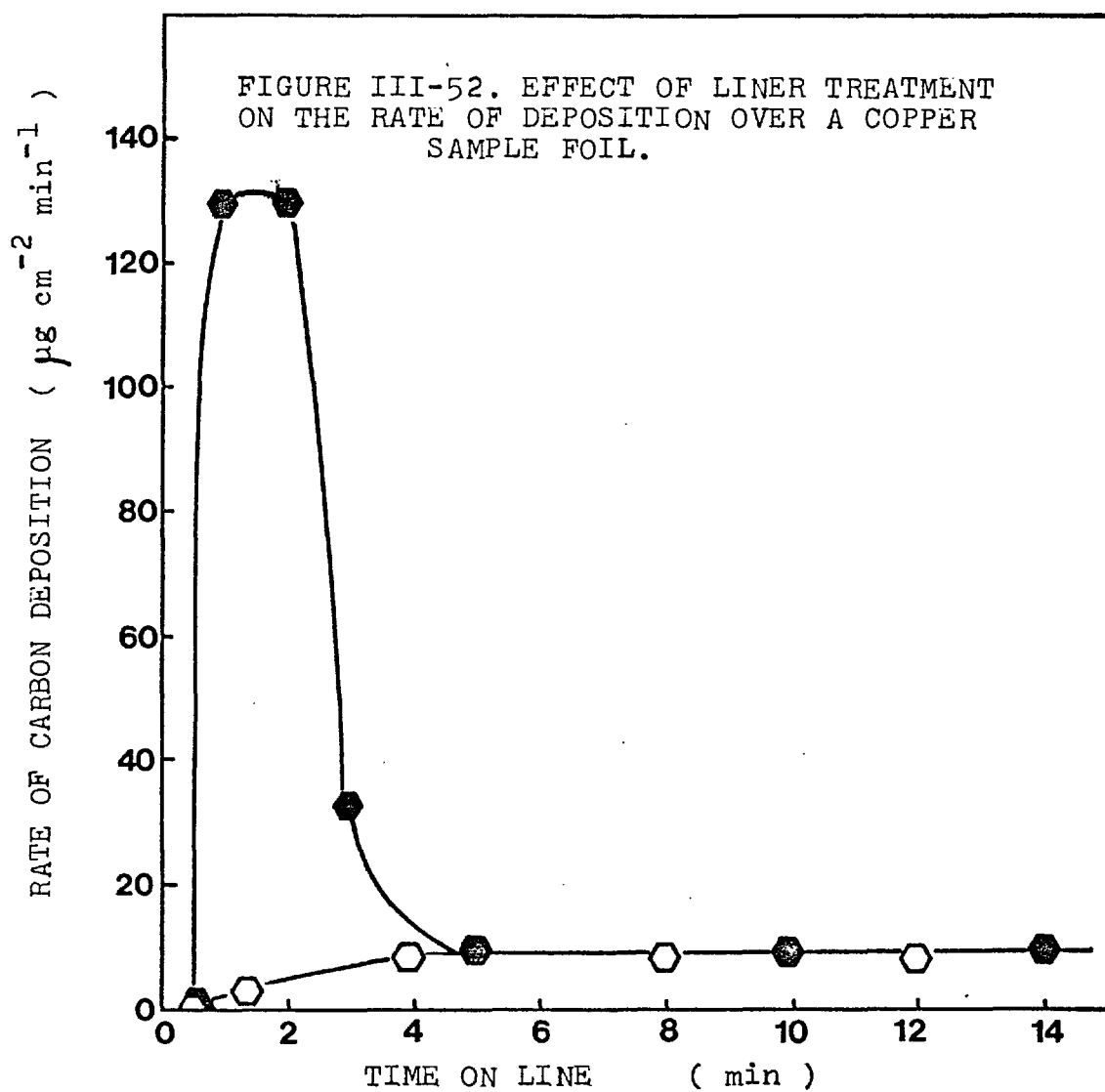
e- Effect of temperature on the rate of carbon deposition on copper sample foils.

A study of the effect of temperature was performed in series I and II experiments. During series II, on-line analysis of the exit gases was made simultaneously.

Figure III-53 show the effect of temperature on the rate-residence time plot. An increase of the rate is observed with increments of temperature, at all levels of residence time. Gas product spectra







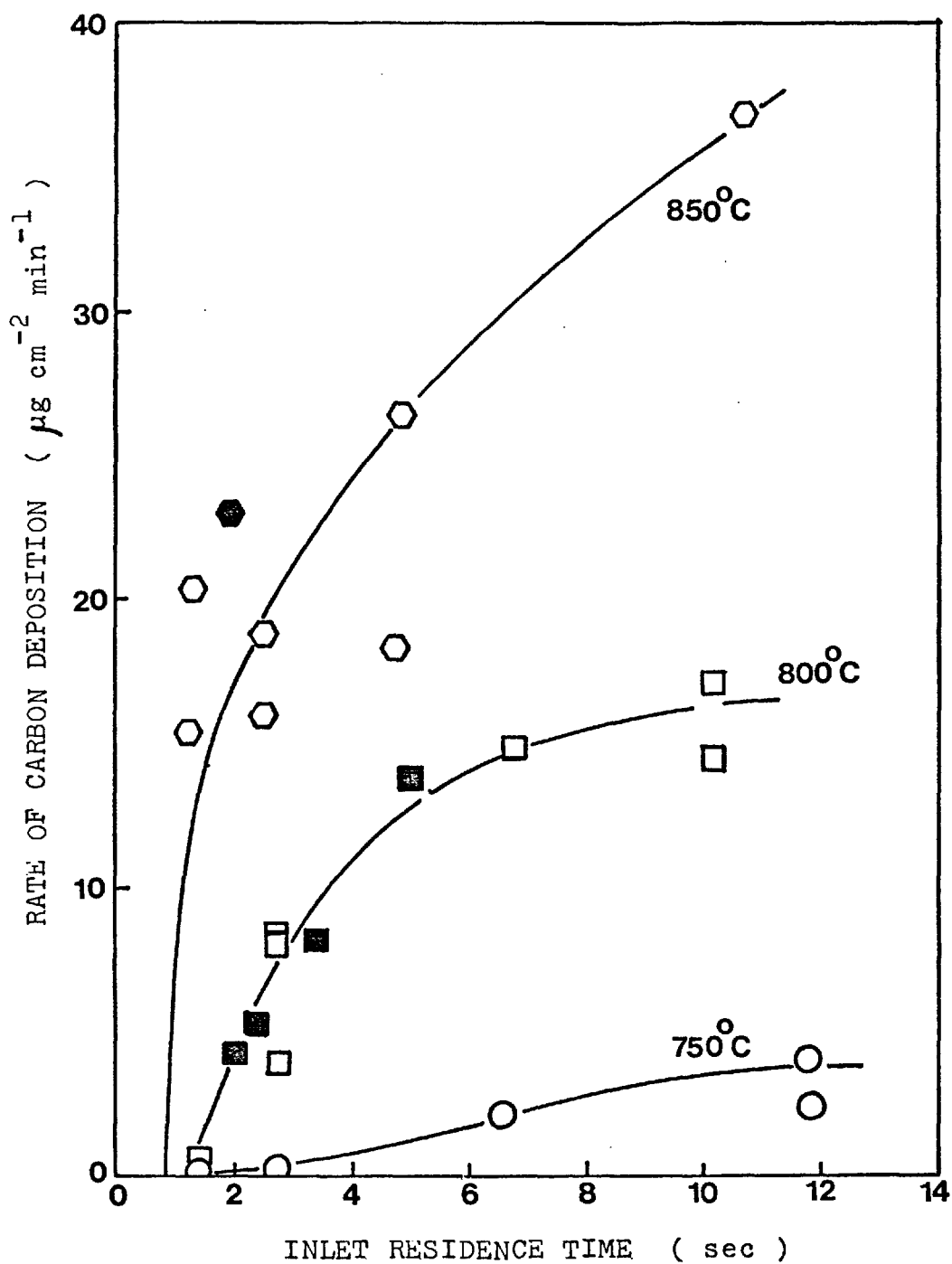


FIGURE III-53. EFFECT OF RESIDENCE TIME AND TEMPERATURE ON THE RATE OF DEPOSITION OVER COPPER FOILS.

corresponding to these experiments are shown in figures III 18,19 and 20.

Results of carbon deposition at different temperatures at two residence times has been presented with a "zero order" kinetics assumption, in the form of an Arrhenius plot (see fig. III-54). The points fall on straight lines. The apparent activation energies obtained from slope measurements were 80.34 Kcal/mole (for  $\tau=2$ ) and 53.49 Kcal/mole (for  $\tau=11$  secs.).

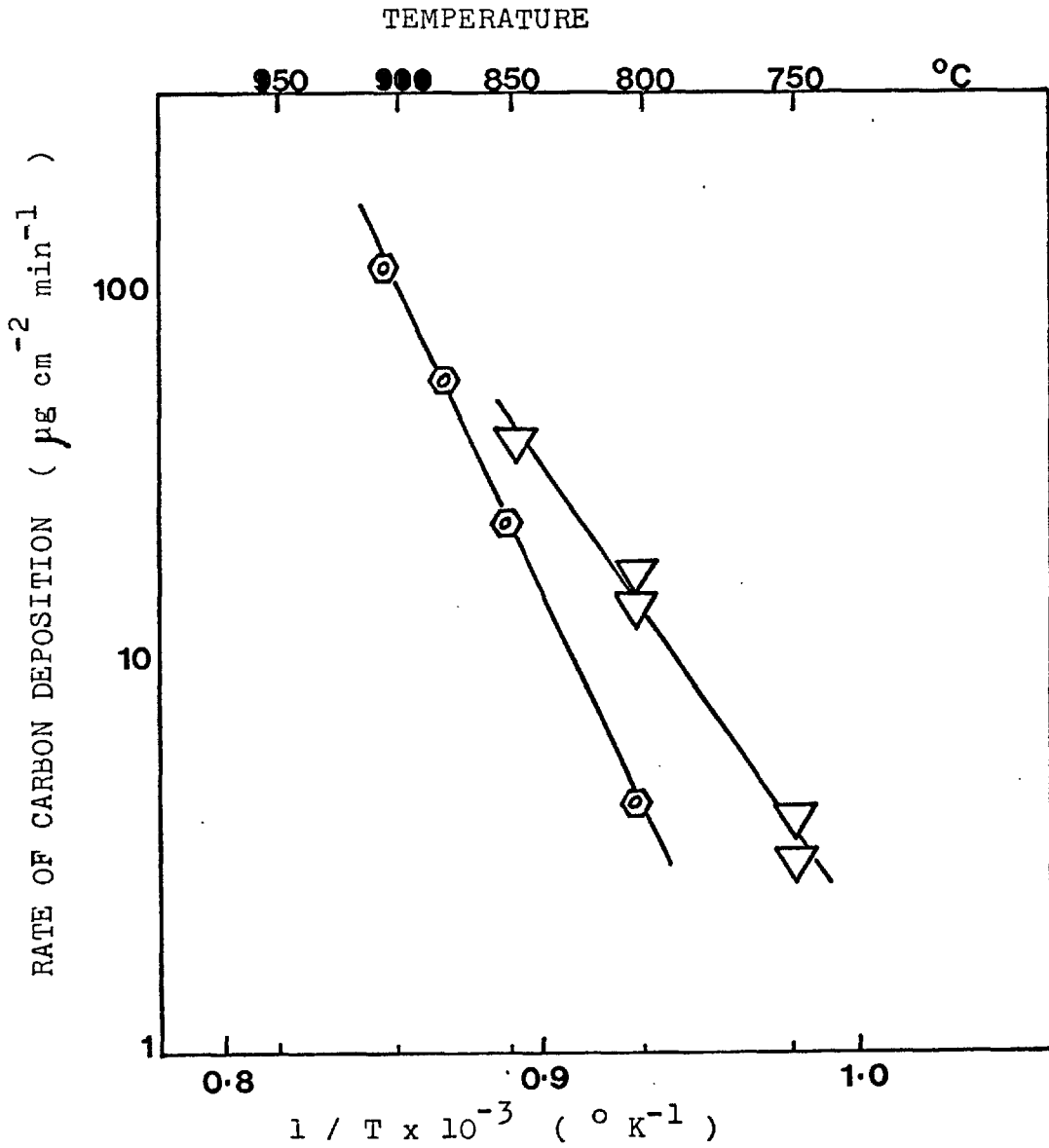


FIGURE III-54. EFFECT OF TEMPERATURE ON THE RATE OF CARBON DEPOSITION OVER COPPER SAMPLE FOILS.

2- EXPERIMENTS WITH BUTANE DILUTED WITH HYDROGEN AND HELIUM

The results detailed in this section correspond to the study of the effect of hydrogen and a diluting inert, helium, on the carbon deposition over different metal foils. Results are reported from two different series of runs, series II and III. In series II, the microbalance reactor was the same as was used previously in the first series of runs (pure butane), but an on-line gas chromatographic analyzer was attached to the system to analyze hydrocarbon gases and hydrogen. In series III, a cold trap was included in the system to collect the aromatic compounds that were formed during the reaction. These fractions were analyzed by gas-chromatography.

a- The effect of hydrogen and residence time on the deposition over copper.

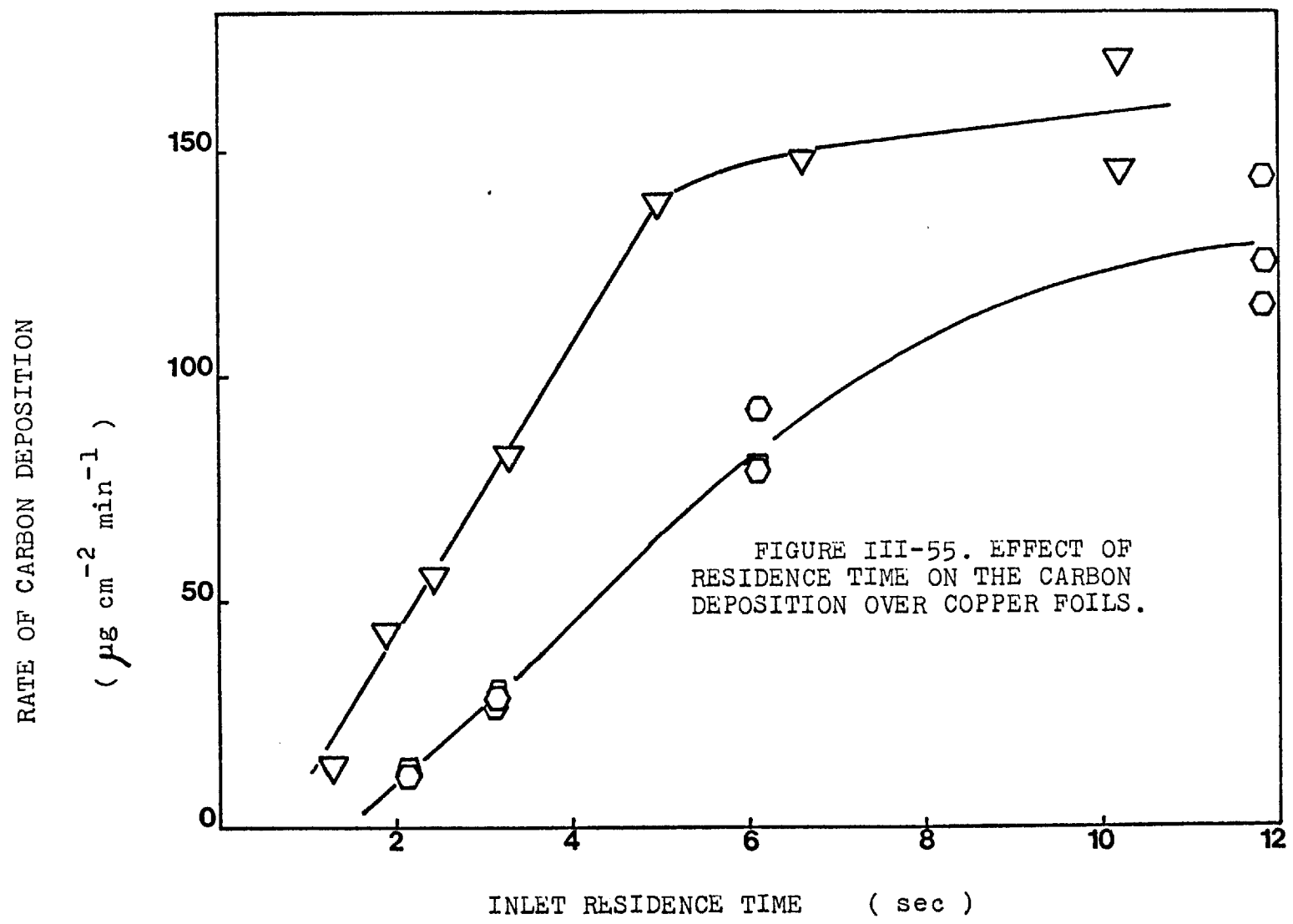
When rates of carbon deposition from pyrolyzing butane-hydrogen mixtures are compared with results obtained from reacting pure butane, the shape of the curve of the rates as a function of residence times is approximately the same, but the dilution with hydrogen decreases the magnitude of the rates of carbon deposition. (Figure III-55).

The gas products composition corresponding to the pure butane experiments are shown in figure III-19 and the product spectra when hydrogen is used as a diluent in figure III-21. Information regarding aromatics formation and composition are given in figures III-25, 26 and 27.

b- The effect of hydrogen on the carbon deposition over different metals.

Experiments that were detailed previously failed to





show significant differences in the rates of carbon deposition from pure reacting butane on foils of different metals. The present results were obtained from a study performed to see whether hydrogen could change the reported behaviour significantly.

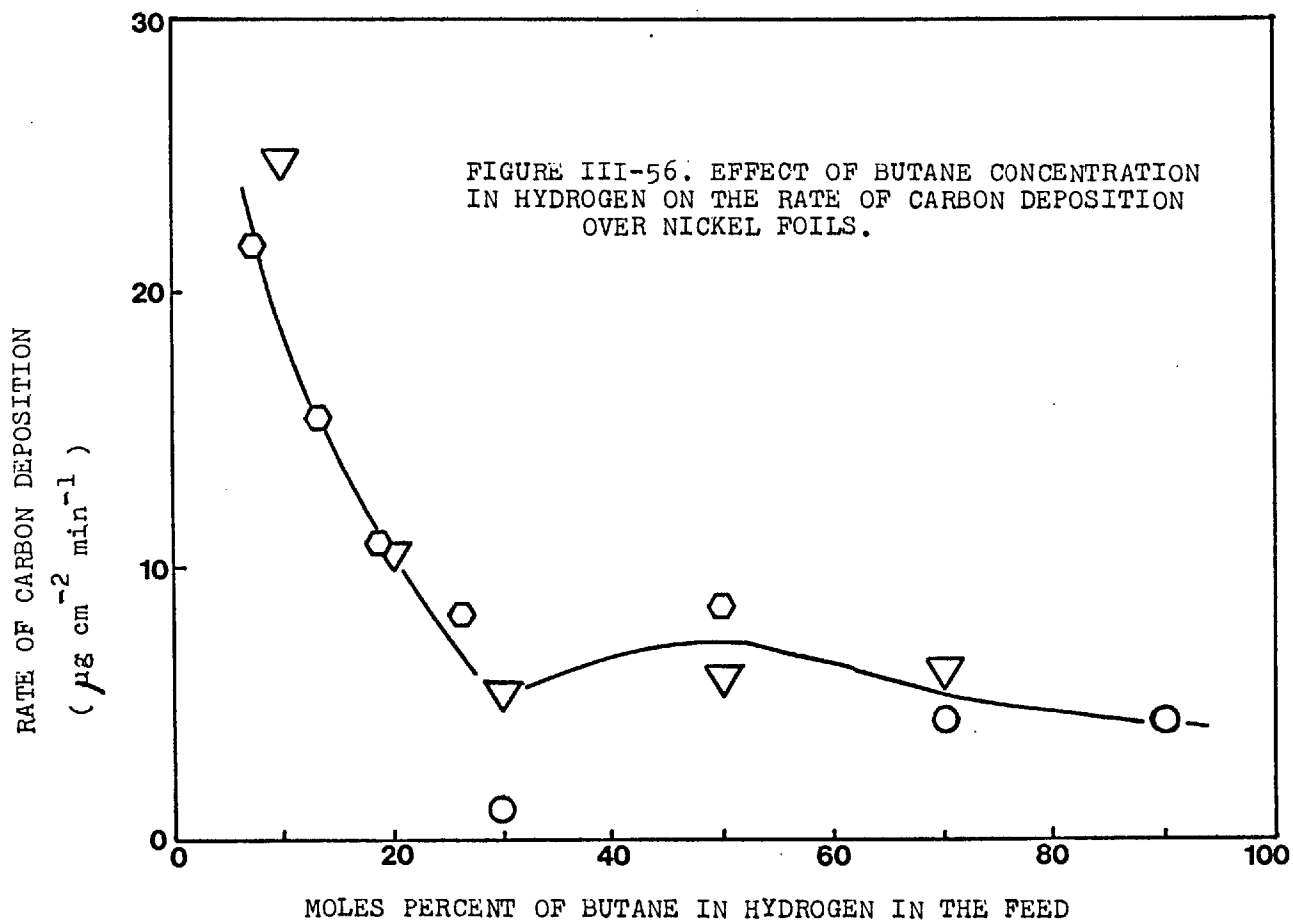
Some experiments were performed with mixtures of butane and hydrogen, where the ratio of flows were changed to give from 10 to 100% of butane in the mixture with the total flow being kept constant. In others, the concentration of butane was kept constant, and appropriate flows of hydrogen and helium were provided to change the concentration of hydrogen, while the overall inlet flow was kept constant.

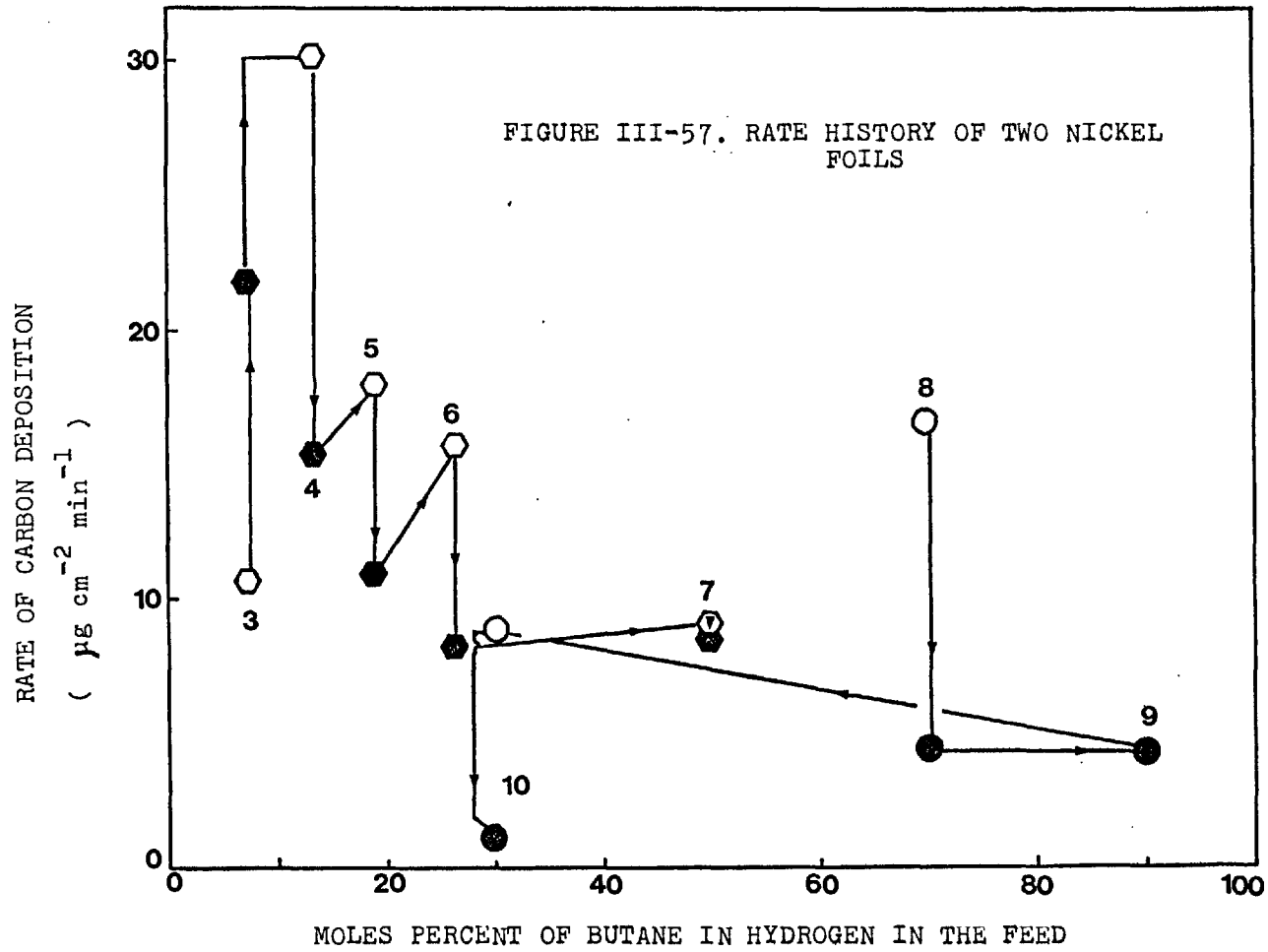
The effect of butane concentration, in mixtures with hydrogen, on the deposition over nickel foils is shown in figure III-56. The concentration of butane is seen to have a negative effect on the rate of carbon formation at low concentrations. The rate of deposition presents a minimum at about 30 % and a maximum at 50 % butane. Results at 10 % lack reproducibility and range from 0.025 to 0.065 mg/cm<sup>2</sup> min. The gas products spectrum that correspond to this figure are given in fig. III-13.

The form in which the steady state rate of deposition was reached in the runs performed with two different nickel foils has been represented in figure III-57. At low butane concentration (8 % in run 3) the deposition on a new foil starts with a low initial rate and increases until it reaches the steady state. At 10 % butane, the deposition starts with a low initial rate, increases to a high maximum rate and later decays to a steady rate. (Not shown).

At 70 %, the deposition on a new foil starts with a fast rate and later decays to the steady value (see 8).

When the same foil is used to obtain different values of rate at different concentrations, the initial rate of deposition is higher at





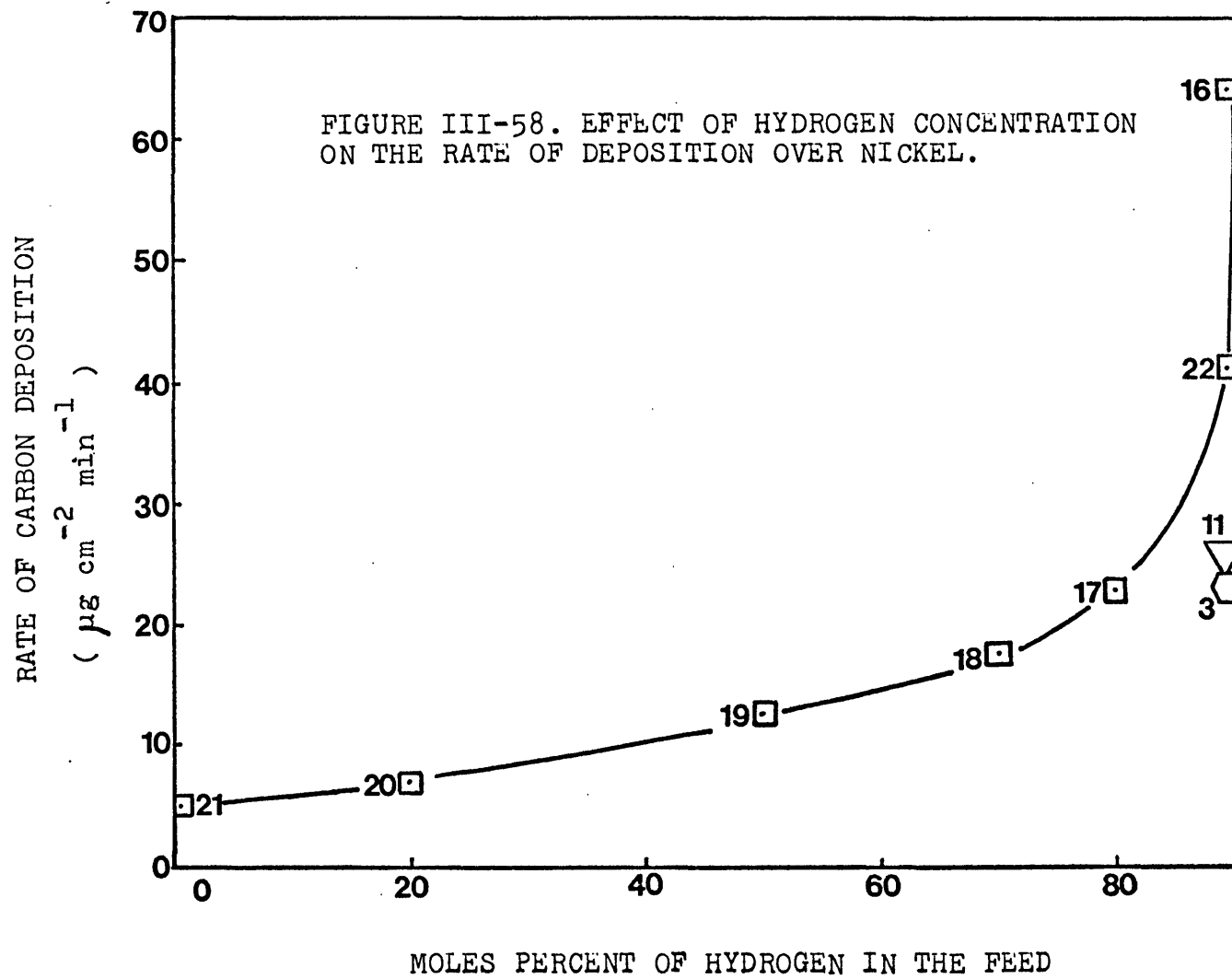
the beginning of the run, except at higher butane concentrations (runs 7 and 9).

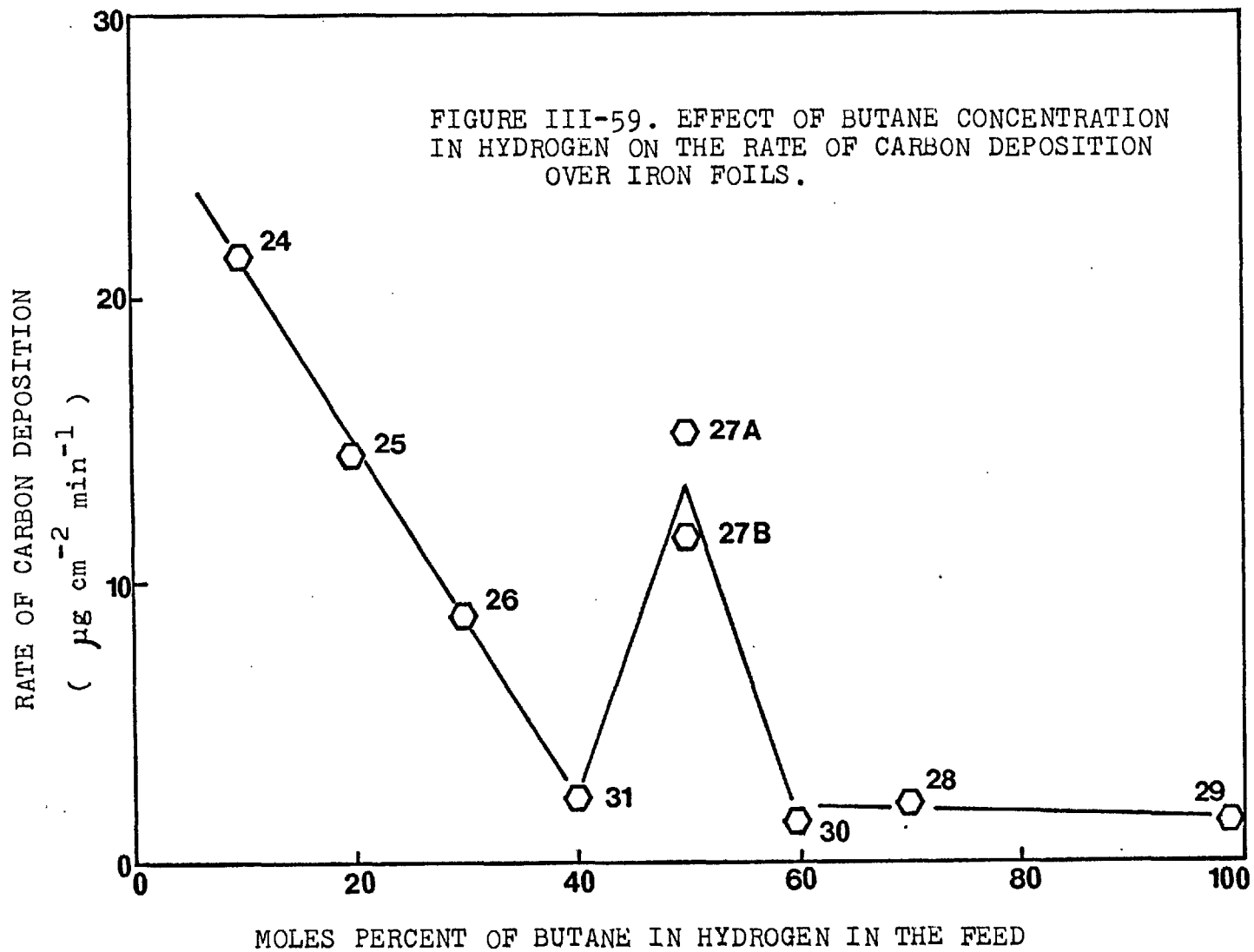
In some cases the steady state rate of deposition was found to be dependent on the history of the deposition surface. The sequence of runs 8-9-10 gave a rate of  $0.001126 \text{ mgr} / \text{cm}^2 \text{ sec}$  ( see figure III-57 ), while the sequence 11-12-13 (from 10 % to 20 % to 30 % of butane) gave a value of  $0.005387 \text{ mgr} / \text{cm}^2 \text{ sec}$  at the same concentration of 30 % of butane.

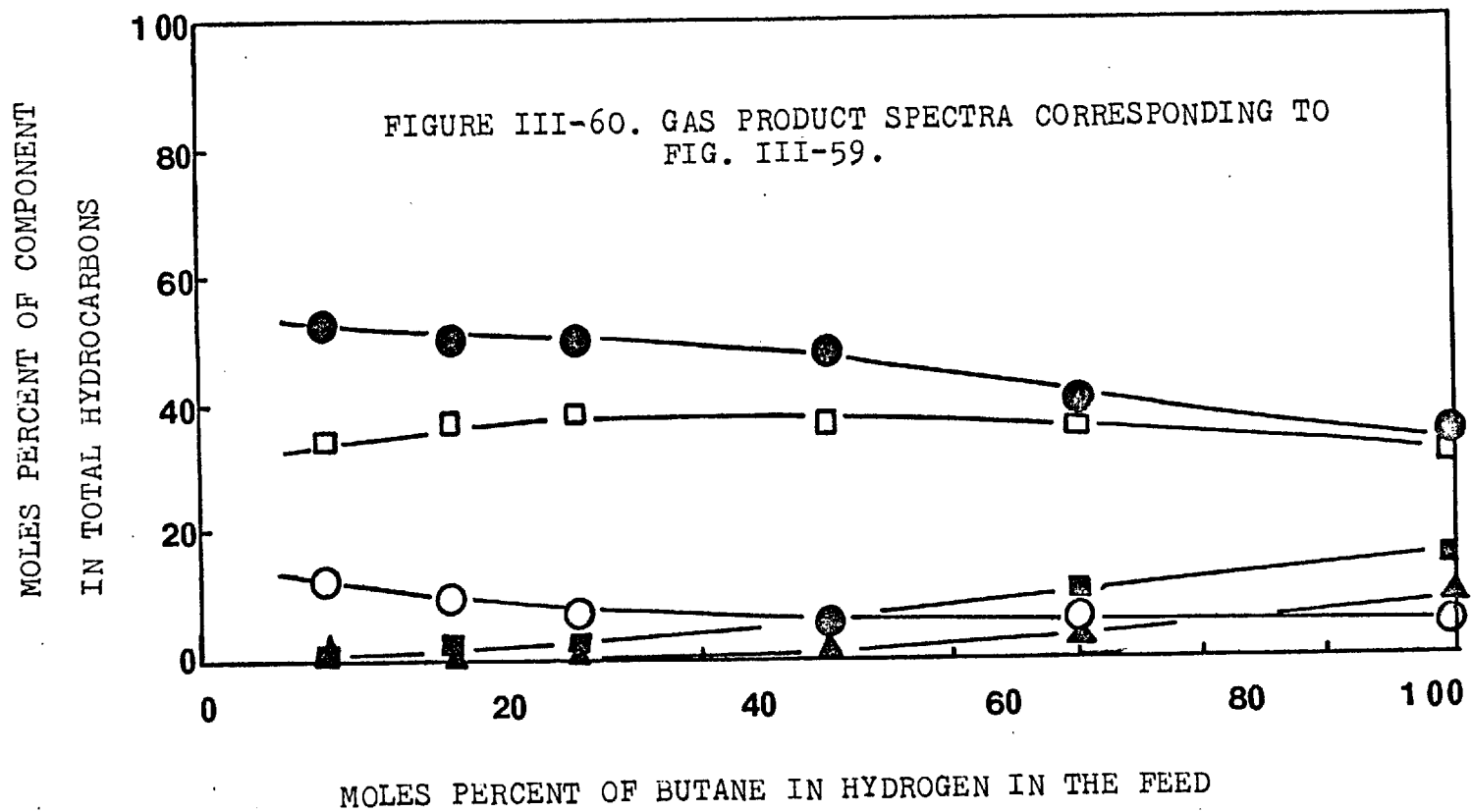
The previous results show the very important influence of dilution with hydrogen on the carbon deposition over nickel foils. It may be in doubt whether the observed effect is due to the dilution of the reactant or to the chemical nature of hydrogen. Figure III-58 show the result of a series of experiments where the concentration of hydrogen was varied and the butane concentration was kept constant. From the figure it is evident that hydrogen positively accelerates the deposition of carbon and does not act only as a diluent. The gas composition corresponding to this last situation was given in Fig. III-14.

A study of the effect of the concentration of butane in hydrogen was performed using iron foils. The result of the study is presented in figure III-59. The features are similar to those previously noticed when studying carbon deposition on nickel foils. A minimum of rate is observed at 40 % butane and a maximum at 50 %. Also in this case the rate of deposition is very high at 10 %. Figure III-60 shows the gas products spectrum and figure III-61, the rate-history of several iron foils.

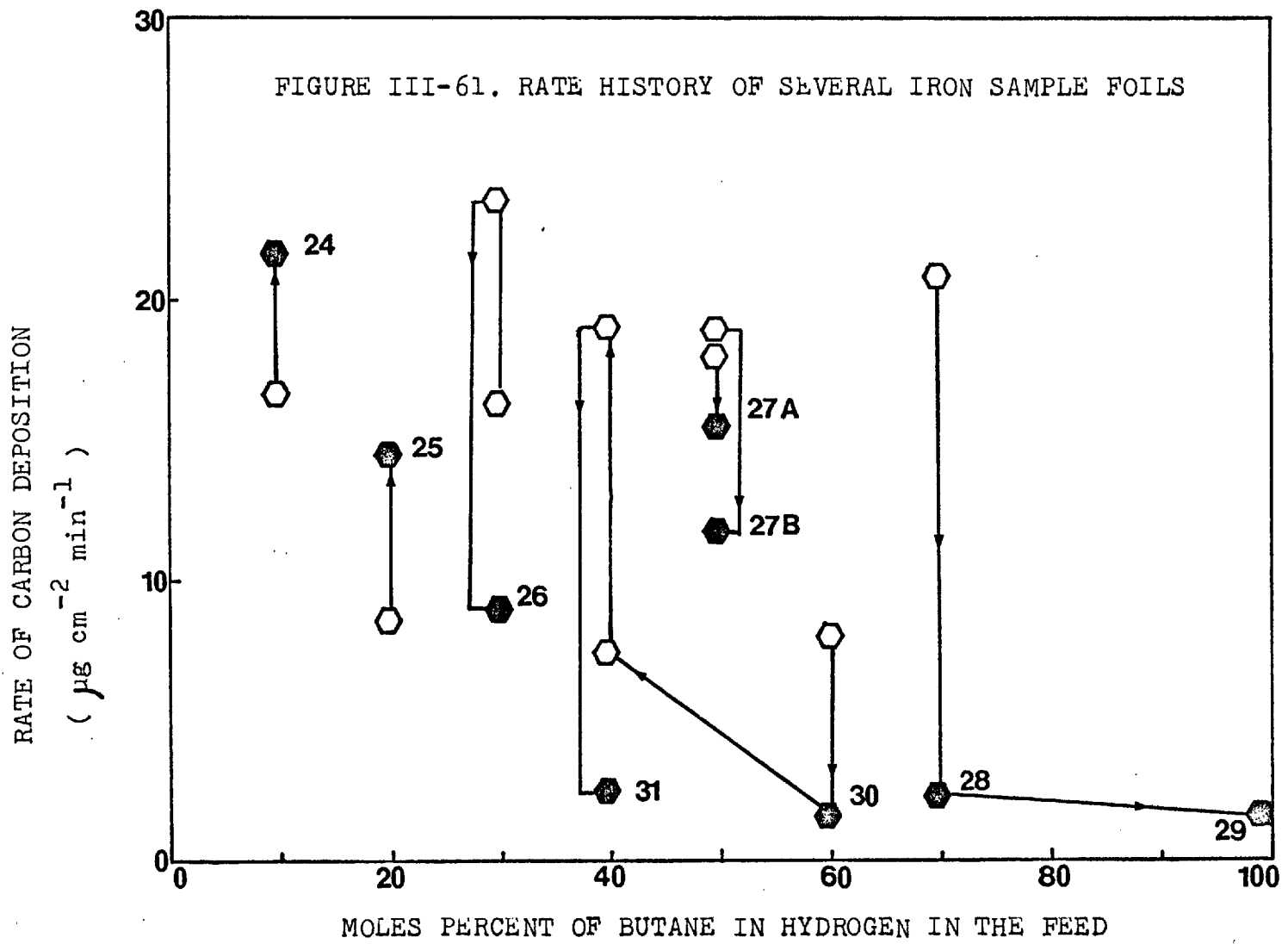
Another study was performed over copper foils, on the effect of butane concentration in hydrogen. The results are presented in figure III-62. In comparison with the results obtained with nickel and iron foils, the shape of the curves are completely different, especially in











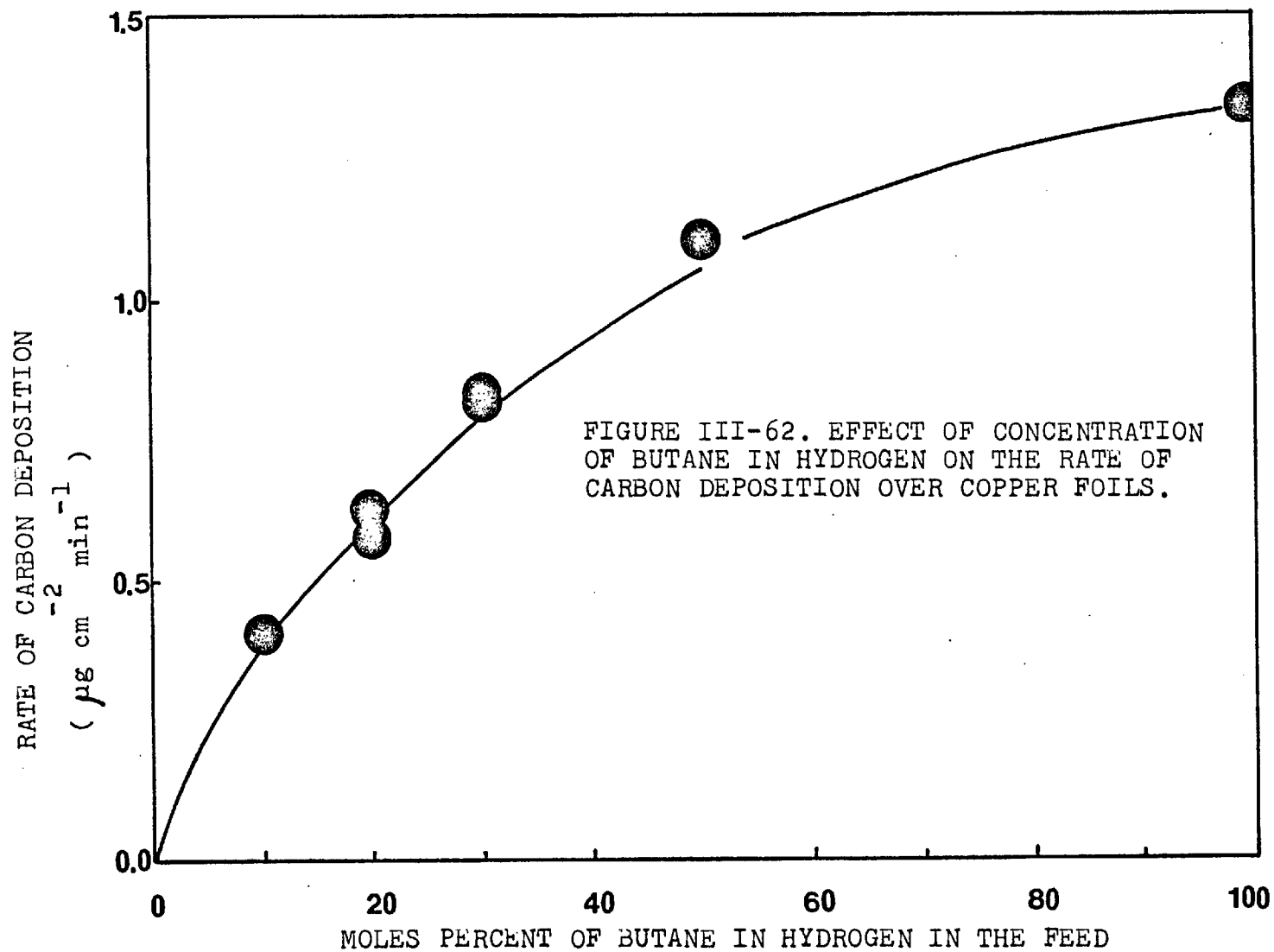
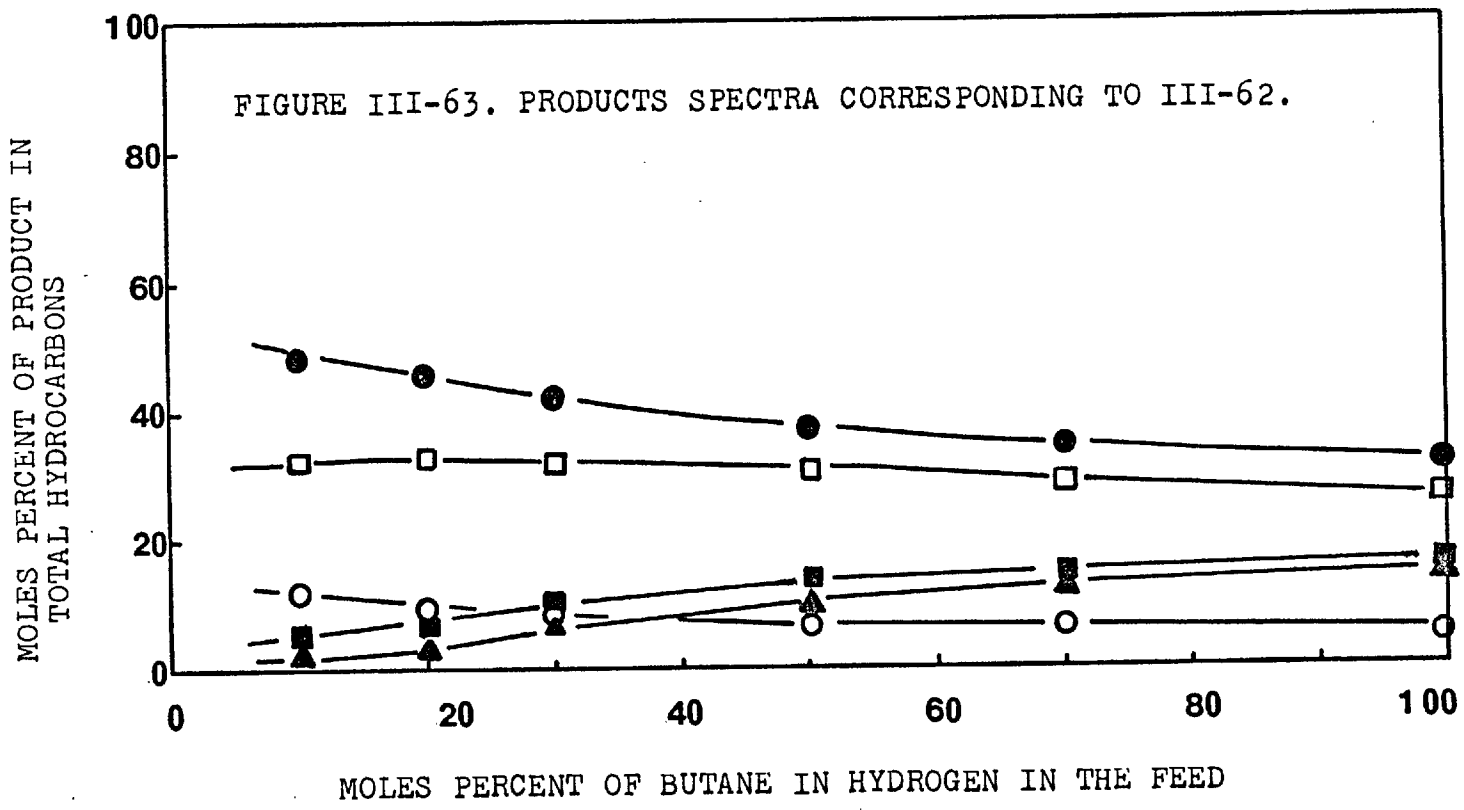


FIGURE III-62. EFFECT OF CONCENTRATION OF BUTANE IN HYDROGEN ON THE RATE OF CARBON DEPOSITION OVER COPPER FOILS.



the low concentration region. In this case the rate depends on a positive kinetic reaction order with respect to butane. The curve presents a maximum at the 50% concentration, which is similar to the curves of nickel and iron. Also in the low concentration region, the initial rates are higher than in the steady state. The products composition corresponding to this case are given in figure III-63.

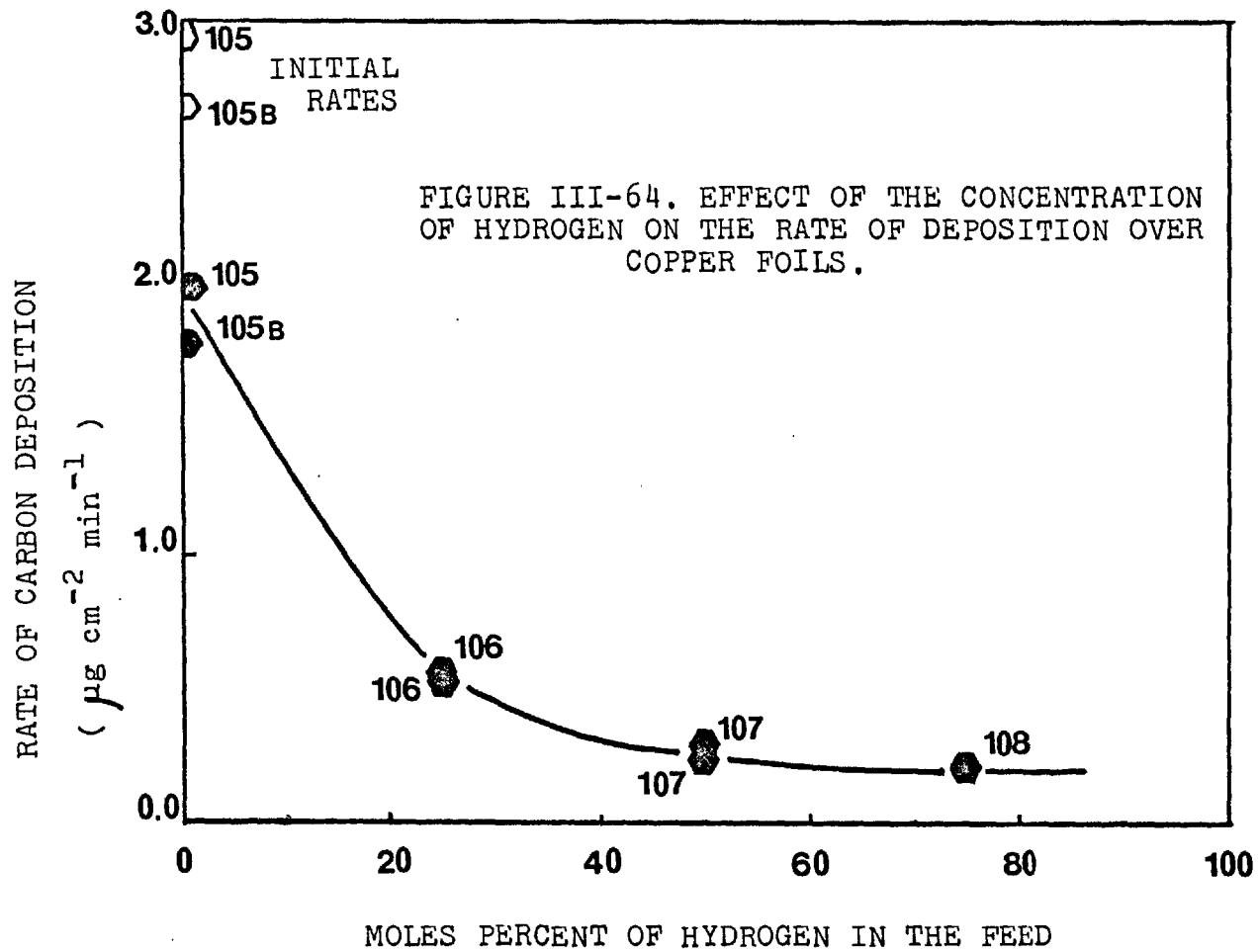
The effect of hydrogen concentration when the concentration of butane is kept constant is shown in figure III-64. There, a marked inhibitory effect of hydrogen on the rate of carbon deposition can be appreciated, opposite to the strong enhancing effect observed in the case of nickel or iron. Gas products compositions corresponding to this case are given in figure III-65. Aromatics production and composition are reported in figures III-28,29 and 30.

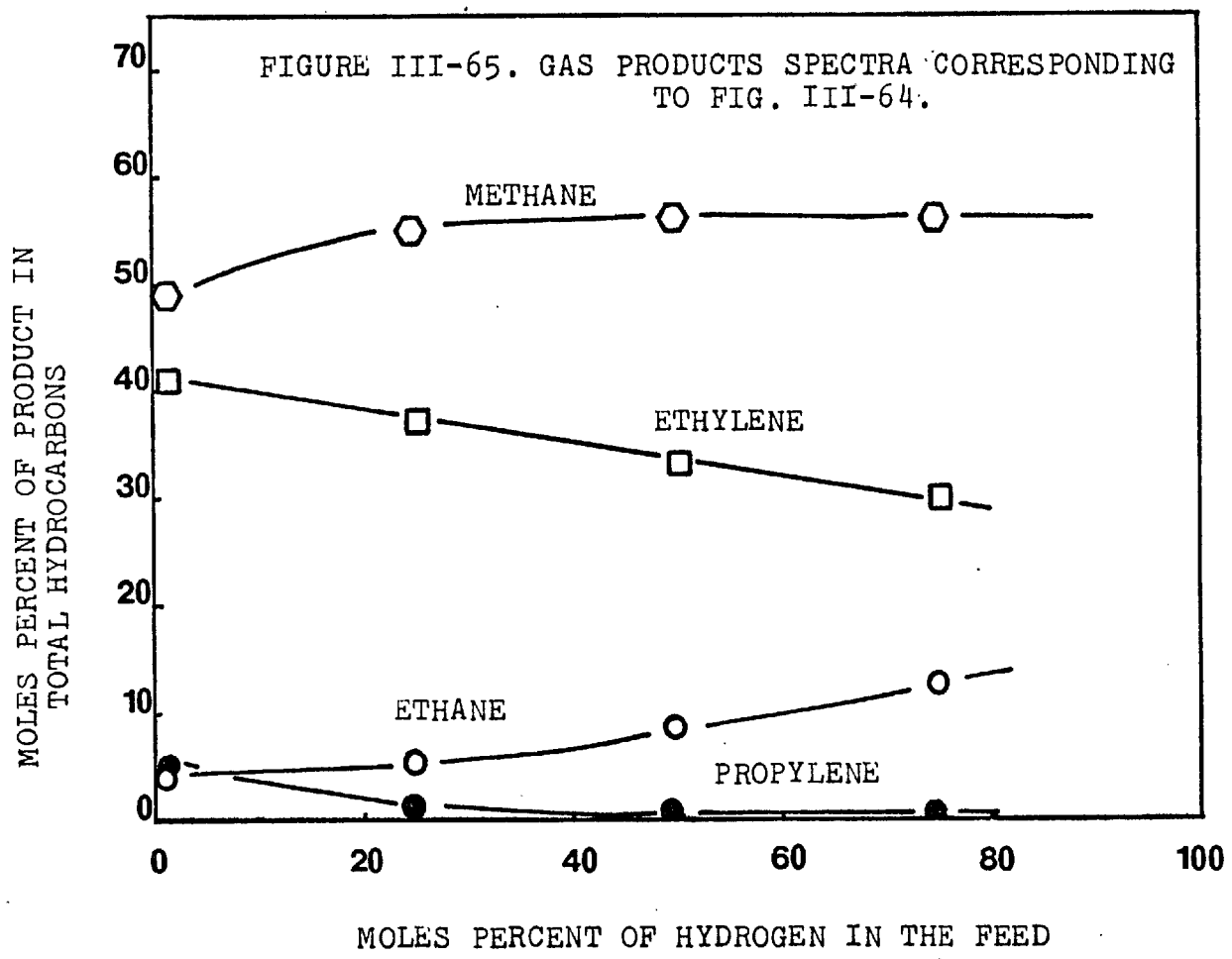
c- Effect of temperature on the deposition over nickel and copper

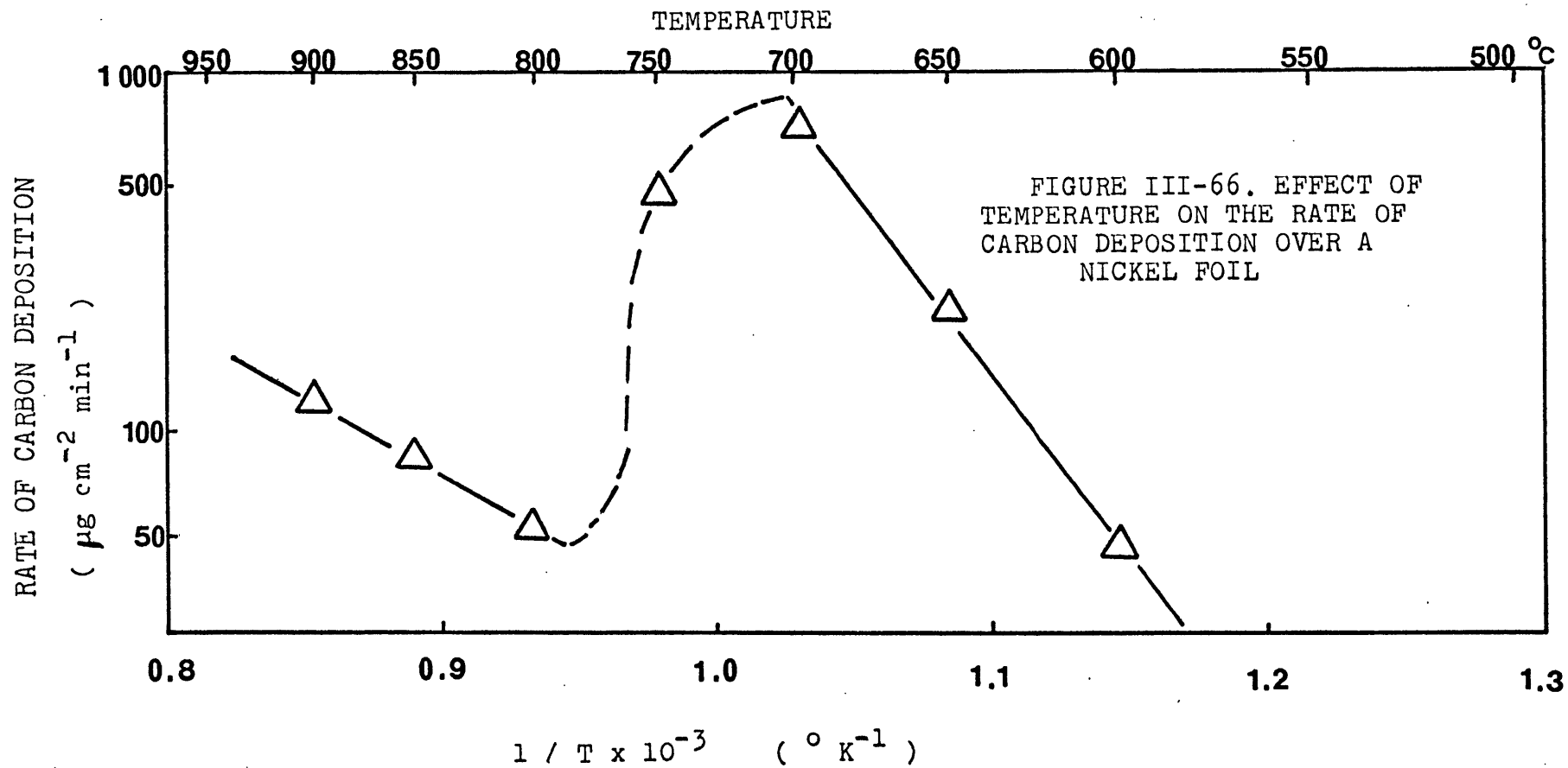
The experiments described in this section were performed to test the combined effect of hydrogen and temperature on the rates of carbon deposition on metal foils. Iron was excluded from this study because magnetic interactions between the foil and the furnace interfered with the microbalance measurements below 800 °C.

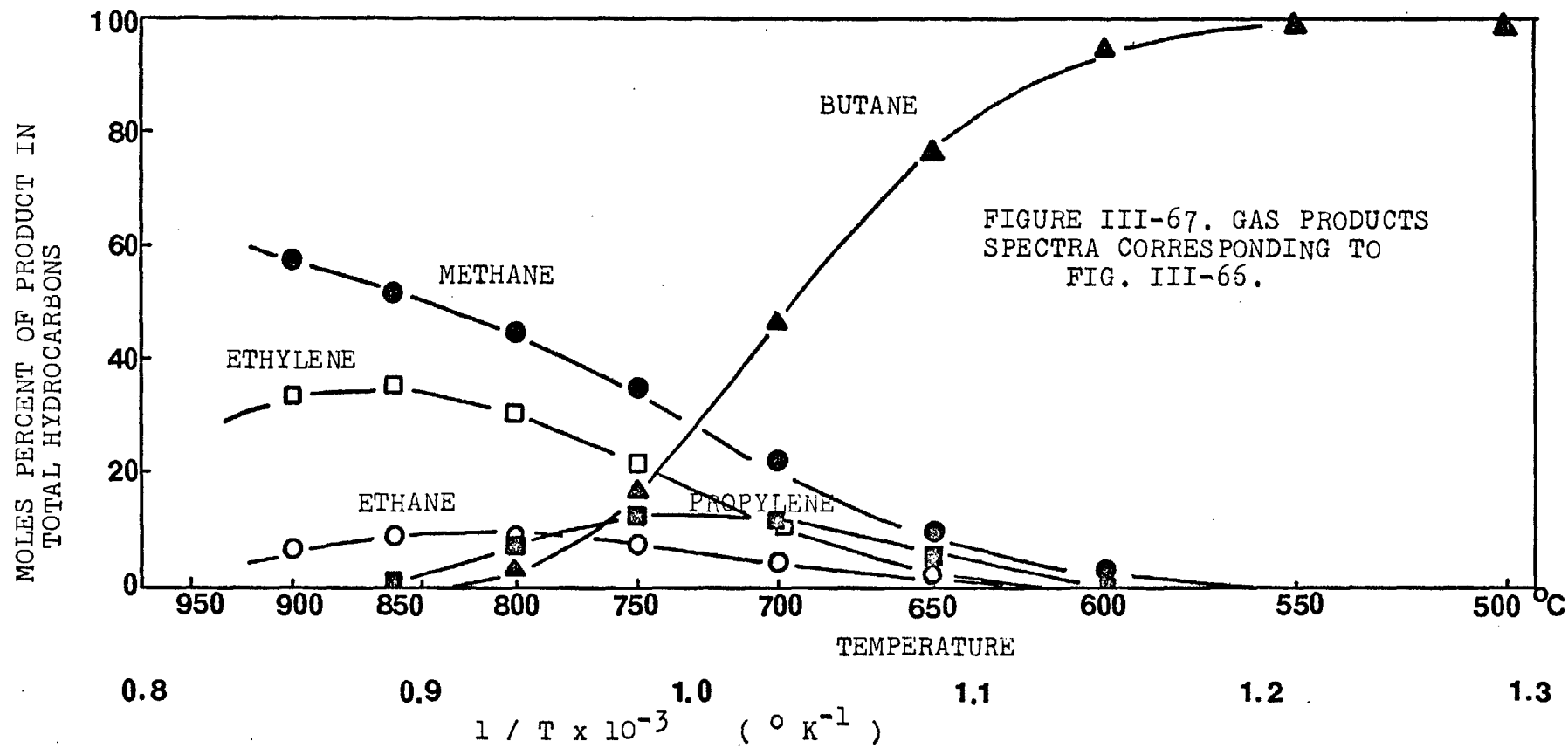
Figure III-66 shows the results in the form of an Arrhenius plot. Three zones can be identified from the plot, a low temperature region where the rate rises continuously with the reaction temperature, an intermediate region where the rate drops with temperature increases, and a third region, where the rate again increases with temperature. These changes are accompanied by changes in the nature of the gas phase products, as shown in figure III-67.

When helium is used as diluent, the plot changes to the form in figure III-68. The three zones are still present, but are less

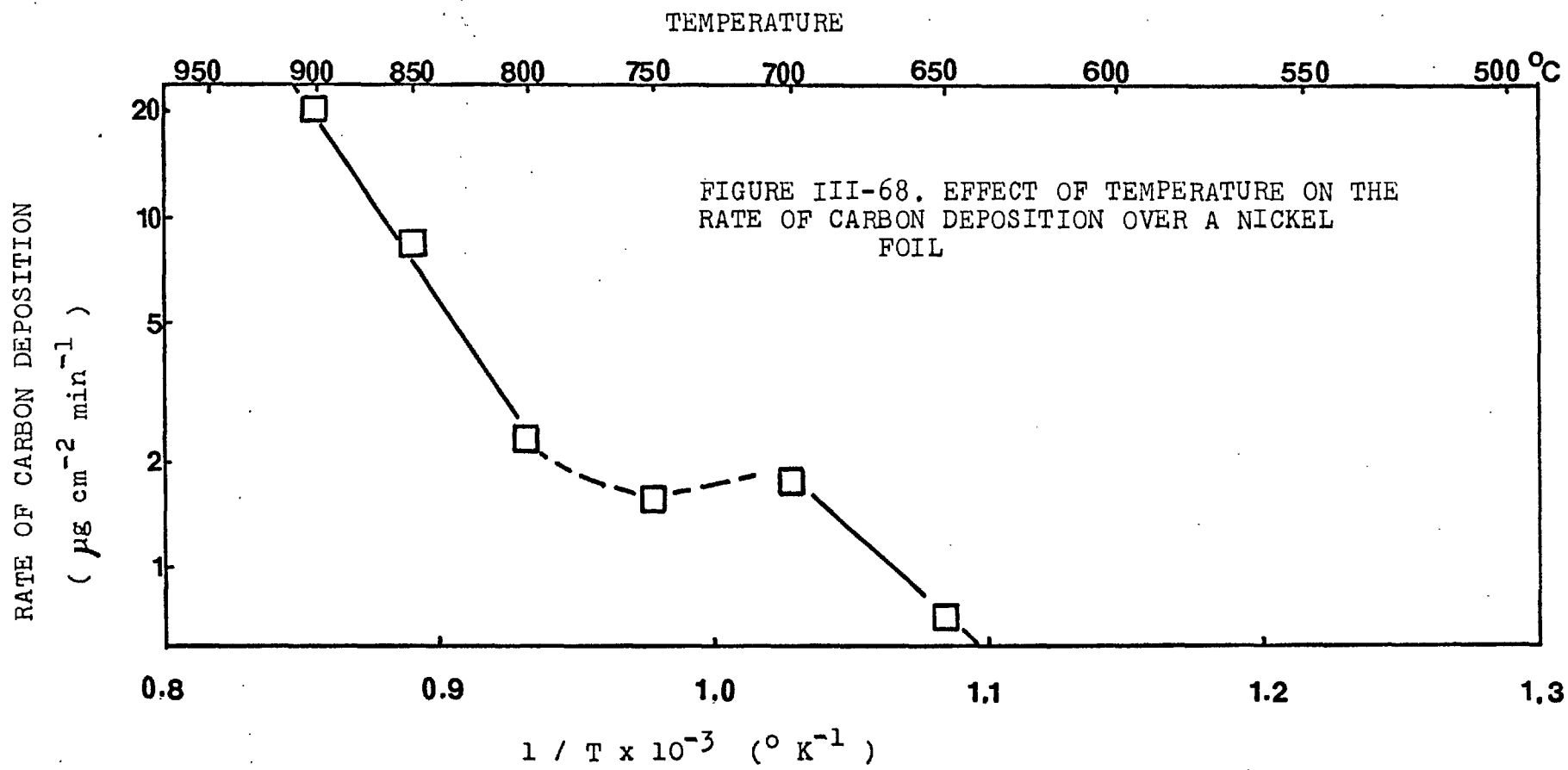




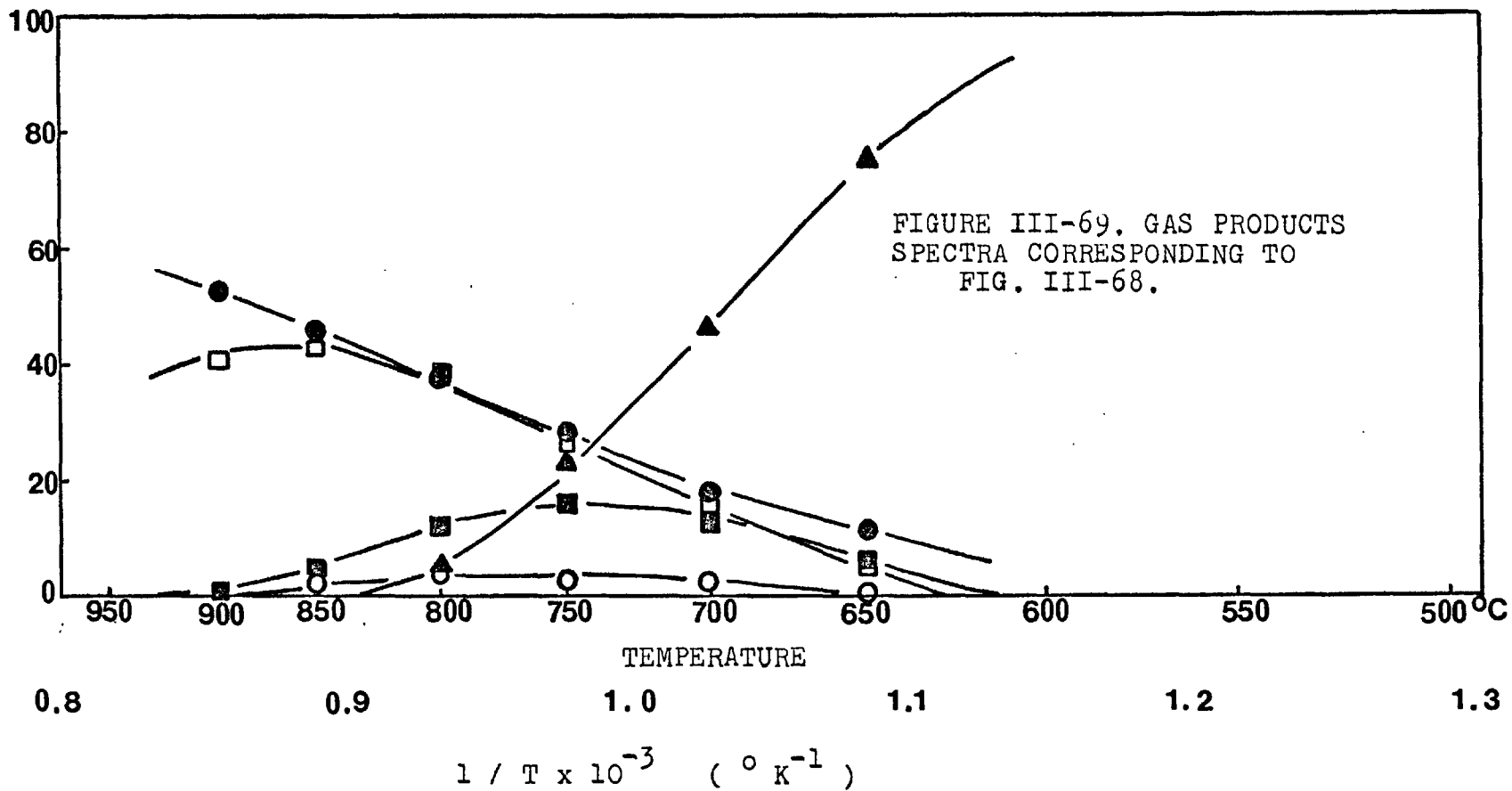








MOLES PERCENT OF PRODUCT IN  
TOTAL HYDROCARBONS



marked than in the previous case. The gas products spectrum is given in figure III-69.

Figure III-70 to 76 gives the results for deposition over copper foils and the corresponding gas products spectra. Figures III-31 to 34 give the aromatics production and composition corresponding to the rate of deposition plots of figure III-74.

The Arrhenius plots obtained with the experiments of deposition over copper are markedly different from those observed in the case of nickel. No deposition is observed at the low temperature region, and hence the first and second zones of deposition observed with nickel are absent in this case.

The presence of hydrogen has the effect of decreasing the rate of carbon deposition (see fig. III-74), while the opposite effect has been observed with nickel foils.

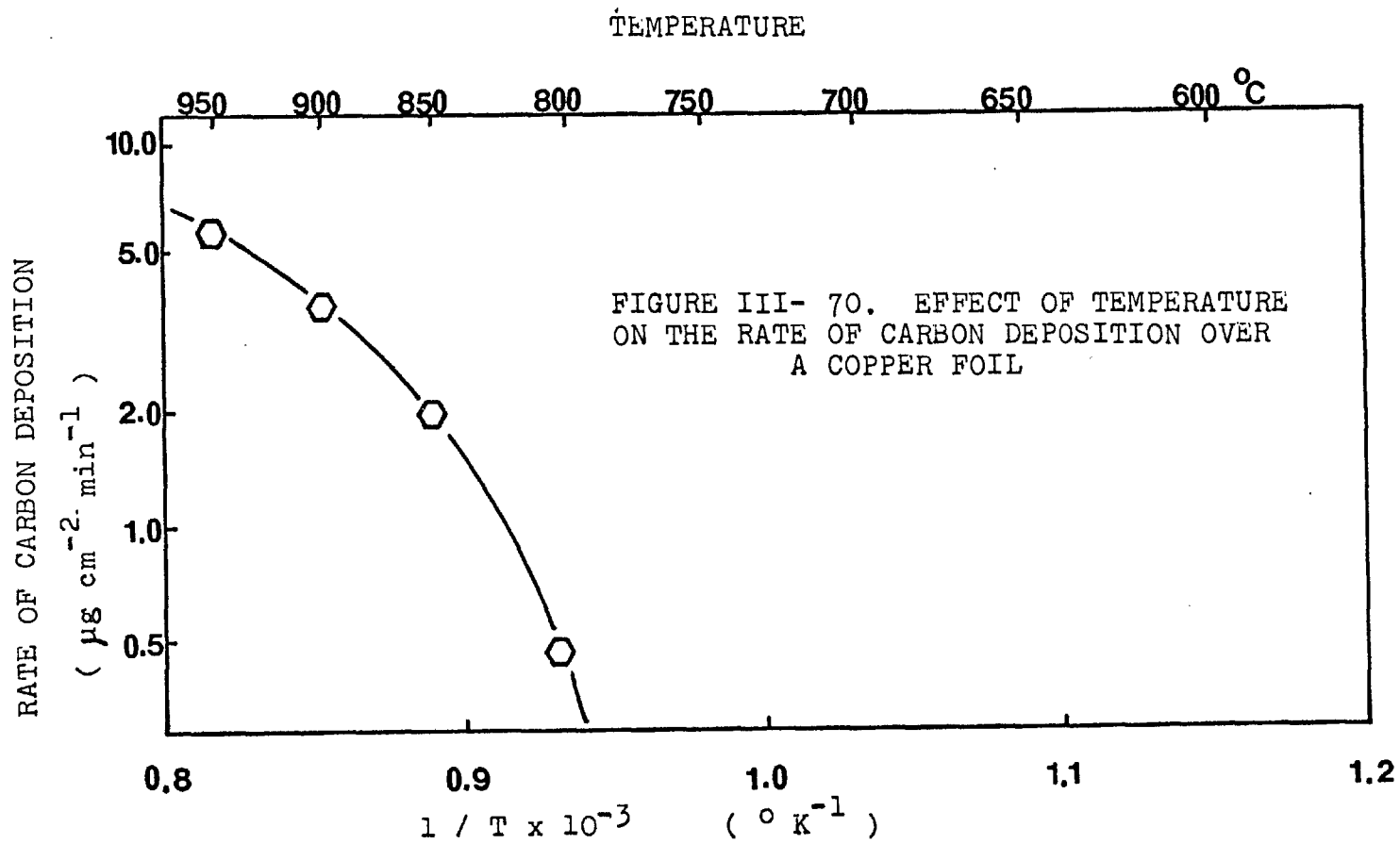
Figure III-77 compares the behaviour of nickel and copper foils in the presence and absence of initial hydrogen when, carbon is deposited from mixtures of 20% butane in hydrogen.

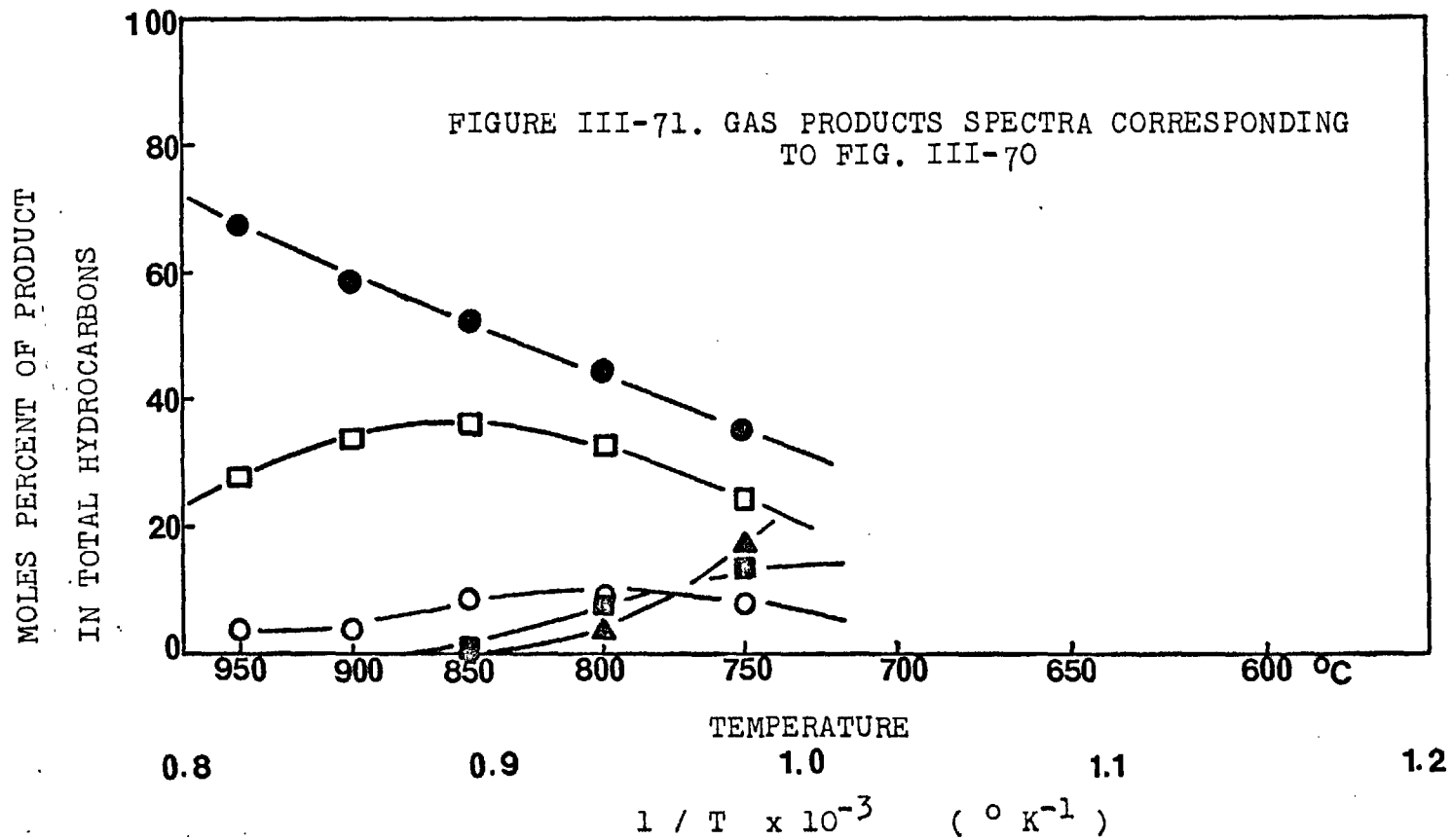
d- Results of experiments with the reactor-condenser scheme.

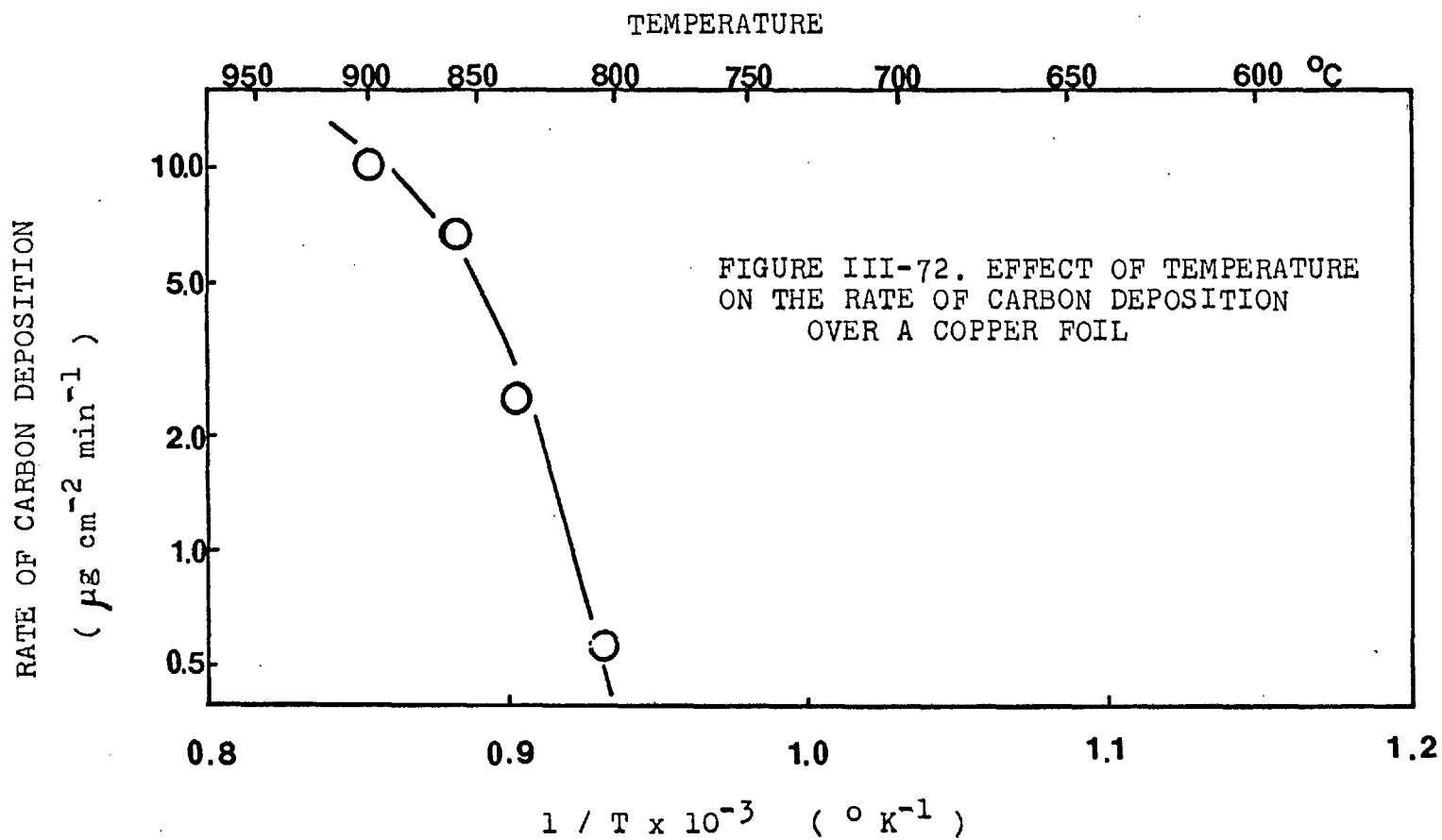
The results described in this section correspond to experiments where the temperature of carbon deposition was varied independently from the temperature at which the pyrolysis reaction was performed.

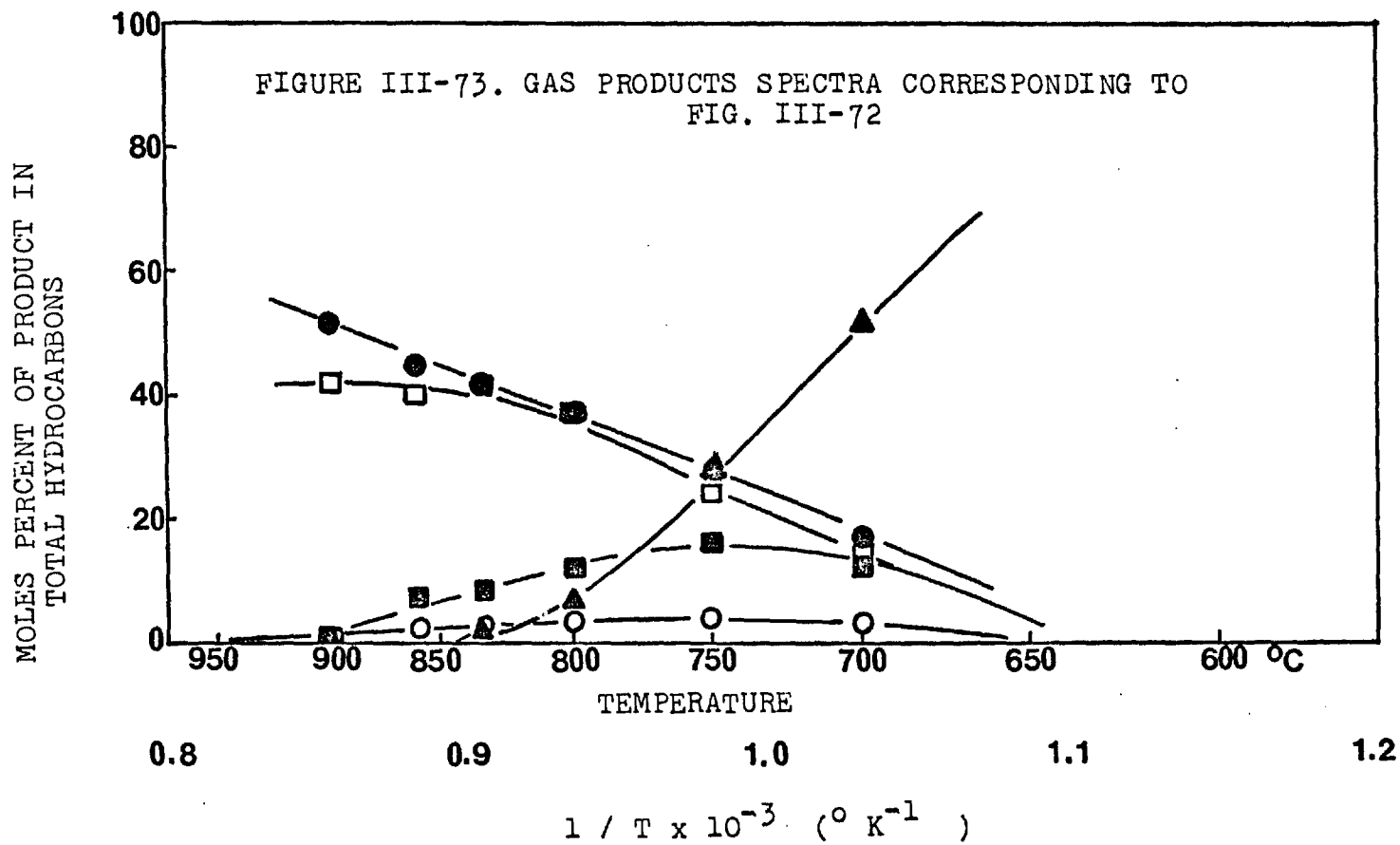
The study was carried on in connection with verifications of the "condensation theory", summarised in a previous chapter.

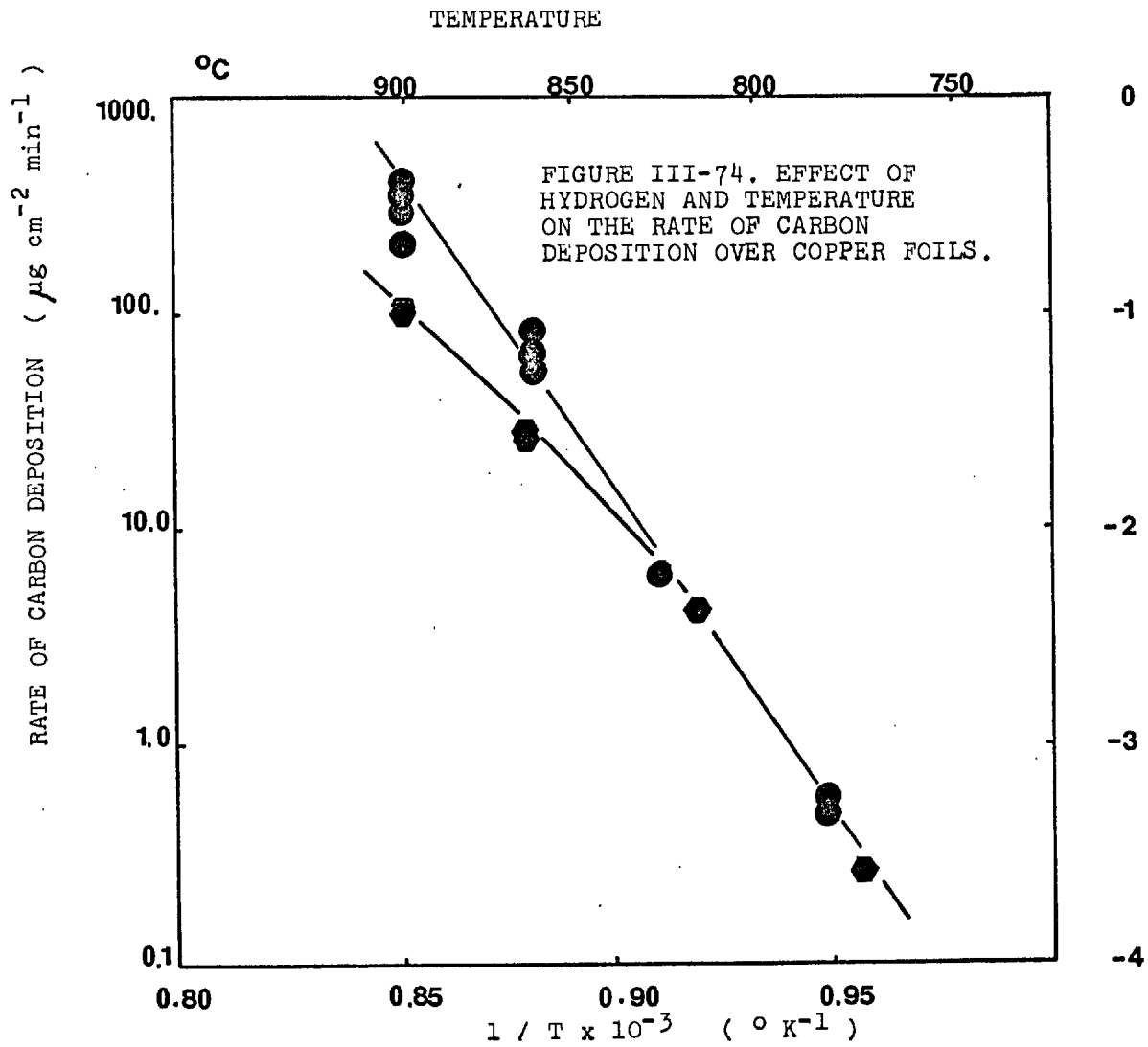
The system used was described previously and corresponds to figure II.6. The reaction zone was held at 950 °C. and temperatures in the "collection" zone varied between 400 and 900 °C in one series of runs and 250 to 900 °C in the other. Copper foils were used to collect



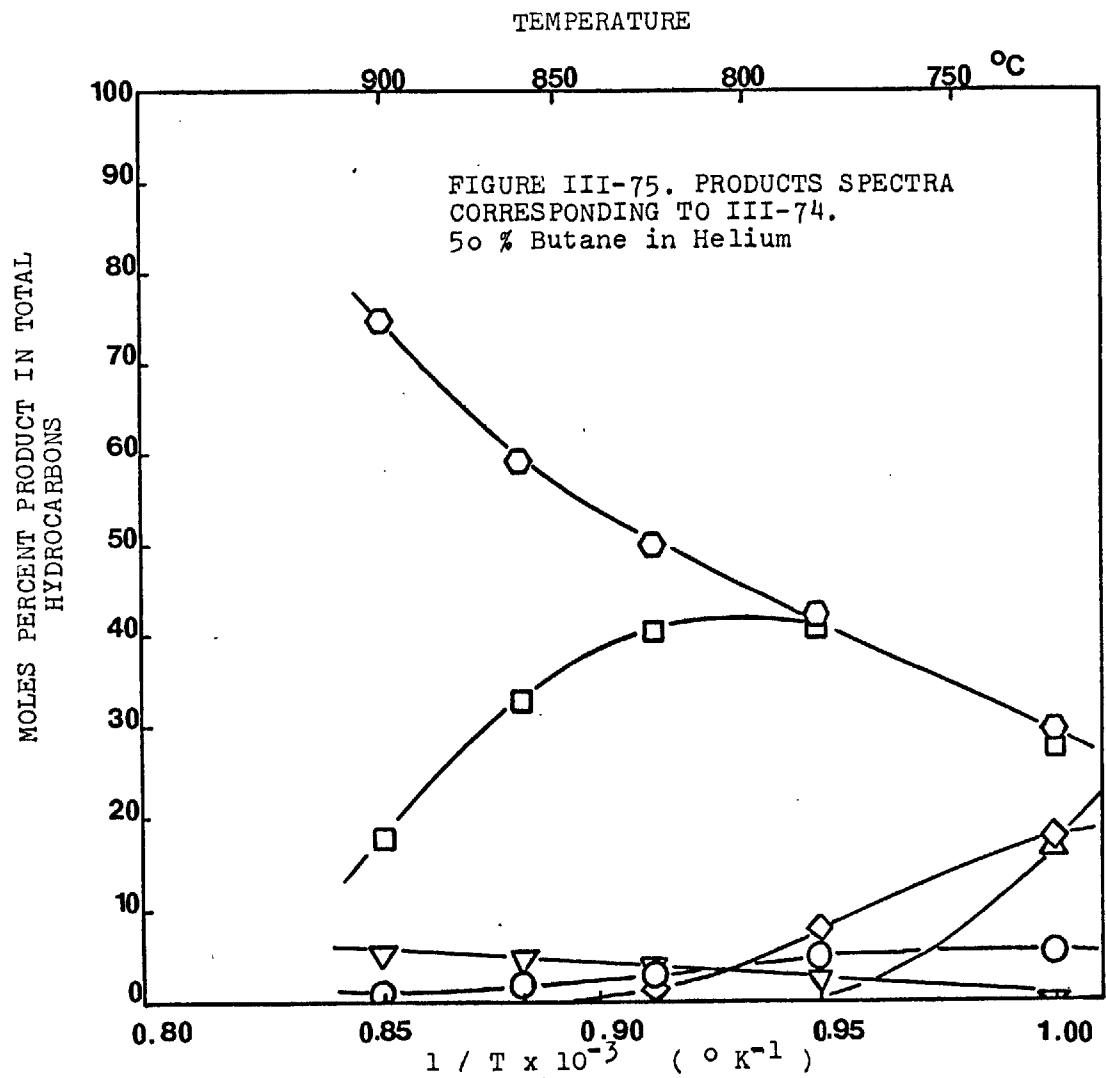


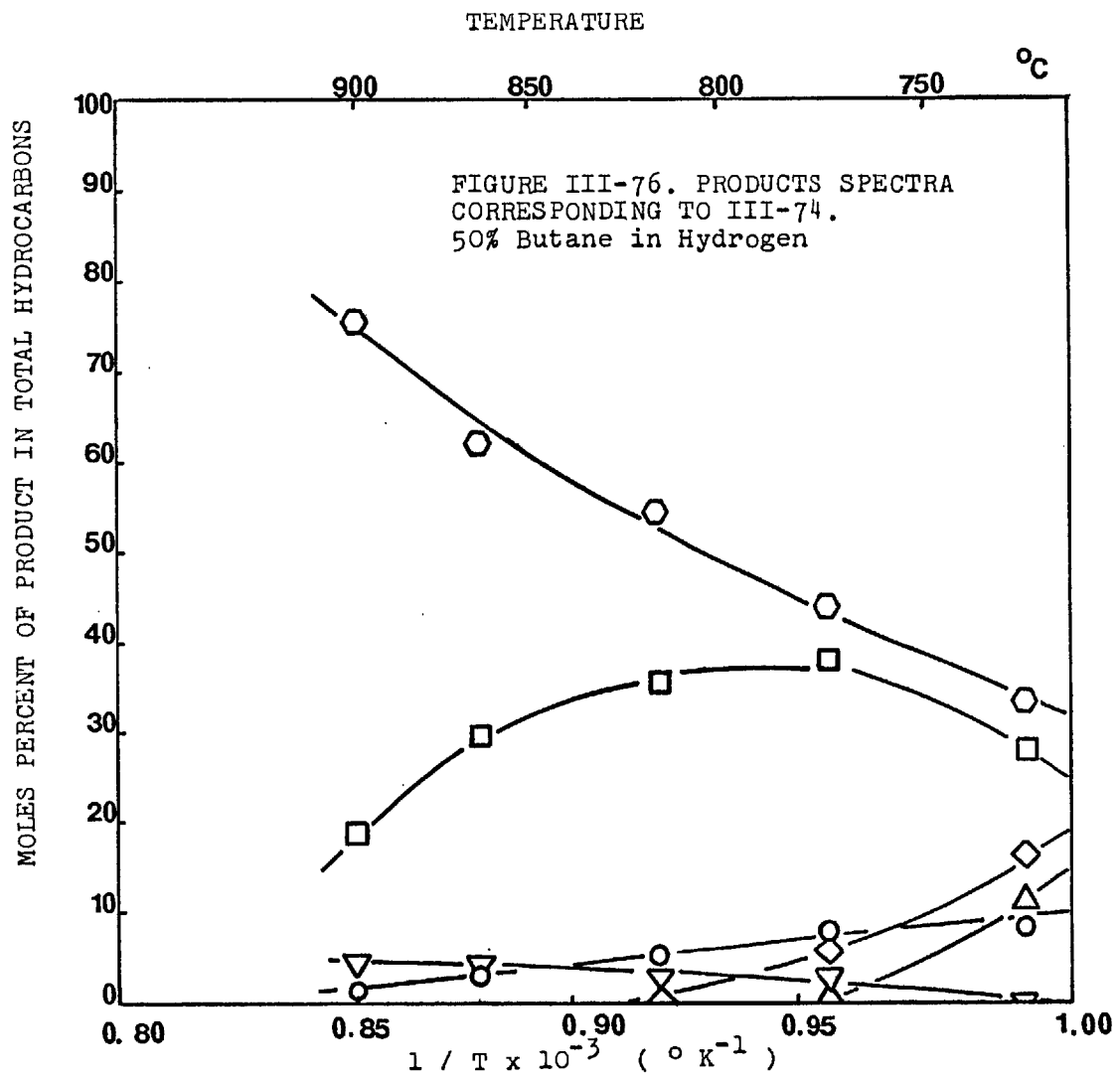


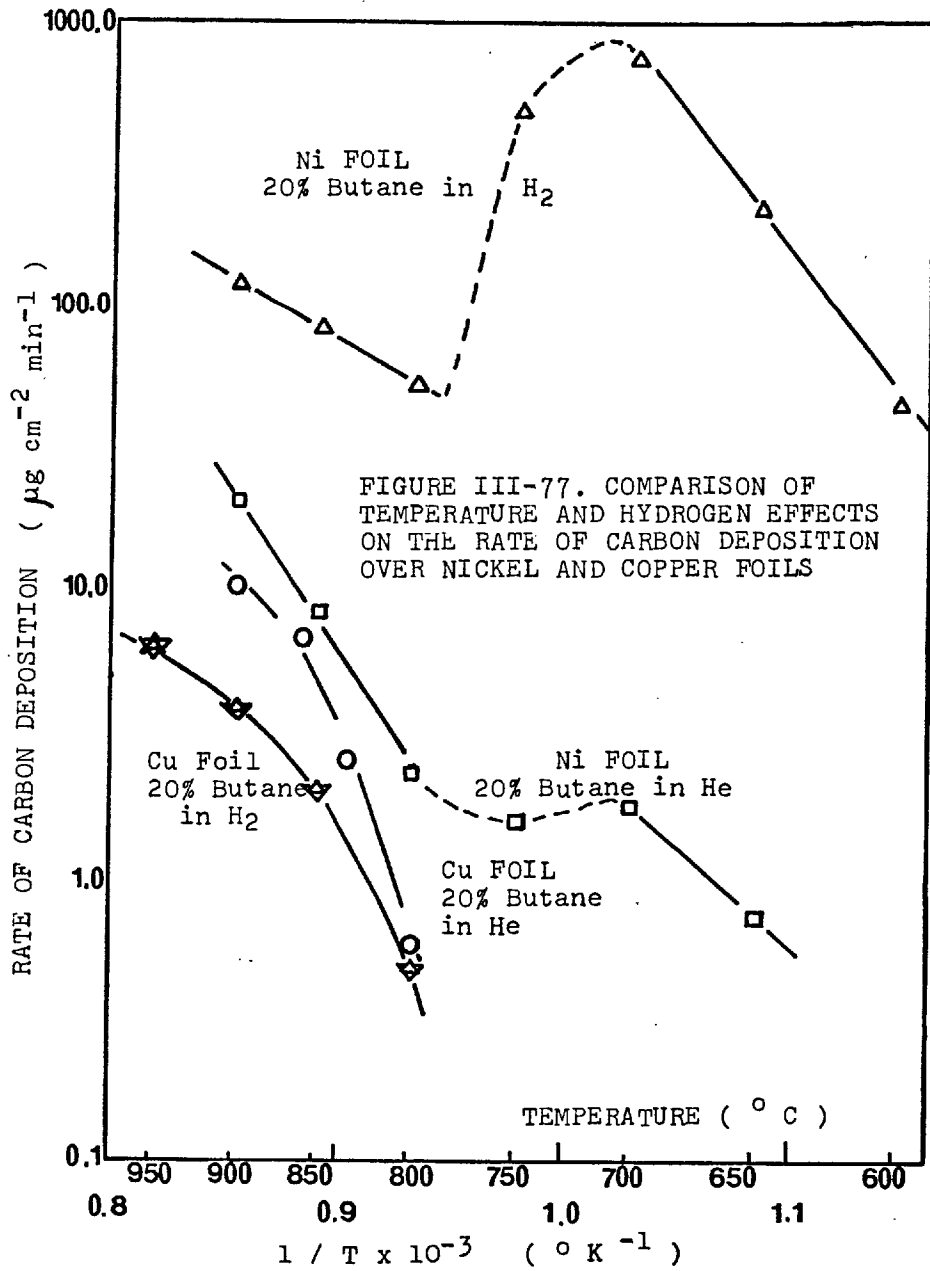












carbon and runs with pure and diluted butane were performed.

Results are shown in figure III-78 in the form of an Arrhenius plot. Two regions can be identified in both cases, with a change over at about 700 ° C. At higher deposition temperatures the process is characterized by positive apparent activation energies. These positive energies identify a chemical reaction process and not a physical condensation (see chapter IV ). Lower temperature results exhibit negative apparent activation energies, which may come from a condensation process.

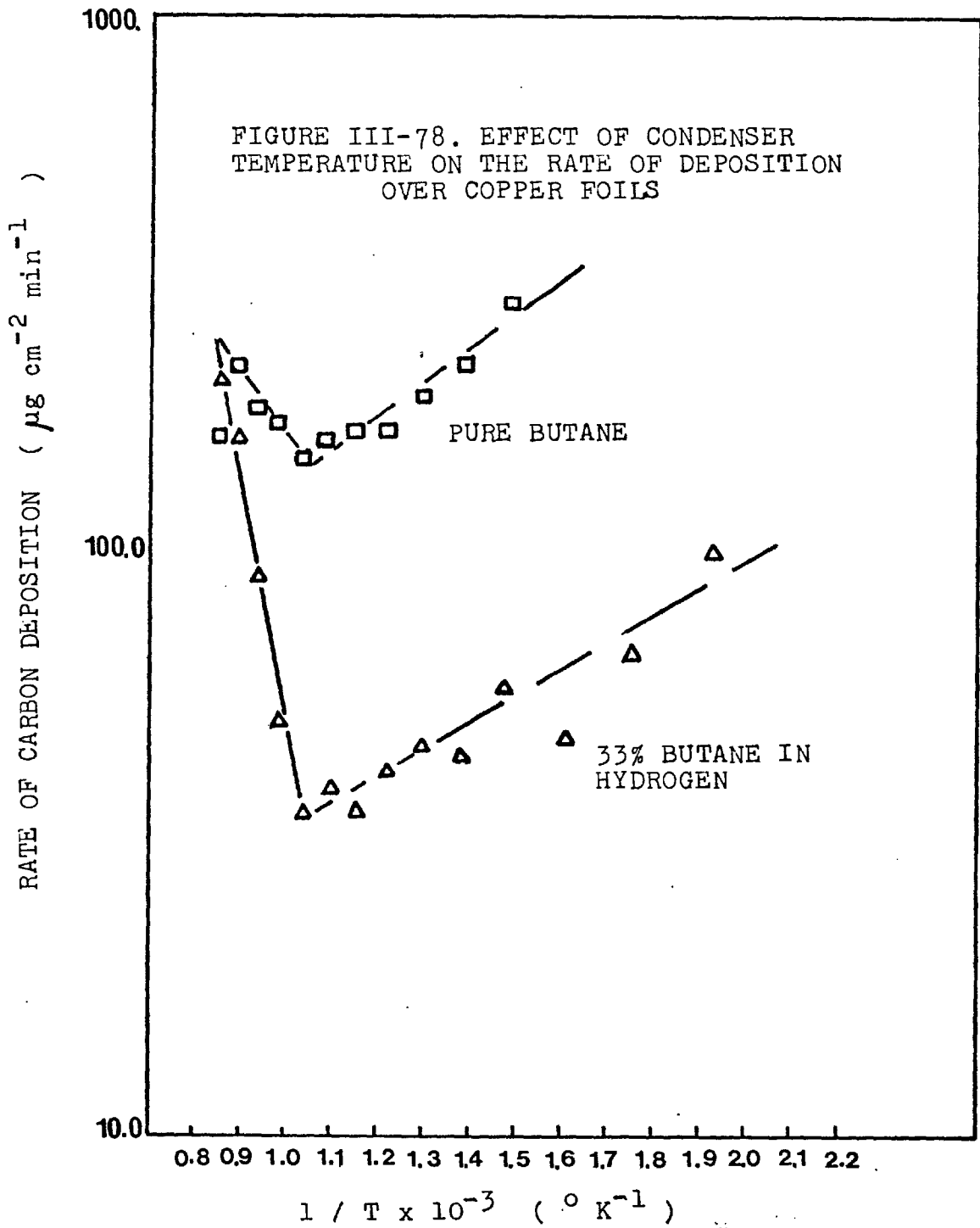
Foils that were subjected to deposition at low temperatures with chloroform and the extract analyzed by gas chromatography. Large amounts of 3-4 benzopyrene and higher polynuclear aromatics were found to be present in the deposit. (See figure III-79 ).

Hydrogen was found to decrease the rates of carbon deposition in both regions. The presence of hydrogen seemed to increase markedly the activation energy in the high temperature zone.

#### e- Transient phenomena during carbon deposition

Hydrogen was found to influence the form in which the steady rate of carbon deposition was established. Figure III-80 show the time behaviour of two nickel foils treated with different concentrations of butane in hydrogen. At low concentrations of hydrocarbon, it takes some time to reach the steady state, as if the surface was being activated with time. At higher concentrations, the activation is fast, but is followed by a period of deactivation. These patterns of behaviour were found in nickel and iron foils. (See figures III-57 and III-61).

A similar transient behaviour was observed when iron foils were used as liners for the reactor and the rate of deposition over copper



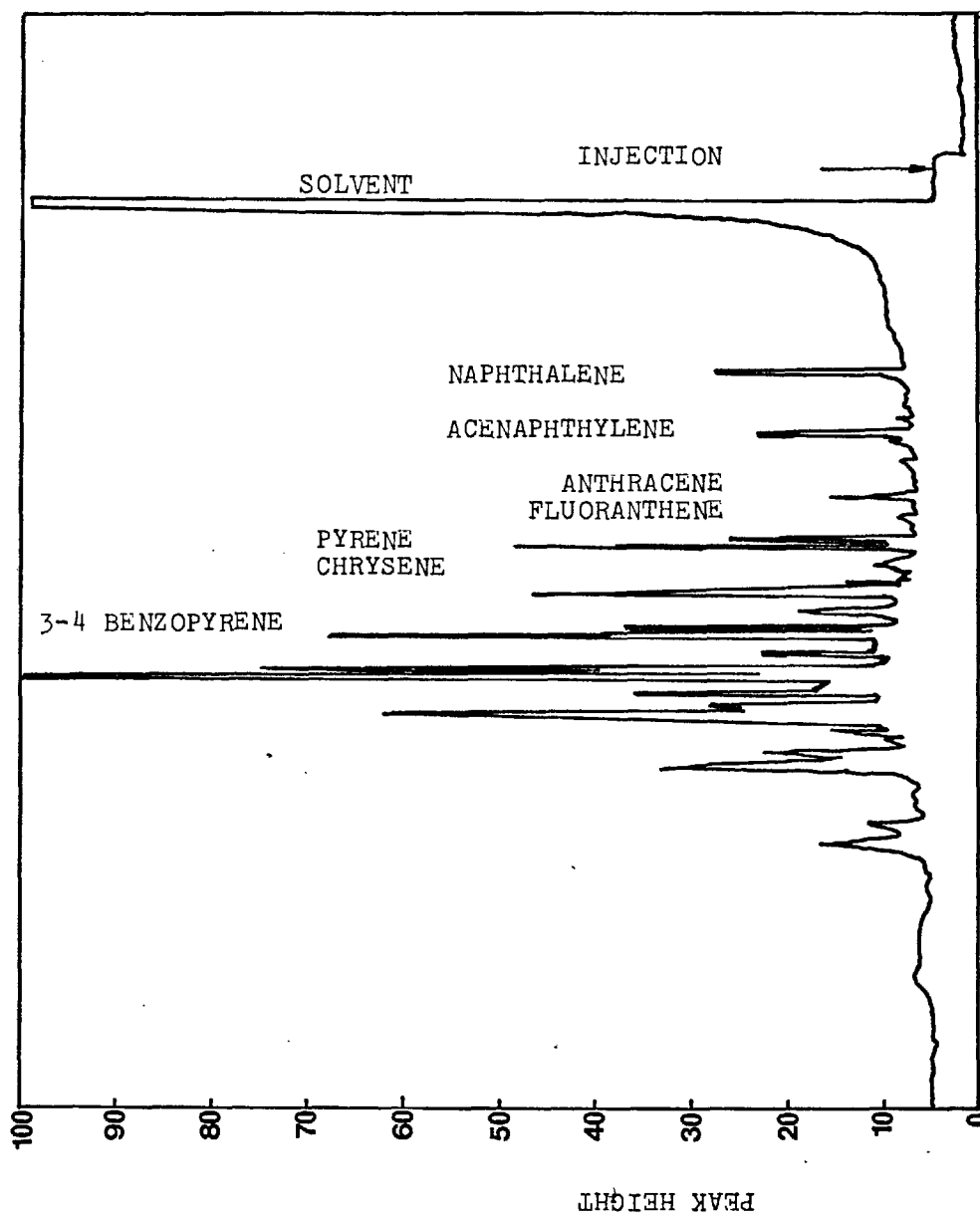
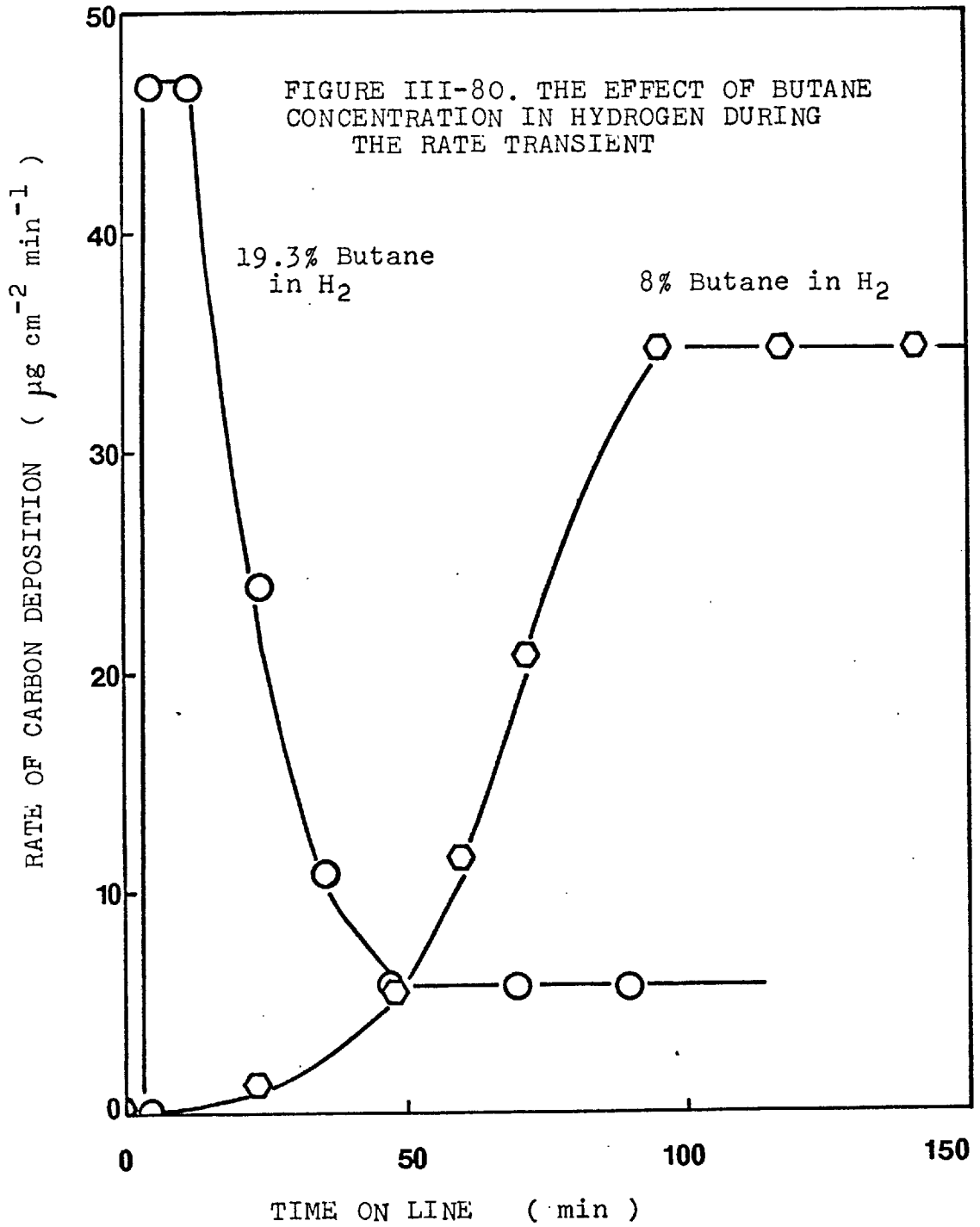


FIGURE III-79. CHROMATOGRAPHIC TRACE OF THE ANALYSIS OF THE EXTRACT OF THE DEPOSIT FROM THE METAL FOIL USED IN FIG. III-78



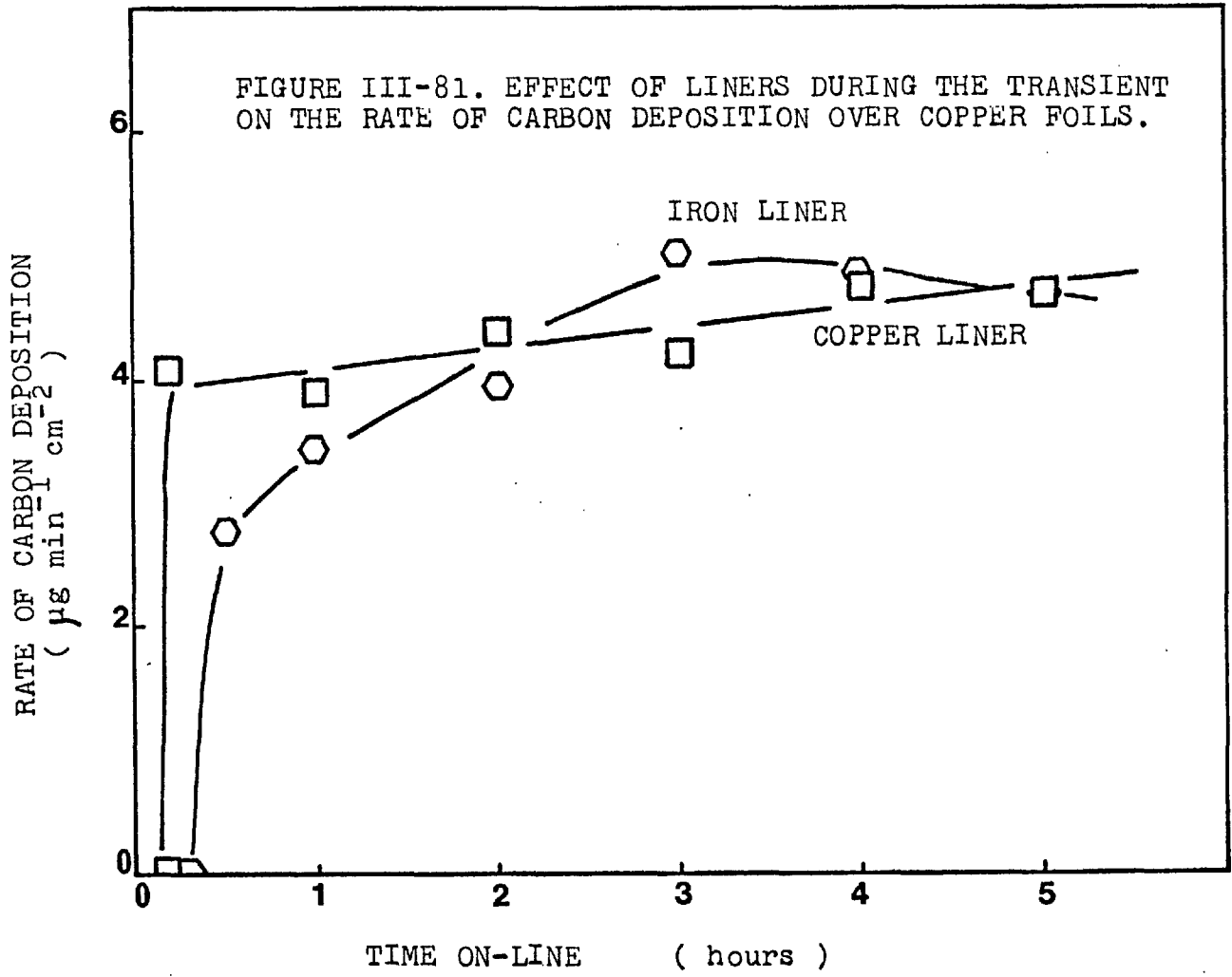
foils was studied. Figure III-81 show the difference observed during the transient when copper and iron foils were used as liners. Iron results gave lower rate of deposition at the early stages, higher in the intermediate zone and equal rates to the copper results at longer times on-line.

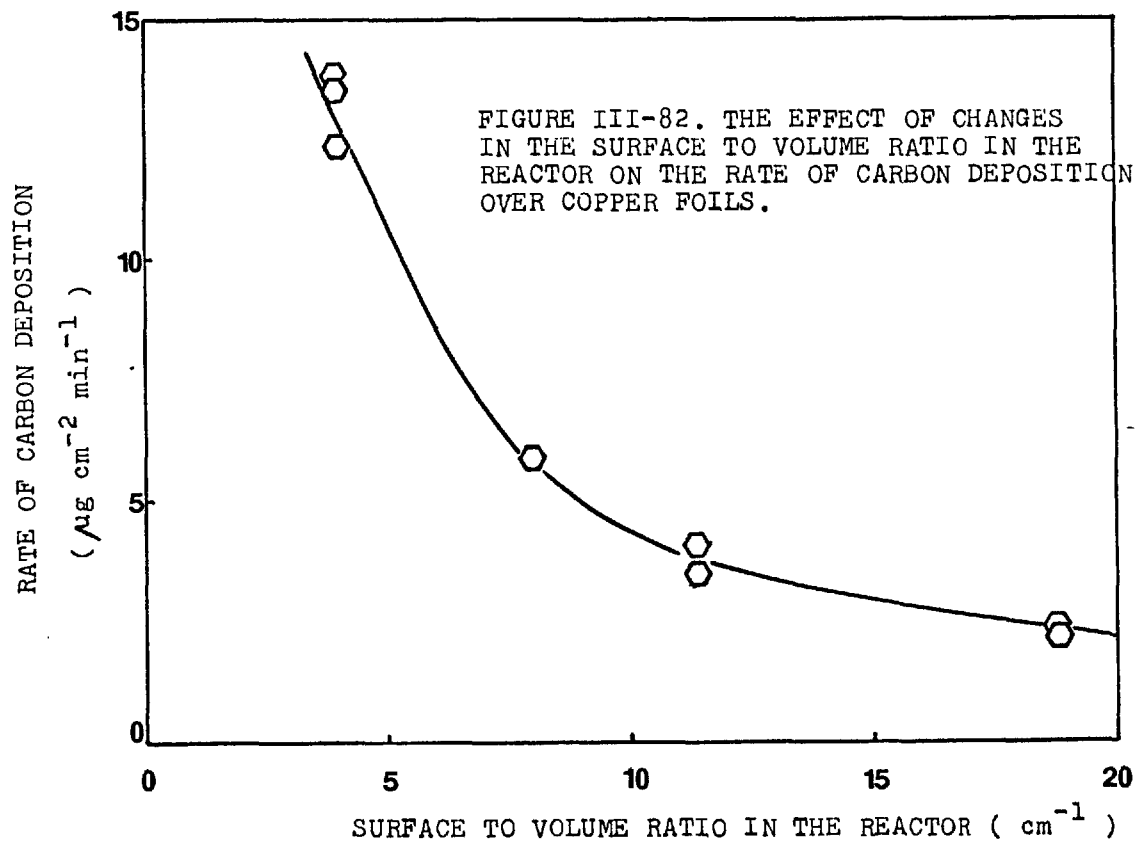
Gas product compositions corresponding to figure III-81 are given in figure III-22. Aromatic production and compositions are given in figures III-35 to 38.

f- The effect of surface to volume ratio on the rate of carbon deposition on a copper sample foil.

The change of the surface to volume ratio in the reactor was found to affect very significantly the rate of carbon deposition on a copper sample foil. The results are shown in figure III-82. A decrease of the order of 70 % in the rate was observed in the range of surface to volume studied.







D-

REFERENCES TO THE FIGURES OF CHAPTER III.

III-1 Products composition from the thermal reaction of ethane in a jet-stirred reactor

	Ethane		Ethylene
	Hydrogen		Methane

Temperature : 700° C

Feed : Pure ethane

III-2 Products composition from the thermal reaction of ethane in a jet-stirred reactor.

Key as in figure III-1

Temperature : 750° C

Feed : Pure ethane.

III-3 Products composition from the thermal reaction of ethane in a jet-stirred reactor.

Key as in figure III-1

Temperature : 800° C

Feed : Pure ethane

III-4 Products composition from the thermal reaction of ethane in a jet-stirred reactor.

Key as in figure III-1

Temperature : 830° C

Feed : Pure ethane.

III-5 Products composition from the thermal reaction of ethane in a jet-stirred reactor.

Key as in figure III-1

Temperature : 700° C

Feed : 56 % ethane in hydrogen.

III-6 Products composition from the thermal reaction of ethane in a jet-stirred reactor.

Key as in figure III-1

Temperature :  $750^{\circ}$  C

Feed : 56 % ethane in hydrogen

III-7 Products composition from the thermal reaction of ethane in a jet-stirred reactor.

Key as in figure III-1

Temperature :  $800^{\circ}$  C

Feed : 56 % ethane in hydrogen.

III-8 Products composition from the thermal reaction of ethane in a jet-stirred reactor.

Key as in figure III-1

Temperature :  $850^{\circ}$  C

Feed : 56 % ethane in hydrogen.

III-9 Products composition from the thermal reaction of ethane in a jet-stirred reactor

Key as in figure III-1

Temperature :  $900^{\circ}$  C

Feed : 56 % ethane in hydrogen.

III-10 Products composition from the thermal reaction of ethane in a jet-stirred reactor.

Key as in figure III-1





Temperature :  $950^{\circ}$  C

Feed : 56 % ethane in hydrogen.

III-11 The effect of temperature and the addition of hydrogen on the yield of ethylene and methane during the thermal reaction of ethane.

Inlet residence time( at  $800^{\circ}$  C ) : 2.5 sec.



Jet-stirred reactor.

-  Ethylene - Feed pure ethane.
-  Ethylene - 55 % ethane in hydrogen.
-  Methane - Feed pure ethane.
-  Methane - 55 % ethane in hydrogen.

III-12. The effect of temperature and addition of hydrogen on the thermal decomposition of ethane.

Inlet residence time(at 800° C)  $\tau$ : 2.5 sec.

Jet-stirred reactor.

-  Ethane conversion. Feed: pure ethane.
-  Ethane conversion. 55 % ethane in hydrogen.

III-13. Effect of the concentration of butane in hydrogen on the product spectra.


The concentrations in the ordinate are expressed as a "free of hydrogen" basis.


Tubular reactor .


Nickel sample foil.


T : 800° C ;


$\tau$  : 2.14 sec

 Methane

 Ethylene

 Butane

 Ethane

 Propylene

III-14. Effect of hydrogen concentration on the product spectrum from butane thermal decomposition.

The concentrations in the ordinate are expressed as a "free of hydrogen" basis.

Tubular reactor .

Nickel sample foil.


T : 800° C ;

$\tau$  : 1.66 sec


Helium as a diluent.


10 % butane in the feed


mixture.

 Methane

 Propylene

 Ethane


 Butane


 Ethylene.

III-15 The effect of hydrogen and temperature on butane conversion.

Tubular reactor. Nickel sample foil

Residence time (800° C) : 1.314 sec


 20 % butane in hydrogen at the feed.


 20 % butane in helium at the feed.


III-16. Effect of temperature and hydrogen addition on the yields of olefins and methane from the thermal reactions of butane. The concentrations in the ordinate are expressed as a "free of hydrogen" basis.


Tubular reactor . Nickel sample foil.


Residence time (800° C) : 1.314 sec.


 Methane . 20 % butane in hydrogen at the feed.

 Ethylene . 20 % butane in hydrogen at the feed.

 Propylene. 20 % butane in hydrogen at the feed.

 Methane . 20 % butane in helium at the feed.

 Ethylene. 20 % butane in helium at the feed.

 Propylene. 20 % butane in helium at the feed.

III-17. The effect of temperature and sample foil material.


The concentrations are expressed as a "free of hydrogen" basis.


Tubular reactor . Residence time(800° C) : 1.314 sec.


Feed . : 20 % butane in hydrogen.

Open symbols : Nickel foil


Closed symbols : Copper foil

 butane

 Ethane

 propylene







 Methane

 ethylene

III-18 Gas product spectra from the thermal reaction of butane.

Tubular reactor . Copper sample foil.

Feed : pure butane.

	butane		ethane
	propylene		methane
	ethylene		hydrogen

T : 750° C

III-19. Key as in figure III-18

T : 800° C

III-20 Key as in figure III-18

T : 850° C

III-21 Effect of residence time and hydrogen on the gas phase composition.

Tubular reactor . Copper sample foil.

Feed : 50 % butane in hydrogen.

T : 800° C.

Concentrations are given as a "hydrogen-free" basis.

	Methane		Ethylene
	Ethane		Propylene

III-22. The effect of metal liners. Gas composition changes during transient.





Tubular reactor . Copper sample foil.

Feed : 50 % butane in hydrogen.

Open symbols : Copper liner

Closed symbols : Iron liner.

T : 800° C ; Residence time : 6 seconds.






	Methane		Ethylene
	Hydrogen		Ethane.

III-23. Concentration trends of minor compounds that could be intermediates in the route towards aromatics.

Tubular reactor . Copper sample foil.

Residence time (800° C) : 6 sec

Feed : 50 % butane in hydrogen.

-  benzene
-  butadiene
-  unidentified (probably alkyl cyclopentene)
-  propylene
-  cyclohexene






III-24. The effect of surface to volume ratio in the reactor on the gas composition.

Tubular reactor . Copper sample foil.

Residence time : 6 sec

Feed : 50 % butane in hydrogen.

T : 800° C. Copper screen used to change S/V.

-  Methane
-  Ethylene
-  Ethane
-  Benzene
-  Propylene

III-25. The effect of residence time on the outlet concentration of total aromatics.








Tubular reactor . Copper sample foil.

Feed : 50 % of butane in hydrogen

T : 800° C.



III-26. Effect of residence time on the composition of the aromatic liquid collected at the reactor outlet.  
Conditions as in III-25.

	Benzene		Diethylbenzene
	Toluene		Acenaphthylene
	Ethylbenzene		Anthracene and Phenanthrene.
	Naphthalene		

III-27. Effect of residence time on the concentration of aromatics calculated at the reactor outlet.  
Conditions as in III-25.  
Key as in III-26.

III-28. Effect of hydrogen concentration on the outlet concentration of total aromatics.









Tubular reactor. Copper sample foil.

Residence time : 5 sec

T : 800° C.

Feed : 25 % butane. Helium as diluent.

III-29. Effect of hydrogen concentration on the composition of the aromatic liquid collected at the reactor outlet.  
Conditions as in III-28.

	benzene		diethylbenzene
	toluene		acenaphthylene
	Ethylbenzene		anthracene and phenanthrene
	Naphthalene		fluorene.

III-30. Effect of hydrogen concentration on the composition of aromatics calculated at the reactor outlet.

Conditions as in III-28.




Key as in III-29.

III-31. Effect of butane concentration in hydrogen on the production of major aromatics.

Tubular reactor . Copper collection foil.









Residence time : 6 sec ; T : 800° C

Feed : butane in hydrogen.

 total aromatics  
 benzene  
 naphthalene.

III-32. Effect of butane concentration in hydrogen on the production of minor aromatics.



Conditions as in III-31.

 toluene       anthracene and  
 ethylbenzene      phenanthrene  
 diethylbenzene       pyrene  
 acenaphthylene       chrysene.  
 fluorene

III-33. Effect of temperature and hydrogen on the outlet concentration of total aromatics produced.

Tubular reactor . Copper collection foil.

Residence time (800° C) : 6 sec






 50 % butane in helium at the feed.  
 50 % butane in hydrogen at the feed.

III-34. Effect of temperature on the composition of the aromatic

liquid collected at the reactor outlet.

Tubular reactor .                      Copper sample foil

Residence time (800° C) : 6 sec

	benzene		diethylbenzene
	toluene		naphthalene
	ethylbenzene		

Feed : 50 % butane in hydrogen.

III-35. As in III-34


Feed : 50 % butane in helium.

III-36. Effect of temperature and hydrogen on the production of benzene and naphthalene.

Conditions as in III-34.

Open symbols : 50 % butane in hydrogen.

Closed symbols : 50 % butane in helium.

	benzene		naphthalene.
---	---------	---	--------------

III-37. Effect of liners during the transient in the formation of total aromatics.

Tubular reactor .                      Copper sample foil.

Residence time : 6 sec ; T : 800° C

Feed : 50 % butane in hydrogen.

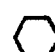


	Cu liner		Fe liner
---	----------	---	----------

III-38. Effect of liners during the transient in the composition of the liquid aromatics collected at the reactor outlet.

Conditions as in III-37.

Open symbols : Cu liner

Closed symbols : Fe liner

	benzene		toluene
	naphthalene.		

III-39 Effect of liners during the transient on the outlet concentration of major aromatics.

Conditions as in III-37.

Open symbols : Cu liner

Closed symbols : Fe liner





 benzene       naphthalene

III-40. Effect of liners during the transient on the outlet concentration of minor aromatics.

Conditions as in III-37.

Open symbols : Cu liner

Closed symbols : Fe liner

 toluene       diethylbenzene  
 ethylbenzene       anthracene and  
phenanthrene.




III-41. Effect of changes in the surface to volume ratio in the reactor on the production of total and major aromatics.

Tubular reactor . Copper sample foil.

Copper metal screen used to change surface to volume ratio.







Residence time : 6 sec ; T : 800° C



Feed : 50% butane in hydrogen.

 total aromatics       naphthalene  
 benzene

III-42. Effect of changes in the surface to volume ratio in the reactor on the production of minor aromatics.

Conditions as in III-41.

 toluene       fluorene  
 ethylbenzene       anthracene  
 diethylbenzene       pyrene

 acenaphthylene       chrysene

III-43. Rates of carbon deposition on a silica foil :


Ageing effect.


Tubular reactor .


Silica foil.

T : 800° C.

Feed : pure butane.

 Run I-2

 Run I-4

 Run I-3


 Run I-5


III-44 The effect of the nature of the collection foil on the rate of carbon deposition.


Tubular reactor .


T : 800° C


Feed : pure butane.

 Run I-6 - Ni foil

 Run I-7 - Ni foil

 Run I-8 - Fe foil

 Run I-9 - Cu foil

 Run I-2 - Silica , not aged.


 Run I-5 - Silica , aged.


III-45. Effect of copper liner on the rate of deposition over a copper sample foil.


Tubular reactor .

T : 800° C

Feed : pure butane.

 Run I-9 - No liner (silica wall)

 Run I-10 - Cu liner , initial rates


 Run I-10 - Steady state rates



III-46. Effect of iron liner on the rate of deposition over a copper sample foil.

Tubular reactor ;

T : 800° C

Feed : pure butane.





 Run I-9 - No liner

-  Run I-11 - Fe liner Initial rate  
 Run I-11 - Fe liner Steady state rate.

III-47 Effect of different liners on the steady state rate of carbon deposition over a copper foil.

Tubular reactor ; T : 800° C

Feed : pure butane.

-  Run I-9 - No liner  
 Run I-13 - Cu liner  
 Run I-12 - Ni liner  
 Run I-11 - Fe liner.



III-48, Effect of the sequence of operation on the rate of carbon deposition.

Tubular reactor . Iron liner.

T : 800° C

Copper collection foil

Feed : pure butane.

-  Run I-14 - Performed sequentially: decreasing the residence time.  
 Run I-11 - Performed sequentially: increasing the residence time.



III-49. Effect of the sequence of operation on the rate of carbon deposition.

Tubular reactor . Nickel liner

T : 800° C

Copper collection foil

Feed : pure butane.





-  Run I-15 - Performed sequentially: decreasing residence time.  
 Run I-12 - Performed sequentially: increasing residence time.

III-50. Transient rates of carbon deposition on different materials.

Tubular reactor . T : 800° C

Residence time : 2 sec

Feed : pure butane.


-  Run I-2 - Silica foil, not aged.
-  Run I-7 - Nickel foil.
-  Run I-8 - Iron foil.
-  Run I-9 - Copper foil.


III-51. Effect of the liner treatment on the rate of deposition over a copper sample foil.

Tubular reactor . T : 800° C

Residence time : 5 sec

Feed : pure butane.

-  Ni liner . New foils. Treated with hydrogen.  
Run I-15 first experiment.


-  Ni liner . Foil and liner after carbon deposition. Treated with hydrogen.  
Run I-15. last experiment.

III-52. Effect of liner treatment on the rate of deposition over a copper sample foil.

Tubular reactor . Iron liner.

Residence time : 1.95 sec , T : 800° C

Feed : pure butane.

 New liner. Pretreated with hydrogen.

 After carbon deposition (Run I-14 ).

Carbon burned with air; metal reduced later with hydrogen.

III-53. Effect of residence time and temperature on the rate of deposition over copper foils.

Tubular reactor . Feed : pure butane.


Open symbols : Runs II-64 to 75.


Closed symbols : Runs I-9 and 10.

 850° C       700° C  
 800° C

III-54. Effect of temperature on the rate of carbon deposition over copper sample foils.


Tubular reactor . Feed : pure butane

 2 sec residence time


 11 sec residence time.

III-55. Effect of residence time on the carbon deposition on copper foils.

Tubular reactor . T : 800° C

 Feed : 50 % butane in hydrogen.

Series III runs.

 Feed : pure butane .

Series I and II runs.



III-56. Effect of butane concentration in hydrogen on the rate of carbon deposition over nickel foils.

Tubular reactor , T : 800° C

Residence time : 1.66 sec

⬡ Runs II-3 , 4 , 5 , 6 and 7

○ Runs II-8 , 9 , 10

▽ Runs II-11 , 12 , 13 , 14 and 15

III-57. Rate history of two nickel foils.

Series II runs. Passing hydrogen between experiments.

Open symbols : initial rates.

Closed symbols : steady rates.

Conditions as in III-56.

III-58. Effect of hydrogen concentration on the rate of deposition over nickel.

Tubular reactor , T : 800° C

Residence time : 1.66 sec

Feed : 10% butane. Helium used as diluent.

Series II runs.






III-59. Effect of butane concentration in hydrogen on the rate of carbon deposition over iron foils.

Tubular reactor , T : 800° C

Residence time : 1.31 sec

Series II runs.

III-60 Product spectra corresponding to III-59.

	Methane		Propylene
	Ethane		Butane
	Ethylene.		

III-61. Rate history of several iron sample foils.

Corresponding to figure III-59.

Open symbols : initial or intermediate rates.

Closed symbols : final or steady rates.

III-62. Effect of concentration of butane in hydrogen on the rate of carbon deposition over copper foils.

Tubular reactor , T : 800° C

Residence time : 1.31 sec

Series II runs.

III-63 Products spectra corresponding to III-62

Key as in fig. III-60.

III-64. Effect of the concentration of hydrogen on the rate of deposition over copper foils.

Tubular reactor ; T : 800° C

Residence time : 5.25 sec

Feed : 25% butane. Helium as diluent.

III-65. Gas products spectra corresponding to III-64.

Key as in fig. III-60.

III-66. Effect of temperature on the rate of carbon deposition over a nickel foil.

Tubular reactor .            Series II runs.

Residence time (800° C) : 1.31 sec

Feed : 20 % butane in hydrogen.

III-67. Gas products spectra corresponding to III-66.

Key as in fig. III-60.

III-68. Effect of temperature on the rate of carbon deposition over a nickel foil.

Tubular reactor .            Series II runs.

Residence time (800° C) : 1.31 sec

Feed : 20 % butane in helium.

III-69. Gas products spectra corresponding to III-68.

Key as in fig. III-60.

III-70. Effect of temperature on the rate of carbon deposition over a copper foil.

Tubular reactor .            Series II runs.

Residence time :            1.31 sec

Feed : 20 % butane in hydrogen.

III-71. Gas products spectra corresponding to III-70.

Key as in fig. III-60.

III-72. Effect of temperature on the rate of carbon deposition over a copper foil.

Tubular reactor .            Series II runs.

Residence time :            1.31 sec

Feed : 20 % butane in hydrogen.


III-73. Gas products spectra corresponding to III-72.


Key as in fig. III-60.

III-74. Effect of hydrogen and temperature on the rate of carbon deposition over a copper foil.

Tubular reactor . Series III runs.


Residence time (800° C) : 6.13 sec


 50 % of butane in helium


 50 % of butane in hydrogen.


III-75. Products spectra corresponding to III-74.


50 % of butane in helium.


 methane

 ethane

 ethylene

 propylene

 butane

 benzene.

III-76. Products spectra corresponding to III-74.

50 % of butane in hydrogen.

Key as in III-75.

III-77. Comparison of temperature and hydrogen effects on the rate of carbon deposition over copper and nickel foils.

Tubular reactor . Series II runs.

Residence time (800° C) : 1.31 sec

 Nickel foil . 20 % butane in hydrogen

 Nickel foil . 20 % butane in helium

 Copper foil . 20 % butane in helium



 Copper foil . 20 % butane in hydrogen.

III-78. Effect of condenser temperature on the rate of deposition over copper foils.

Reactor- condenser scheme. Series II runs.

Reactor temperature : 900° C

Flow : 90 ml min<sup>-1</sup>

-  Pure butane  
 33 % butane in hydrogen.

III-79. Chromatographic trace of the analysis of the extract of the deposit from the metal foil used in III-78.

Conditions as in text. ( Chapter II ).

III-80. The effect of butane concentration in hydrogen during the rate transient.

Tubular reactor . Nickel foils.

Residence time : 4.4 sec , T : 800° C

Series II runs.

○ Feed : 19.3 % butane in hydrogen

⬡ Feed : 8 % butane in hydrogen

III-81. Effect of liners during the transient on the rate of carbon deposition over copper foils.

Tubular reactor . Residence time : 6 sec

Feed : 50 % butane in hydrogen , T : 800° C.

 Cu liner                       Fe liner

III-82. The effect of changes in the surface to volume ratio in the reactor on the rate of carbon deposition over copper foils.

Tubular reactor . Copper metal screen used to change the surface to volume ratio.

Residence time : 6 sec , T : 800° C

Feed : 50 % butane in hydrogen.

## CHAPTER IV

DISCUSSION

1- <u>GENERAL</u>	.....	216
2- <u>THE FORMATION OF THE MAIN GAS PRODUCTS</u>	.....	218
a- Free-radical model at high conversions in the presence of hydrogen : The thermal reaction of ethane...		219
b- The effect of hydrogen on the rate of the thermal decomposition of hydrocarbons.	.....	232
c- Semi - empirical modelling of thermal hydrogenation reactions (hydrogasification).	.....	237
d- Effect of reactor surfaces on the production of the major compounds.	.....	241
3- <u>THE PRODUCTION OF AROMATIC COMPOUNDS</u>	.....	242
a- Introduction	.....	242
b- The synthesis of aromatics from paraffins.	.....	243
c- Modelling of aromatics synthesis.	.....	249
d- Further reactions leading to the formation of polycyclic aromatics.	.....	251
e- The effect of hydrogen on aromatics formation.	.....	256
f- The effect of surface to volume ratio in the reactor.		257
4- <u>THE FORMATION OF CARBONACEOUS DEPOSITS ON SURFACES</u>	....	258
General	.....	258
4-A <u>The formation of carbon deposits without the intervention of catalytic metals</u>	.....	259
a- General discussion of the experimental results.....		259
b- A model for non - catalytic carbon deposition.	.....	262
c- Simplified mathematical model. The effect of the operational variables.	.....	264

d-	The effect of surface to volume ratio on carbon deposition.	273
e-	Mathematical modelling of the growth of coke particles by carbon deposition in a fluid bed during thermal hydrogenation.	277
f-	The deposition of carbonaceous material by physical condensation.	285
4-B	<u>The formation of carbon deposits on surfaces in the presence of catalytic metals.</u>	287
a-	Introduction	287
b-	Description of a qualitative model for carbon formation on catalytic metals.	288
I-	<u>Experiments with pure butane</u>	290
c-	Carbon deposition on different metals.	291
d-	The effect of lining the reactor wall with different metals.	291
e-	Transient effects during the early stages of deposition.	293
f-	Effect of temperature on the deposition of carbon over nickel.	293
II-	<u>Experiments with butane diluted with hydrogen and helium.</u>	294
g-	The effect of hydrogen on the carbon deposition over different metals.	294
h-	Transient phenomena in the presence of hydrogen.	296
5-	<u>THE INTER-RELATION AMONGST GAS MAJOR PRODUCTS, AROMATIC COMPOUNDS AND CARBON FORMATION.</u>	297
6-	<u>CONCLUSIONS</u>	301
	<u>APPENDIX I</u>	307

1- GENERAL

The present studies have been focused on the pyrolysis of hydrocarbons in the absence and presence of hydrogen. The reaction leads to gas phase products such as light olefins, to liquid phase products such as alkylaromatics and to carbon. Work has been directed towards studies of the mechanism and kinetics of the reactions and towards the effect of surfaces on the product spectrum.

A simplified picture of the main reaction paths proposed here to explain the thermal reaction of a paraffinic hydrocarbon is presented in figure IV-1. The initial hydrocarbon is supposed to break down into hydrogen, low molecular weight paraffins and to olefins following a free-radical homogeneous chain mechanism. These fragments could not react, or could be hydrogenated to form the main stream of products that leaves the reactor as a gas.

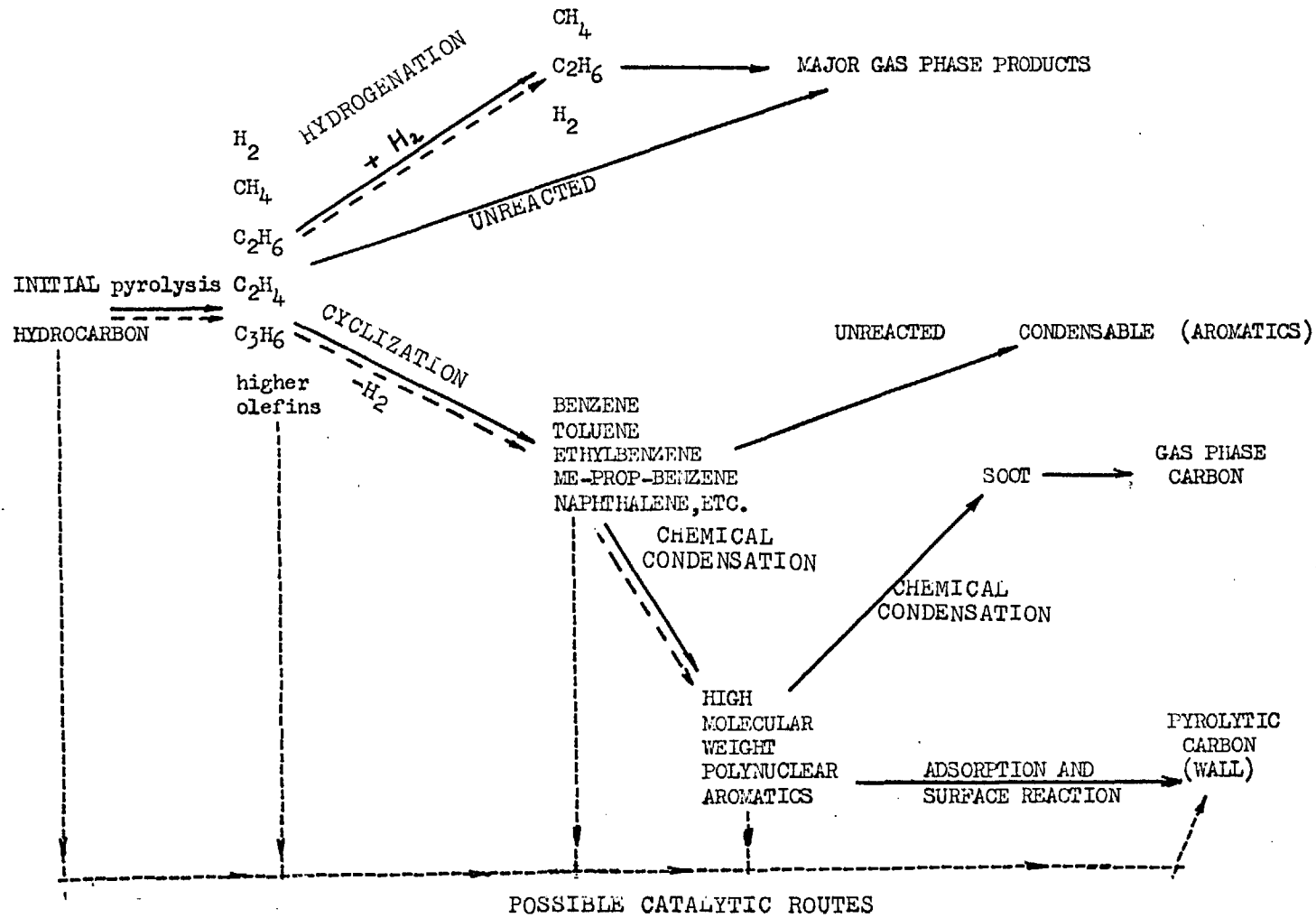
Some of the olefins produced in the primary breakdown could undergo cyclisation and dehydrogenation reactions, together with some reactions involving side chains. These reactions would lead to the production of long-lived, relatively stable aromatic molecules that would leave the reactor to form a "condensate" or "aromatic tar", rich in benzene, alkylbenzenes, naphthalene, pyrene and some other undercomposed aromatics.

The more reactive and short-lived aromatics could undergo reactions of further condensation, until the size of the aromatic polymer is such that a partial pressure large enough to provoke the adsorption of the molecule on the reactor surface is established. This molecule could then lose hydrogen in a carbonization process, establishing a carbon surface able to adsorb new molecules of aromatic polymer.

Alternatively, in the case in which the surface to volume ratio in the reacting system is very low or when the reaction conditions are very severe, polynuclear molecules could grow by chemical condensation



FIG. IV. 1 POSSIBLE GAS PHASE PHENOMENA



to a certain critical size while suspended in the gas phase. Here they could act as a nuclei for further growth, by surface chemical reaction, physical condensation and agglomeration.

In figure IV -1 , the dotted lines indicate the reaction paths that may be set in operation by surfaces in contact with the gas.

In this chapter, the complex system of reactions has been divided, for the convenience, as reactions that lead to major gas products, aromatics and carbon. Each type of reaction is discussed separately and are linked together in the last section of the chapter.

## 2- THE FORMATION OF THE MAIN GAS PRODUCTS

The use of free-radical models of the pyrolysis of hydrocarbons to describe the reaction at low conversion has been summarised in a previous chapter. In the case of light paraffins, these models are well established and essentially describe the initial behaviour and initial rates of the reactions involved.

Reactions produced under conditions of industrial interest, however, are far from being at low conversions. Secondary reactions involving the products are increasingly important in industrial cracking and thermal hydrogenation, and the chemical mechanism of the reactions involved cannot be explained by the same free-radical mechanisms as used at zero conversions.

The effect of hydrogen dilution on the thermal reactions has also received little attention. The general effect has been explained qualitatively, but no attempt has been made to model quantitatively the free-radical mechanism of the hydrogen-hydrocarbon pyrolysis.

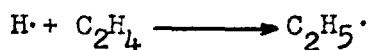
The quantitative explanation of both pyrolysis and thermal hydrogasification reactions, under conditions of practical interest, involves an extension of the well-established low-conversion mechanisms and models, to include secondary reactions and those where hydrogen

participates at relatively high concentrations. This has been carried out using a model of the high - conversion thermal reaction of ethane in the absence and presence of hydrogen as an example. The procedure and conclusions are detailed below.

a- Free-radical model at high conversions in the presence of hydrogen:

The thermal reaction of ethane.

The basic low-conversion mechanism was similar to that proposed by Pacey and Furnell (1972). The reactions of hydrogenation of ethylene:



and decomposition of propylene:



were included in the scheme, together with some minor termination reactions. Polymerization and aromatization reactions were neglected. The complete set of free-radical reactions used is presented in the Scheme I and Table IV-1 gives the values of kinetic parameters obtained from the literature.

The model was applied to simulate the operation of the jet-stirred reactor used in the experiments on ethane reactions, where results were available as in Chapter III.

## SCHEME I

## THE FREE RADICAL REACTION MODEL

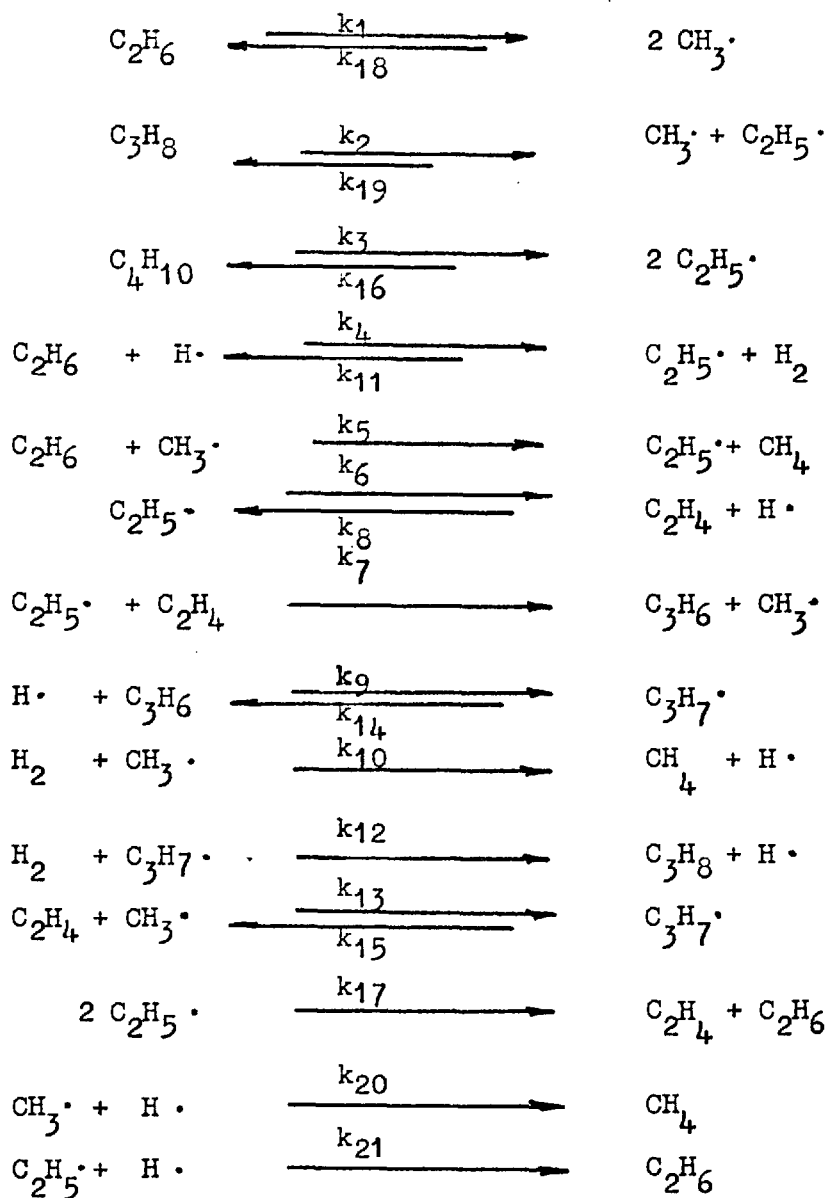


TABLE IV-2: PARAMETERS OF THE MODEL.

<u>Constant</u>	<u>Literature</u>	<u>Value</u>	<u>Source</u>	<u>After Regression</u>	<u>Activation Energy</u>
	<u><math>k_{oi}</math></u>			<u><math>k_{oi}</math></u>	<u><math>E_i</math></u>
1	6.3 x 10	<sup>16</sup>	Snow (1966)	4.32 x 10	86.0
2		<sup>18.2</sup>	Kunugi , et.al. (1970)	1.83 x 10	85.0
3		<sup>17.9</sup>	Pacey, et.al. (1972)	10	86.3
4	3.8 x 10	<sup>12</sup>	Snow (1966)	1.90 x 10	7.0
5	2.5 x 10	<sup>11</sup>	Snow (1966)	8.24 x 10	10.8
6	5.3 x 10	<sup>14</sup>	Snow (1966)	7.48 x 10	40.8
7		<sup>9.6</sup>	Pacey, et.al. (1972)	3.36 x 10	19.0
8	5.4 x 10	<sup>13</sup>	Snow (1966)	8.15 x 10	5.4
9	6.3 x 10	<sup>10</sup>	Blackmore, et.al. (1969)	6.3 x 10	4.5
10	1.9 x 10	<sup>11</sup>	Snow (1966)	1.9 x 10	9.5
11	1.8 x 10	<sup>12</sup>	Snow (1966)	2.69 x 10	11.4
12		<sup>9</sup>	Kunugi, et.al. (1970)	10	8.0
13		<sup>8</sup>	Blackmore, et.al. (1969)	10	7.0
14	2.6 x 10	<sup>14</sup>	Blackmore, et.al. (1969)	2.6 x 10	39.5
15	5.0 x 10	<sup>11</sup>	Blackmore, et.al. (1969)	5.0 x 10	25.0
16	6.0 x 10	<sup>13</sup>	Snow (1966)	9.14 x 10	0.0
17		<sup>13</sup>	Snow (1966)	10	0.0
18	7.0 x 10	<sup>13</sup>	Snow (1966)	7.0 x 10	0.0
19	7.0 x 10	<sup>13</sup>	Snow (1966)	4.44 x 10	0.0
20		<sup>8</sup>	Blackmore, et.al. (1969)	10	0.0
21		<sup>12</sup>	Blackmore, et.al. (1969)	10	0.0

To obtain the mathematical model of the free-radical reactions in a jet-stirred reactor and to solve the model, the following procedure was used:

The general equation of conservation of the  $i^{\text{th}}$  species in a multicomponent homogeneous system was integrated over the macroscopic volume of reaction assuming constant temperature and pressure and perfect mixing inside the reactor. The result of the integration is

$$\kappa C_i - C_{i0} = \tau R_i \quad i = 1, \dots, N \quad 2-a-1$$

where  $\kappa = \rho/\rho_0$  is the relative expansion due to changes in density caused by the chemical reaction and  $\tau = V_r/q_0$  is the residence time calculated at conditions in the inlet of the reactor.  $R_i$  is obtained from the reaction scheme and depends on the free-radical mechanism chosen. The general form of the rate equations for a system with first and second order reactions is

$$R_i = a_{ij} C_j + b_{ijk} C_j C_k \quad \begin{array}{l} i = 1, \dots, N \\ j = 1, \dots, N \\ k = 1, \dots, N \end{array} \quad 2-a-2$$

where the index summation convention is applied.

The set of equations 2-a-1, coupled with the chemical kinetics expressed in 2-a-2, can now be solved. The usual procedure is to use an accelerated Newton technique, but these techniques were found to be very time consuming, and a different approach was developed.

A closer analysis of the kinetic equations 2-a-2 showed the advantage of considering equations for molecular species separately from equations for free-radicals. The assumption that molecular species do not undergo second order reactions amongst themselves was made, but the procedure

described can be easily modified to remove this assumption. The general form of free-radical kinetics is then

$$R_{Bi} = h_{ik} A_k + r_{ij} B_j + s_{ikj} A_k B_j + t_{ijl} B_j B_l \quad 2-a-3$$

and the molecular species equation form is

$$R_{Ai} = d_{ij} A_j + e_{ik} B_k + f_{ikj} B_k A_j + g_{ilk} B_l B_k \quad 2-a-4$$

These equations can be rearranged to give

$$R_{Bi} = (r_{ij} + s_{ijk} A_k) B_j + h_{ik} A_k + t_{ijl} B_j B_l \quad 2-a-5$$

$$R_{Ai} = (d_{ij} + f_{ikj} B_k) A_j + e_{ik} B_k + g_{ilk} B_l B_k \quad 2-a-6$$

Replacing 2-a-5 and 2-a-6 in 2-a-1 and putting the result in matrix notation, the two subsets of equations to be solved are

$$\frac{K}{\tau} \underline{B} = \underline{\Psi}(\underline{A}) \cdot \underline{B} + \underline{E}(\underline{A}) + \underline{S_c}(\underline{B}) \quad 2-a-7$$

$$\frac{K}{\tau} \underline{A} - \frac{1}{\tau} \underline{A} = \underline{\phi}(\underline{B}) \cdot \underline{A} + \underline{D}(\underline{B}) \quad 2-a-8$$

Equation 2-a-8 is linear with respect to  $\underline{A}$ . Equation 2-a-7 is linear with respect to  $\underline{B}$ , with the exception of second order terms in  $\underline{B}$  that have been grouped in  $\underline{S_c}(\underline{B})$ .

The method of solution of 2-a-7 and 2-a-8 is to find  $\underline{A}$  and  $\underline{B}$  alternatively from 2-a-7 and 2-a-8 until convergence is reached. The algorithm is as follows

- 1- Start with  $\underline{A}^n = \underline{A}$  and  $\underline{B}^n = \underline{E}$
- 2- Find  $\underline{B}^{n+1}$  as the value of convergence of the following algorithm, starting with  $\underline{B}^s = \underline{B}^n$

$$\begin{aligned} (\underline{B}^{s+1} - \underline{B}^s) &= \left[ \frac{\underline{K}}{\underline{\tau}} \underline{I} - \underline{\Psi}(\underline{A}^n) - \left( \frac{\partial \underline{Sc}(\underline{B}^s)}{\partial \underline{B}} \right) \right]^{-1} \\ &\quad \left[ - \left( \frac{\underline{K}}{\underline{\tau}} \underline{I} - \underline{\Psi}(\underline{A}^n) \right) \underline{B}^s + \underline{E}(\underline{A}^n) + \underline{Sc}(\underline{B}^s) \right] \end{aligned}$$

3- Find  $\underline{A}^{n+1}$  from the set of linear equations

$$\underline{A}^{n+1} = \left[ - \frac{\underline{K}}{\underline{\tau}} \underline{I} - \underline{\phi}(\underline{B}^{n+1}) \right]^{-1} \cdot \left[ \frac{\underline{A}_0}{\underline{\tau}} + \underline{D}(\underline{B}^{n+1}) \right]$$

4- Continue steps 2 and 3 until total convergence is reached.

This algorithm was found to be very efficient and stable, the step size being increased up to 1 second without convergence problems. Comparisons drawn with the conventional approach using Newton methods showed a considerable time saving, the present method needing only 26 seconds of CDC 6400 computer time for a real time interval of up to 13 seconds.

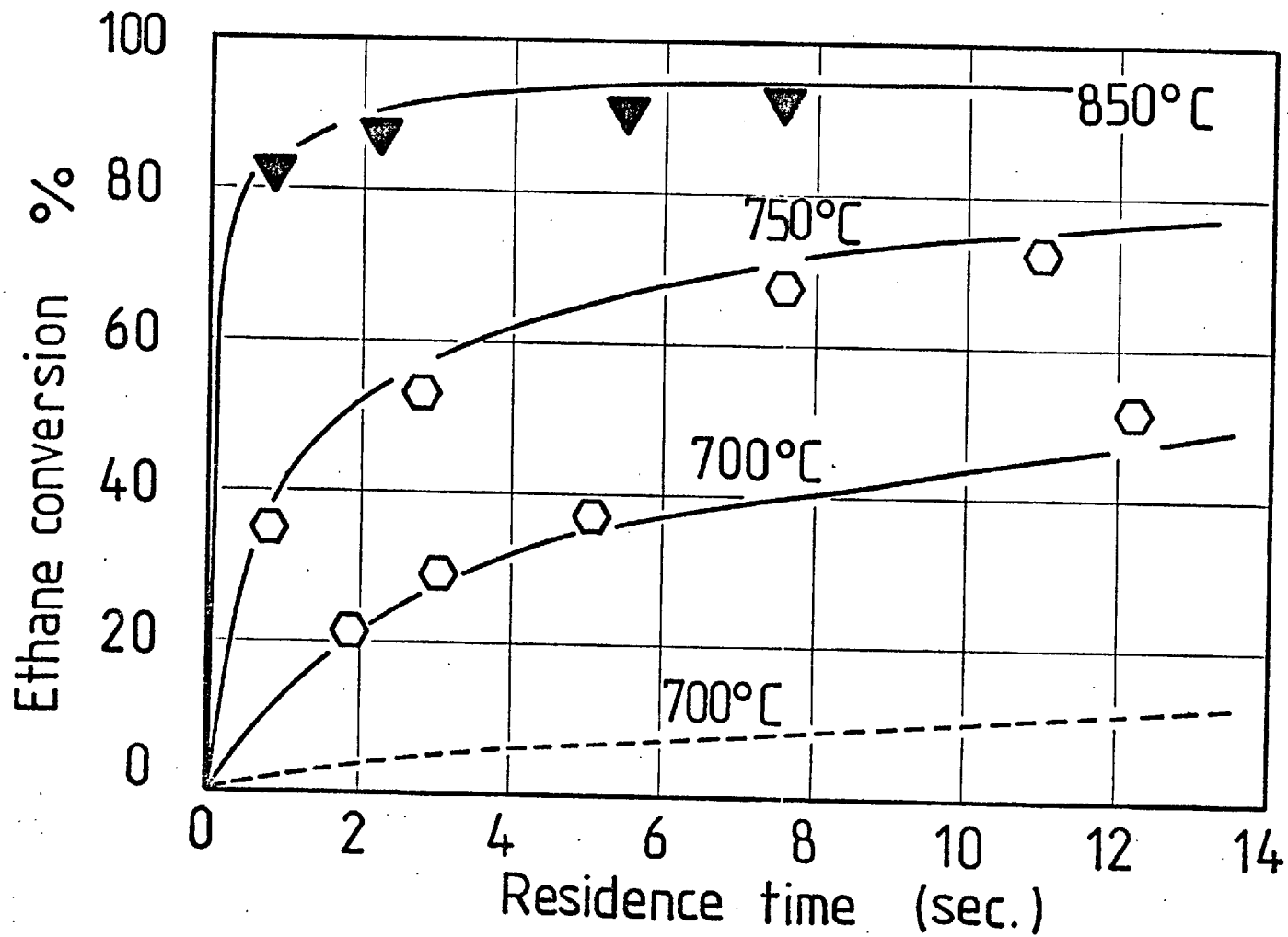
The mathematical model gives predictions of the amount of ethane reacted and the concentration of different products as a function of the residence time.

Comparisons are drawn between experimental results (Chapter III) and computer prediction (broken line) in figure IV-2. As can be seen, the prediction differs markedly from experimental results, a difference attributed to the fact that the model was based on kinetic parameters obtained from the literature and used without correction: this resulted in an extremely short chain length.

A decision was made to adjust the pre-exponential parts of the parameters while leaving the activation energy unchanged, for two reasons. In the first place, the activation energy of a reaction can be estimated from thermochemical information with a certain degree of accuracy while, generally, a less accurate prediction can be made of the pre-exponential



FIGURE IV-2. COMPARISON OF COMPUTER MODELLING AND EXPERIMENTAL RESULTS. FULL LINES: MODEL WITH PARAMETERS AFTER REGRESSION. BROKEN LINES: MODEL WITH LITERATURE INITIAL PARAMETERS.



factor. The second reason is that, for most cases, the kinetic constant is more sensitive to changes in the pre - exponential factor. For small changes in parameters:

$$\delta k = e^{-\frac{E}{RT}} \delta k_0 - \frac{k_0}{RT} e^{-\frac{E}{RT}} \delta E$$

defining  $k_0 = 10^B$

$$\delta k_0 = 10^B \ln 10 \delta B$$

then

$$\delta k = \left\{ 2.3 \cdot 10^B e^{-E/RT} B \right\} \frac{\delta B}{B} - \left\{ 10^B e^{-\frac{E}{RT}} \frac{E}{RT} \right\} \frac{\delta E}{E}$$

where  $\delta B/B$  and  $\delta E/E$  are relative changes in the parameters. The terms between brackets are the relative sensitivities with respect to both parameters:

$$B \frac{\partial k}{\partial B} = S_{RB} = 2.3 \times 10^B e^{-E/RT} B$$

$$- E \frac{\partial k}{\partial E} = S_{RE} = 10^B e^{-E/RT} \frac{E}{RT}$$

The value of the ratio  $|S_{RB}/S_{RE}|$  was calculated for all the parameters of the model at 1100 °K and is presented in Table IV-2. In most cases the ratio is larger than one, indicating that  $k$  is more sensitive to relative changes of  $B$  and hence that this parameter should be selected for an estimation procedure.

TABLE IV - 2

<u>CONSTANT</u>	<u>S<sub>RB</sub> / S<sub>RE</sub></u>
1	0.98
2	1.08
3	1.04
4	11.04
5	4.17
6	1.97
7	3.06
8	14.90
9	12.07
10	6.0
11	4.63
12	5.69
13	5.78
14	1.84
15	2.37

The parameter estimation procedure used was a non-linear regression technique, based on the Gauss - Siedel method for algebraic models (Seinfeld, 1970). It was applied to obtain the "best fit" minimising a function that involved the squares of the residuals on 16 points, taken at 4 residence times and 4 temperatures and including 4 values of concentration per point. The regression procedure was applied to points where undiluted ethane was used as reactant, and the parameters obtained were used to predict the spectrum composition of experiments where the reactant was diluted with hydrogen.

The simulation prediction and experimental results for both diluted and undiluted ethane are shown in figures IV-2,3 and 4. Good agreement (less than 4 % difference) between model prediction and experiments was observed for most conditions.

The final set of parameters of the model are tabulated in table IV-1, and a comparison is shown with the range of values found in the literature in table IV-3. The values obtained are seen to be within the orders of magnitude of parameters previously estimated by several authors.

This successful attempt at modelling for high conversions indicates that the concepts used in building the free-radical sequence of secondary reactions are essentially correct, and that more complicated models can be built in the same form to explain the high-conversion thermal reaction of higher paraffins. The procedure has, however, some disadvantages that are discussed below.

When building a free-radical model that includes several elementary steps, the kinetic parameters that are assumed for each reaction are either estimated by thermochemical data and kinetic theories or are adopted from values given in the literature. In any case, the parameters are subjected to a certain degree of uncertainty and error. When a model is built that includes a large list of elementary reactions, there is a very low possibility that the predictions of such model could represent the experimental information, due to the propagation of errors introduced with the parameters (as seen for the original model). This fact would lead to modification of the parameters of the model to allow a better fitting with experiments, and here some other problems arise. The first of these is that there are too many parameters that could be modified, and is only too well known that, with many parameters to modify, most models would fit the experimental results. Another problem is that

FIGURE IV-3. COMPARISON OF COMPUTER MODEL AND EXPERIMENTAL RESULTS.  
FULL LINES: MODEL WITH PARAMETERS AFTER REGRESSION.

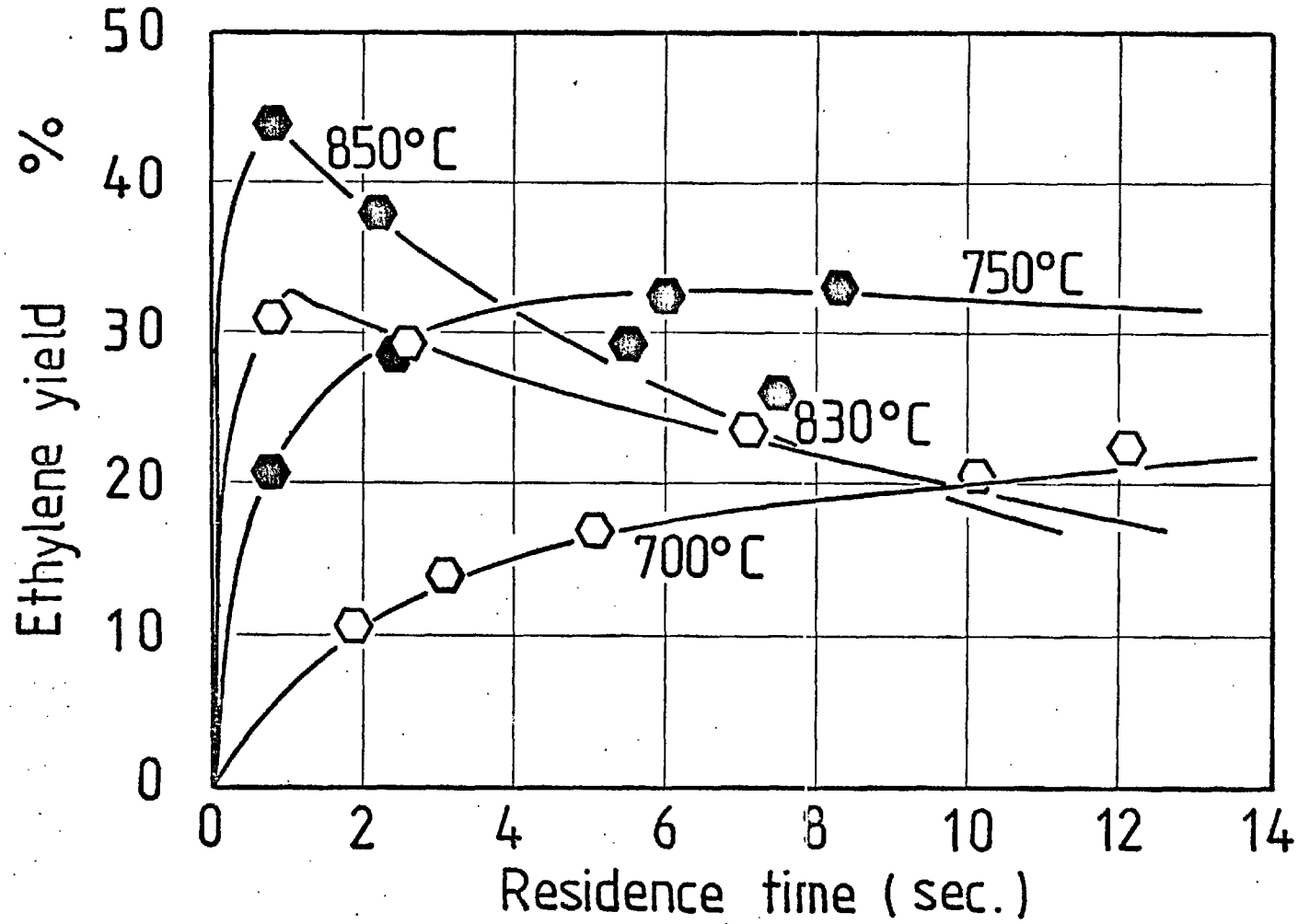


FIGURE IV-4. COMPARISON OF COMPUTER MODEL AND EXPERIMENTAL RESULTS.  
FULL LINES: MODEL WITH PARAMETERS AFTER REGRESSION.

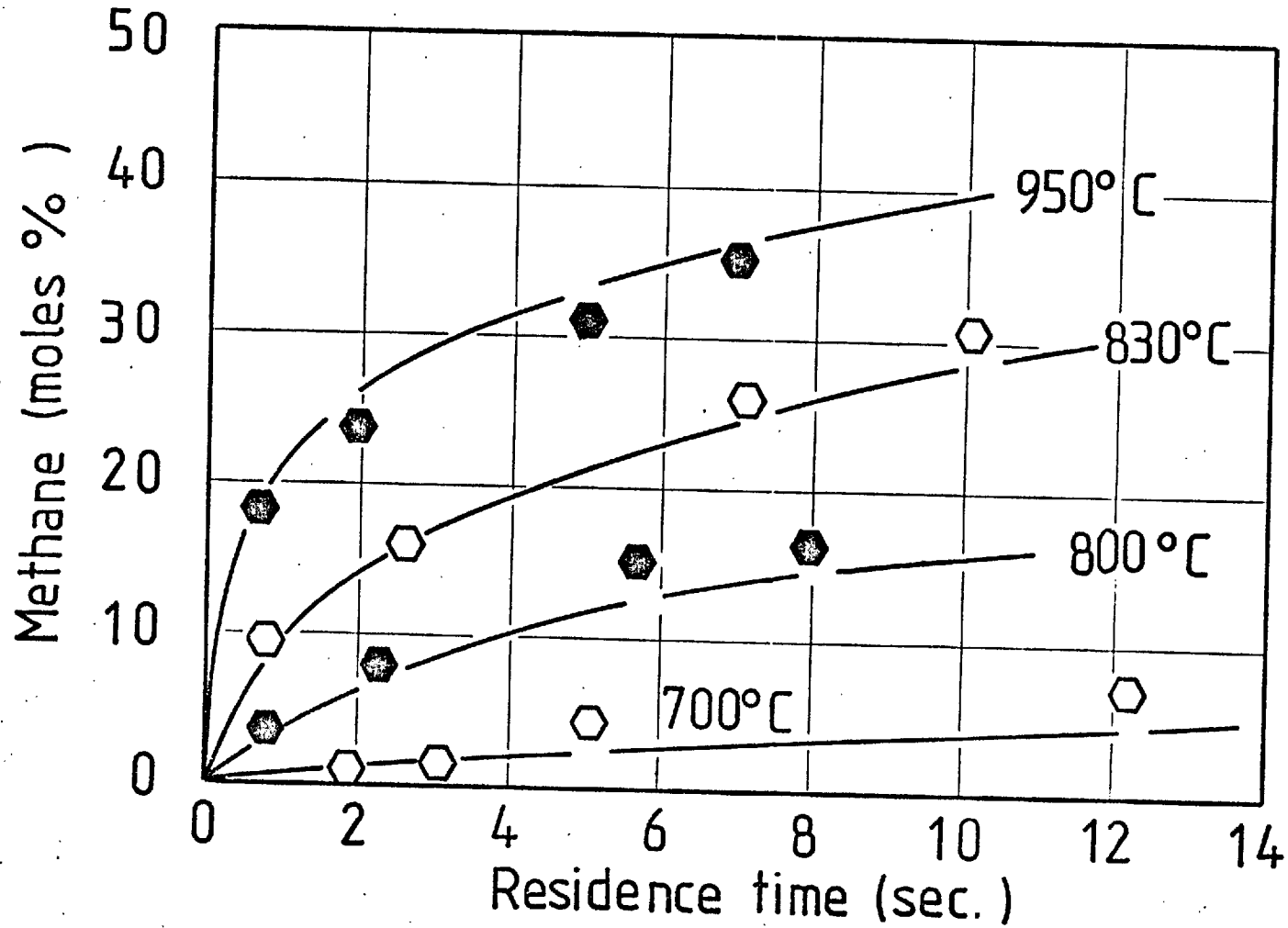


TABLE IV-3  
COMPARISON OF THE PARAMETERS OBTAINED WITH  
LITERATURE VALUES.

<u>Parameter</u>	<u>Log <math>k_{o_i}</math> (regression)</u>	<u>Log <math>k_{o_i}</math> (literature)</u>
1	16.53	16.29 Leathard , et.al. (1970)
		16.70 Pacey ,et.al.(1972)
2	18.26	18.2 Kunugi,et.al. (1970)
4	15.27	14.32 Ratajczak,et.al.(1967)
5	8.91	12.2 Kunugi,et.al.(1970)
		8.50 Pacey,et.al.(1972)
6	15.87	14.0 Kunugi,et.al.(1970)
		14.72 Snow (1966)
7	11.52	9.6 Pacey,et.al.(1972)
		12.8 Ratajczak,et.al.(1967)
8	15.91	14.1 Kunugi,et.al.(1970)
		13.8 Ratajczak,et.al.(1967)
11	10.43	11.7 Kunugi,et.al.(1970)
16	13.96	12.88 Ratajczak,et.al.(1967)
		13.78 Snow (1966)
19	14.65	13.40 Ratajczak,et.al.(1967)
		13.85 Snow (1966)

no "best fit" parameter estimation procedure or regression ensures that the parameters correspond to any physical actuality and, when the procedure is finished, the parameters obtained could predict the experimental facts without necessarily being the parameters that should be associated with each individual free-radical reaction.

Another difficulty is the complexity of the mathematics involved in solving large free-radical models. Unless termination reactions are oversimplified, the system leads to a set of stiff differential equations, which would be very time consuming to solve with a computer. This difficulty is increased by an order of magnitude when an iterative-non-linear parameter estimation technique is used to obtain the "best fit".

The above considerations would rule out free-radical modelling as a procedure to predict products composition and behaviour of reactions involving more complicated systems operating at high conversions, such as reactions of industrial interest. Semiempirical approaches, such as the modelling proposed by Murata, et.al. (1975), would be much more practical and easier to use than the equivalent, more realistic free-radical mechanisms.

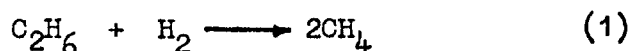
However, it is true to say that the predictions of the model here presented are in good agreement with the experimental results, even when the model has not been developed on the basis of the reaction for which results are available. The wider applicability of the model, or further corrections to the model, should be made for a wider range of experimental results.

b- The effect of hydrogen on the rate of the thermal decomposition of hydrocarbons.

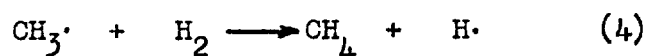
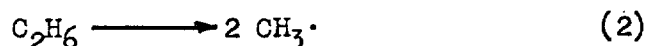
The experimental findings reported in Chapter III indicate that the presence of hydrogen may produce changes both in the products composition and in the rate of the original hydrocarbon breakdown.



A rather surprising result (observed also by Brooks, 1967), is that the hydrogenolysis of ethane:



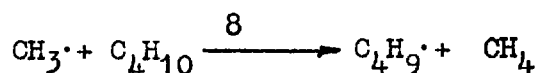
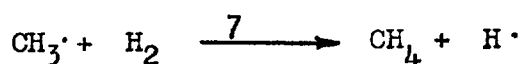
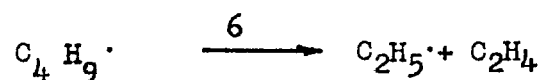
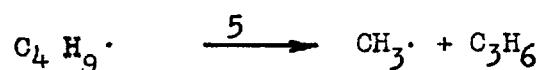
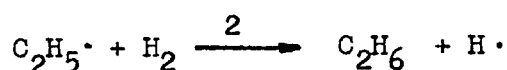
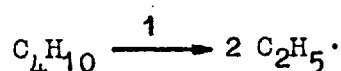
is not affected by the concentration of hydrogen. This result is evident from the mechanism of ethane decomposition:

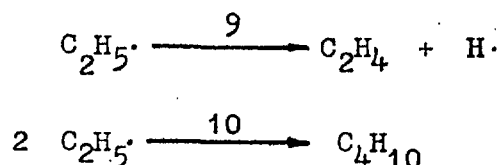


which is dominated by the first step in the sequence. The reaction is first order in ethane and the rate constant corresponds to reaction (2).

However the rate of breakdown of butane and of higher hydrocarbons is known to be accelerated by the presence of hydrogen. Such an effect has been attributed to the transfer of chains from radicals  $\text{C}_2\text{H}_5\cdot$  and  $\text{CH}_3\cdot$  to  $\text{H}\cdot$ . One suggested mechanism of the action of hydrogen on the breakdown of butane at low conversions is presented below.

Consider the sequence of reactions:





The use of a steady - state assumption for the concentration of free-radicals allows one to obtain the following expressions for the radical concentrations:

$$[\text{C}_2\text{H}_5\cdot] = \left(\frac{k_1}{k_{10}}\right)^{\frac{1}{2}} [\text{C}_4\text{H}_{10}] \quad 2-b-1$$

$$[\text{H}\cdot] = \frac{1}{k_4[\text{C}_4\text{H}_{10}]} \left\{ k_2 [\text{C}_2\text{H}_5\cdot][\text{H}_2] + k_7 [\text{CH}_3\cdot][\text{H}_2] + k_9 [\text{C}_2\text{H}_5\cdot] \right\} \quad 2-b-2$$

$$[\text{C}_4\text{H}_9\cdot] = \frac{[\text{C}_4\text{H}_{10}]}{(k_5 + k_6)} \left\{ k_3 [\text{C}_2\text{H}_5\cdot] + k_4 [\text{H}\cdot] + k_8 [\text{CH}_3\cdot] \right\} \quad 2-b-3$$

$$[\text{CH}_3\cdot] = \frac{k_5 [\text{C}_4\text{H}_9\cdot]}{k_7 [\text{H}_2] + k_8 [\text{C}_4\text{H}_{10}]} \quad 2-b-4$$

The overall rate of  $\text{C}_4\text{H}_{10}$  breakdown is then given by:

$$r = k_3 [\text{C}_4\text{H}_{10}] [\text{C}_2\text{H}_5\cdot] + k_4 [\text{H}\cdot] [\text{C}_4\text{H}_{10}] + k_8 [\text{CH}_3\cdot] [\text{C}_4\text{H}_{10}] \quad 2-b-5$$

Substitution of 2-b-1, 2-b-2, 2-b-3, and 2-b-4 in 2-b-5 gives an expression of the rate as a function of concentrations. Since this is very complex, two limiting cases have been considered, one in which  $[\text{H}_2] \gg [\text{C}_4\text{H}_{10}]$  and another in which  $[\text{C}_4\text{H}_{10}] \gg [\text{H}_2]$ . The analytical expression of both cases is shown in figure IV-5. The rate of reaction is seen to increase linearly with the concentration of hydrogen in both cases, as has been observed experimentally (Brooks, 1967).

Hydrogen also affects the product distribution through a series of reactions involving the primary products of breakdown, such as the

FIGURE IV - 5

1-  $[H_2] \gg [C_4H_{10}]$  ; assumed also  $k_8 [CH_3] \ll k_4 [H]$

$$R = k_3 \left( \frac{k_1}{k_{10}} \right)^{\frac{1}{2}} [C_4H_{10}]^{\frac{1}{2}} + \frac{(k_5 + k_6)}{k_6} \left\{ k_9 \left( \frac{k_1}{k_{10}} \right)^{\frac{1}{2}} [C_4H_{10}]^{\frac{1}{2}} + \frac{k_5 k_3}{(k_5 + k_6)} \left( \frac{k_1}{k_{10}} \right)^{\frac{1}{2}} [C_4H_{10}]^{\frac{3}{2}} + k_2 \left( \frac{k_1}{k_{10}} \right)^{\frac{1}{2}} [C_4H_{10}]^{\frac{1}{2}} [H_2] \right\}$$

2 -  $[C_4H_{10}] \gg [H_2]$

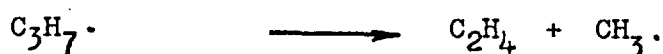
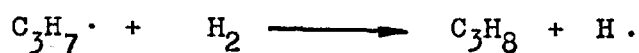
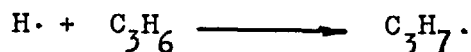
$$R = k_3 \left( \frac{k_1}{k_{10}} \right)^{\frac{1}{2}} [C_4H_{10}]^{\frac{1}{2}} + k_9 \left( \frac{k_1}{k_{10}} \right)^{\frac{1}{2}} [C_4H_{10}]^{\frac{1}{2}} + \left\{ k_2 \left( \frac{k_1}{k_{10}} \right)^{\frac{1}{2}} + \frac{k_7 k_5 k_3}{k_8} \left( \frac{k_1}{k_{10}} \right)^{\frac{1}{2}} \right\} [C_4H_{10}]^{\frac{1}{2}} [H_2] + k_5 k_3 \left( \frac{k_1}{k_{10}} \right)^{\frac{1}{2}} [C_4H_{10}]^{\frac{3}{2}}$$

$$+ \frac{k_5}{k_4} \left\{ k_9 \left( \frac{k_1}{k_{10}} \right)^{\frac{1}{2}} [C_4H_{10}]^{\frac{3}{2}} + k_2 \left( \frac{k_1}{k_{10}} \right)^{\frac{1}{2}} [C_4H_{10}]^{\frac{3}{2}} [H_2] + \frac{k_7 k_5 k_3}{k_8} \left( \frac{k_1}{k_{10}} \right)^{\frac{1}{2}} [C_4H_{10}]^{\frac{3}{2}} [H_2] \right\}$$

hydrogenation of olefins:



and



In addition a secondary process can enhance, in some circumstances, the production of propylene:



This series of reactions could explain the presence of propylene at high temperature in the presence of hydrogen, as shown in figure III-16.

Thus, the overall action of hydrogen on the reaction involving the major components is an acceleration of the rate of breakdown of initial hydrocarbons, followed by hydrogenation and hydrogenolysis of the olefinic fragments produced. This picture explains qualitatively the experimental results obtained in the present work.

c- Semi - empirical modelling of thermal hydrogenation reactions  
( hydrogasification )

Reference was made, in a previous chapter, to successful attempts at modelling pyrolysis reactions on a semi-empirical basis (Murata, M. et. al. 1975). This model was shown to represent, approximately, the experimental information for high - conversion pyrolysis of hydrocarbons and the model together with kinetic equations and parameters are presented in APPENDIX I.

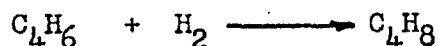
Some modifications would be required to apply this model to the thermal hydrogenation of hydrocarbons. If the primary reaction of decomposition is accelerated by the presence of hydrogen, then the rate equation has the form : (Thompson, et. al. , 1975)

$$r_n = k_1 (n) \left\{ 1 + b [H_2] \right\} [P_F (n)]$$

and the value of b can be calculated from Brooks (1967) :

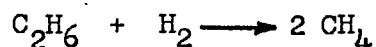
<u>Paraffin:</u>	<u>b (lt / mole)</u>
Ethane	0
Isobutane	1.799
Neobutane	4.498
n- Butane	5.398
Cyclopentane	7.198

Some secondary reactions also should be considered, such as hydrogenation of butadiene and the destructive hydrogenation of higher olefins:



but unfortunately the kinetics of these reactions is not known.

If ethane is a product from the thermal hydrogenation of ethylene, the hydrogenolysis is an important reaction.



since this is the rate determining step in hydrogasification at long residence times. The kinetics have been given by Brooks (1967) and can be represented by the equations:

$$r = k [\text{C}_2\text{H}_6] \quad k = 10^{17.5} \exp(-90000 / RT)$$

Another slow reaction, involving very stable compounds, is the hydrogenolysis of aromatics:



Assuming first order reaction, the kinetic constant can be estimated using experimental information published by Thompson et.al. (1975) :

$$r = k [\text{C}_6\text{H}_6] \quad k = 1.11 \times 10^{10} \exp(-70587 / RT)$$

With the inclusion of these reactions, it is possible to expect that the semi empirical model would be able to predict the product composition under conditions of industrial thermal hydrogasification. This would involve only the solution of the set of differential equations that result from the multicomponent mass-balance in the reactor. The solution of the set can be performed with any conventional method of integration (such as the Runge - Kutta method) as no unstabilities or stiffness could be expected in the solution.

Moreover, the model can be solved in an approximate form in the case of thermal hydrogasification. The procedure is given below.

Industrial hydrogasification is carried out under severe

TABLE IV - 4

DESCRIPTION	C <sub>4</sub> H <sub>10</sub>	H <sub>2</sub>	CH <sub>4</sub>	C <sub>2</sub> H <sub>6</sub>	C <sub>2</sub> H <sub>4</sub>	C <sub>3</sub> H <sub>6</sub>	REACTION
FEED	1	9	-	-	-	-	_____
C <sub>4</sub> H <sub>10</sub> BREAKDOWN	0	9.3	0.65	0.07	0.65	0.65	C <sub>4</sub> H <sub>10</sub> Products C <sub>4</sub> H <sub>8</sub> + H <sub>2</sub>
C <sub>4</sub> H <sub>8</sub> HYDROGENATION	0	9.28	0.655	0.075	0.655	0.665	0.73(CH <sub>4</sub> + C <sub>3</sub> H <sub>6</sub> ) + 0.27(C <sub>2</sub> H <sub>6</sub> + C <sub>2</sub> H <sub>4</sub> )
C <sub>3</sub> H <sub>6</sub> HYDROGENATION	0	8.615	1.330	0.075	1.330	0	C <sub>3</sub> H <sub>6</sub> + H <sub>2</sub> → CH <sub>4</sub> + C <sub>2</sub> H <sub>4</sub>
C <sub>2</sub> H <sub>4</sub> HYDROGENATION	0	7.285	1.330	1.405	0	0	C <sub>2</sub> H <sub>4</sub> + H <sub>2</sub> → C <sub>2</sub> H <sub>6</sub>
C <sub>2</sub> H <sub>6</sub> HYDROGENOLYSIS	0	6.949	2.000	1.069	0	0	C <sub>2</sub> H <sub>6</sub> + H <sub>2</sub> → 2CH <sub>4</sub>
% MOLES PRODUCT		69.36	19.96	10.67			

Reaction  $C_2H_6 + H_2 \rightarrow 2 CH_4$ ;  $r = k C_2H_6$ ; at  $753^\circ C$   $k = 0.0182$  and  $x = 23.86\%$

(x = conversion)

$$x = 100 (1 - e^{-kt}); t = 15 \text{ seconds}$$

conditions, where most of the reactions are carried to full conversion. For the present model, it is assumed that the primary reactions reach full completion and that each of the products is fully hydrogenated, with the exception of ethane, which is partially converted following a first - order kinetics.

To illustrate the procedure, predictions were obtained for a mixture of one mole of  $C_4H_{10}$  and nine moles of hydrogen reacting at  $753^\circ C$  and 650 psig and the results of this simulation can be compared with experiments of Brooks (1966). The calculation sequence is summarised in Table IV-4. The comparison between the predicted and the experimental results is shown below :

	<u>Predicted</u>	<u>Experimental</u> (Brooks, 1966)
$H_2$	69.36 %	68 %
$CH_4$	19.96 %	20.6 %
$C_2H_6$	10.67 %	11.4 %
$CH_4 / C_2H_6$	1.90	1.80

The agreement between prediction and experiments is good enough to ensure that the modelling procedure is essentially correct.

To summarise, the thermal hydrogasification of hydrocarbons under industrial conditions, can be predicted with the use of a semiempirical model of the decomposition of hydrocarbons. The procedure is simplified further considering that, at long residence times, most of the reactions reached full conversion and that the hydrogenolysis of ethane is the limiting step.



d- Effect of reactor surfaces on the production of  
major compounds

During the experimental work performed in connection with the present research, attention was paid to the nature of the surface on the major products distribution. The presence of catalytic metals, such as foils and wall liners, seemed to have negligible effect on the gas products, as shown, for example, in figure III-17. There was, however, a noticeable effect at the beginning of the reaction, but the phenomena disappeared rapidly.

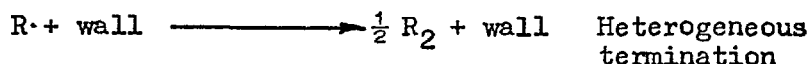
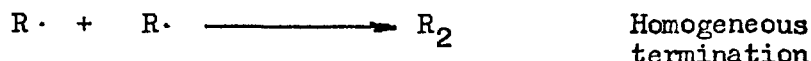
Metals used, such as nickel and iron, would be expected to have some catalytic effect on the reactions that are being carried on in the gas phase. The lack of difference between various metals can be interpreted as a fast deactivation of the metal active centres as a result of encapsulation with carbon. Thus, the catalytic activity of the metal would be present at the early stages of the reaction, and would decay rapidly with time (i.e. with coverage). These changes during the transient were observed in the experiments of figure III-22.

However, an effect of surface (rather than nature of surface) would still be expected and, in agreement with this a more significant effect was observed in experiments where the surface to volume ratio was changed inside the reactor, as shown in the results of figure III-24.

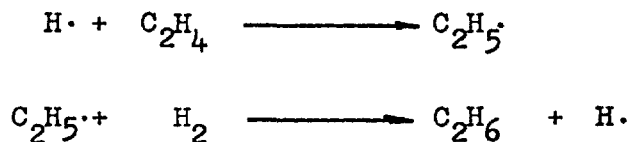
The general effect observed on the main product distribution is as if the reaction were being inhibited slightly by the wall, whose surface was increased by the introduction of a copper wire screen. Some calculations were performed to check whether this effect was not due to changes in the residence time provoked by the modification of the reaction volume. The change in residence time could account for a change in 0.6% of  $\text{CH}_4$  and 0.37% of  $\text{C}_2\text{H}_4$ , values that are at least one order of magnitude less than

the observed changes.

The inhibiting action of the surface can be explained by termination of chains on the walls of the reactors, competing successfully with homogeneous termination reactions:



In systems where hydrogen is a main component in the gas, the termination of hydrogen atoms against the wall is favoured with respect to homogeneous termination, for reasons of energy transfer. An increase in the surface to volume ratio would decrease the concentration of H· in the system and reactions such as



would be inhibited. The increased production of ethylene with the surface to volume ratio noticed in figure III-24 could be attributed to this effect.

To summarise the effect of surfaces, it could be stated that catalytic effects were found to be short lived, probably due to encapsulation of the active centers with polymers or carbon. The surface to volume ratio in the reactor, on the other hand, was found to influence the products distribution, and the effect was attributed to heterogeneous termination being enhanced at high S / V ratio.

### 3- THE PRODUCTION OF AROMATIC COMPOUNDS

#### a- Introduction

The fact that minor amounts of aromatic liquids or

"tars" are found as products of the pyrolysis and thermal hydrogenation of hydrocarbons has been known for a long time. However, the nature of the reactions involved in the "thermal synthesis" of aromatics is still open to question and the mechanism is not yet established. Moreover, the present research shows that there is a sequence of reactions that produce further condensation of the aromatic compounds to form polynuclear molecules of high molecular weight. This sequence of reactions are considered to be very important in the route towards carbon formation.

This part of the discussion is devoted to consideration of some features of the reactions that produce or involve aromatics, since they play a very important role in the processes under study.

b- The synthesis of aromatics from paraffins.

Aromatics are not primary products in the pyrolysis of paraffins. During this research, for example, it was noticed that aromatics appeared only after some time had elapsed. (See for example, figure III-26) and this is an indication that aromatics are produced in a sequence of reactions involving one or several intermediates.

According to Brooks (1967) , the production of aromatics from several hydrocarbons seems to correlate approximately with the initial amount of olefins produced during the primary breakdown. This fact seems to indicate olefins as intermediates in the formation of aromatics.

When considering the decomposition of olefins, Kunugi, et.al. (1970,1969) found that, again, aromatics were not among the primary products, but appeared at relatively low conversions. This is an indication that primary products from olefin decomposition react further to form aromatics. The products formed from the primary decomposition of ethylene and propylene ( at conversions extrapolated to zero) are given in the following table:

TABLE IV - 5

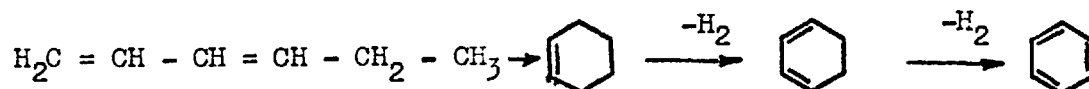
calculated from

(Kunugi et.al. , 1969,1970)

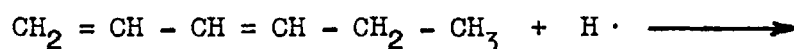
PRODUCT	MOLES PRODUCT / 100 MOLES OF	
	ETHYLENE (750° C)	PROPYLENE
METHANE	2	30
HYDROGEN	7	10
ETHANE	16	1
ETHYLENE	-	50
ACETYLENE	2	2
PROPYLENE	10	-
1-BUTENE	7.5	12
1-3 BUTADIENE	20.0	12
CYCLOPENTENE	2	1.5
ME-CYCLOPENTANE	-	5
HEXADIENES	1	2.5

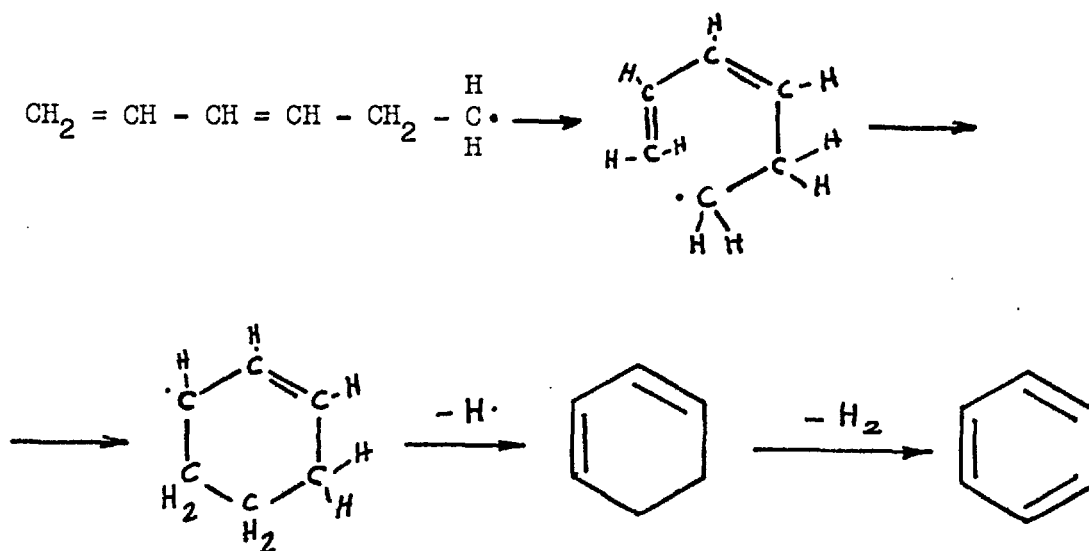
The main reactions involving the above compounds that could produce aromatics are :

- 1- Cyclization and dehydrogenation of hexadienes (Fitzer, et.al. , 1971)

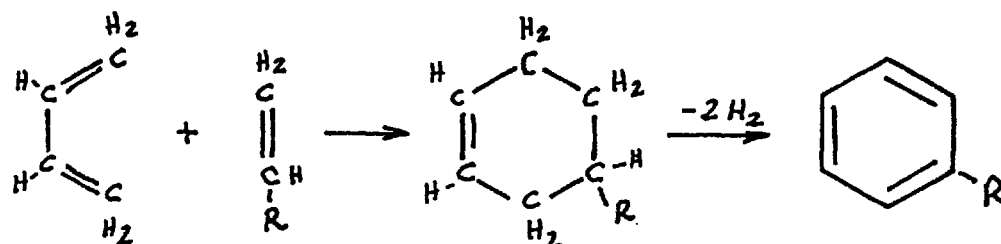


The mechanism of this reaction is unknown. A free-radical series of reactions be proposed, as follows.

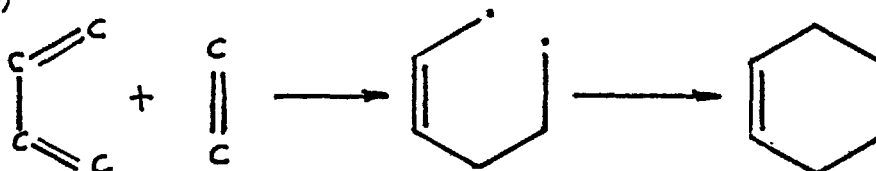




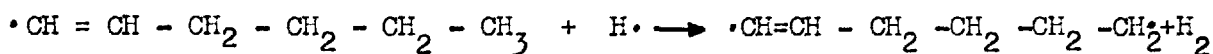
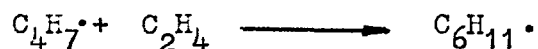
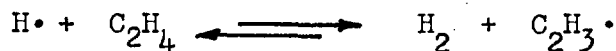
2- Diels - Adler addition of butadiene to olefins (Fitzer, et.al., 1971)



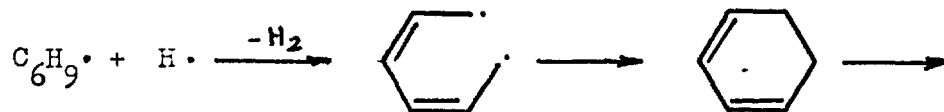
This reaction should be more important than (1) because the amount of butadiene present in olefin decomposition is quite high. The mechanism is usually interpreted as a molecular reaction, although a birradical could be the intermediate in the closure of the ring (Benson, 1968)



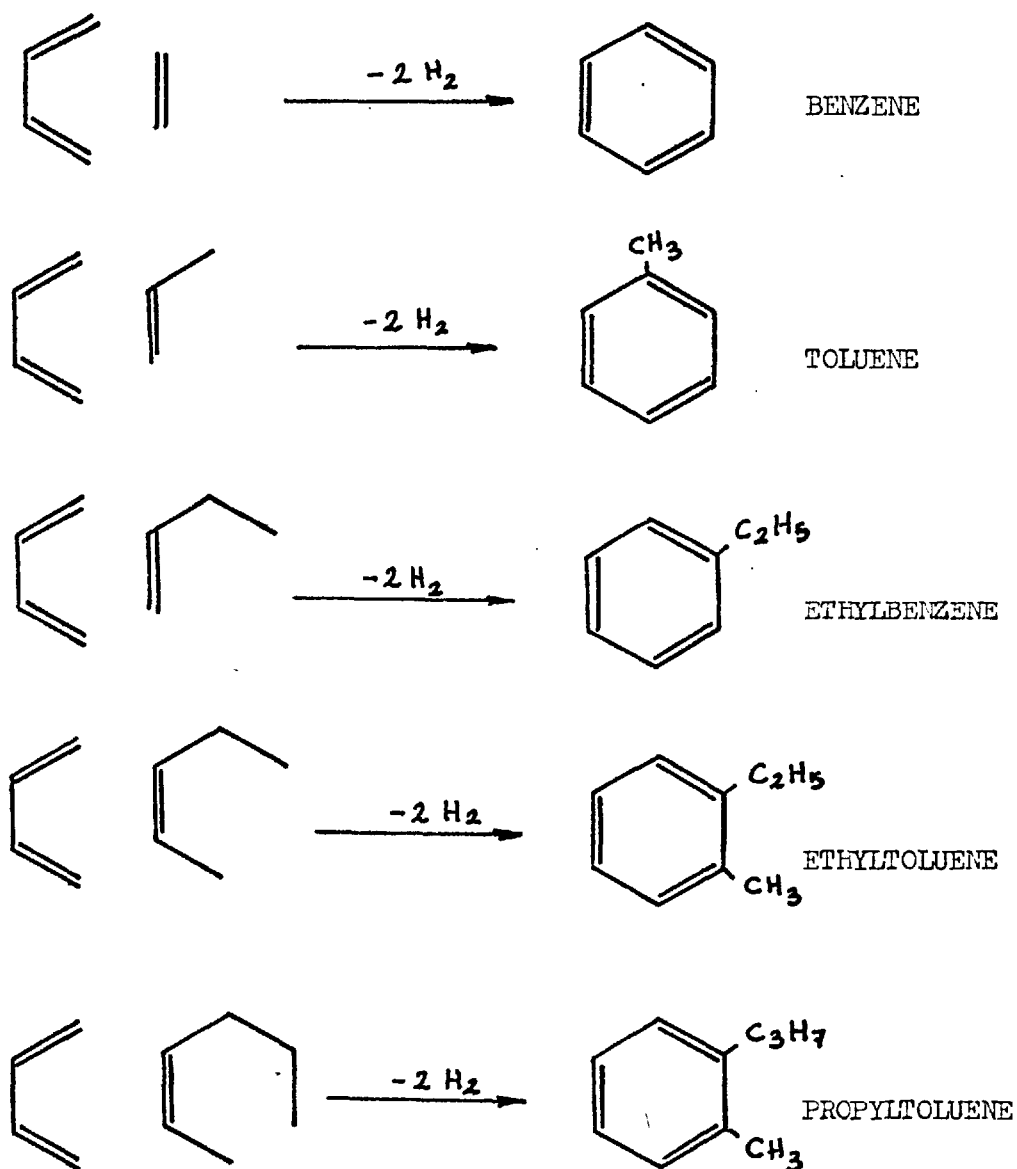
Under the conditions at which the thermal reaction takes place, however, a free-radical mechanism is more likely to occur. The sequence of reactions that follows is proposed to explain the synthesis through a free-radical path :



and



The same type of reactions may involve propylene, butenes, pentenes or hexenes. The products of the reaction would be toluene, ethylbenzene, ethyltoluene and propyltoluene, according to the additions:



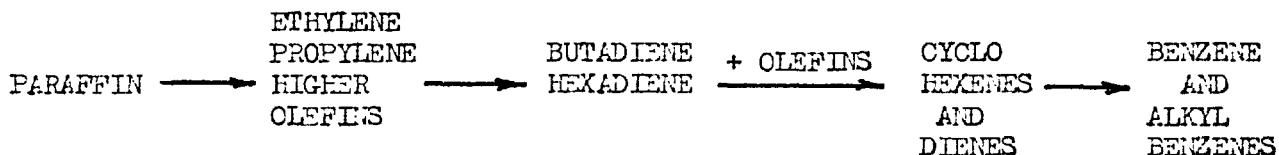
These compounds are actually present among the aromatics formed from pyrolysis of hydrocarbons, and constitute the primary products of the synthesis. The following table gives the initial composition of the aromatics produced during the pyrolysis of butane. (From figure III-26).

TABLE IV - 6

PRIMARY PRODUCTS IN THE SYNTHESIS OF AROMATICS  
FROM n - BUTANE (800° C )

COMPOUNDS	MASS PERCENT IN TOTAL AROMATICS
BENZENE	55
TOLUENE	20
ETHYLBENZENE	15
PROPYL TOLUENE	10

From the previous discussion, the path that leads to the synthesis of aromatics from paraffins pyrolysis is reasonably clear. The following scheme gives a picture of the overall process.



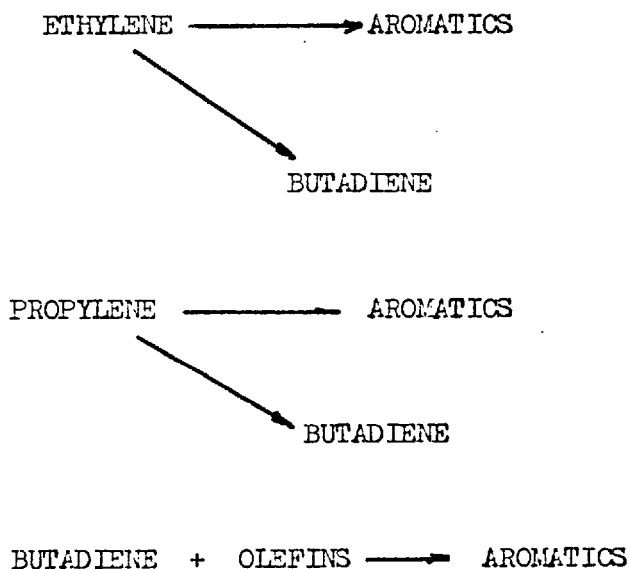
In the experiments performed during this research, most of the suspected intermediates were identified in the gas phase, although some of them in small quantities. Figure III-23 gives a typical trend of composition of these intermediates.

As can be seen, the trends observed are in good agreement with the proposed reaction path, with olefins going to dienes, to cyclo-olefins and to aromatics.



c- Modelling of aromatic synthesis

A simplified representation of the kinetics of aromatics formation can be obtained from the reactions : (Murata, et.al. 1975)



Values of some parameters for the above reactions can be obtained from a simulation model of Murata et.al. , (1975).

Information from rates of total aromatics formation can be calculated from data obtained by Turner (1976). Since his experiments were performed in a jet-stirred reactor, the format of the kinetic equations is very convenient for verification purposes.

A preliminary estimation indicate that, under the conditions studied by Turner (1976) , the main production of aromatics originates from the decomposition of propylene. The rate of production of aromatics is given by

$$r = b_8 k_3 [\text{C}_3\text{H}_6]^{3/2}$$

and at a temperature of 1100° K :

$$r = 1.98 \times 10^{-3} X_{\text{C}_3\text{H}_6}^{1.5} \quad \left( \frac{\text{moles}}{\text{et}^{-1} \text{ sec}^{-1}} \right)$$

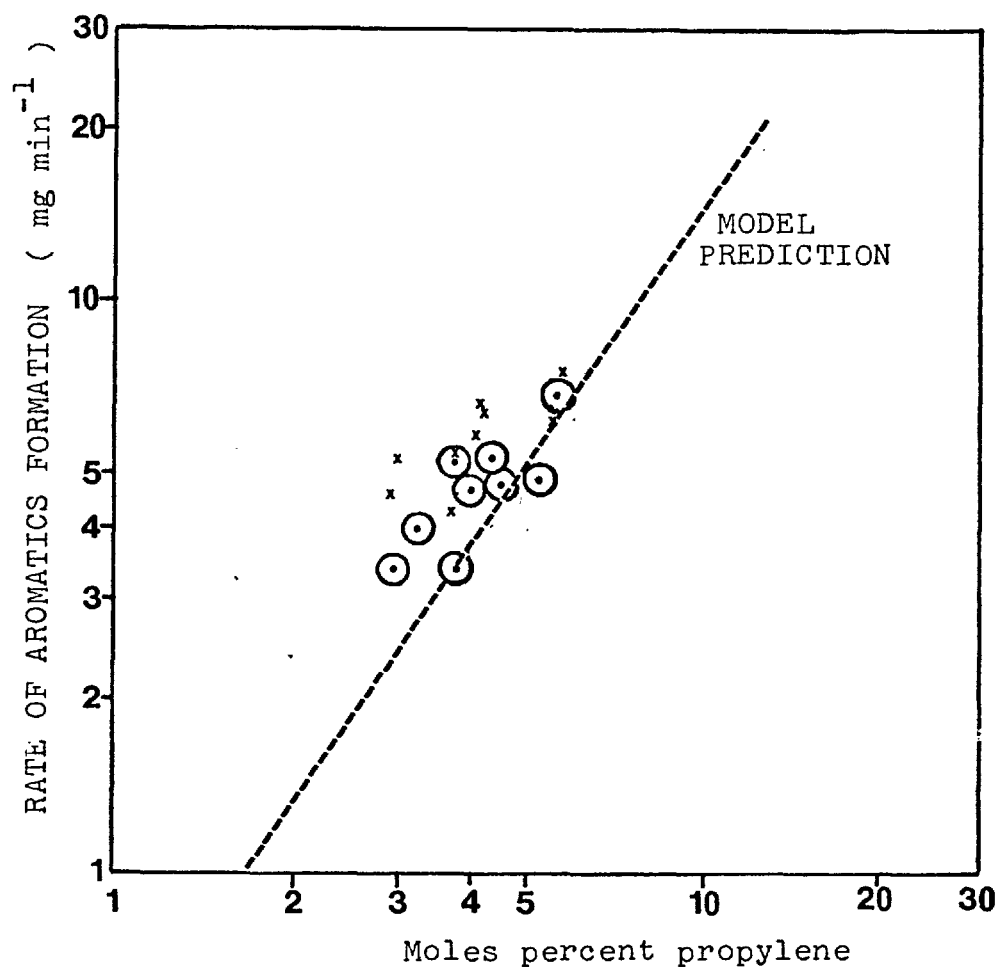


FIGURE IV-6. COMPARISON OF MODEL PREDICTION AND EXPERIMENTS FROM TURNER (1976)

Both, the rates of production predicted by the model and the experimental results are presented in figure IV - 6. The agreement between both is good and indicates that the semiempirical model can be used to predict total aromatic productions.

d- Further reactions leading to the formation of polycyclic aromatics.

During the present research, attention was focused on the identification and the determination of the concentration of several compounds that were condensed in the reactor outlet. Figure IV - 7 gives the molecular structure of some of the compounds that were identified.

The reactions that lead to the production of polycyclic aromatics during conditions of thermal decomposition of alkanes and alkenes has received little attention in the literature. Most of the compounds are present in minor or perhaps in trace amounts, but they have been considered important during the course of the present research, as they may act as precursors in the formation of carbon.

Thompson et.al. (1973) and Virk et.al. (1974) assume that the formation of polycyclic aromatics takes place according to the mechanism:

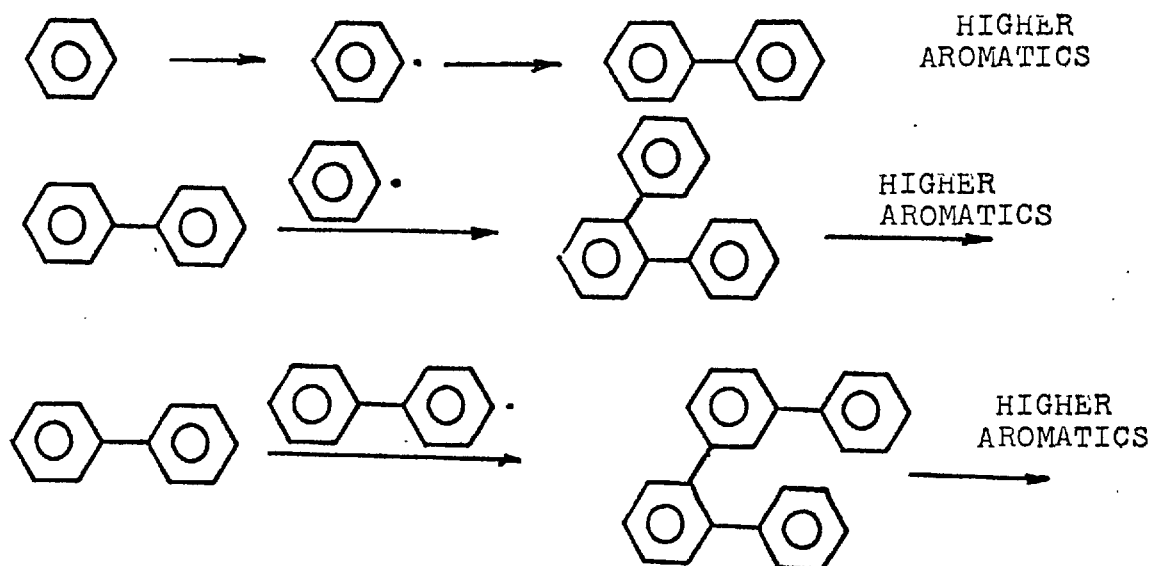
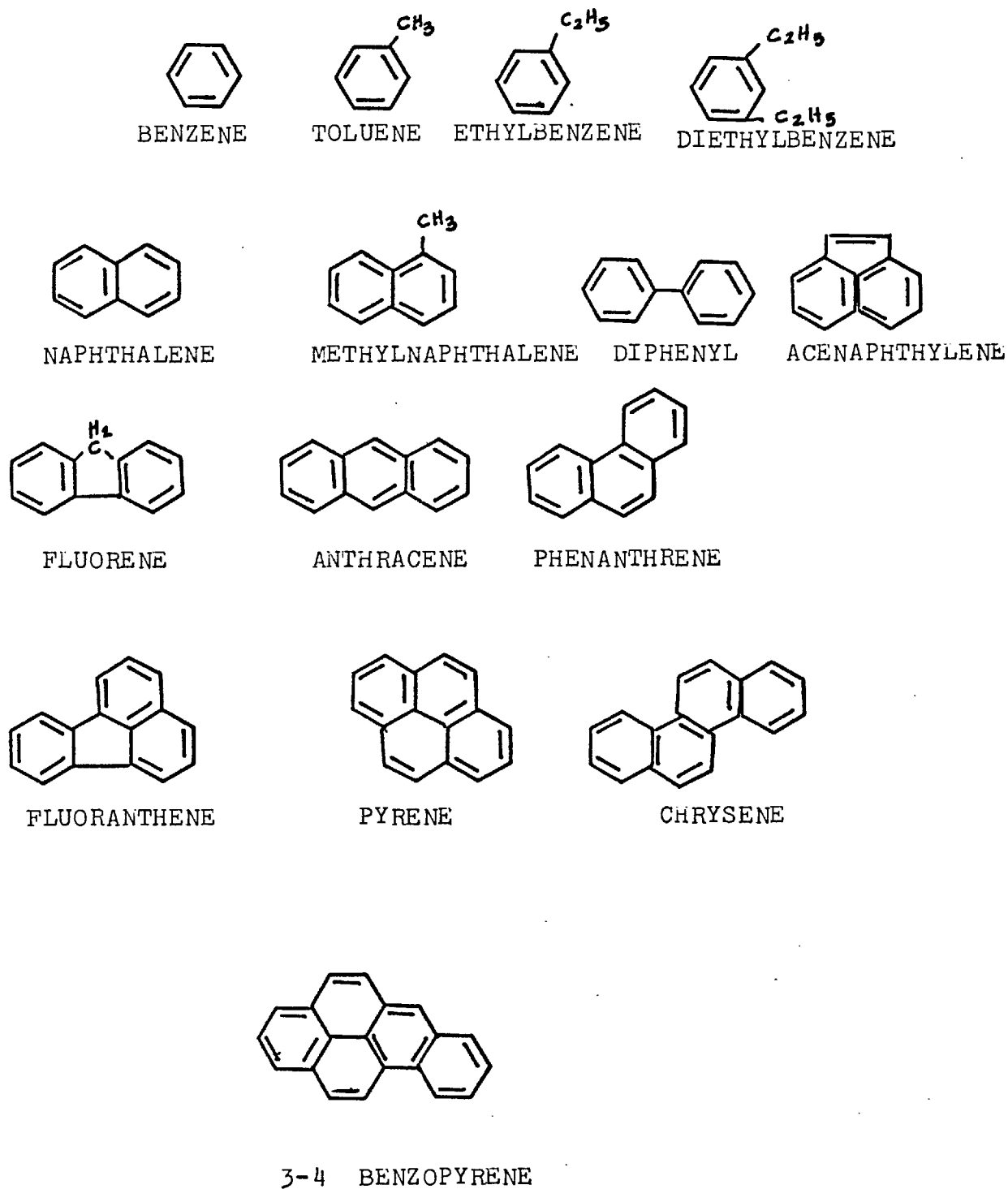
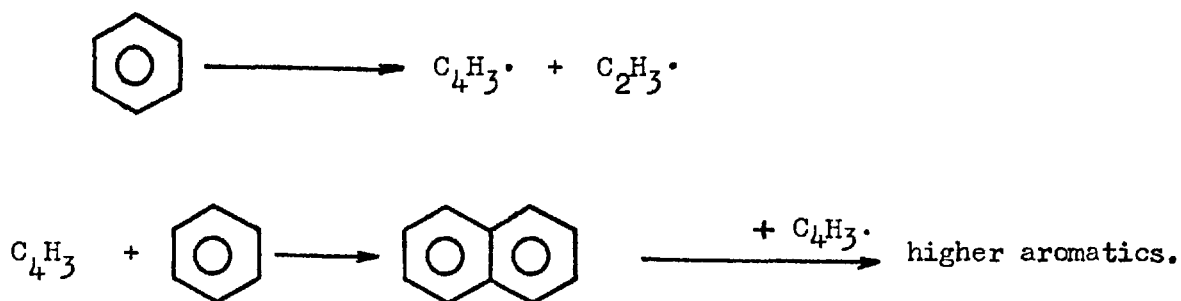


FIGURE IV-7. TYPICAL AROMATICS FROM HYDROCARBON PYROLYSIS



In fact, some diphenyl was found in the aromatic products, but in minor quantities. A path as shown above depends on the formation of diphenyl, which is kinetically very slow (Thompson et.al. 1973) and hence is very unlikely to be important under the conditions of this study.

Another possibility is that the reaction would involve the breakdown of the benzene ring : (Thompson et.al. , 1973)



This path is more likely to be operative at relatively high temperatures, since the first step involves the destabilization and breakdown of the benzene ring, which is very stable. Calculations indicate that the half life time for decomposition of benzene at 1000° K is of the order of 500 seconds, which is very large compared with the residence times used in pyrolysis and hydrogasification. As a result this mechanism cannot be very important in the conditions under study.

The presence of alkyl and di - alkyl aromatics in small amounts indicate that they may act as intermediates in the production of polycyclic compounds. Side chains can be produced by thermal alkylation:

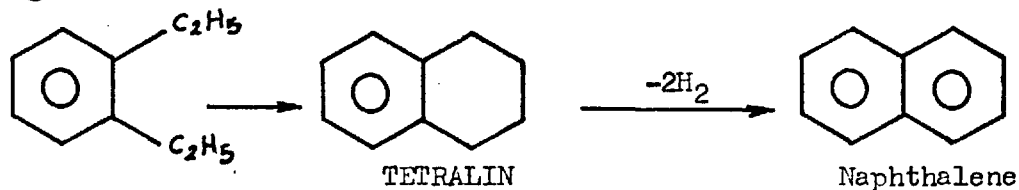


by growth of side chains :

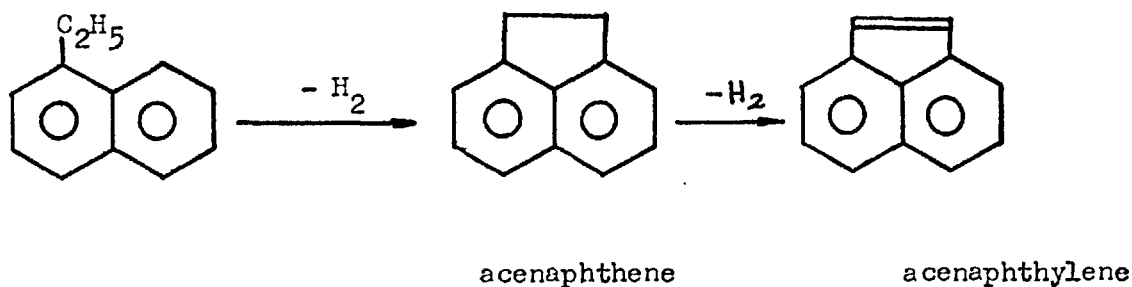


In addition, alkyl - aromatics can be produced from the synthesis reactions of butadiene and olefins, as discussed above.

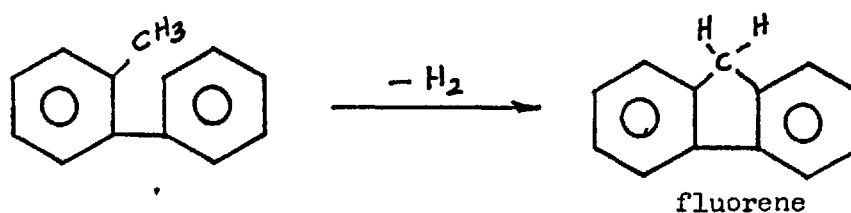
Side chains may then undergo cyclisation reactions to produce higher aromatics :



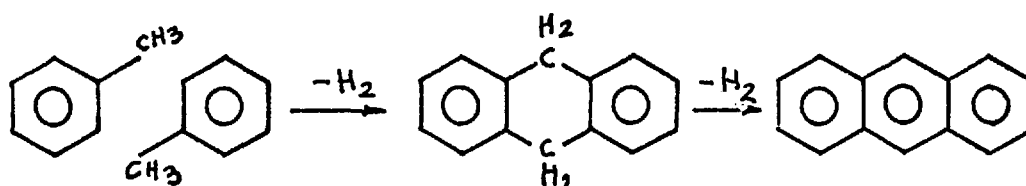
Acenaphthene and acenaphthylene can be produced by a side reaction of an alkylnaphthalene :



Fluorene can be produced by a methyl - diphenyl :



Anthracenes can be formed from alkylbenzenes



Fluoranthrene can be formed by a Diels - Adler synthesis :



and pyrene from side - chain cyclisation



The above mechanisms would explain the type of products that were found during the present research.

A further comment can be made with regard to the stability of the aromatics that are synthesised during thermal reactions. The stability of molecules larger than benzene decreases (approximately) with the number of rings present in the molecule ; hence, they tend to decompose faster, the bigger they are. The half life time of several molecules at  $1000^{\circ}$  K are given in the following table :

(Virk et.al. , 1974)

<u>Compound</u>	<u><math>T^{\frac{1}{2}}</math></u>	(seconds)
Benzene	499	
Diphenyl	118	
Naphthalene	171	
Chrysene	43	
Anthracene	20	

Molecules of aromatics that could be produced by further condensation of the compounds observed would be very short - lived, suffering themselves an accelerated series of further condensation

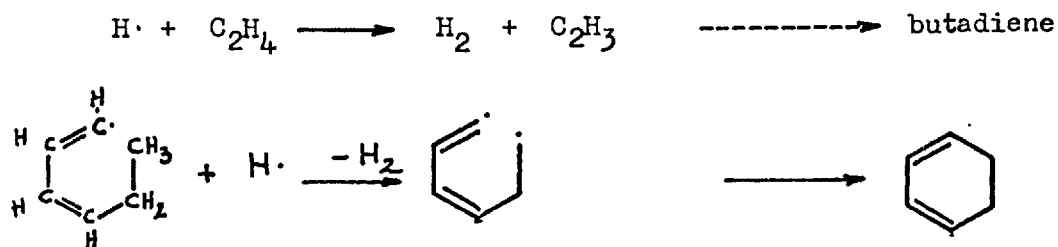
reactions to form graphite - like structures.

This mechanism of growth and chemical condensation of the aromatic molecules into larger polycyclic structures is not only important to explain the large variety of aromatics synthesized during the reaction, but also helps to understand the mechanism of carbon formation under the conditions studied. Graphite can be considered as the limiting case of a polycyclic aromatic molecule of infinite number of aromatic rings and can be formed with the same mechanism as any other large polycyclic aromatic molecule. Further evidence to support this model of non catalytic carbon formation is presented in the discussion of the link between aromatics and carbon formation at the end of this chapter.

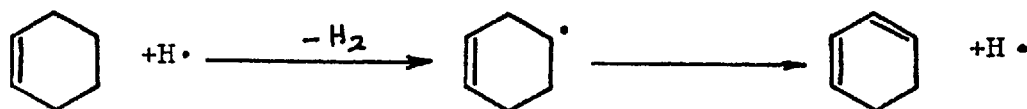
e- The effect of hydrogen on aromatics formation

During the experimental part of this research, it was found that hydrogen can play a complex role in the formation of aromatic compounds (Chapter III). At low concentrations, hydrogen enhances the production of total aromatics, while at higher proportions it tends to reduce it.

The enhancing effect could be explained by the presence of the hydrogen atom as a radical, that can help in the aromatization chain in some of the following steps :

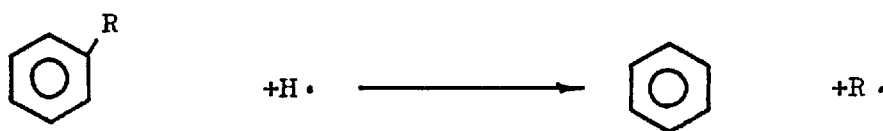


or through dehydrogenation :

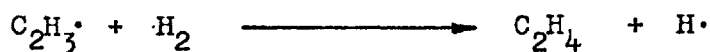




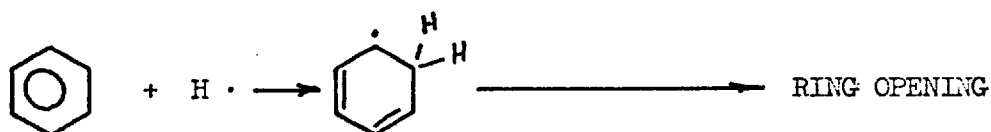
or could increase the total amount of benzene through dealkylation.



At higher hydrogen concentrations, hydrogenation reactions would tend to decrease the production of aromatics :



or yet, under severe conditions



Thus the synthesis of high molecular weight aromatics would be decreased in the presence of hydrogen. Dealkylation reactions would tend to cut the path of condensation through side chains. The aromatic mixture of products would contain more proportions of benzene and less of the other aromatics. This fact has been observed in the experiments of figure III - 28.

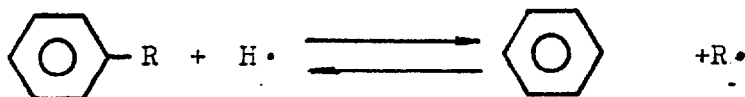
#### f. Effect of surface to volume ratio in the reactor

The effect of increased surface to volume ratio in the reactor on the production of aromatics seemed to be an overall decrease of their concentration in the reactor outlet (Fig. III - 41). This effect cannot be attributed to the change in residence time. Preliminary estimations indicate that this would account only for 2% of the 20% of total

change observed. The main possibility appears to be a reaction on the surface to produce carbon :



This scheme would be favoured particularly by aromatic compounds of high molecular weight, able to adsorb easily on the carbon surface. Alkyl benzenes may also undergo dealkylation reactions such as :



Reactions such as the above would be sensitive to the surface to volume ratio through the effect on the concentration of  $\text{H}\cdot$ . This will be decreased by surface terminations, as was discussed previously, and the above reaction would be driven to the left hand side. This consideration could explain why some alkyl - aromatics were increased by the surface to volume ratio, at the expense of the yield of benzene and other aromatics.

Thus, the increase of surface to volume ratio produces a decrease in the total aromatics produced and increases the production of some alkyl substituted benzenes. The first effect is attributed to the "trapping" of heavy aromatic molecules and the second to the heterogeneous recombination of hydrogen atoms, which suppress some of the dealkylation reactions .

#### 4- THE FORMATION OF CARBONACEOUS DEPOSITS ON SURFACES

##### General

In addition to the gaseous and tar-like products discussed above, the pyrolysis of butane also results in the formation of significant quantities of coke, a mixture of carbon and high molecular weight

carbon-like polymers. As expected, the present studies have confirmed that coke formation is influenced by both gas phase reactions and by the nature and amount of available surface, and have shown that coke-formation phenomena on different surfaces may interact.

It is convenient to consider coke formation on surfaces that do and do not influence the process catalytically although, for example, interactions such as the effect on catalytic surfaces on the formation of coke on non - catalytic surfaces are known to be significant. In addition, it is necessary to define carefully the word catalytic. Surfaces have been found to affect the product spectra to differing extents. At low surface to volume ratios on some surfaces (e.g. carbon, copper) the effect appears to be independent of the nature of the surface, and these are defined as non - catalytic surfaces. This does not necessarily mean that the surface is not influencing the reaction, but that - as opposed to catalytic surfaces - that the nature of the surface does not appear to influence the product spectra.

#### 4-A THE FORMATION OF CARBON DEPOSITS WITHOUT THE INTERVENTION OF CATALYTIC SURFACES.

##### a - General discussion of the experimental

Experimental results show that silica and copper can generally be considered as non - catalytic surfaces. However, silica foils were found to show an "ageing" effect, that affected the reproducibility of results in consecutive runs. This effect could be attributed to conditioning of the silica surface by the consecutive treatments of deposition of carbon and oxidation at 800° C. After several treatments, the results began to be reproducible, but were in any case different from those obtained in the deposition over any of the metals studied. Due to the lack of reproducibility of the deposition over silica, most of the experiments

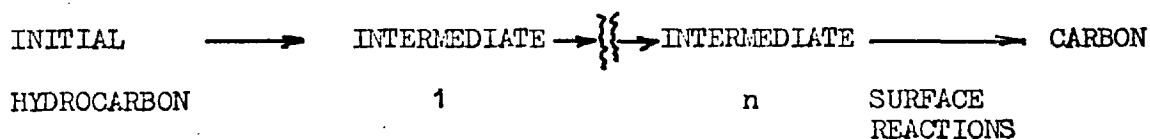
discussed in this section were performed with the use of copper sample foils.

When considering the effect of residence time on the rate of carbon deposition ( figures III-39,48 and 50 ), a certain threshold residence time was found to be required before carbon was formed at an appreciable rate. From that point the rate increase with residence time, first in a linear form and then with decaying slope .

The shape of the curve indicates the important fact that carbon is not being formed directly from the initial hydrocarbon, but requires the formation of an intermediate in the gas phase which is responsible for the deposition. If appreciable amounts of carbon were formed from the initial reactant, the rate of carbon formation should be greater than zero when extrapolating the plot to  $\tau \rightarrow 0$ , which does not happen in the present case.

The existence of an induction period in residence time indicates also that carbon is not formed from the primary products of the decomposition of butane. If it was, then no threshold would be required and the rate of deposition would start to increase from  $\tau$  equals to zero, since a primary intermediate would be produced immediately in the reaction.

The observed behaviour suggests that a series of intermediates are being formed consecutively before carbon starts to be deposited :



This is an important observation, since it requires a complete series of chemical reactions to occur in the homogeneous phase as an important step in the production of surface carbon.

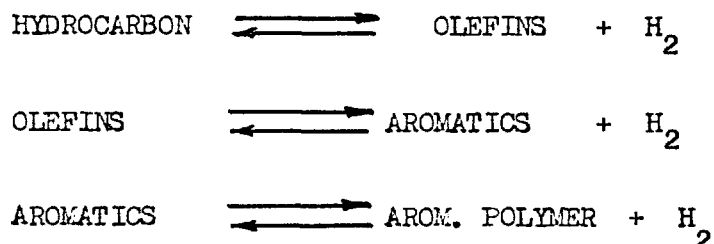
The above series of reactions is not the only explanation of the behaviour of the system. An "induction" residence time could also be caused by a reaction of order higher than one of the primary products (intermediate 1) to give surface carbon. Some other type of evidence, however, such as the polycyclic aromatics chain towards carbon (see later), tends to support the suggestion of several intermediates taking part in the reaction. In any case, there is little doubt that, from the above discussion, carbon formation is a phenomena that results from the interaction of a homogeneous process (production of intermediates) and a heterogeneous surface chemical reaction.

Temperature was found to increase the rate of carbon deposition in all conditions (figure III-54) and also affected the value of residence time at which the deposition of carbon started (figure III-53). Both effects can be explained by an acceleration of the rates of production of intermediates, through an Arrhenius type of effect of temperature on one or more of the set of reactions. The reaction on the surface would also be affected by temperature.

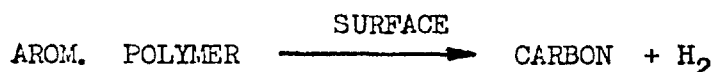
The dependence of the rate on temperature can be expressed in a pseudo - zero order Arrhenius plot. Experimental points were found to follow, in most cases, a straight line or a line where the slope decayed slowly at lower values of  $1/T$ . No specific significance was assigned to the slopes of the graphs, due to the complexity of the overall phenomena (see later). This system is very different from the phenomena studied by Lobo et.al. (1972), in which the activation energy calculated from the Arrhenius plot had a precise physical signification.

Dilution with hydrogen had a strong inhibiting effect on the rate of carbon deposition. (figure III-64). The effect was also noticed by Tesner (1973), during the pyrolysis of methane. This effect

can be attributed to two sources : on one side, the chain of reactions that lead to the formation of intermediates involve dehydrogenation steps, in the form :



where, in each reaction, hydrogen can inhibit the path towards carbon. Secondly, the reaction



can also be affected by the presence of hydrogen.

The concentration of butane in mixtures with hydrogen in the reactor feed was found to affect the rate of carbon formation (figure III-62). The dependence of rate on initial concentrations seemed to be of reaction order less than one. This would indicate either a complex gas phase mechanism with inhibition or an adsorption process on the reaction surface.

#### c- 2. b A model of non - catalytic carbon deposition

To build an accurate model of the whole phenomena of carbon deposition or formation on surfaces would require a detailed knowledge of the processes in the gas phase that lead to the production of carbon forming intermediates and the surface reactions that transform these intermediates to carbon. The state of knowledge of these processes is, however, very limited, and only very simplified models, incorporating the most essential features, can be proposed.

From the discussion of the general features of the previous section, it has to be concluded that a series of reactions leading to carbon forming intermediates are necessary to explain the behaviour of the system. With regards to the nature of these intermediates, under the conditions of the present study, they are probably heavy aromatic molecules or aromatic polymers (Fitzer, 1971). The reasons for this proposal are as follows :

- 1- A complete series of stable polycyclic aromatics are present as products of the reaction, (Chapter II). These could well be by-products of a series of reactions involving short-lived aromatic intermediate that would lead eventually to heavy aromatic structures and to carbon.
- 2- The tendency towards carbon formation, and the rate at which carbon is formed, increases with the number of rings in the aromatic structure and with the molecular weight of the compound. (Virk, et.al., 1974).
- 3- Aromatization and chemical condensation of aromatic molecules are necessary steps in the chain towards graphite. (Fitzer et.al. 1971). High molecular weight polycyclic aromatics are similar to graphite in chemical structure.

Further evidence in support of the polycyclic aromatics route to carbon formation will be presented later in this chapter.

Once the intermediate molecules have been formed, they have to deposit on the surface and decompose further to carbon. There are two ways in which this process can take place. In the first, the concentration of molecules in the gas phase can increase with residence time until the saturation point, when heterogeneous physical condensation occurs. Molecules are then deposited on the surfaces and carbonization

continues through liquid pyrolysis towards graphitic structures. This process is the heterogeneous equivalent to the "condensation theory", recently revived by Lahaye et.al. (1974).

There are some reasons to believe that this process is not operative in the reaction conditions of interest in the present study. One of these is that if such a process was important, then an apparent negative activation energy should be observed under conditions of constant concentration of intermediates : this other is that physical condensation should show a certain dependence on diffusional transfer that is not exhibited, at least by the process of growth of coke particles in a fluidized bed during thermal hydrogasification. Both tests will be analyzed in detail in following sections.

The other mechanism that could transfer the intermediate molecules to the surface is adsorption. The process does not require the partial pressure of the intermediates to reach the saturation point but envisages molecules adsorbed on the surface, where they could react by dehydrogenation to produce a layer of carbon. This layer, in turn, would adsorb more intermediates and carbon would continue to grow.

This representation of the phenomena seems to be fairly good way of explaining the mechanism of carbon formation over non - catalytic surfaces. In essence, the proposed model postulates a mechanism that is a homogeneous reaction, followed by a heterogeneous reaction on the reactor surface, that would be, in most cases, carbon.

c- Simplified quantitative model. The effect of operation variables

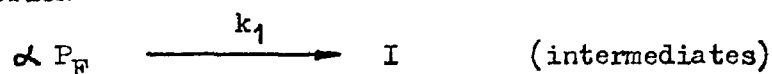
The qualitative model described in the previous section can now be put in a mathematical form. The mathematical description given below is the simplest possible explanation of the phenomena that incorporates the most essential features. A large number of more complex, and perhaps more realistic models could be constructed incorporating more detailed information on each of the reaction steps.



This model was developed under the assumption of low surface to volume ratio in the system. The effect of S / V ratio is discussed later.

- 1- The production of intermediates (polycyclic aromatics) was approximated with a first order kinetics reactions. This assumption was also used previously by Lahaye et, al. (1974) and is equivalent to assume that the curves in figures III-31 and 32 are approximated by straight lines. The hypothesis also assume that the effect of hydrogen on polycyclic aromatics is small. (The effect of hydrogen on the overall carbon formation was attributed to inhibition of the surface reaction. In fact, this simplification was suggested by figures III-30 and III-64).

GAS PHASE REACTION



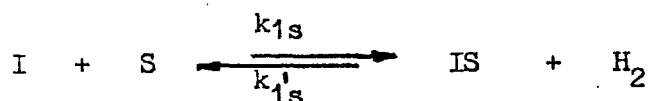
The first order kinetics reaction , integrated over the volume of the tubular reactor is :

$$[I] = \alpha [P_F^0] \left\{ 1 - e^{-k_1 \tau} \right\} \quad c-1$$

This simplified model of the gas phase production of intermediates assumes that the residence time required to start producing intermediates is very small.

- 2- Surface reactions were expressed in two steps :

- a- Adsorption and dehydrogenation



- b- Carbon formation and regeneration of the carbon surface



The solution of the model would give an expression for the rate of carbon deposition per unit area of surface in contact with the gas phase at a certain residence time  $\tau$ .

The hypothesis of steady - state applied to the active species IS on the surface, and assuming that the number of vacant plus occupied surface centers remain constant, leads to the following rate of carbon formation per unit area :

$$W_{cf} = \frac{k_{2s} k_{1s} [I]}{\left(1 + \frac{k_{1s}}{k_{2s}} [I] + \frac{k'_{1s}}{k_{2s}} [H_2]\right)} \quad c-2$$

Equation c-2 has to be used together with c-1 for a complete description of the phenomena. The effect of the different variables on the deposition of carbon is discussed below.

#### I- The effect of hydrogen concentration in the feed

When the initial concentration of reactant, residence time and temperature are kept constant, equation c-1 predicts that the concentration of intermediates will be constant. Under this condition equation c-2 can be reduced to the form :

$$\frac{1}{W_{cf}} = A_1 + A_2 [H_2] \quad c-3$$

which predicts that the inverse of the deposition rate would change linearly with the concentration of hydrogen. Data from figure III-60 has been plotted in figure IV-8, and the shape of the plot indicates that this prediction is correct.

#### II- The effect of the residence time.

When considering relatively short residence times, equation c-1 can be expanded in a Taylor series and, taking only up to the first power of the series, the equation is simplified to :

$$[I] \approx \alpha [P_f^0] k_1 \tau \quad c-4$$

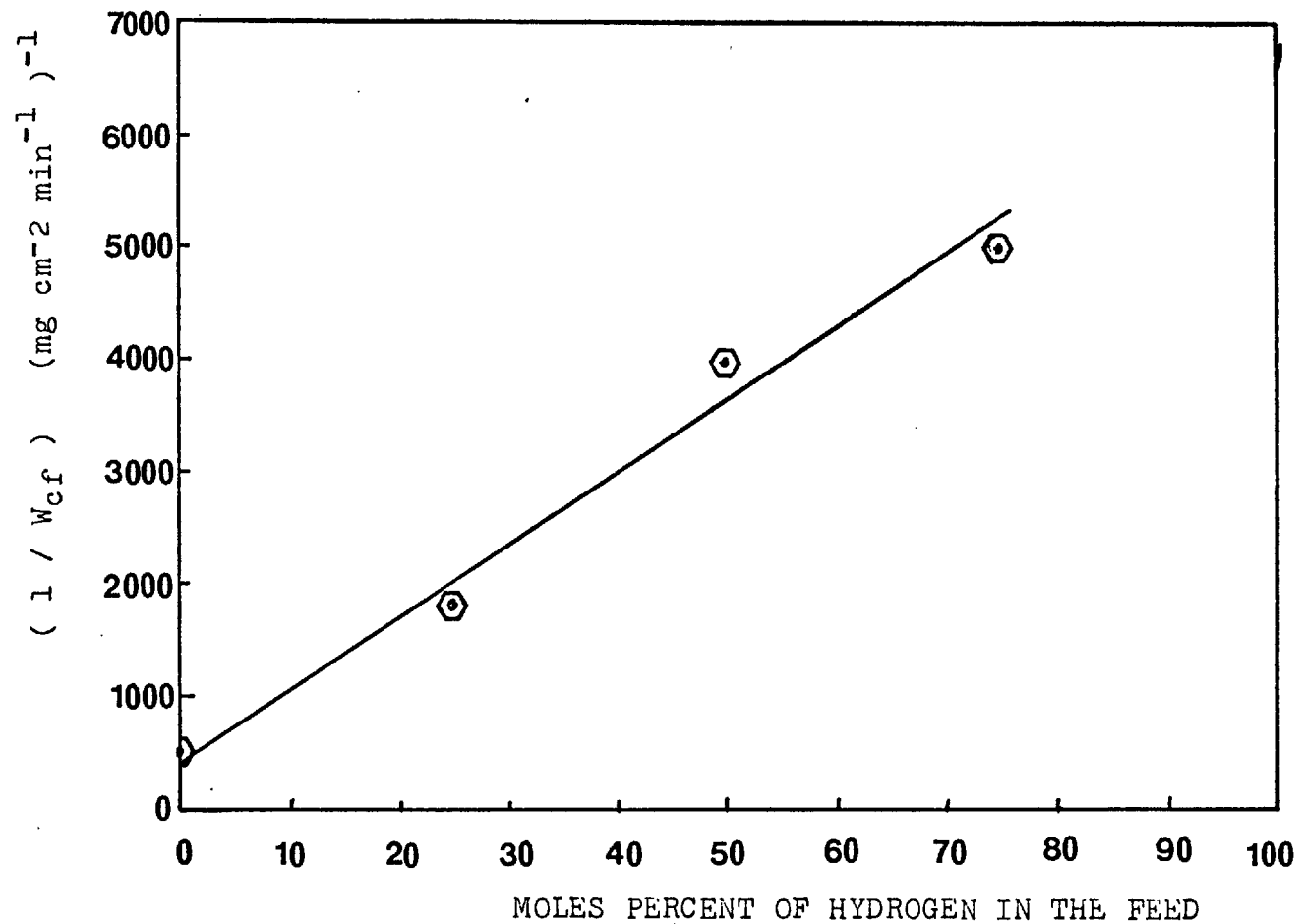


FIGURE IV-8. THE EFFECT OF HYDROGEN CONCENTRATION IN THE FEED AT CONSTANT RESIDENCE TIME, REACTANT CONCENTRATION AND TEMPERATURE. ( Data from Fig. III-60)

Substituting c-4 in c-2, and considering the changes of hydrogen concentration with residence time to be negligible and at constant initial reactants concentration and temperature, it is possible to obtain the following expression on rearrangement :

$$\frac{\tau}{W_{CF}} = A_3 + A_4 \tau \quad c-5$$

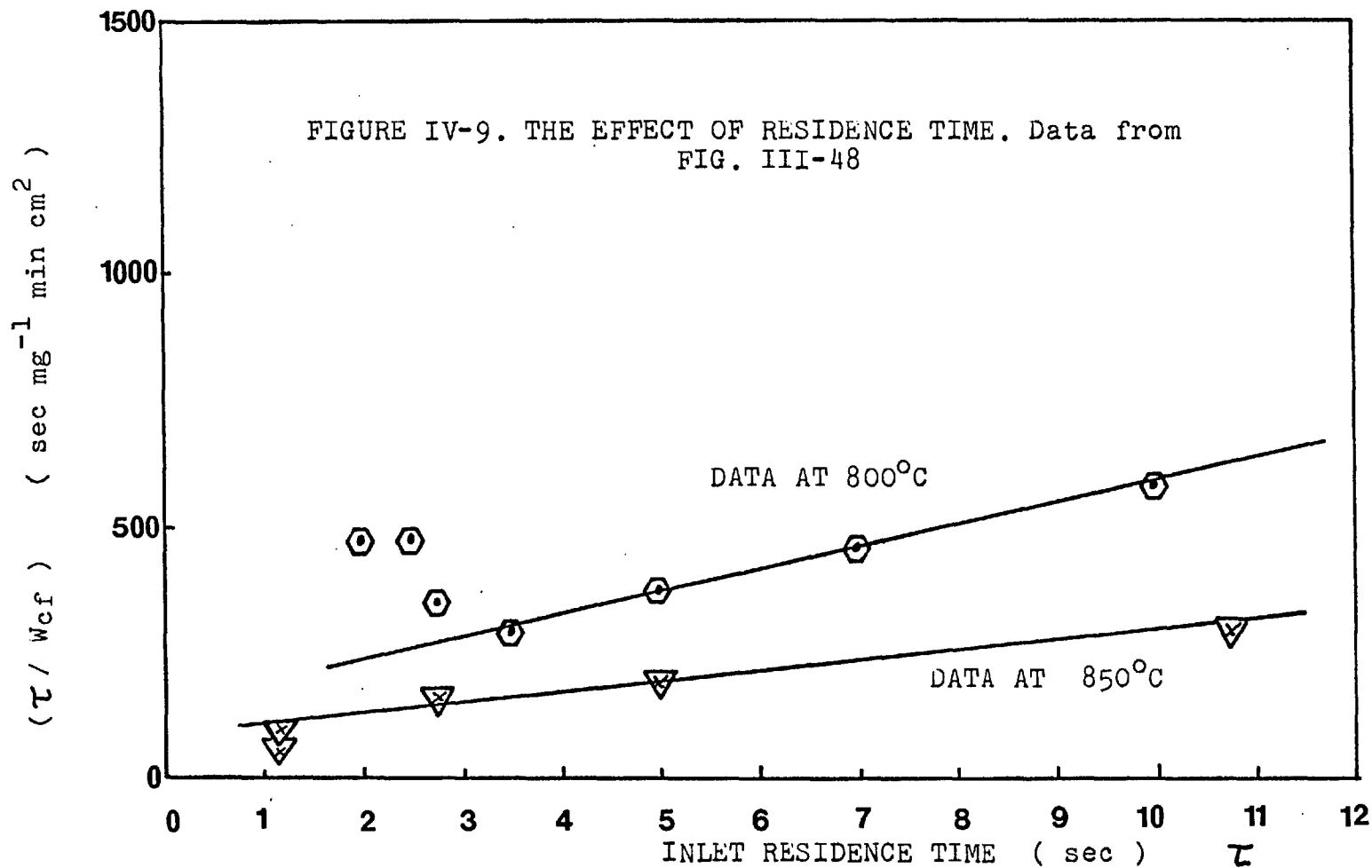
Information from figure III-48 was plotted as  $\tau / W_{CF}$  as a function of  $\tau$ . The plots are shown in figure IV-9. Most of the data fall in the form predicted by equation c-5. At 800° C and at low residence times, however, the points do not fall on the same line. This effect can be attributed to the presence of a significant value of residence time required to start forming the intermediates I. Under these conditions, the model is oversimplified and fails to represent the experimental behaviour.

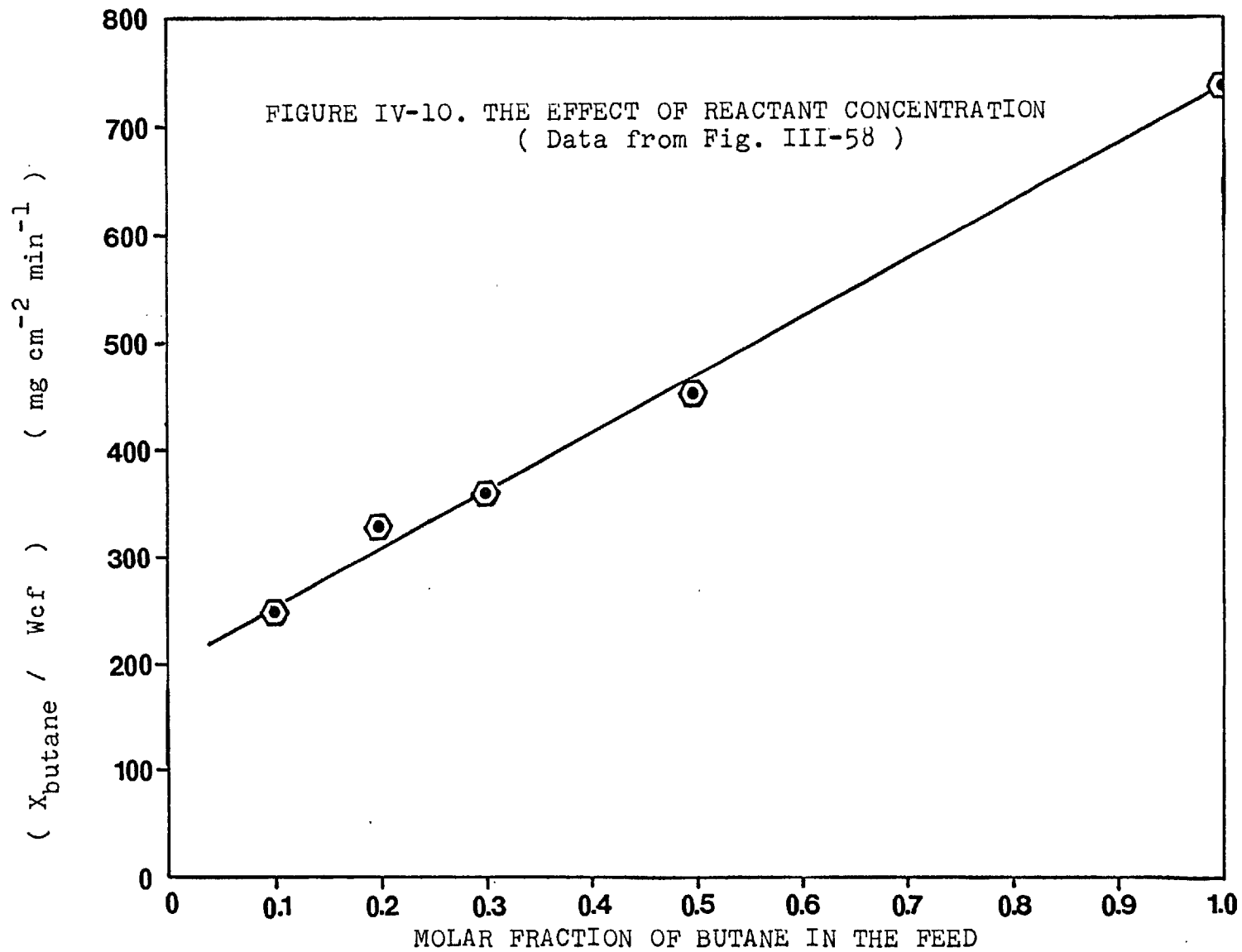
### III- Effect of reactant concentration

When mixtures of different proportions of the initial hydrocarbons and hydrogen are reacted at constant residence time and temperature, from equations c-1 and c-2 the following equation can be deduced : this the rate of deposition with the initial concentration of reactant:

$$\frac{[PF^{\circ}]}{W_{CF}} = A_5 + A_6 [PF^{\circ}] \quad c-6$$

To deduce c-6 it is necessary to put the concentration of hydrogen as a function of the concentration of initial reactant. Data from figure III-58 has been plotted in the form of  $X^{\circ}BUTANE / W_{CF}$  as a function of  $X^{\circ}BUTANE$ , to show that the prediction of equation c-6 is correct. (See fig. IV-10)





IV - Effect of temperature

When substituting equation c-4 in c-2, the expression of the rate is :

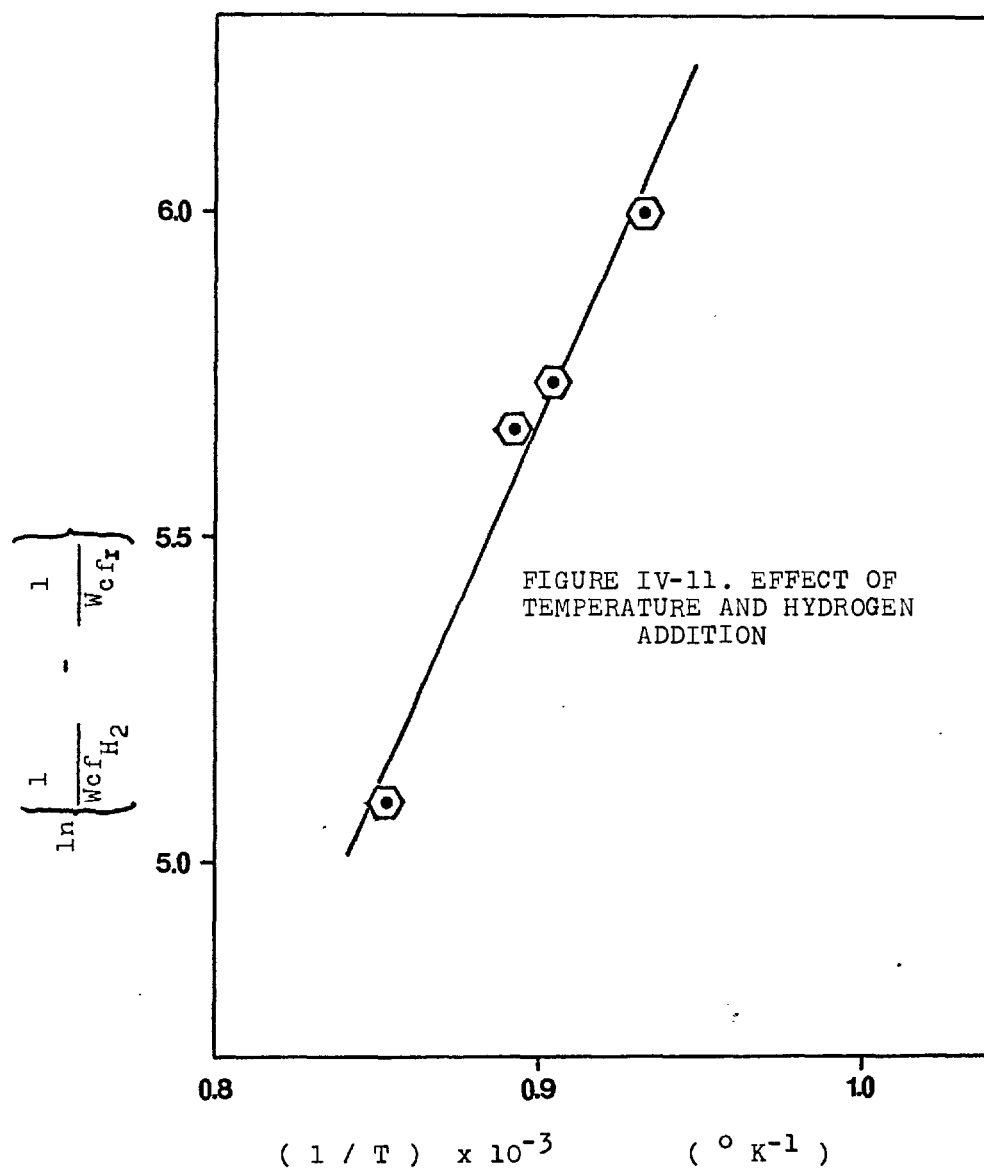
$$W_{CF} = \frac{k_{2s} k_{1s} k_1 \propto [PF^o] \tau}{\left[ 1 + \frac{k_{1s}}{k_{2s}} k_1 \propto [PF^o] \tau + \frac{k_{1s}}{k_{2s}} [H_2] \right]} \quad c-7$$

Considering that each constant would follow an Arrhenius - type of temperature dependence, equation c-7 would predict a complicated relationship of rate with temperature. In some limiting cases, it may be possible that plots of  $\log W_{CF}$  as a function of  $(1/T)$  might give a straight line, but generally it would be expected that the slope of the plot would change with  $(1/T)$ . This prediction has been confirmed in many cases during the experimental work, and can be observed in the plots presented in the experimental section.

A further test can be made on the basis of the simple model presented. Data was obtained experimentally for the rate of carbon deposition as a function of temperature in two series of runs performed under the same concentration of reactant in the feed and the same residence time, but differing in that hydrogen was used as diluent in one case and an inert in the other. This data was presented in figures III - 66 and III-68.

When the constants in equation c-7 are expressed in the Arrhenius form, and the inverses of the rates of deposition with and without hydrogen are combined in one equation, the following result is obtained :

$$\left\{ \frac{1}{W_{CF} (H_2)} - \frac{1}{W_{CF} (INERT)} \right\} = \frac{k_{1s}^o e^{(2 E_{2s} + E_{1s} + E_1 - E_{1s}) / RT}}{k_{2s} k_{1s}^o k_1^o} \propto \frac{[H_2^o]}{[PF^o]} \tau \quad (c-8)$$





Equation c-8 predicts that the logarithm of the difference of the inverse of rates should give a straight line as a function of  $(1/T)$ .

As shown in figure IV-11, the points do fall in a straight line, and from the slope it was estimated that

$$2 E_{2s} + E_{1s} + E_1 - E_{1s} = 22.58 \text{ Kcal / mole}$$

This concludes the study of the simplified model of carbon formation through a non-catalytic mechanism. Predictions of the effect of the different variables of the system on the rate have been found correct in most cases. This indicates that the model incorporates most of the essential features of the phenomena and represents a good first approximation to the mechanism.

d- The effect of surface to volume ratio on carbon deposition

The simplified model described in the previous section was based in the assumption that the surface to volume ratio was small and hence that the surface had little influence on the final rate of deposition of carbon on the reactor surface. An increase in the internal surface of the reactor would offer a larger surface where the intermediates of carbon formation could adsorb and react, and hence the intermediates would be depleted from the gas phase and the rate of deposition per unit area would decrease.

To find the mathematical relationship between the rate of carbon formation and the surface to volume ratio, the principle of mass conservation is applied to a differential element of volume in a cylindrical flow reactor, which may contain surfaces other than the walls. The resultant differential equation is as follows :

$$\frac{dI}{d\xi} = - \tau \left( \frac{S}{V} \right) W_{CF} + \tau R_v \quad d-1$$

where:  $I$  : concentration of intermediates

- $\xi$  : dimensionless distance = Z / L  
 L : reactor length  
 $\tau$  : residence time = V / q\_0  
 $W_{CF}$  : = rate of carbon deposition per unit area  
 q : volumetric flow through reactor  
 S : surface inside the reactor  
 V : reactor volume  
 $R_v$  : rate of generation of intermediates per unit volume

Applying the same assumption as in (c)

$$R_v = \alpha k_1 [P_F^0] e^{-k_1 \tau \xi} \quad d-2$$

$$W_{CF} = \frac{k_{2s} k_{1s} [I]}{1 + \frac{k_{1s} [I]}{k_{2s}} + \frac{k_{1s} [H_2]}{k_{2s}}} \quad d-3$$

To obtain an analytical solution, equation (d-3) is linearized (for low concentrations of I) and, together with d-2, is substituted in d-1. The resulting equation is integrated with the condition that the concentration of intermediates is zero at the reactor inlet. The result is:

$$[I] = \left\{ \frac{\alpha [P_F^0]}{1 - \left(\frac{S}{V}\right) \frac{k_{2s} k_{1s}}{\left(1 + \frac{k_{1s} [H_2]}{k_{2s}}\right) k_1}} \right\} \left[ e^{-\left(\frac{S}{V}\right) \frac{k_{2s} k_{1s} \tau \xi}{\left(1 + \frac{k_{1s} [H_2]}{k_{2s}}\right) k_1} - k_1 \tau \xi} - e^{-k_1 \tau \xi} \right] \quad (d-4)$$

Equation d-4 could be substituted in d-3 to give a complicated expression of the rate of deposition with the surface to volume ratio. However, simplified equations can be obtained for limiting cases. When

the surface to volume ratio is zero, equation d-4 transforms into c-1, reducing the model to the previously discussed in section c.

At small values of  $(S / V)$  and  $\tau$ , the exponentials in d-4 could be linearised and, after simplification, d-4 is transformed into :

$$[I] = \alpha [P_F^0] k_1 \tau \xi \quad \text{d-5}$$

Equation d-5, substituted into d-3, shows that the rate of carbon formation per unit area is insensitive to changes of  $(S / V)$  at low values of surface to volume ratio.

At very large values of  $(S / V)$ , equation d-4 becomes :

$$[I] = \frac{k_1 \alpha [P_F^0] \left( 1 + \frac{k_{1s}}{k_{2s}} [H_2] \right) e^{-k_1 \tau \xi}}{\left( \frac{S}{V} \right) k_{2s} k_{1s}} \quad \text{d-6}$$

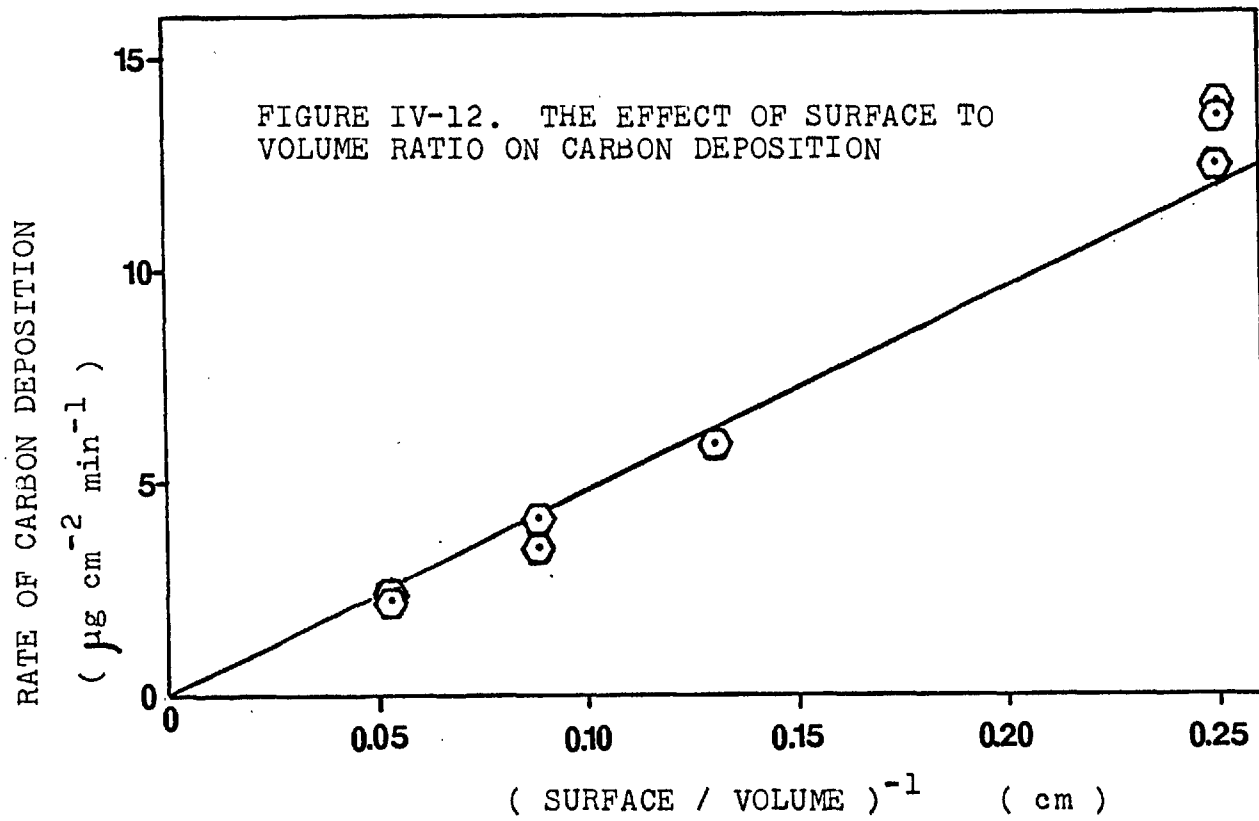
Substituting d-6 into the linearised version d-3, the resulting equation is :

$$W_{CF} = \left( \frac{S}{V} \right)^{-1} \alpha k_1 [P_F^0] e^{-k_1 \tau \xi} \quad \text{d-7}$$

which predicts that the rate of carbon deposition per unit area should be inversely proportional to the surface to volume ratio at large  $S / V$ .

Data for the rate of deposition at different  $S/V$  ratios has been plotted as a function of  $(S / V)^{-1}$  and are presented in figure IV-12. The prediction of equation d-7 is correct, as the points fall in a straight line at large  $S / V$  ratios.

Finally, it is possible to suggest that the rate of carbon formation can be controlled by the  $S/V$  ratio in a reacting system. An increased surface would "trap" the intermediates, avoiding the deposition



of carbon in inconvenient places, such as pipes, valves and nozzles.

e- Mathematical modelling of the growth of coke particles by carbon deposition in a fluid bed during industrial thermal hydrogasification

Reference has been made to the fact that the growth of carbon does not appear to be limited by diffusional effects (section 4A-b). Evidence for this originates from the treatment of the data obtained using fluid beds of coke particles during thermal hydrogasification. (Murthy et.al. , 1963).

In section 4-A.d , the mechanism of controlling carbon deposition by means of a high surface to volume ratio was analyzed, and it is very likely that the fluid bed of coke particles play a similar role, offering a large surface where the intermediates for carbon deposition can be trapped.

Particles in the fluid bed grow by carbon deposition, a process that can be simulated mathematically. When modelling the particle growth, it is interesting to notice that the shape of the size distribution function growth is sensitive to the mechanism of deposition. In this sense, if particles grow by physical condensation of a heavy intermediate, the shape of the distribution of particle size would be different from that obtained for particles that grow by chemical reaction on the surface.

This fact offers the possibility of testing the applicability of the adsorption - reaction mechanism and the condensation theory. In this section, a model of particle growth is developed for each mechanism. The model is applied to the simulation of the growth of particles in an industrial hydrogasifier and the predictions are compared with the experimental results.

Modelling of particle growth

Given the initial distribution function of particle sizes, the particles can be considered to grow by different mechanisms of deposition.

a- Deposition by condensation of polynuclear aromatics.

This mechanism should be limited by diffusional resistances only. The rate of volume deposition on a particle in a fluid bed will be :

$$R = \frac{dv}{dt} = S k_L (C_G - C_p) = \frac{SK}{D_p} f(C_G) \quad (e-1)$$

R : rate of volumetric deposition

S : surface area

V : volume of a particle

$k_L$  : mass transfer coefficient

$C_G$  : concentration of condensable in the gas

$C_p$  : Saturation concentration in surface.

$D_p$  : particle diameter

The simplification in (e-1) has been carried out knowing that mass transfer to small particles in a fluid bed can be written as

$$k_L = \text{CONSTANT} / D_p \quad (e-2)$$

This gives the following differential dependence of diameter with time:

$$\frac{dD_p}{dt} = 2 \frac{K}{D_p} f(C_G) \quad e-3$$

which on integrating, gives

$$D_p = \left[ D_p^2 + 4 K f(C_G) t \right]^{\frac{1}{2}} \quad e-4$$

$4 K f (C_G) t$  can be replaced by only one parameter  $\Theta'$  to give

$$D_p = ( D_p^2 + \Theta' )^{\frac{1}{2}} \quad e-5$$

- b) Deposition of droplets of an aerosol on the particles of a fluid bed.

This mechanism will be diffusion - limited, since the droplets of the aerosol would be of the order of 100 - 800 Å . The growth will be governed by an equation such as (e-1)

( Prado , 1973)

- c) Deposition by chemical reaction on the surface of the particles

This mechanism will be described by

$$R = \frac{dv}{dt} = S k_K f' ( C_G ) \quad e-6$$

Equation (e-6) gives the differential equation :

$$\frac{dD}{dt} = 2 k_K f ( C_G ) \quad e-7$$

which integrated gives

$$D = D_0 + 2 k_K f ( C_G ) t \quad e-8$$

Again ,  $2 k_K f ( C_G ) t$  can be replaced by one parameter ,  $\Theta$

$$D = D_0 + \Theta \quad e-9$$

#### The experimental size distributions of coke particles

Analysis of coke particle sizes, performed before and after carbon deposition, are given by Murthy et.al. (1963). The initial particle size distribution function was found by a fitting procedure

described below. The function was used as an initial value to simulate the growth by carbon deposition.

The experimental information on particle size distributions is given in figure IV - 13. To find a theoretical size distribution function that would fit the initial experimental data, a non linear iterative parameter estimation technique was used. A series of standard statistical functions were tested, which included normal and lognormal distributions, and these multiplied times  $X_i$ ,  $X_i^2$  and  $X_i^3$ . Some of the more successful fittings are shown in table IV - 7. The best fit is provided by the normal distribution times  $X_i^2$ , that fitted the experimental results with a 2.52 % standard error. This function, and the parameters estimated, were used in the later development of growth models.

#### Growth simulation

Growth was simulated by applying equations ( e-5 ) and ( e-9 ) to small discreet intervals in the distribution of particle sizes. Particles were considered as spheres. In each small interval, all particles were assumed to be of a diameter equal to the mean of the interval and were modelled on the basis of diffusional or kinetic mechanisms to a selected value of  $\Theta$  or  $\Theta'$ . From the new situation, the cumulative distribution function was calculated.

The results of both models compared with the initial and final experimental distributions are given. In both cases  $\Theta$  and  $\Theta'$  is a parameter that is proportional to the reaction time and a group of unknown parameters that will remain constant during the operation; and  $\Theta$  can thus be considered as a reaction " time" in both cases. (See figures IV-14 and IV-15).

The process of growth by physical condensation does not follow the pattern required by the final experimental distribution . The chemical growth mechanism fits the final distribution with good



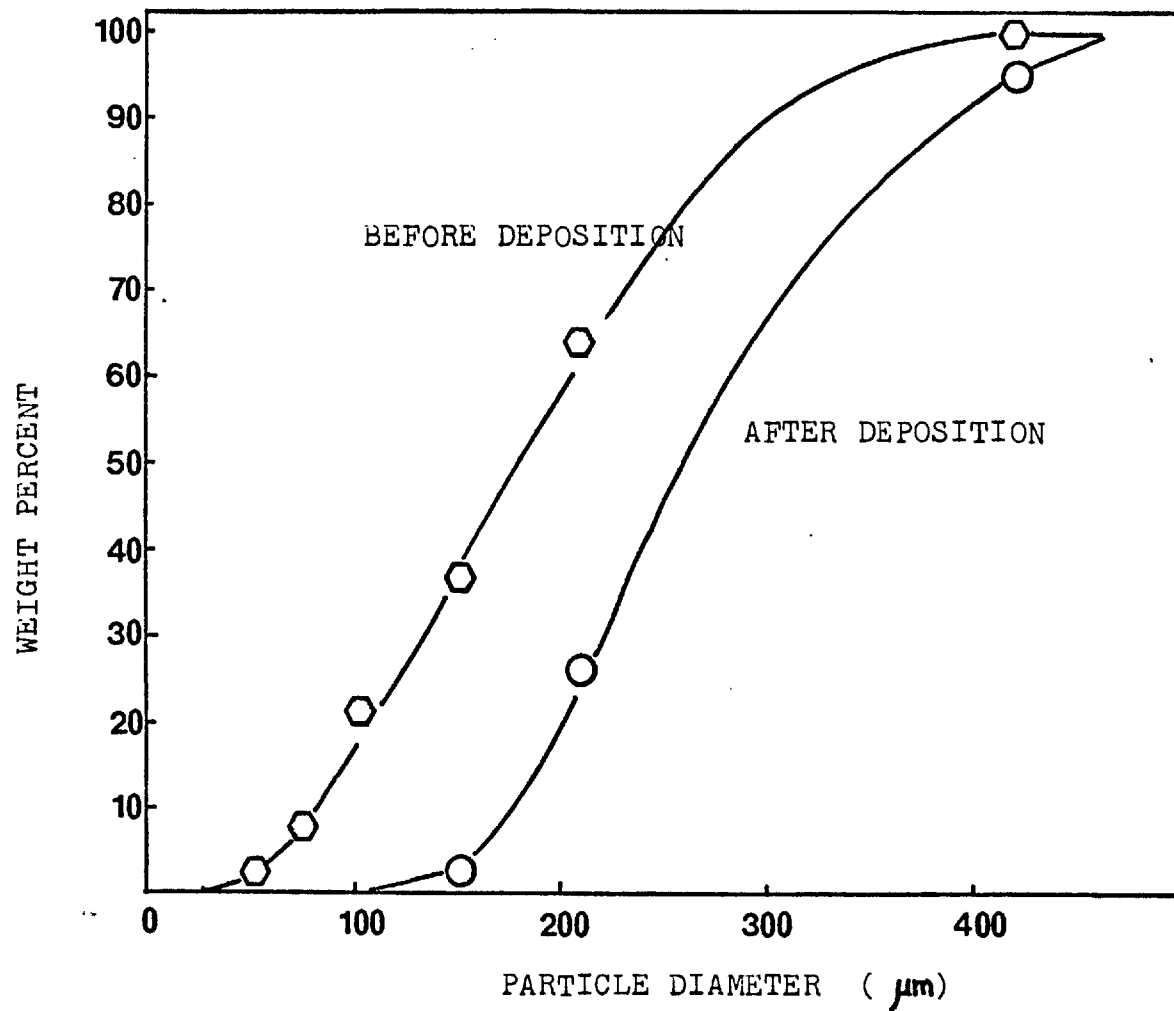


FIGURE IV-13. EXPERIMENTAL CUMULATIVE DISTRIBUTION FUNCTIONS FOR COKE PARTICLES BEFORE AND AFTER CARBON DEPOSITION IN A FLUIDIZED BED.  
 ( From Murthy, et. al., 1963 )

TABLE IV - 7

FITTING THE INITIAL SIZE DISTRIBUTION WITH A THEORETICAL FUNCTION

FUNCTION		$\alpha$	B	STAND. DEV. RESIDUES (%)
(1 / B )	x EXP $(-(X_i - \alpha)^2 / 2B^2)$	$7.14 \times 10^{-3}$	$1.28 \times 10^2$	31.25
(X <sub>i</sub> / B )	x EXP $(-(X_i - \alpha)^2 / 2B^2)$	$1.86 \times 10^{-3}$	$1.28 \times 10^2$	8.7
(X <sub>i</sub> <sup>2</sup> / B)	x EXP $(-(X_i - \alpha)^2 / 2B^2)$	$1.85 \times 10^{-3}$	$1.150 \times 10^2$	2.52
(X <sub>i</sub> <sup>3</sup> / B)	x EXP $(-(X_i - \alpha)^2 / 2B^2)$	$5.71 \times 10^{-1}$	$1.409 \times 10^2$	18.83
(X <sub>i</sub> <sup>2</sup> / B)	x EXP $(-(\log X_i - \alpha)^2 / 2B^2)$	$6.73 \times 10^{-3}$	6.033	32.40

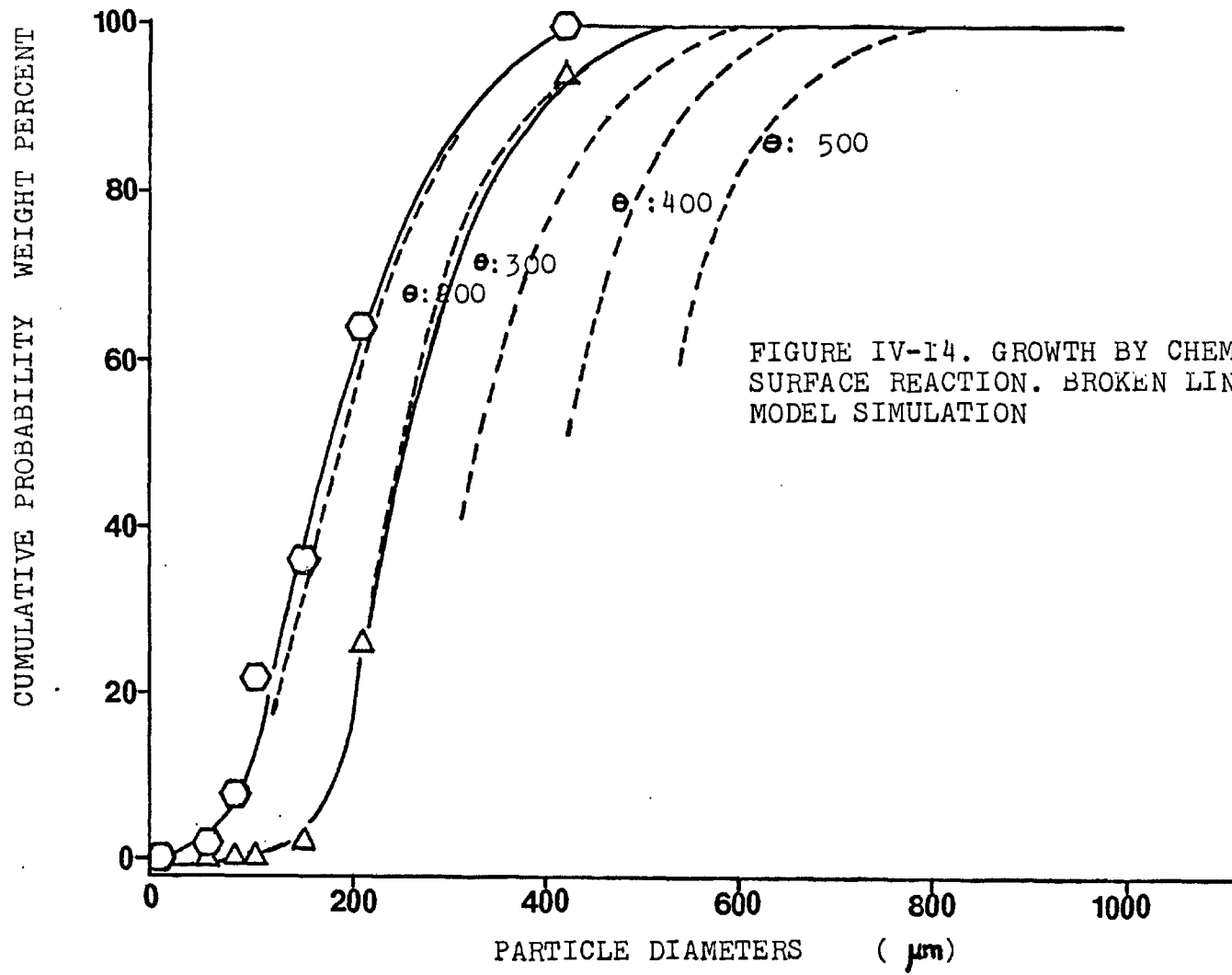
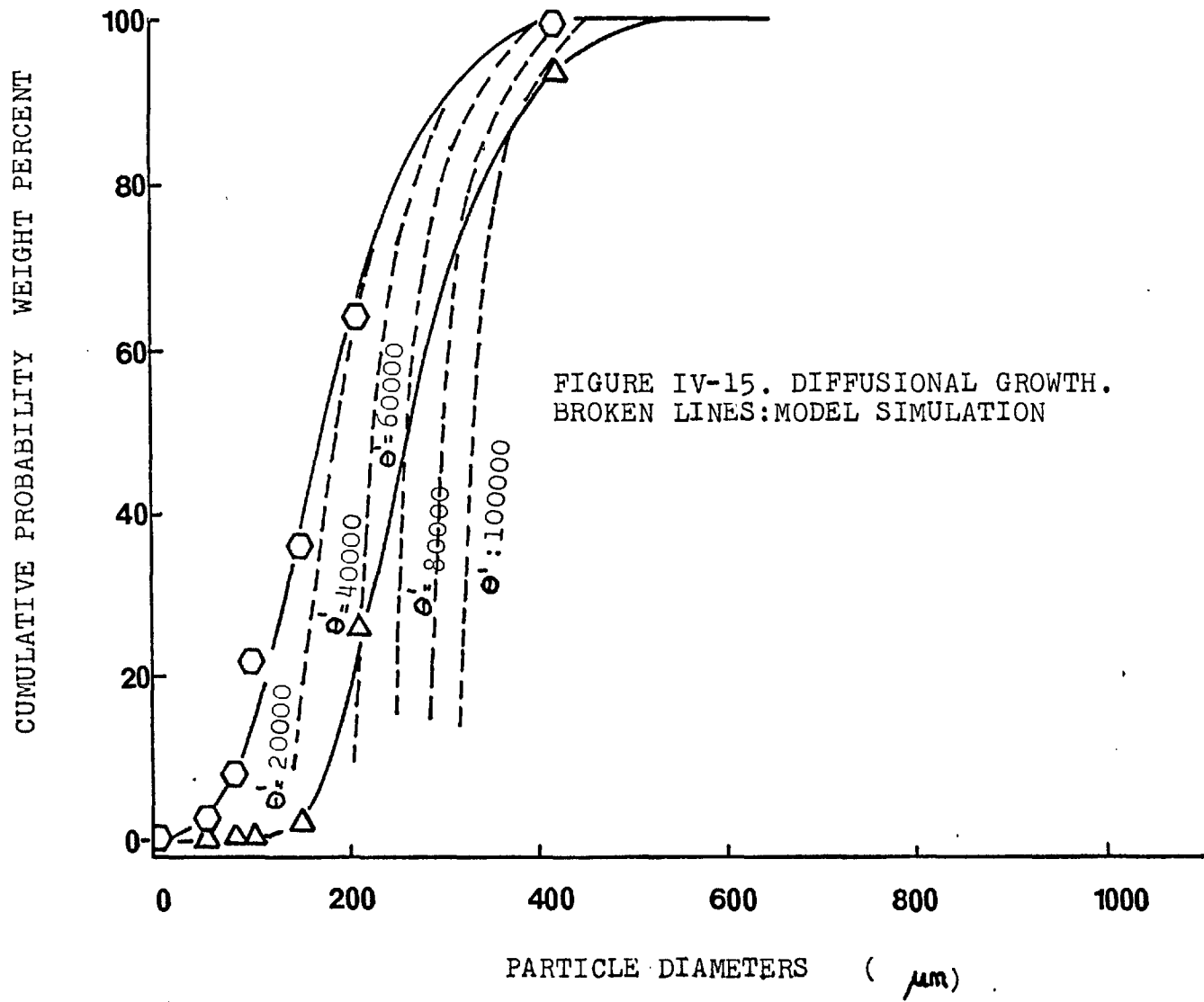


FIGURE IV-14. GROWTH BY CHEMICAL SURFACE REACTION. BROKEN LINES: MODEL SIMULATION



accuracy to the data available. (  $\Theta = 200$  ).

The conclusion from this modelling study is that the surface reaction model represents very closely the growth pattern of the coke particles in the fluid bed hydrogenator under industrial operation conditions, while a condensation type of mechanism does not give good predictions of the growth. The former mechanism is probably in operation during industrial conditions, although further evidence is necessary before the model is finally accepted.

f- The deposition of carbonaceous material by physical condensation

The so called " condensation theory " was revived recently by Lahaye et.al. (1974). The theory postulates the formation of carbon particles as the result of physical condensation of high molecular weight polycyclic aromatic hydrocarbons. One immediate extension of this theory is the idea that in some conditions, heterogeneous condensation could be the rate controlling mechanism of carbon formation from a pyrolyzing gas. Heterogeneous condensation would be thermodynamically favoured with respect to the homogeneous process at low supersaturations, and carbon would be formed by further cross - linking and dehydrogenation of the liquid intermediate condensate.

Experiments were performed in a system where intermediates for carbon deposition were generated in one section of the reactor tube at constant conditions and at high temperature (900 - 950° C ). The products were then passed into a second section of the tube that was held at lower temperature and where a copper sample foil was used to collect the amount of material present. The second section was considered to act as a "condenser" , where the heavy intermediates would be condensed. Results of these experiments were reported in figure III-78.

In a condensation regime, the rate of deposition on a surface

would be given by the expression :

$$W_{CF} = k_G (I - I_s) \quad f-1$$

$$I_s = I_s^0 e^{-\frac{\Delta H_v}{RT}} \quad f-2$$

where  $k_G$  : mass transfer coefficient in the gas phase  
 $I$  : concentration of intermediates  
 $I_s$  : saturation concentration of intermediates  
 $\Delta H_v$  : heat of vaporisation of the intermediates  
 $I_s^0$  : integration constant.

In the kinetic regime, the rate of deposition would be given by an expression such as

$$W_{CF} = e^{-\frac{E(T)}{RT}} f(I) \quad f-3$$

where  $E(T)$  : apparent activation energy,  
 (function of temperature)  
 $f(I)$  : a function of the concentration of the intermediates.

Equations f-1, f-2 and f-3 predict different behaviour with respect to the temperature when the concentration of intermediates is held constant. According to f-1, f-2, the rate of deposition would increase with a decrease in temperature, while from f-3, the behaviour should be the opposite, decreasing rate with temperature.

According to figure III-78, both predictions are correct but each in a different range of temperatures.

The complete behaviour of the system can be explained as follows. In the higher temperature region, intermediates do not reach the dew point but adsorb on the surface and react through an activated chemical mechanism that is favoured by an increase in temperature. At lower temperatures, the

surface reaction decreases and, at about 700° C, the dew point of the heavier aromatics is reached and the condensation deposition starts ; this is favoured by further temperature decreases. The presence of aromatics in the lower temperature range has been verified by dissolving the deposit on the sample foil and analyzing it by gas chromatography. The presence of 3-4 benzopyrene and higher unidentified aromatics has been verified. ( See figure III-79)

As a result, and in agreement with the previous discussion, the condensation mechanism cannot be considered operative under pyrolysis conditions, where the mechanism of carbon deposition most probably involves a chemical reaction on the surface. Condensation deposition, however, may be an important source of carbon formation after the reactor, in coolers or condensers or on any cold surface that may be exposed to the outlet gas.

### c-3 THE FORMATION OF CARBON DEPOSITS ON SURFACES IN THE PRESENCE OF CATALYTIC METALS

#### a- Introduction

The existence of a catalytic path for carbon formation from hydrocarbons on metals was reviewed in the Introduction, from which it is possible to expect catalytic effects to affect the deposition of carbon during pyrolysis and thermal hydrogasification of hydrocarbons in the presence of some metal surfaces.

The experimental part of this work has shown that catalytic effects are present under some conditions, although the main body of the experiments show that they are short - lived and are replaced by a " non - catalytic " deposition after some time has elapsed. In some cases, however, catalytic carbon deposition continued for prolonged periods of time, mainly in the presence of high proportions of hydrogen or in the lower temperature range.

Observation of the composition of the gas in contact with the metallic surface under study shows that catalytic carbon formation starts to be inhibited in the range of temperatures where the conversion of reactants by gas phase homogeneous reactions is significant. This may suggest some sort of interaction between a gas-phase generated compound and the loss of activity of the catalyst, or more possibly that the active surfaces are poisoned by some type of compound produced by the gas-phase reaction. If this is the case, then the experimental observation that significant quantities of polynuclear compounds are produced could suggest that these condense and react on the surface in some way to encapsulate the active metal.

The picture of poisoning by encapsulation may explain why carbon deposition occurs at essentially the same rate in some experiments performed on different metal liner foils. After some time, the catalytic centre will be covered by a layer of carbon, and the deposition will continue on essentially the same surface (carbon), following the mechanism described in 4-A-c.

A realistic model of carbon deposition should be able to describe the phenomena in the catalytic and non - catalytic regimes, as well as in the intermediate region between both mechanism. Such a model would have to take in to account several processes, whose nature has yet to be elucidated. A qualitative description and discussion of a simplified model is presented in the following section ; due to the uncertainties involved, no attempt has been made to build a more quantitative, mathematical model.

b- Description of a qualitative model for carbon formation on catalytic metals

If the experimental rates of carbon formation at various temperatures are used to construct a pseudo Arrhenius plot (e.g

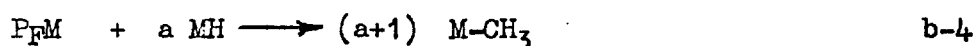
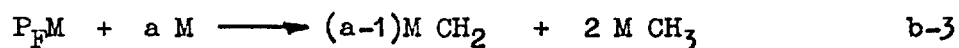


figure III-62) , the dependence is seen to be complex and to show that there appears to be more than one mechanism involved. Considering first the low temperature region, it has been suggested that the rate determining step is the diffusion of carbon through metal (Lobo et.al, 1972). The first steps of the process were thought to involve the adsorption of hydrocarbon specie and hydrogen on the surface :



followed by the breakdown of the hydrocarbon to fragments of one or two atoms of carbon..

The breakdown would probably be enhanced by hydrogenolysis reactions, of the form :

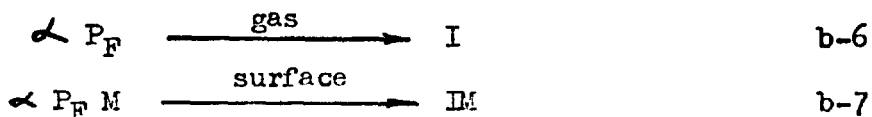


Once the hydrocarbon has been reduced to small fragments, a dehydrogenation reaction could take place and carbon atoms would then be produced on the metal lattice :



These atoms could then dissolve in and diffuse through the metal crystallite to deposit graphitic carbon at the rear of the crystallite. The diffusion of carbon through the metal is assumed to be the rate - limiting step.

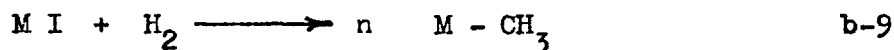
In the intermediate region of temperature, conditions are such as to postulate that the formation of polymers or aromatic hydrocarbons would start to be important in the system. These may be generated either in the gas phase, or on the surface by a catalytic fashion :



An adsorption - desorption equilibrium of the intermediate I would then be established :



If I is either a polymer or an aromatic molecule of high molecular weight, it would be strongly adsorbed on the metal sites and would act as a surface poison. Hydrogen, however, would tend to keep the surface clean, breaking down the polymer or aromatic rings by a series of hydrocracking reactions :



The small fragments would then be dehydrogenated, forming carbon catalytically and regenerating the surface active site. The balance between generation and breakdown of I would thus control the amount of surface that will be poisoned with I. If I remains on the surface, the polymer may be expected to grow and to dehydrogenate and reorganise to produce carbon.

At still higher temperatures, the rate of generation of polymers and aromatic molecules can be expected to increase, and the balance would favour encapsulation of the metal. Under these conditions, the surface would rapidly become covered with polymer and carbon, and the particular activity of a given surface would tend towards the common activity of a carbon surface.

It is convenient to discuss the experimental results in the light of this qualitative model, and this is carried out in the sections below.

#### I - Carbon formation from pure butane

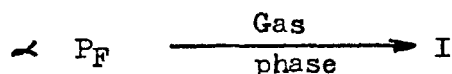
c - Deposition on nickel and iron

Steady state rates of deposition on different materials are shown in figure III-39, and although the rates are markedly different in the early stages of deposition, after some time of reaction the rates tend to be nearly the same for all materials.

At high concentrations of hydrocarbon and with little hydrogen to keep the surfaces clean, the concentration of aromatic intermediates on the surface would be very high and, after some time, all the surface would become covered with a layer of carbon that will poison any catalytic activity of the metal surface. Any further deposition would then occur on carbons of very similar nature, and very little difference would be observed among initially different substrates. Complete encapsulation of active sites with carbon thus explains why nickel, iron and copper exhibit the same final rate of deposition.

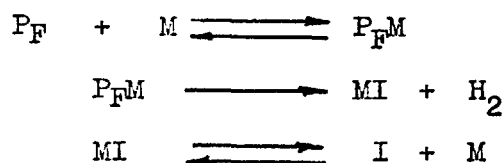
-d The effect of lining the reactor wall with different materials

The fact that the rate of deposition of carbon on an inert copper foil can be affected by the nature of the reactor wall is very significant. Deposition on an inert foil was discussed in a previous section, and the process was suggested to require that a series of heavy intermediates be produced by a homogeneous reaction :



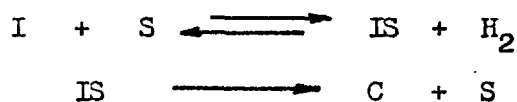
On a catalytic surface (in this case the reactor wall), the concentration of intermediates in the gas phase may be enhanced by two possible routes. Firstly, the metal surface may react to produce carbon forming intermediates directly. These may then desorb to increase the

concentration of gas phase intermediates e.g.



Alternatively, the metal surface may interfere with the free radical reaction in the gas phase in some way, for example, by selectively terminating or initiating different chains. The effect of this interference could be to increase the amounts of carbon forming intermediate, I, subsequently produced in the gas phase.

In both cases, the increase of concentration in the gas will bring an acceleration of the deposition in the inert foil, via the reactions on the inert surface S :



The above arguments explain the experimental observation that iron and nickel walls in the tubular reactor enhance the rate of carbon deposition over copper, as compared with silica or copper walls, provided that at least some parts of the surface should remain unencapsulated by carbon during a long period of time. In a tubular reactor, these conditions can be expected near the inlet, in that intermediates require a period of residence time to reach a significant concentration in the gas phase.

Experiments reported by Turner (1976), show that the enhancing effect of catalytic walls on the rate of carbon deposition on copper in a stirred reactor disappears after some minutes of reaction. This effect can be explained in terms of the deactivation of all the surface by backmixing of heavy aromatic intermediates. As a result, none of the surface remains clean.

e- Transient effects during the early stages of deposition

The steady state deposition of carbon on different metals were discussed in c-3-c, where the encapsulation of the metal active sites was considered to be responsible for the lack of difference in the rates of deposition over metals. During the initial stages of deposition, however, important differences were noted : Figure III-45 shows the transient rates of deposition on different materials. Iron and nickel show an increase of the rate at the beginning of the run, followed at longer times on line by a fall to the steady - state value. The acceleration period may be attributed to the nucleation of the catalytic growth of carbon, when centres of growth are generated on the surface . The deceleration stage can be explained as the gradual deactivation of the centres to cause the rate to fall to the " deposition on carbon " level. The effect is more noticeable for iron than in nickel, under the conditions studied.

The generation of intermediates on the wall follows the same behaviour, as shown in figure III-46. Treatment with hydrogen after carbon deposition did not make the wall behave as a new surface, indicating that most of the centres are irreversibly poisoned by the deposit.

Treatments of the surface, such as deposition - oxidation-reduction with hydrogen, may disrupt the surface and enhance the activity of an iron wall for generation of intermediates, as shown in figure III-47. The effect, as in the other cases, disappeared rapidly with time.

f- Effect of temperature on the deposition of carbon  
over nickel

The effects observed during the present work are similar

to previous reports in the literature for the deposition of carbon over nickel from several hydrocarbons. The three zones of deposition were present, although the temperatures for each region were found to be much higher in the case of butane than in the case of the olefins studied by Lobo (1971) and Figueiredo (1975).

A strong effect of the presence of hydrogen is observed in the experiments with butane, which could be attributed to the contribution of hydrocracking reactions on the surface.

## II- Experiments with butane diluted with hydrogen and helium

### g- The effect of hydrogen on the isothermal deposition over different metals

Since encapsulation is producing such a marked effect on the properties of a metal surface, it was decided to investigate deposition from mixtures of hydrocarbon and hydrogen. Under these circumstances, hydrogen would be expected to gasify carbon and to stop encapsulation. Experiments with helium were carried out to check the importance of dilution effects.

The change of the butane to hydrogen ratio in the reactor feed acted in a complicated form on the rates of deposition of carbon over iron and nickel at 800° C. In both cases, low butane to hydrogen ratios gave a pronounced increase in the rate of deposition, which was found to be proportional to the hydrogen concentration to the first or higher power. Under these conditions, it seems that the cleaning of the surfaces with hydrogen (thus favouring the catalytic growth of carbon) is the rate - determining step.

The cleaning effect of hydrogen of the metal active sites is not very well understood at the present. It has been suggested

(Figueiredo , 1975) that hydrogen could burn some surface carbon leaving the surface clean. This hypothesis has been discarded by thermodynamic reasons, in that the equilibrium is reached with very small amounts of methane in the gas. The hypothesis that hydrocracking reactions provoke the rupture of polymers allowing migration of the smaller fragments into the metal, is worthy to be subjected to further tests.

At higher concentrations of butane, intermediates for non-catalytic carbon formation could induce surface growth if the catalytic formation is being suppressed by encapsulation of the metal. A whole range of intermediate stages , combining features of both mechanisms, may be expected.

It is difficult, however, to explain why the results for iron and nickel show a minor maximum in the rate at about 50 % butane in hydrogen. Changes in composition of the gas phase products, and their interaction with surface processes, may account for this effect, but no simple explanation can be proposed at this stage.

Experiments performed with mixtures of butane, helium and hydrogen at constant initial concentration of the hydrocarbon have shown that the acceleration effect of the presence of hydrogen is not due to a dilution of the hydrocarbon but to an effect coming from the chemical action of hydrogen.

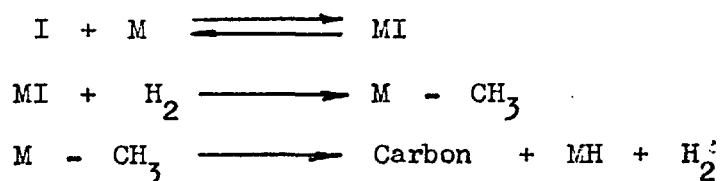
The rate of deposition on nickel and iron foils were found, as expected, to depend on the previous history of the foil. Treatment with hydrogen after deposition produced higher initial rates when the deposition was re - started. Foils that were first subjected to deposition at high hydrocarbon concentrations gave lower rates in the following runs as compared to those which were only treated at the lower butane concentrations, indicating that parts of the surface

were poisoned irreversibly.

#### h- Transient phenomena in the presence of hydrogen

The transient of deposition over nickel at different butane concentrations in hydrogen is shown in the figure III - 75. Higher butane concentrations promote faster initial rates of deposition, and the steady rate is low due to poisoning with polymers or aromatics. Lower butane concentrations mean higher hydrogen concentration, a cleaner surface and hence a higher steady state rate. The time taken to reach the faster rate is longer, as a result of the fact that heterogeneous nucleation stage that starts the reaction on the surface depends on the hydrocarbon concentration.

When iron was used as liner in the reactor (figure III-76), it was found that the rate took quite a long time to reach the same level as the equivalent experiments with copper liners. No noticeable enhancement of the rate of deposition was found by the use of the iron wall, as opposed to the results with pure butane in which an important acceleration was obtained. The possible explanation is that, in the presence of hydrogen, the iron wall was able to produce catalytic carbon from the intermediates and keep clean by the reactions :



As a result, light hydrocarbons and heavy intermediates would be depleted from the gas phase, which would, in turn, decrease the rate of deposition on the inert foil. The surface production of intermediates would also be greatly reduced through their destruction



by hydrocracking or catalytic carbon formation on the surface.

5- The inter relation amongst gas major products, aromatic compounds and carbon formation

The forms in which aromatic hydrocarbons are synthesized during the thermal reaction of paraffins and olefins were discussed in detail in section IV-B of this chapter. Paraffins would suffer cracking rendering light olefins, which in turn would form butadiene and hexadiene. These would react further to give cyclohexenes, cyclohexadienes and aromatics.

The detailed mechanism of the synthesis is not known, although it is probable that it is carried on through free - radicals reactions.

The formation of polycyclic aromatics from simple aromatic molecules can be produced through several mechanisms that were discussed above (Chapter IV, section 3-B). Side chains cyclisation and aromatisation could be responsible for the formation of large polycyclic aromatic structures.

With respect to the link between major gas and aromatic products and carbon formation, the correlation is not very simple.

The formation of carbon on catalytic metals from pure paraffins and olefins under conditions of nonhomogeneous reaction has been verified previously. (Lobo, 1972, Figueiredo, 1975 and Derbyshire, 1976). One could say that, in the presence of the appropriate metal (Ni, Fe, Co), carbon will be formed from almost every possible hydrocarbon.

In the absence of catalytic metals, however, the situation is different. Carbon is deposited in conditions where the homogeneous reaction has reached a high conversion and hence is undoubtedly associated with one or more intermediates formed in the gas phase. The

nature of these intermediates has been subjected to controversial discussion in the bibliography ( see Chapter I, section 6 ) and every hypothesis has been found difficult to prove. In the present research, attempts to plot the rates of carbon deposition as a function of any of the components in contact with the deposition surface failed to show an accurate correlation, and hence failed to prove that any of the observed compounds was the definitive intermediate for carbon formation. ( A similar reluctance of the rates of carbon deposition to correlate with gas composition was observed by Liebermann et.al. , 1974 ). This behaviour indicated that either more than one compound acts as intermediate or that, for some reason, the real intermediate was not detected with the analytical techniques used during this research.

One of the samples of tar collected during series II experiments was analysed for heavy polycyclic aromatics by British Gas (London Research Station). The technique used was mass spectrometry, with a Varian 311 A mass spectrometer. The electron impact spectrum shown in figure IV-16 was taken at 500° C. The sample was found to be a complex mixture of polycyclic aromatic hydrocarbons, ranging from one to eleven rings, and containing alkyl side chains with up to six carbon atoms. Table IV-8 lists some of the possibilities for many of the  $m/e$  values.

The mass spectrum shows clearly that the chromatographic technique used during this research was not able to detect all the compounds of molecular weight higher than about 250. A complete and continuous series of polycyclic aromatics are present covering the range of up to eleven aromatic rings. These higher molecular weight compounds are insoluble in most of the organic solvents, have very high melting points, and hence could be considered as carbon for all practical purposes.

These observations leave little doubt that aromatics, through

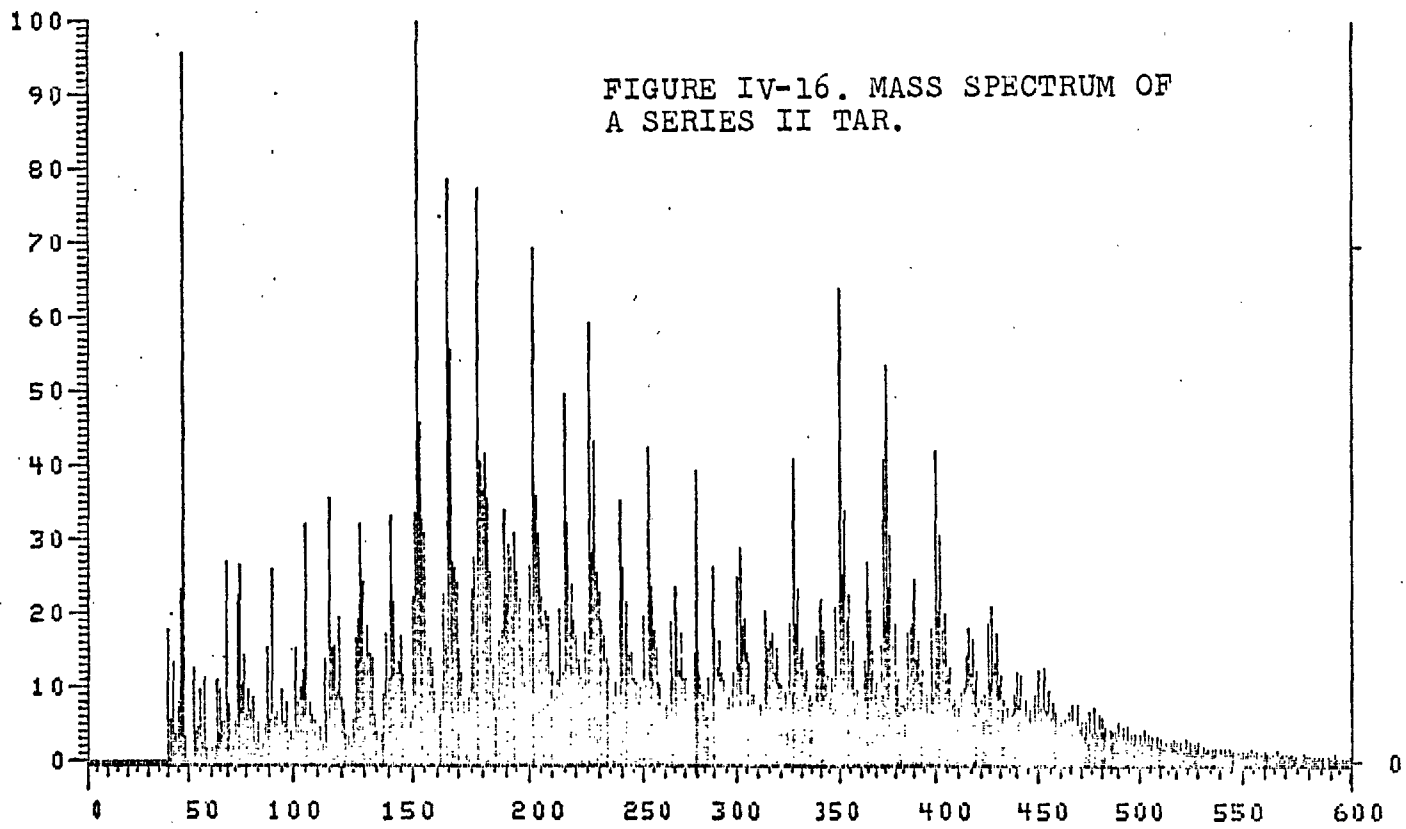


FIGURE IV-16. MASS SPECTRUM OF  
A SERIES II TAR.

SPEC# 5100 LM NDP/MS/4 AT 500C

STEP MASS=1, I/B/S = 1%

m/e	Possible compound	No. of rings	m/e	Possible compound	No. of rings
128	Naphthalene	2	302	Dibenzopyrene	6
142	Methylnaphthalene	2	326	Benzanthanthrene	7
152	Diphenylene	2	328	Dibenzochrysene	6
154	Diphenyl	2	340	Dibenzonaphthanthrene	7
166	Fluorene	2	350	Benzocoronene	8
168	Methyldiphenyl	2	352	Tribenzpyrene	7
178	Phenanthrene, Anthracene	3	354	Dihydrodibenzopentacene	7
180	Methylfluorene	2	364	Methylbenzocoronene	8
182	C <sub>2</sub> -Diphenyl	2	366	Methyltribenzpyrene	7
192	Methylphenanthrene	3	374	Dibenzoperopyrene	9
194	C <sub>2</sub> -Fluorene	2	376	Dibenzanthranthrene	8
202	Pyrene	4	378	Tribenzochrysene	7
204	Dihydropyrene	4	390	Methyldibenzanthranthrene	8
216	Methylpyrene	4	400	Dibenzocoronene	9
218	Methyldihydropyrene	4	402	Tetrabenzopyrene	8
226	Benzofluoranthene	4/5	404	C <sub>2</sub> -Dibenzanthanthrene	8
228	Chrysene	4	426	Tribenzanthranthrene	9
230	p-Terphenyl	3	428	Octacene	8
240	Naphthanthrene	5	440	Methyltribenzanthranthrene	9
252	Benzopyrene	5	442	Methylocacene	8
254	Methylnaphthanthrene	5	450	Tribenzocoronene	10
266	Naphthoperinaphthene	5	452	Pentabenzopyrene	9
276	Anthanthrene	6	478	Nonacene	9
278	Benzochrysene	5	528	Hexabenzotriphenylene	10
290	Benzonaphthanthrene	6	578	Undecacene	11
300	Coronene	7			

TABLE IV- 8

reactions of ring condensation, are the intermediates in the formation of non - catalytic carbon under the conditions of this study. The whole chain of intermediates, while they grow into graphite - like structures, can be traced through the spectrum in figure IV . 16

To summarise the above discussion, while the deposition of carbon on catalytic metals do not require the formation of intermediates in the gas phase, non - catalytic carbon deposition requires the presence of polycyclic aromatic structures that grow towards carbon by condensation reactions. These molecules, in turn, will adsorb or react with other species in the reaction surfaces to provoke the growth of carbon on the walls.

## 6- CONCLUSIONS

- 1- A successful free - radical modelling and parameter estimation procedure was carried on for the high conversion pyrolysis of ethane in the presence of hydrogen, based on experimental information obtained from a jet stirred reactor.

The procedure could be extended to the modelling of other hydrocarbons, although errors in the estimation of kinetic parameters through regression and the complexity and excessive computer time consumption of the mathematical procedures involved, would suggest that for practical or industrial purposes, a simplified or semiempirical model could be used.

- 2- Hydrogen was found to accelerate the rate of butane breakdown in the experiments. This phenomena was reported previously in the literature. In this work, a series of free-radical reactions are proposed to explain the effect of hydrogen in the thermal decomposition of butane at low conversions, and the resulting kinetic equations were solved using the steady - state approximation for

the free-radical concentrations. The final equations show a linear relationship with hydrogen concentration, which is in agreement with literature experimental results.

- 3- Thermal hydrogasification reactions under industrial conditions were modelled with the use of a slightly modified version of a semiempirical pyrolysis model reported in the literature. The predictions of composition agree with literature experimental results, the procedure of calculation is simple and requires little computational effort.
- 4- The presence of catalytic metals (nickel and iron) in the reactor, such as foils and wall liners, was found to have little effect on the composition of the major gas products. A study of the transient effects, however, showed that there is an influence in the beginning of the reaction, but the effect disappears rapidly. The deactivation of the metal active centres during the transient was attributed to the encapsulation of these with aromatic polymers or carbon.
- 5- Changes of the surface to volume ratio inside the reactor were found to affect the composition of the major gas products, as if the reaction was being inhibited. The effect was attributed to heterogeneous terminations being enhanced with increasing surface to volume ratios.
- 6- Minor amounts of aromatic tars were produced during the thermal reaction of butane. Analysis of the tar by gas chromatography revealed the presence of benzene, alkyl benzenes, naphthalene and other polycyclic aromatics ranging at least up to 3-4 benzopyrene. The presence of carcinogenic compounds as products of pyrolysis, indicates that proper precautions should be taken in manipulating

reaction products.

- 7- The concentration of aromatic tars was found to increase with residence time at short times and to go through a maximum and decay at longer residence times ( $\tau \approx 10$  sec.). Hydrogen was found to increase the production of total aromatics at low concentration, but effectively decreased it at higher hydrogen proportions. Increasing the concentration of butane in hydrogen increased the production of aromatics by a non-linear relationship. Within the range of conditions studied, increases in temperature produced increases in the rate of aromatics production. Hydrogen was found to decrease the rate of formation of tars at temperatures below  $800^{\circ}$  C.
- 8- The presence of catalytically active metal liners in the reaction affected the production of aromatic tars at the beginning of the reaction. The effect was found to disappear at longer times on-line, a fact that was attributed to the encapsulation of the active centres of the catalytic metal.
- 9- The increase in the surface to volume ratio in the reactor was found to decrease the production of total aromatics. The effect was attributed to increased heterogeneous termination of free-radical chains and to the trapping of polycyclic aromatics by the surfaces to produce carbon.
- 10- The mechanism of aromatics synthesis during pyrolysis was discussed. There is experimental evidence to support the hypothesis that olefins are intermediates in the synthesis, and that they could react to form dienes, cyclohexenes and cyclohexadienes. These may further dehydrogenate to produce benzene and alkyl-benzenes. At

the temperatures of interest, the mechanism probably involves free - radical reactions. Some possible free -radical mechanism of aromatization are proposed.

- 11- The mechanism of formation of polycyclic aromatics was discussed. The presence of side alkyl chains in the aromatics produced, could indicate that these are intermediates between simple aromatics and heavier, complex polycyclic structures.
- 12- The use of a tubular microbalance reactor was found very convenient to obtain information on the rates of carbon deposition over sample surfaces suspended in the atmosphere of the reactor. The behaviour of catalytic metal surfaces was found to be, under some operation conditions, very different from non - catalytic surfaces.
- 13- Carbon deposition over non - catalytic surfaces (copper) was found to increase with increases of residence time. The effect of increasing temperature was to increase continuously the rate of deposition, giving only one zone in a pseudo - zero order Arrhenius plot. Increasing the concentration of hydrogen decreased the rate of carbon deposition.
- 14- The deposition of carbon over catalytic metals (nickel, iron ) presented differences relative to non - catalytic surfaces in the presence of hydrogen . Temperature was found to have a complex effect on the rate of deposition, which gave three zones in the zero order Arrhenius plot. Hydrogen was found to accelerate the rate of deposition.



- 15- When pyrolyzing pure butane in a reactor lined with a catalytic foil, the rate of carbon deposition over a non - catalytic sample was found to increase noticeably. During the thermal reaction of butane - hydrogen mixtures, the presence of catalytic liners was found to have an effect on the transient rate of deposition over non catalytic surfaces.
- 16- Some experiments were performed in which the tubular reactor was heated with two furnaces to simulate a reactor followed by a cooler section (condenser) . The temperature in the " reactor" was kept constant and the temperature in the "condenser" was used as a variable. An Arrhenius plot of the results showed two regions. At higher temperatures, a zone was found that presented a positive apparent activation energy. At lower temperatures the other zone gave a negative activation energy. The positive activation energy region was attributed to the chemical reaction of intermediates produced in the "reactor" with the surface to form carbon. The negative activation energy region was attributed to a mechanism of condensation of the intermediates on the surface to form " condensation " carbon. The experiment showed that the "condensation" region happens at a lower temperature than reaction; hence, under reaction conditions, the deposition of carbon occurs by chemical reaction between the intermediates and the surface. Carbon could be formed by condensation, however, when cold surfaces are exposed to the flow.
- 17- A simplified explanation of the mechanism of carbon deposition over non - catalytic surfaces is presented. Initial hydrocarbons would react in the gas phase, through a series of intermediates, to form carbon precursors (probably polycyclic

aromatics). These precursors would adsorb on the surfaces and suffer further reactions towards carbon on the surface. Hydrogen may inhibit both the homogeneous and the heterogeneous process. A simple mathematical model, based upon the proposed mechanism, was found to explain most of the experimental data.

- 18- Experimental data from the literature on the growth of coke particles by carbon deposition during oil hydrogenation in an industrial plant, was used to discriminate between surface chemical growth and diffusional - condensation growth models. The mathematical simulation of the growth of the size - distribution function shows that the surface chemical reaction growth predicts accurately the final size distribution function.
- 19- The surface to volume ratio in the reactor was found to affect significantly the rate of carbon deposition over non - catalytic surfaces. A model is presented to explain the effect and is solved mathematically. At high surface to volume ratios, the rate of deposition of carbon per unit area is inversely proportional to the surface to volume ratio. This theoretical conclusion is confirmed by experiment.
- 20- A qualitative explanation of the deposition of carbon on catalytic surfaces is proposed. At the low temperature zone of catalytic carbon formation, the initial hydrocarbon is adsorbed in the metal surface. There it is cracked into small fragments, probably by the participation of hydrogenolysis reactions. Once the hydrocarbon is reduced to small fragments, these can be dehydrogenated and the carbon atom formed can diffuse through the metal to deposit graphite at a

growth centre.

In the intermediate region of temperature, the homogeneous reaction can produce polycyclic aromatics. These would tend to adsorb on the active centres and poison the surface, decreasing the rate of catalytic carbon formation.

At the higher temperature region, the metal active centres become encapsulated with polycyclic aromatics, and the non - catalytic carbon deposition mechanism starts to operate.

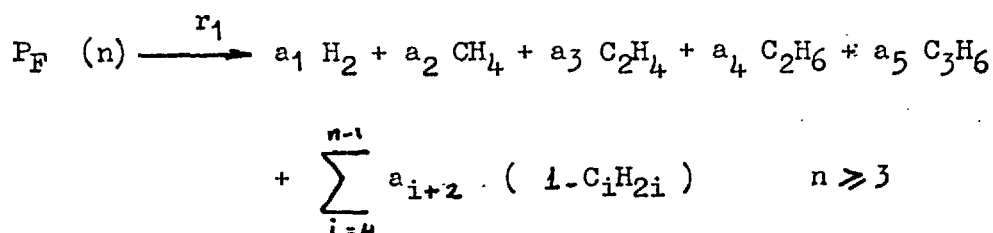
Further experimental evidence is required to verify this proposed mechanism.

- 21- A study of the polycyclic aromatics obtained in the experiments by mass spectrometry revealed the presence of a continuous spectrum of aromatics ranging up to ten or eleven rings in the molecules. This finding supports the hypothesis that polycyclic aromatics are intermediates in the route towards non - catalytic carbon formation.

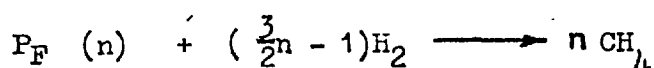
#### APPENDIX I

##### Model for pyrolysis and hydrogenolysis of hydrocarbons

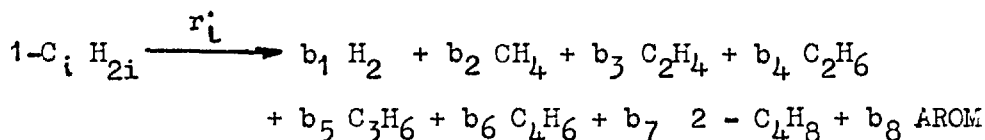
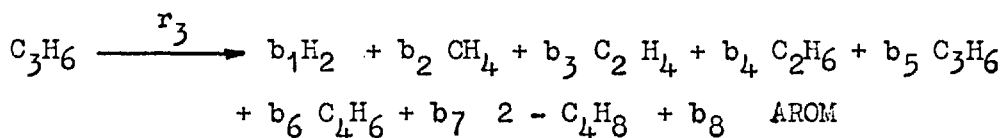
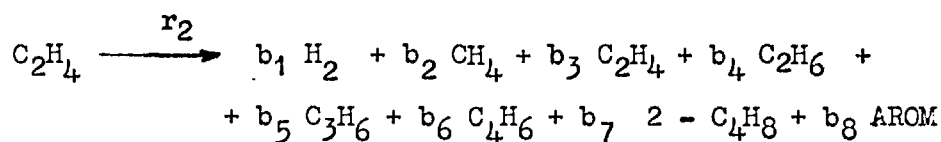
- a) Primary reaction (Murata, et.al.,1975)



- b) Hydrogenation (olysis) reaction (Thompson, et.al.,1973)

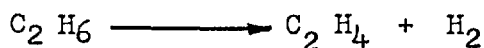


c) Decomposition of olefin (Murata, et.al. 1975)

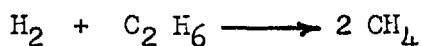


$$+ \sum_{j=4}^{n-2} b_{j+5} (1 - \text{C}_j \text{H}_{2j})$$

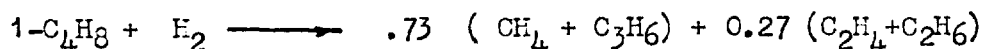
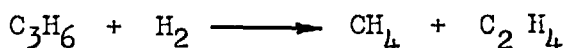
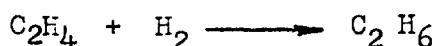
d) Decomposition of ethane (Murata, et.al. 1975)



e) Hydrogenolysis of ethane (Thompson et.al. 1973)



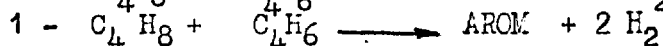
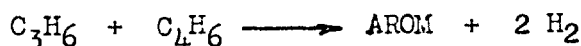
f) Hydrogenation of olefins (Murata, et.al. 1975)



g) Hydrogenation of butadiene (Murata, et.al. 1975)



h) Diels - Adler aromatization (Murata, et.al. 1975)



2- Kinetics and constantsa- Primary reaction

(Murata et.al. , 1975)

$$-r_1 = k_1 (n) [P_F (n)]$$

$$k_1(n) = k_1 (no) / (1 + \alpha x) \quad x = \text{conversion.}$$

$$k_1(no) = 5.99 \times 10^3 n^{2.68} \exp \left\{ - \frac{60000}{R} \left( \frac{1}{T} - \frac{1}{973} \right) \right\}$$

<u>n- Paraffin</u>	<u><math>\alpha</math></u>
Propane	5.3
n-Butane	8.7
n-Hexane	4.9
n-Heptane	3.3
n-Octane	8.3

b- Hydrogenolysis reaction

(Thompson et.al. , 1973)

$$r_H = k_H [H_2] [P_F (n)]$$

We assume that these affect the rate of breakdown but that the initial product composition does not change.

Assume

$$r_1 = k_1(n) \{ 1 + b [H_2] \} [P_F(n)]$$

Known values of b are calculated from

(Thompson et.al.,1973)

<u>Paraffin</u>	<u>b (lt / mole)</u>
Ethane	0
Isobutane	1.799
Neopentane	4.498
n-butane	5.398

## Cyclopentane

7.198

( Murata , et.al. , 1975)

c- Decomposition of olefins

$$r_2 = k_2 [C_2H_4]^{3/2}$$

$$k_2 = 1.70 \times 10^{10} e^{\frac{-49600}{RT}}$$

$$r_3 = k_3 [C_3H_6]^{3/2}$$

$$k_3 = 3.63 \times 10^{13} e^{\frac{-63200}{RT}} f_1$$

(  $f_1$  : inhibition parameter )

$$r_n = k_{ol}(n) [1 - C_nH_{2n}] \quad n \geq 4$$

$$k_{ol}(n) = 4.08 \times 10^{-3} n^{3.77} \exp \left\{ -\frac{55000}{R} \left( \frac{1}{T} - \frac{1}{973} \right) \right\}$$

Selectivity coefficients for olefin pyrolysis

( From Murata et.al. , 1975)

	$C_2H_4$	$C_3H_6$	$C_4H_8$	$1-C_5H_{10}$	$C_6H_{12}$	$C_7H_{14}$
b <sub>1</sub>	0.084	0.10	-	-	0.04	0.09
b <sub>2</sub>	-	0.30	0.46	0.15	0.23	0.11
b <sub>3</sub>	-	0.50	0.21	0.81	0.64	0.90
b <sub>4</sub>	0.17	0.01	0.05	0.13	0.03	0.08
b <sub>5</sub>	0.11	-	0.46	0.41	0.54	0.41
b <sub>6</sub>	0.22	0.12	0.30	0.26	0.24	0.16
b <sub>7</sub>	-	-	0.10	-	0.02	0.02
b <sub>8</sub>	0.034	0.14	-	0.05	0.14	0.18
b <sub>9</sub>	-	0.10	-	0.14	0.17	0.29
b <sub>10</sub>	-	-	-	-	0.07	0.14
b <sub>11</sub>	-	-	-	-	-	0.01

## PRIMARY PRODUCTS IN HYDROCARBON PYROLYSIS

Values of  $a_i$  (Murata, et.al  
1975)

PRODUCTS	PROPANE	n - butane	n- PENTANE	n - HEXANE	n- HEPTANE	n- OCTANE	n-NONANE	n- DECANE
H <sub>2</sub>	.48	.30		0.33	0.43	0.41		0.31
CH <sub>4</sub>	.45	.65		0.56	0.47	0.44		0.53
C <sub>2</sub> H <sub>4</sub>	.45	.65		0.95	1.25	1.24		1.23
C <sub>2</sub> H <sub>6</sub>	-	.07		0.08	0.17	0.14		0.19
C <sub>3</sub> H <sub>6</sub>	.52	.65		0.51	0.44	0.43		0.45
C <sub>3</sub> H <sub>8</sub>	-	-		-	-	-		-
1 - C <sub>4</sub> H <sub>8</sub>	-	.02		0.27	0.27	0.21		0.20
1 - C <sub>5</sub> H <sub>10</sub>	-	-		0.08	0.15	0.17		0.19
1 - C <sub>6</sub> H <sub>12</sub>	-	-		-	0.07	0.16		0.19
1 - C <sub>7</sub> H <sub>14</sub>	-	-		-	-	0.09		0.15
1 - C <sub>8</sub> H <sub>16</sub>	-	-		-	-	-		0.12
1 - C <sub>9</sub> H <sub>18</sub>	-	-		-	-	-		0.04
TOTAL EXPANS.	1.9	2.34		2.78	3.26	3.31		3.61

Ethane decomposition

(Murata et.al. , 1975)

$$r_1' = k_1' [C_2H_6] \quad k_1' = 4.40 \times 10^{15} e^{\frac{-75900}{RT}}$$

Hydrogenolysis of ethane

(Thompson et.al. , 1975)

$$r = k [C_2H_6]$$

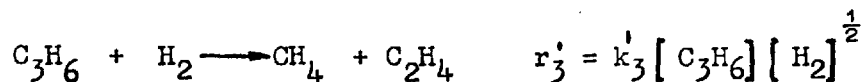
$$k = 10^{17.5} \exp(-90000 / RT)$$

f- Hydrogenation of olefins

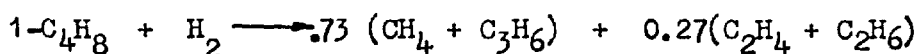
(Murata , et.al., 1975 )



$$k_2' = 2.5 \times 10^7 \times \exp(-32300 / RT)$$



$$k_3' = 1.19 \times 10^{12} \exp(-57200 / RT) f_2$$



$$r_4' = k_4' [1-C_4H_8] [H_2]^{\frac{1}{2}}$$

$$k_4' = 2.67 \times 10^{15} \exp(-62400 / RT)$$

g- Hydrogenation of butadiene

$$r = k [C_4H_6] [H_2]^{\frac{1}{2}}$$

$$k = 2.67 \times 10^{15} \exp(-62400 / RT)$$

(Assumed equal to  $k_4$ )



h- Diels - Adler aromatization

(Assumed as polymer

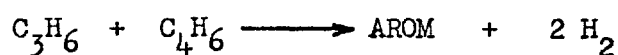
formation in Murata et.al.,

1975)



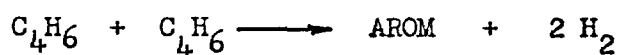
$$r'_5 = k'_5 [\text{C}_4\text{H}_6][\text{C}_2\text{H}_4]$$

$$k'_5 = 9.58 \times 10^7 \exp(-28800 / RT)$$



$$r'_6 = k'_6 [\text{C}_3\text{H}_6][\text{C}_4\text{H}_6]$$

$$k'_6 = 5.02 \times 10^7 \exp(-29700 / RT)$$



$$r'_7 = k'_7 [\text{C}_4\text{H}_6]^2$$

$$k'_7 = 2.57 \times 10^7 \exp(-24800 / RT)$$



$$r'_8 = k'_8 [1 - \text{C}_4\text{H}_8][\text{C}_4\text{H}_6]$$

$$k'_8 = 9.36 \times 10^{12} \exp(-52700 / RT)$$

NOTATIONCHAPTER I

- $C_1, C_2$  Constants.
- [ ] Indicate concentration of the species considered.
- S/V Surface to volume ratio. (  $\text{cm}^{-1}$  )

CHAPTER II

- $\tau$  Residence time, defined as the volume of the reactor divided by the gas volumetric flow at inlet conditions ( sec )

CHAPTER IVSection 2.a

- $a_{ij}$  Kinetic coefficient of the  $j^{\text{th}}$  species reacting in a first order reaction to produce the  $i^{\text{th}}$  species ( sec )
- $b_{ijk}$  Kinetic coefficient of the  $k^{\text{th}}$  and  $j^{\text{th}}$  species reacting in a second order reaction to give the  $i^{\text{th}}$  species. (  $\text{cm}^3 \text{sec}^{-1} \text{g-mole}^{-1}$  )
- $h_{ik}, r_{ij}$  First order kinetic coefficient. ( Similar meaning as  $a_{ij}$  ). (  $\text{sec}^{-1}$  )
- $d_{ij}, e_{ik}$
- $q_0$  Volumetric flow at the conditions at the reactor inlet. (  $\text{cm}^3 \text{sec}^{-1}$  )
- $s_{ijk}, t_{ijl}$  Second order kinetic coefficients. ( Similar meaning as  $b_{ijk}$  ). (  $\text{cm}^3 \text{sec}^{-1} \text{g-mole}^{-1}$  )
- $f_{ikj}, g_{ilk}$

$k_{oi}$	Pre-exponential factor in the Arrhenius expression for a kinetic constant, ( $\text{sec}^{-1}$ ) or ( $\text{cm}^3 \text{sec}^{-1} \text{g-mole}^{-1}$ )
$k_i$	Kinetic constant. ( $\text{sec}^{-1}$ ) or ( $\text{cm}^3 \text{sec}^{-1} \text{g-mole}^{-1}$ )
$A_i$	Concentration of the $i$ th molecular species ( $\text{g-mole cm}^{-3}$ ).
$B$	Logarithm of the Arrhenius pre-exponential factor.
$B_i$	Concentration of the $i$ th free-radical species. ( $\text{g-mole cm}^{-3}$ )
$E_i$	Activation energy. ( $\text{Kcal g-mole}^{-1}$ )
$C_i$	Concentration of the $i$ th species. ( Either free-radical or molecule ). ( $\text{g-mole cm}^{-3}$ ).
$R$	Gas law constant. ( $\text{Kcal g-mole}^{-1} \text{ } ^\circ\text{K}^{-1}$ )
$R_i$	Rate of appearance of the $i$ th component. ( $\text{g-mole cm}^{-3} \text{sec}^{-1}$ )
$R_{Ai}$	Rate of appearance of the $i$ th molecular species. ( $\text{g-mole cm}^{-3} \text{sec}^{-1}$ ).
$R_{Bi}$	Rate of appearance of the $i$ th free-radical species. ( $\text{g-mole cm}^{-3} \text{sec}^{-1}$ )
$S_{RB}$	Relative sensitivity of $k$ with respect to $B$ .
$S_{RE}$	Relative sensitivity of $k$ with respect to the activation energy.
$T$	Temperature. ( $^\circ\text{K}$ )
$V_r$	Reactor volume. ( $\text{cm}^3$ )

- $\underline{A}$  Vector of concentration of molecular species.
- $\underline{B}$  Vector of concentration of free-radicals.
- $\underline{D}(\underline{B})$  Vector function of the concentration of free-radicals.
- $\underline{E}(\underline{A})$  Vector function of the concentration of the molecular species.
- $\underline{R}_A$  Vector of reaction rates of molecular species.
- $\underline{R}_B$  Vector of reaction rates of free-radical species.
- $\underline{S}_c(\underline{B})$  Vector whose elements are nonlinear functions of the concentration of free-radical species.
- $\delta$  Increment operator.
- $\kappa$  Relative expansion of a reactant gas mixture.
- $\rho$  Density of the homogeneous mixture. (  $\text{gr cm}^{-3}$  )
- $\tau$  Inlet residence time of the reactor. ( sec )
- $\underline{\Psi}(\underline{A})$  Matrix function of the concentration of molecular species.
- $\underline{\phi}(\underline{B})$  Matrix function of the concentration of free-radicals.
- $\underline{\epsilon}$  Vector of elements of small magnitude.
- $\circ$  Initial conditions in the variable considered
- Vector or matrix quantity.
- $n$  Value at the  $n$ th iteration.

Section 2.c

- b kinetic parameter that describes the acceleration produced by hydrogen on the rate of decomposition of hydrocarbons. (  $\text{lt g-mole}^{-1}$  ).
- $P_F$  (n) Paraffinic hydrocarbon of n carbon atoms.

Section 4-A.c

- $A_1, A_2$   
 $A_3, A_4,$   
 etc. General groups of constants.
- I Intermediate in the route towards carbon.
- IS Intermediate adsorbed on a surface site.
- S Surface site for adsorption of intermediates. Assumed to be part of the carbon wall.
- $W_{CF}$  Rate of surface carbon deposition. (  $\mu\text{g cm}^{-2} \text{min}^{-1}$  )
- $\alpha$  Stoichiometric coefficient for the production of intermediates from paraffins.

Section 4-A.e

- $f(C_G),$   
 $f'(C_G)$  Functions that depend on the concentration of intermediates in the gas.

$\theta, \theta'$  Parameters formed by a group of constants multiplied by time.

$k_K$  kinetic constant of reaction between molecules of intermediate and the surface of the particle.

Section 4-B.b

M Metal catalytic surface site.

S Non-metal surface site. ( Assumed generally to be the carbon surface )

REFERENCES

- Badger, G.M. (1965)  
"Pyrolysis of hydrocarbons", p.1. in "Progress in Physical Organic Chemistry ", Vol. 3 (Interscience) New York
- Benson, S.W. (1968)  
"Thermochemical Kinetics"  
John Wiley and Sons, London.
- Blackemore J.E. and Corcoran W.H. (1969)  
Ind. Eng. Chem. Proc. Res. & Dev. 8, 206
- Blackemore, J.E., J.R. Barker and W.H. Corcoran (1973)  
Ind. Eng. Chem. Fundam., Vol 12, N<sup>o</sup> 2, 147.
- Böckros, J.C. (1969)  
in "Chemistry and Physics of Carbon", Vol. 5, p.1  
( P.L. Walker Jr. Ed.) Dekker, New York.
- Brooks, C.T. (1966)  
J. Inst. Gas Eng. 7, 492.
- Brooks, C.T. (1967)  
IEC Prod. Res. Dev., 6, 236.
- Brooks, C.T. Cunnings, C.P.R. and S.J. Peacock (1971)  
Trans. Farad. Soc., 67, 3265.

- Bush, S.F. (1966)  
Trans. Inst. Chem. Eng. 47, T59.
- Denis, G.H. and T.E. Daubert (1974)  
AIChE Journal, 20, 720
- Dent, F.J., R.F. Edge, D. Hebden, F.C. Wood, T.A. Yarwood (1957)  
Trans. Inst. Gas Eng., Vol. 106, 194 (1956-1957)
- Derbyshire, F.J. (1974)  
Ph.D. Thesis, London University
- Figueiredo, J.L.C.D.C., (1974)  
Ph.D. Thesis, London University.
- Fitzer, E., K. Mueller and W. Schaefel, (1971)  
"The Chemistry of the Pyrolytic conversion of Organic  
Compounds to Carbon", in "Chemistry and Physics of Carbon"  
(Marcel Dekker Inc. N.Y.)
- Graham, S.C., J.B. Homer and J.L.J. Rosenfeld (1975)  
2nd. European Combustion Symposium, Orlean, France, p.374.
- Hardley, D.J. and L. Turner (1973)  
"The production of petroleum chemical intermediates", in  
"Modern petroleum technology", 4th. Edition, G.D. Hobson (editor),  
Applied Science Publishers Ltd., Barking (Essex, England), p440



- Hebden, D. and G. Percival (1972)  
I.G.E. Journal, 12, 229
- Herriot, G.E., R.E. Eckert and L.F. Albright (1972)  
AIChE Journal, 18, 84
- Himmelblau, D.M. (1970)  
"Process design by statistical methods",  
New York, John Wiley)
- Kaiser, R. (1963)  
"Gas Phase Chromatography", translated by P.H. Scott, Butterworths.
- Khan, M.S. and B.L. Crynes (1970)  
Industrial and Engineering Chemistry, 62, (10), 54 (1970)
- Knight, W.N.N. and M.L. Pensitton-Bird (1973)  
"Cracking and Reforming", in "Modern Petroleum Technology",  
4th. Edition, G.D. Hobson (editor), Applied Science Publishers Ltd.  
Barking ( Essex, England), p.278.
- Kunugi, T., T. Sakai, K. Soma and Y. Sasaki (1969)  
IEC Fundamentals, 8, 374
- Kunugi, T., T. Sakai, K. Soma and Y. Sasaki, (1970)  
IEC Fundamentals, 9, 314.
- Kunugi, T., K. Soma, T. Sasaki (1970a)  
Ind. Eng. Chem. Fundamentals, 9, 319.

- Lahaye, J., H.B. Palmer and R.K. Sharma (1968)  
"Carbon", 6, 419
- Lahaye, J., G. Prado and J.B. Donnet (1974)  
"Carbon", 12, 27
- Leathard, D.A. and J.H. Purnell (1970)  
Ann. Rev. Phys. Chem., 21, 197.
- Lieberman, M.L. and G.T. Noles, (1974)  
Carbon, 12, 689.
- Lobo, L.S. (1971)  
Ph.D. Thesis. London University
- Lobo, L., D.L. Trimm and J. Figueiredo (1972)  
5th. Int. Congr. Catalysis, Palm Beach (U.S.A.)
- Lom, W.L. and A.F. Williams (1976)  
"Substitute Natural Gas. Manufacture and Properties"  
Applied Science Publishers Ltd. London.
- Makarov, K.I. and V.K. Pechick (1969)  
"Carbon", 7, 279
- Makarov, K.I. and V.K. Pechick (1974)  
"Carbon", 12, 391

- Moignard, L.A. and K.D. Stewart (1959)  
Trans. Inst. Gas Eng., 108, 528 (1958-1959)
- Murata, M. and S. Saito, (1975)  
Journal of Chemical Engineering of Japan, 8, 39.
- Murthy, P.S. Edge, R.F. (1963)  
I.G.E. Journal, 3, 459
- Nelson, W.L. (1958)  
"Petroleum refinery engineering",  
McGraw Hill Book Company, London.
- Nonhebel, D.C. and Walton, J.C. (1974)  
'Free - Radical Chemistry'  
(Cambridge, at the University Press)
- Oltay, E., J.M.L. Penninger and W.A.N. Konter, (1973)  
J. Appl. Chem. Biotechnol., 23, 573.
- Pacey, P.D. and Purnell J.H. (1972)  
IEC Fundamentals, 11, 233
- Palmer, H., Cullis, C.F. (1965)  
in "Chemistry and Physics of Carbon",  
Vol. 1, p.266 (P.L. Walker Jr. Ed. ) Dekker, New York.
- Penninger, J.M.L. and H.W. Slotboom (1973)  
Erdol und Kohle, Erdgas, Petrochemie 26, 445-47.

- Penninger, J.M.L. and H.W. Slotboom (1973)a  
Rec. Trav. Chim. Pays - Bas 92, 513.
- Penninger, J.M.L. and H.W. Slotboom (1973)b  
Rec. Trav. Chim. Pays - Bas 92, 1089.
- Prado, G. (1973)  
Ph.D. Thesis, Le Centre Universitaire du Haut Rhin et  
L'Universite Louis Pasteur de Strasbourg.
- Quinn, C.P. (1963)  
Proc. Roy. Soc. London, A275, 190.
- Ratajczak and Trotman - Dickenson, A.F. (1967)  
"Supplementary tables of bimolecular gas reactions",  
(Cardiff, University of Wales Institute of Science and Technology).
- Robertson, R.W.J. and D. Hanesian (1975)  
Ind. Eng. Chem. Process Des. Dev. 14, 216.
- Rostrup - Nielsen, J.R. (1975)  
"Steam reforming catalysts". "An investigation of catalysts for tubular  
steam reforming of hydrocarbons". Teknisk Forlag A/S  
(Danish Technical Press Inc.) COPENHAGEN, 1975.
- Seinfeld, J.H.,  
"Industrial and Engineering Chemistry" 62, 32
- Seinfeld, J.H., Lapidus, L. and Hwang, M. (1970)  
Ind. Eng. Chem. Fund. 9, 266.

- Slotboom and J.M.L. Penninger (1974)  
Erdol und Kohle - Erdgas - Petrochemie , 27, 410-412.
- Slotboom, H.W. and J.M.L. Penninger (1974)a  
Ind. Eng. Chem. Process Res. Develop. 13, 296.
- Snow, R.H., R.E. Peck, and C.G. Von Fredersdorf (1959)  
AIChE Journal, 5 304.
- Snow, R.H. (1966)  
The Journal of Physical Chemistry, 70, 2780.
- Tesner, P.A. (1973)  
Faraday Symposium, Chemical Society, 7 104.
- Thompson, B.H. and C.T. Brooks (1973)  
Paper presented to the 165th Amer. Chem. Soc. National Meeting,  
Dallas (U.S.A.).
- Trimm, D.L. (1974)  
"Comments from a visit to a steam cracking industrial plant",  
Private communication.
- Turner, C.E. (1976)  
Ph.D. Thesis, University of London.
- Virk, P.S., L.E. Chambers and H.N. Woebcke, (1974)  
Advances in Chemistry, 131, 237.

Weiss, A.H., L. Friedman (1963)

IEC Process Res. Dev. , V2, 163.

Zdonik, S.B., E.J. Green and L.P. Halle (1970)

"Manufacturing ethylene", The Petroleum Publishing Company,  
Tusla, Oklahoma, (U.S.A.).